GEOTECHNOLOGIEN

GEOTECHNOLOGIEN
Science Report

Early Warning Systems for Transportation Infrastructures

Workshop 9-10 February 2009
Fraunhofer IITB Karlsruhe
Karlsruhe Institute of Technology (KIT)

Programme & Abstracts

No. 15

GEOTECHNOLOGIEN
Science Report

Early Warning Systems
for Transportation Infrastructures

Workshop
9–10 February 2009
Fraunhofer IITB Karlsruhe
Karlsruhe Institute of Technology (KIT)

Programme & Abstracts

No. 15

Impressum

Editorship / Schriftleitung
Dr. Ute Münch, Dr. Alfons Buchmann

ISSN 1619-7399

Die Deutsche Bibliothek – CIP Einheitsaufnahme

GEOTECHNOLOGIEN
Workshop Early Warning Systems for Transportation Infrastructures

9–10 February, 2009
Fraunhofer Institute for Information and Data Processing (IITB)
Karlsruhe Institute of Technology (KIT)
Geophysical Institute and the Institute for Road and Railway Engineering

Programme & Abstracts –
Potsdam: Koordinierungsbüro GEOTECHNOLOGIEN, 2010
(GEOTECHNOLOGIEN Science Report No. 15)
ISSN 1619-7399

Distribution / Bezug
Koordinierungsbüro GEOTECHNOLOGIEN
Heinrich-Mann-Allee 18/19
14473 Potsdam, Germany
Fon +49 (0)331-288 10 71
Fax +49 (0)331-288 10 77
www.geotechnologien.de
geotech@gfz-potsdam.de

Preface

International Workshop on Early Warning Systems for Transportation Infrastructures

On February 9–10, 2009 an international Workshop on "Early warning systems for transportation infrastructures" was held at the Fraunhofer Institute for Information and Data Processing (IITB) in Karlsruhe. The Workshop was organized by the Geophysical Institute and the Institute for Road and Railway Engineering both at the University of Karlsruhe (TH), and the Fraunhofer Institute for Information and Data Processing (IITB). The meeting was funded by the geoscientific research and development programme GEOTECHNOLOGIEN.

The Workshop focus was on the specific safety requirements of railbound transportation systems. For the latter, early warning is crucial not only because of the long braking times of trains but also because of the high demands on track geometry and stability necessary for safe train operation. In addition, after a natural disaster, reliable and fast information about the state of the railway infrastructure (damage map) is of utmost importance in order to mitigate the consequences of the disaster.

During two days experts from the fields of seismology, sensor technology, railway engineering, computer science, and railway safety reviewed the state of the art and the potential of early warning for transportation systems. Major workshop topics were

- seismic early warning and sensors,
- early warning of endangered trains,
- damage assessment for railway infrastructure,
- modern geo-standard based information systems,
- train control and safety strategies.

Another purpose of the workshop was to delineate the possibilities and limitations of a railway infrastructure integrated network of accelerometers that can be used for permanent structural health monitoring and earthquake early warning.

The organizers wish to thank the speakers for their efforts in preparing interesting contributions as well as the attendants for participating in the discussions. We also thank the exhibitors, who displayed their latest sensor and railway technology products during the Workshop. Their names and addresses can be found in this volume.

Table of Contents

Workshop Program
»Early Warning Systems for Transportation Infrastructures«

Monday, 9 February 2009

Topic: Introduction

10:00 E. Hohnecker, University of Karlsruhe, Karlsruhe, Germany
Opening of Workshop

10:15 *Keynote:* F. Wenzel, Geophysical Institute, University of Karlsruhe, Germany
Seismic Early Warning – Recent Developments and Perspectives

Topic: Early Warning Systems and Sensors

11:00 Y. Nakamura, System and Data Research, Tokyo, Japan
On successive examples and discussions on earthquake early warning

12:15 M. Erdik, Bogazici University, Department of Earthquake Engineering, Istanbul, Turkey
Istanbul earthquake early warning and rapid response system

12:45 M. Picozzi, GFZ Potsdam, Germany
Self-organizing seismic early warning information network

14:15 C. Arnhardt and T. M. Fernandez-Steeger, Department of Engineering Geology and Hydrogeology, RWTH Aachen University, Germany
Sensor fusion in an ad-hoc multi-hop sensor network for realtime monitoring of landslides endangering human infrastructures

14:45 I. Iervolino, Department of Structural Engineering, University of Naples, Italy
The potential of structural control EEW applications

15:45 T. Titzschkau, A. Buchmann, D. Hilbring, University of Karlsruhe and Fraunhofer IITB Karlsruhe, Germany
Earthquake Early Warning Systems for Transport Lines

16:15 F. Quante, University of Applied Sciences, Bielefeld,
G. Schnellboegl, edilon-sedra GmbH, Munich
Th. Eisenmann, Infab GmbH, Munich
Railway Infrastructure: Type and viability of integrated measurements,
appropriate features of Embedded Rail Systems and applicability of FBG sensors

16:45 Discussion on topic: »Early Warning Systems and Sensors«

End of first day: 17:00

Tuesday, 10 February 2009

Topic: Infrastructure Endangered by Natural Hazards

9:00 K. Pitilakis, Dept. Civil Engineering, University of Thessaloniki. Greece
Seismic risk assessment of lifeline systems with emphasis on transportation systems

9:30 M. Hennecke, Zilch und Mueller, Munich, Germany
Railway infrastructure and seismic loads

10:00 K.-J. Bieger, DB AG, Frankfurt, Germany
Emergency management at Deutsche Bahn AG

11:00 U. Haeusler, Deutsche Bahn AG, Karlsruhe, Germany
Train operation control center and natural disasters

11:30 K. Meskouris, Chair of Structural Statics and Dynamics, RWTH Aachen, Germany
Seismic vulnerability assessment of bridges

12:00 Discussion on topic »Infrastructure Endangered by Natural Hazards«

Topic: Information Systems for Early Warning

13:15 T. Usländer, K. Watson, Fraunhofer IITB, Karlsruhe, Germany
Integration of sensors into early warning systems

13:45 C. Kiehle, J. Mays, lat/lon GmbH, Bonn, Germany
Sustainable spatial infrastructure components as building blocks for early warning system based upon open geospatial platforms

14:45 Stefan Hinz, University of Karlsruhe, Germany
Automated detection and classification of intact road networks in multi-sensorial remote densing data for near-realtime disaster management

15:15 Kai Walter, Frank Niemeyer, Universität Rostock, Rostock, Germany
Delivering data from a wireless sensor network via sensor observation service

15:45 Discussion on topic: »Information Systems for Early Warning«

16:00 F. Wenzel, Geophysical Institute, University of Karlsruhe, Germany
Workshop Summary and Future Developments

End of Workshop: 16:30

On Successive Examples and Discussions on Earthquake Early Warning

Nakamura, Y. (1, 2)

(1) President, System and Data Research, Tokyo, Japan

(2) Visiting Professor, Dept. of Built Environment, Tokyo Institute of Technology, Japan

Email: yutaka@sdr.co.jp

Abstract

This paper describes the concept and a brief history of EEW, which is almost equal to the development of the UrEDAS, Urgent Earthquake Detection and Alarm System. UrEDAS is the first practical P-wave early warning system. And the explanations of early warning systems and the actual example of disaster prevention by this system are also described. Finally I would like to discuss on the role of national or public organization about the earthquake disaster prevention, especially in Japan. The concluding remarks as follows: 1) Network alarm is effective for middle distance area, but risky because of the data interruption caused by the network error, 2) On-site alarm by FREQL or AcCo is useful for anywhere, even in epicentral area, 3) Early Earthquake Information distributed by JMA is full of error and useless for damage area because of too late warning, and 4) the nation-wide-organization must be issued the detailed earthquake information as soon as soon as the earthquake terminated, and issuing alarm is not a role of these organizations.

KEYWORDS: EEW, UrEDAS, Compact UrEDAS, FREQL, Real-Time, P wave Warning

1. Brief History of Earthquake Early Warning

There are two kinds of the earthquake alarm as Figure 1. One is »On-Site Alarm« which is the alarm based on the observation close to the side of the objects to be warned. The other is »Front Alarm« which is the alarm based on the observation near the epicentral area for the warning to possible damage area. Because of using communication networks, the latter is also called »Network Alarm« instead of »Front Alarm«.

For each, there are two more kinds of alarm. One is the alarm exceeding the preset level, so-called »S-wave Alarm« or »Triggered Alarm«. And the other is the alarm during the preliminary motion, so-called »P-wave Alarm«.

As the first stage of the earthquake alarm, the simple triggered alarm had been realized. This is ussued by the alarm seismometer observing the strong motion just near the objective for the alarm, and when the earthquake motion exceeds the preset level, the alarm seismometer issues the alarm. Although because of the anxiety of false alarm, it is impossible to set the alarm level low and the alarm is issued almost same time to the severe strong motion. But even so, it is useful to stop the gas supply or other systems automatically.

Next, to extend the time margin before the strong motion arrival, it was considered the way to observe the earthquake near the focal area, so-called »Front Alarm«. Dr. Cooper originally had offered this idea in 1868. He proposed to utilize the propagation time of the earthquake motion from the epicenter to alarmed area, supporting the activities for escape. More than 100 years after this original idea, the first system realizing the »Front Alarm« was developed as the coast line detection system for Tohoku Shinkansen line in

1982. After this, SAS, Sistema de Alerta Sísmica, for Mexico City started operation in 1991.

The first P wave detection system for practical use, UrEDAS, Urgent Earthquake Detection and Alarm System, was realized as the front alarm system for Tokaido Shinkansen line in 1992, and then almost same system was installed for Sanyo Shinkansen line in 1996. The UrEDAS technology is based on new concepts and methods to realize a real time system for estimating the earthquake parameters as magnitude, location and depth using only the initial motion of P wave at single station.

The 1995 Great Hanshin Disaster triggered to develop earlier P wave alarm system because of the recognition of necessity to construct onsite P wave alarm. This is realized as Compact UrEDAS, that the alarm concept is different from the UrEDAS, and it was installed for Tohoku, Joetsu and Nagano Shinkansen lines and Tokyo metro subway network. The detail of the Compact UrEDAS is described later.

In Japan at 1992, a new information service including »Network Alarm« using UrEDAS technology had been prepared, but it was not born due to objection of JMA, Japan Meteorological Agency. By the same JMA, an information service has been broadcasted in nation wide since the first of October 2007. This implies that our UrEDAS Information Service plan has been correct, and it is my pleasure. However, it shall be rare case in Japan that JMA's information will reach faster than arriving of M7 class or less earthquake at the possible damaged areas, because it takes relatively long time for processing and transmitting. Only for M8 class earthquakes that the occurrence probability is about once in several ten years in Japan, it will be possible to receive the information before arriving of strong shaking in a possible damaged area far from the epicenter.

Paying attention to the abilities of UrEDAS, a local government, Wakayama Prefecture, having coastline decided to install UrEDAS for their own tsunami disaster prevention system and started test operation in 2000.

As the new generation of UrEDAS and Compact UrEDAS, a new small-sized instrument FREQL, Fast Response Equipment against Quake Load, is developed to shorten the processing time for alarm and to combine the functions of UrEDAS and Compact UrEDAS. After P wave detection, FREQL can issue the alarm within one second (minimum in 0.1 seconds as of May 2009) and estimate the earthquake parameters at one second. Since 2005, FREQL has been adopted for the hyper rescue team of Tokyo fire department to save the staffs from the large after shocks during their activity.

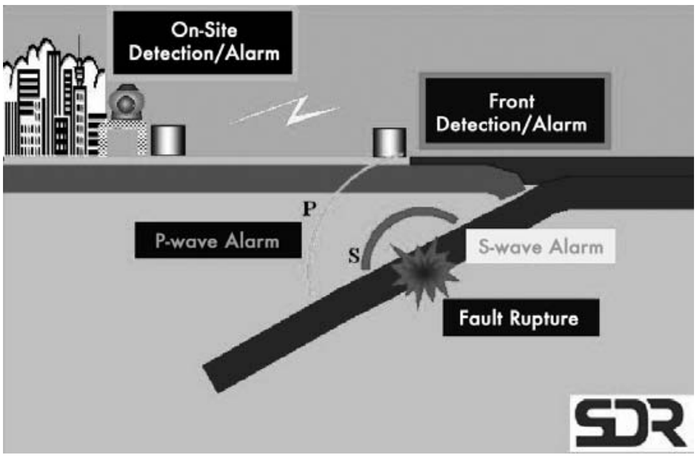

Figure 1: Concept of Earthquake Early Warning

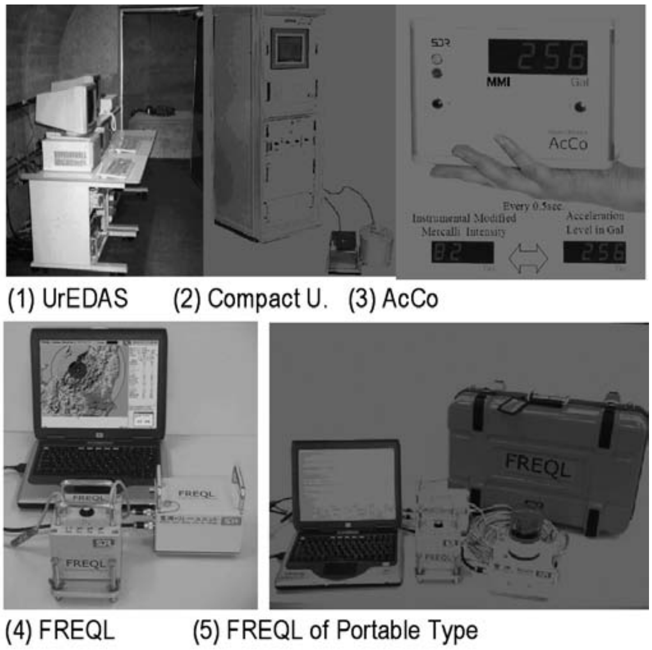

Figure 2: UrEDAS, Compact UrEDAS, FREQL and AcCo

On the other hand, it is necessary for local facilities to grasp immediately their »own« strong motion index for the quick response. For this purpose, a simple seismometer »AcCo«, Acceleration Collector, was developed. This unique palmtop seismometer has a bright indicator, memory, alarm buzzer and relay connecter. On-Site alarm is more important than the network alarm, because the network alarm is sometime missed during data communication.

2. PRINCIPAL EARTHQUAKE EARLY WARNING SYSTEMS

2.1 UrEDAS, Urgent Earthquake Detection and Alarm System

Main UrEDAS functions are estimations of magnitude and location, vulnerability assessment and issuing warning within a few seconds using initial P wave motion at a single station. Unlike the other automatic seismic observation systems, UrEDAS does not have to transmit the observed waveform in real time to a remote processing or centralized system and thus the system can be considerably simplified.

UrEDAS calculates parameters such as back azimuth, predominant frequency for magnitude evaluation and vertical to horizontal ratio for discrimination between P and S waves, using amplitude level for each sampling in real time. These calculations are basically processed in real time without storing waveform data. UrEDAS processes these calculations continuously regardless of whether an earthquake occurs or not, and calculates as filtering, so the number of procedures is not increased in the event of an earthquake. UrEDAS can detect earthquakes in P-wave triggering with the amplitude level, and then estimates earthquake parameters such as magnitude, epicentral and hypocentral distance, depth and back azimuth from the result of real-time calculation in a fixed period. UrEDAS can issue the alarm based on the M-Δ diagram in Figure 3 immediately after the earthquake detection. This new way of alarm is referred to as the M-Δ Alarm. Moreover UrEDAS can support restarting operation based on the detailed earthquake parameters.

The 1995 Hyogoken-Nambu Earthquake also provided the motivation for Compact UrEDAS development. Figure 4 shows several pictures from the VTR shoot in the focal region, initial

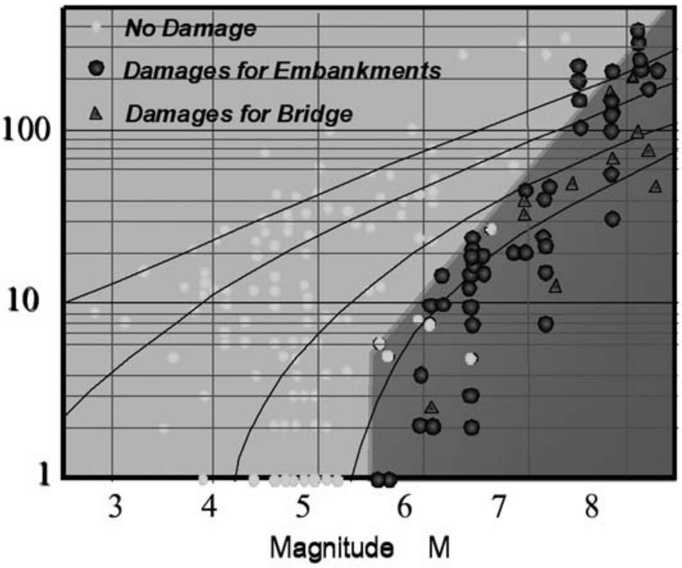

Figure 3: M-Δ Diagram

Figure 4: Video Photos examples at focal region

P wave motion was detected as something happening, and then severe motion started. In an interview with victims, although there were only a few seconds between notification of something happening to earthquake recognition, there was anxiety and fear because they could not understand what happens during this period and felt relieved after recognition of earthquake occurrence. To counter this kind of feeling, earlier earthquake alarm was required. So Compact UrEDAS was developed to issue the alarm within one second of P wave arrival.

2.2 Compact UrEDAS

Compact UrEDAS estimates the destructiveness of the earthquake in realtime from the earthquake motion directly, not from the earthquake parameters as UrEDAS, and then issues the alarm if needed. To estimate earthquake dangerousness, the power density PD (W/kg) of the earthquake vibration is calculated from the inner product of the acceleration vector *a* (cm/s^2) and the velocity vector *v* (cm/s). Hence this value will be large, Destructive Intensity (*DI*) is defined as the logarithm of absolute value of this inner product (*LPD*,

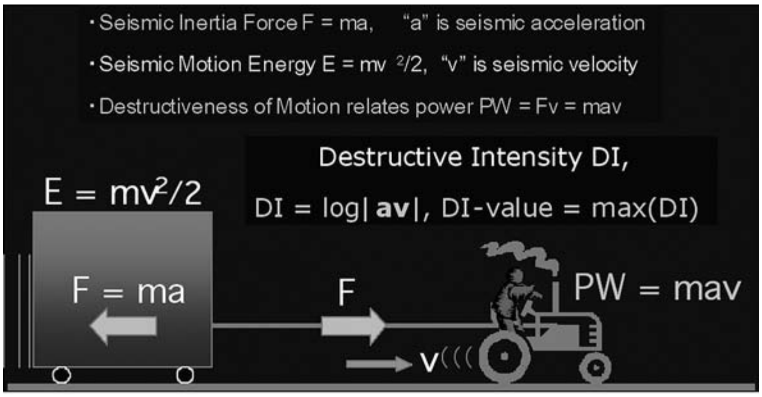

Figure 5: Definition of *DI*

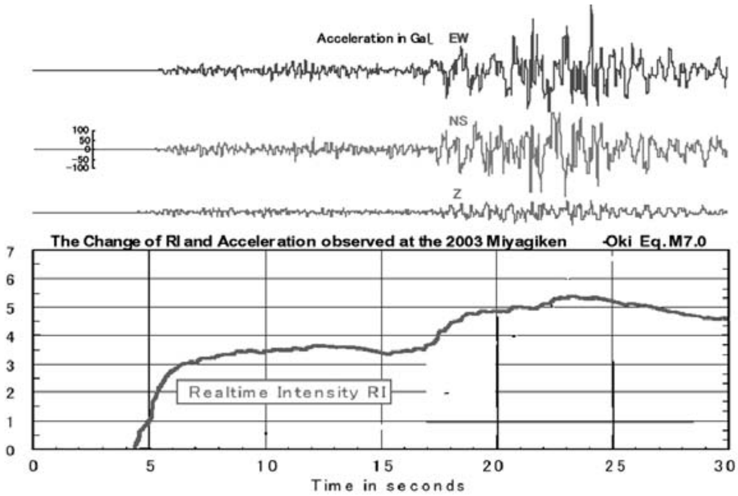

Figure 6: Change of *RI*

logarithm of the power density) as Eq. (2.1), illustrated in Figure 5.

$$DI = \log |\boldsymbol{a} \cdot \boldsymbol{v}| = LPD + 4.0 \qquad (2.1)$$

The maximum value of *DI* during an event, *DI*-value relates to earthquake damage and is similar to the instrumental intensity scale of JMA with the constant difference of 2.4, and corresponds to MMI, Modified Mercalli Intensity. These indexes are referred as *RI*, Realtime Intensity, and *MMI*, respectively.

$$RI = DI + 2.4 \qquad (2.2)$$

$$MMI = (11/7)\, RI + 0.5 = (11/7)\, DI + 4.27 \qquad (2.3)$$

Instrumental JMA seismic intensity can be determined only after the earthquake termination according to its definition. On the other hand, *DI* has a very important practical advantage, because it can be calculated in real time soon after the P-wave arrival with the physical meaning. Figure 6 shows the change of *RI* as a function of time. When the P wave arrives, *RI* increases drastically. *PI*-value is defined as the maximum *RI* within *t* seconds after P-wave detection. This value suggests to be used for P-wave alarm. Subsequently, *RI* continues to increase slowly until the S-wave arrival, and the maximum value of *RI* is called *RI*-value. In other words, with the continuous observation of *RI*, an earthquake alarm can be issued efficiently and the damage can be estimated precisely.

2.3 FREQL, Fast Response Equipment against Quake Load

FREQL is integrated the functions of UrEDAS, Compact UrEDAS and AcCo described later. Which is to say that FREQL can estimate the earthquake parameters one second after the P wave detection faster than UrEDAS, and it can judge the dangerousness of the earthquake motion within one second, minimum in 0.1 seconds, after P wave detection faster than Compact UrEDAS, and can output the information and alarm based on both acceleration and *RI*, Realtime Intensity, in real time same as AcCo.

And all the components of a seismometer, sensors, A/D converter, amplifier, CPU and so on, are put together in small aluminum die-cast vessel of almost 5 inches cube, and the system is electrical isolated. So the FREQL is easy to install and the structure of FREQL is noise proof.

FREQL also has functions to omit the influence of electrical thunder noise and to detect the P wave after rather small pre-shock. Thus it is able to say that FREQL solved the known problems of the ordinary earthquake early warning systems. It is known that there was a pre-shock at the time of the 1994 Northridge earthquake attacked Los Angels and the 1995 Hyogoken-Nanbu Earthquake attacked Hanshin area. It seems to be failing for the early warning system except FREQL that it is not possible to issue the alarm for large earthquake motion if the pre-shock exists just before the destructive earthquake because the pre-shock is recognized as small event. And also it seems to be difficult for the huge system to keep running perfectly under the destructive earthquake motion. It is uncertain only with such remote systems because of information lack. It must be considered to install the onsite warning system for the important facility.

FREQL is toward to the new field for the early warning system, as for the hyper rescue teams of Tokyo fire department under the severe situation with the risk of aftershocks (see Figure 7). Hyper rescue teams made a miraculous activity but the activity was always in a risk of large after shocks. After the activity at the damaged area of the 2004 Niigataken-Chuetsu Earthquake, the Tokyo fire department approached us to adopt FREQL as a support system for the rescue activity, taking notice of the portability, rapidness and accuracy of the warning. The portable FREQL for Tokyo fire department was consists of FREQL main body, power unit with backup battery for three hours, central monitoring system and the portable alarm instrument with more than 105dB loud alarm and rotary light.

Tokyo fire department has equipped the FREQL unit from spring of 2005, and since 2007, three hyper rescue teams is operating. At the time of their rescue activity after the 2005 Pakistan earthquake, they reported that FREQL works in right manner. Also at the Wenchuan earthquake in China, Japanese international rescue team had done the rescue activity with the portable FREQL. Now, there are many FREQL of the portable type equipped at local fire departments in Japan.

And the FREQL of stationary type are used in many field such as subway, nuclear power plant, high-rise building, semiconductor facilities, and etc., in Japan.

Figure 7: New Field for EEW

Now, in Berkeley and in Pasadena, California, FREQL has started test observation. These projects are doing under the support by UC Berkeley and Caltech. I hope this FREQL network growth to Pan-Pacific Tsunami Warning System.

2.4 AcCo, Acceleration Collector

Because usual seismometers were expensive and required an expert of installation and maintenance, they have been installed for limited facilities. After the Kobe earthquake, the number of seismometer was installed but at most thousands sets for whole Japan. It is not so much because it means one set per several tens km^2 or per several ten thousands person. Even so there are many seismometers in Japan, but many hazardous countries have only a few seismometers. So it is difficult to take exact countermeasure against earthquake disasters because it is impossible to grasp and analysis the damage based on the strong motion records and to draw a plan of the city with certain strategy.

AcCo was developed to realize a simple seismometer to issue alarm and record the strong motion in low cost. Since AcCo is just a palmtop size instrument, it can indicate not only acceleration but also the world's first real time intensity. So AcCo can issue alarm with the trigger of both acceleration and intensity. AcCo indicates acceleration and intensity if the 5HzPGA (5 Hz low passed peak ground acceleration) exceeds 5 Gals as in Figure 2(3). Intensity can be chose from *RI*, *MMI* or PEIS, Philippine Earthquake Intensity Scale. AcCo can output the digitized waveform via serial port and also record the waveform for the two largest events with delay memory. AcCo can work with AC power supply and backup battery for seven hours.

Because AcCo indicates acceleration as inertial force and RI as the power of the earthquake motion, it is useful to learn the sense for the meaning of acceleration and intensity from the experience. This sense is required for the exact image against the earthquake motion.

AcCo has been applied for many fields as warning system, education, kindergarten, factory, train operation and so on. And also AcCo is used not only in Japan but also in out side of Japan for a instance, Taiwan, Philippine and etc.

2.5 Alarm timing and margin time gained by EEW

In case of the system requiring the earlier warning with no error or accidental warning, it is necessary to install a system with high reliability and sophisticated as FREQL. But in gen-

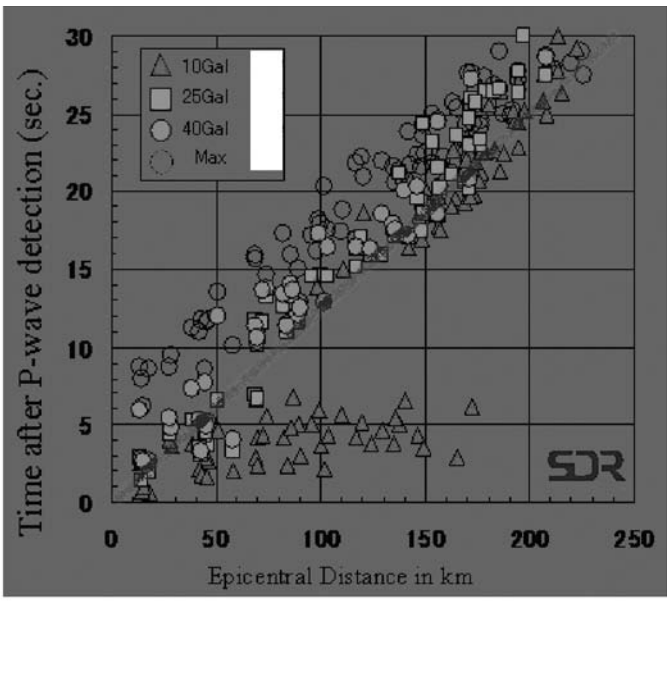

Figure 8: An example of alarm timings by simple triggers in case of the 2000 Tottoriken-Seibu Earthquake

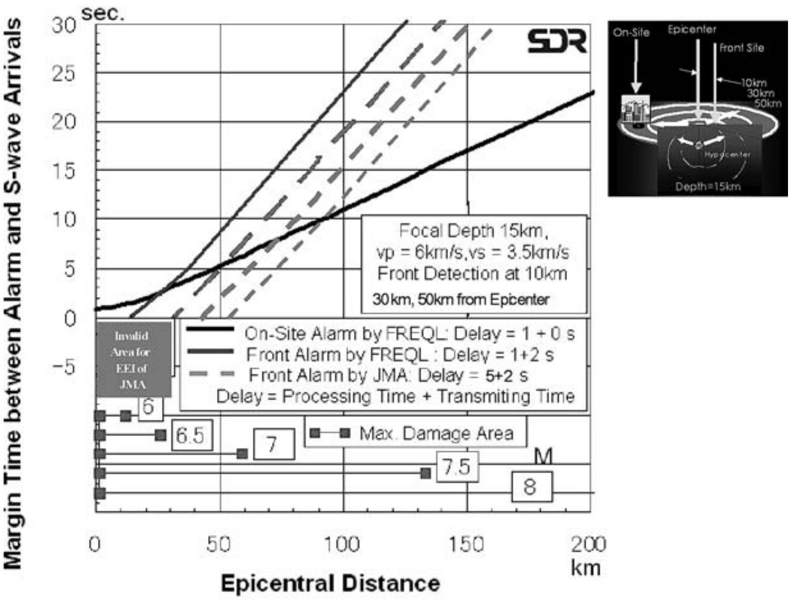

Figure 9: Margin time by EEW

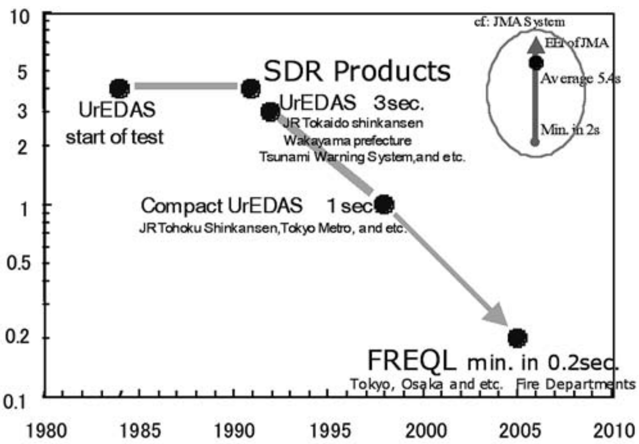

Figure 10: Change of processing time for EEW

eral, it seems to be useful even the simple warning system. This kind of system seems to be useful enough in many cases under the situation of several alarms per year even in higher seismic activity area of Japan. AcCo 10 Gals alarm or RI 2.0 alarm can play the role of this simple early warning. Figure 8 shows the relationship example between the alarm timings. Since the AcCo 10 Gals alarm or RI 2.0 alarm is a little later than the P wave alarm of FREQL, it is enough earlier than the ordinary triggered S wave alarm.

Figure 9 shows gained time margin by EEW. Basic condition for calculating time margin is assumed as follows: focal depth is 15 km, velocity of P-wave and S-wave are vp = 6 km/s and vs = 3.5 km/s, respectively, front detection site at 10 km, 30 km and 50 km from the epicenter.

Based on the calculation for 10km, Earthquake Early information, of JMA comes after S wave arrival within a 30 km radius as confession by JMA. On-Site alarm by FREQL can keep at least more than one second even just above the epicenter; and more time margin than front alarm by JMA within about 55 km radius from the epicenter. This distance corresponds for out line of the damage area for over M7. It means that the EEI of JMA is not available the estimated damaged area up to M7, so it seems that it is not useful for the recent Japanese earthquake in this 20 years. Contrary to this, the on-site FREQL alarm is available even around the focal area; of course the margin time is just a few seconds. So we should take a hard look at the on-site alarm and put it into practical use. It is also useful for popularization of earthquake disaster mitigation. It seems that there are many fields not so affected by false alarm if reset easily. Official information as correct location and magnitude must be informed within few minutes for the exact clear of the alarm. And this kind of information must keep suitable redundancy so there must be informed from several organizations.

3. EXAMPLE OF DISASTER PREVENTION

At the time of the 2004 Niigataken Chuetsu Earthquake, Mjma 6.8, there were four trains running in the focal area. There are four observatories called Oshikiri SP, Nagaoka SSP, Kawaguchi SS and Muikamachi SP, from north to south. Kawaguchi and Nagaoka issued both the P-wave and the S-wave alarms, and the others issued only the S-wave alarm. Every station issued the alarm for the section to the next station (see Figure 11). At first Kawaguchi and then Nagaoka issued the P-wave alarm. Subsequently, Oshikiri and Muikamachi issued the 40 Gals alarm. As the result, trains Toki #325 and #332 received the alarm 3.6 seconds after the earthquake occurred, Toki #406 4.5 seconds after and Toki #361 11.2 seconds. The damaged section was between

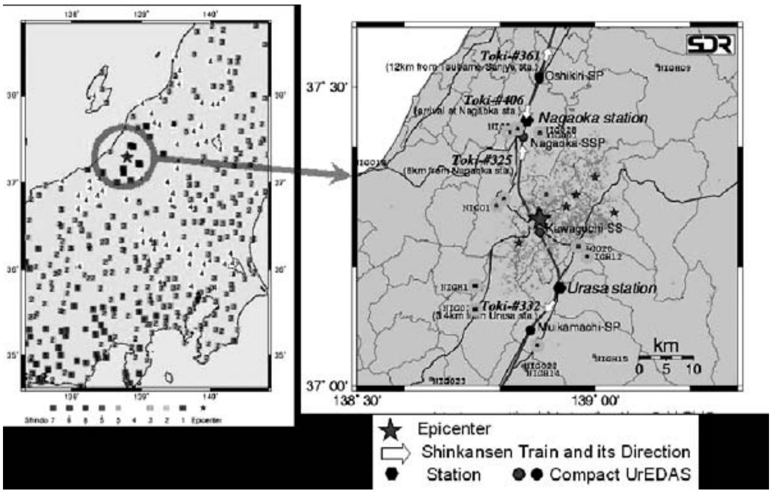

Figure 11: The 2004 Niigata-ken-Chuetsu Earthquake

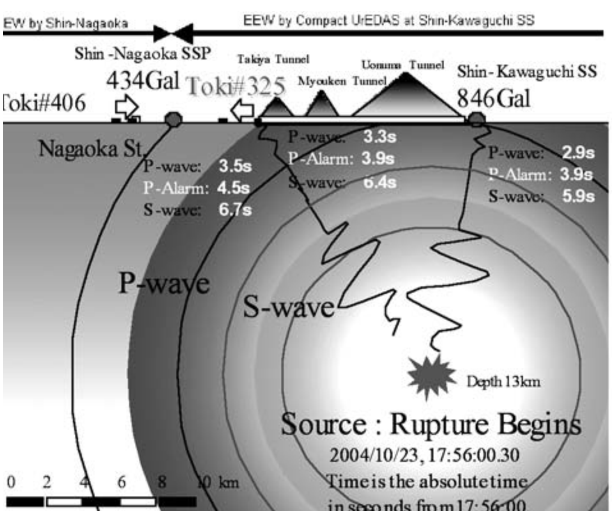

Figure 12: Schematic diagram for this earthquake

Muikamachi and Nagaoka. Trains traveling on this section received the alarm immediately, proving that the alarm system settings were appropriate.

The UD component of earthquake motion predominate at the high frequency more than 10 Hz. The Shinkansen line runs from north to south and the EW component seems to contribute to derailment. In the case of the EW component, there is a peak at 1.5 Hz and the range of 1 to 2.5 Hz predominates. The natural frequency of the Shinkansen vehicle is included in this frequency range.

The Kawaguchi observatory detected the P wave 2.6 seconds after the earthquake occurred, and one second after that, or 3.6 seconds after the occurence, issued a P-wave alarm. When the derailed train, Toki #325, encountered the earthquake motion when traveling at 75 m from the Takiya tunnel exit of 206 km 000 m from Tokyo, the train received the alarm from the Compact UrEDAS and the power supply was interrupted. The Shinkansen train situated automatically to apply the break immediately at the interruption of power supply. The driver put on the emergency brake after recognizing the Compact UrEDAS alarm. The S-wave hit the train 2.5 seconds after the alarm, and more one second later, a strong motion with five seconds duration hit the train. Figure 12 shows the schematic diagram for this earthquake.

As the result of simulation using the strong-motion records at Kawaguchi and Nagaoka, real-time intensity (RI) rose sharply with the earthquake motion arrival and immediately reached the P-wave alarm level. This RI is a real-time value and the maximum value fits to the instrumental intensity of JMA. Because FREQL, improves the reliability of P-wave distinction, FREQL can issue the alarm immediately after exceeting the P-wave alarm threshold. If FREQL had been installed instead of Compact UrEDAS, both Kawaguchi and Nagaoka observatory would issued the P-wave alarm 0.2 and 0.6 seconds after P-wave detec-

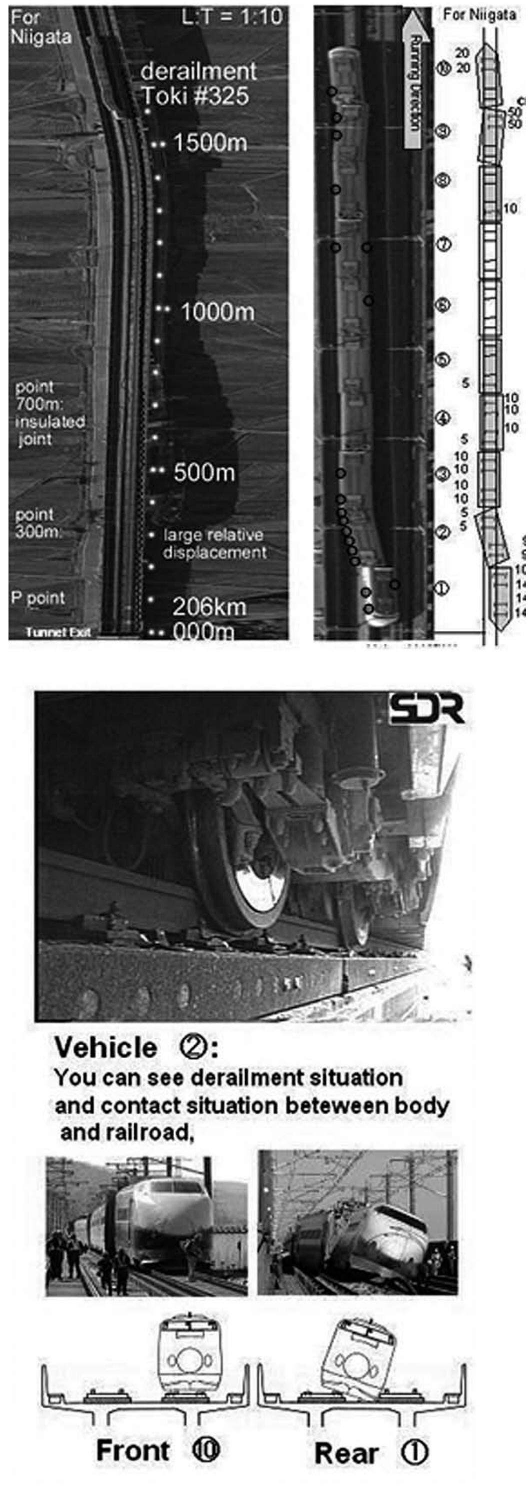

Figure 13: Detail of the derailment

Alarm and Accident Site	Kawaguchi	Tunnel Exit	Nagaoka
5HzPGA (Gal)	846		434
RImax (MMI)	6.6 (10.9)		5.8 (9.6)
Origin Time	17:56:00.3	17:56:00.3	17:56:00.3
Recorded Detecting Time	3 s		4 s
P-wave arrival Time	2.9	3.3	3.5
Time of RI >2	3.1		4.1
P-wave Alarm Time	3.9	3.9	4.5
Time of Max. Acc >10Gal	3.4		4.7
Time of Max. Acc >40Gal	4.2		5.9
Time of 5HzPGA	7.7		9.4
Time of RImax	8.1		9.5

Table 1 Summarize the simulation results

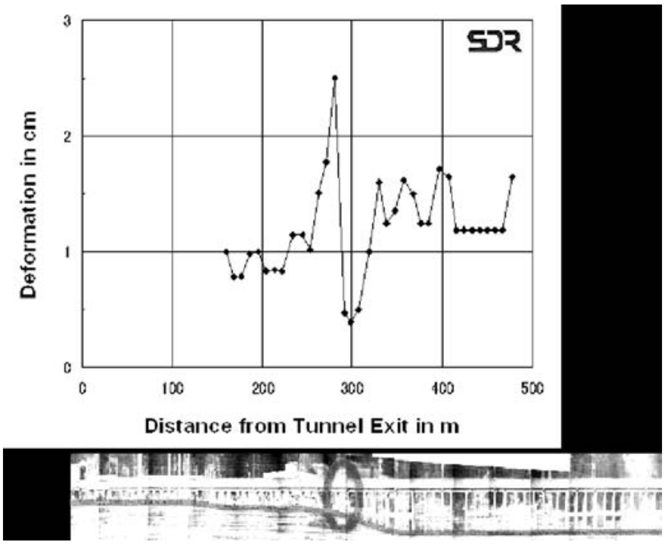

Figure 14: Performance of the deformation

tion, respectively. Table 1 summarizes the simulation results. In this case, the P-wave alarm reached the derailed section before P-wave arrival. Accordingly, FREQL minimizes the process time for alarm.

Figure 13 shows the details of the derailment. The derailed train, Toki #325, consisted of 10 cars, from car #10 to car #1 along the traveling direction. The number of derailed axles is 22 out of a total of 40 axles. The last car, #1, fell down the drain besides the track and tilted by about 30 degrees. The open circle indicates the location of broken window glass. The number of broken grass appears larger on the left due to the something bounce from the sound barrier, and tends to break one or two cars after the derailed car. The number of the broken glass of the car #2 exceeds that of the car #1. If it is assumed that the glass broken of car #2 was caused by the derailment of cars #4 and #3, the paucity of broken glasses from car #1 suggests that car #2 did not derail during the earthquake motion. It is estimated that the frictional heat between the vehicle and the rails caused elongation and slightly rift up at the joints of 206 km 700 m, and car #1 derailed, making car #2 derail.

Deformation performance of viaducts is specified within one cm under the loading of the seismic design force. Although the designed natural frequency corresponding to the deformation performance is 2.5 Hz, in practice it is 3.5 Hz. Thus the viaduct may be considered to behave statically against the earthquake motion less than around 1.5 Hz. Figure 14 shows the relative deformation derived from the dimension of the viaduct columns. The meshed line shows the averaged deformation

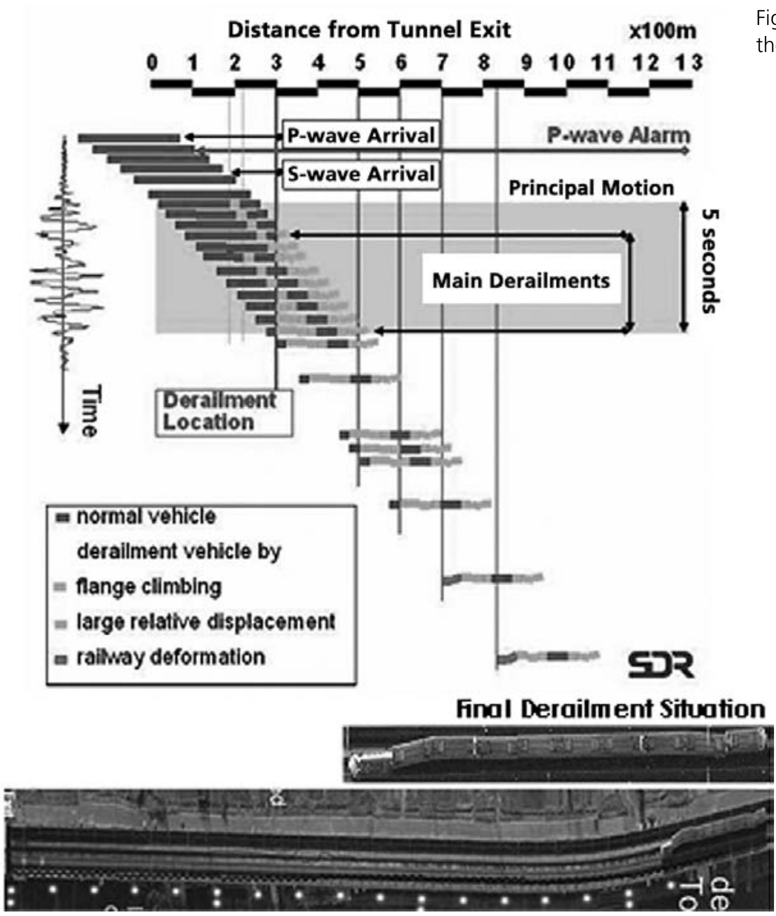

Figure 15: Estimated situation of the derailment

for each viaduct block, and it is estimated that the relative large occurred at the area farther from the tunnel exit. Taking into account the timing of earthquake occurrence, this is the point of derailment.

Figure 15 shows the outlines the circumstances of the derailment. It seems that the derailed cars were on the large displacement section accidentally. The later the alarm reached, the more the number of derailed car, because of the risk of running the large displacement section. As a result, if the friction heat release value were higher, the derailment situations were more severe. On the other hand, the early warning shows decreasing the train speed which means that the main shock hits the train before the large displacement section and decreases while the train travels the section. The number of the derailed cars is thus expected to decrease and the derailment damage must be minor. In this regard, the P-wave alarm of the Compact UrEDAS demonstrates its effectiveness at making the derailment non-catastrophic.

4. DISCUSSION

It seems that the difference between the real time seismology (RTS) and the real time earthquake engineering (RTEE) is the way of contribution indirectly or directly for practical use, as same as the difference between science and engineering. RTS makes the countermeasure soon after the earthquake rational and prompt by sending information universally to be useful for public. And RTEE sends the information for certain customers as a trigger of the countermeasures against the earthquake disaster. From the view of time domain, RTS is required by the rational action after the earthquake terminated and RTEE is necessary for the immediate response just after the earthquake occurrence or earthquake motion arrival.

RTS needs high accuracy on the information but not immediate, so it is possible to utilize effectively the knowledge and experience on seismology and infrastructures as observation networks. The tasks are to be more accurate the information on the earthquake observation and to deliver rapidly to all people.

On the other hand, the most important aim of RTEE is to decrease the degree of the disaster or the possibility of the disaster occurrence so it is necessary to issue alarm rapidly and certainly. For this purpose, at first it must be concerned to install own observation system for the alarm, without relying the information from the other authorities. And then, it is possible to use the other information if it can be received. It is necessary to customize the way of issuing and utilizing the alarm depends on the situation for each customer and fields. Again, it is risky to rely to the information only from the other authorities using the data transmission network under the situation of earthquake.

In Japan, JMA has started delivering on 1st October 2007. It is clear that EEI is belonging to RTS. So it is only a result of earthquake observation and must be delivered widely for public with no restriction for receiving. Since for some case, it may be possible to use it as alarm, but generally to say, EEI is mainly for the rational countermeasures after earthquake termination. People must use it for quick release of the EEW by themselves if the alarm is not needed. From the view point of this, the most important point is accuracy and the delay of few seconds is not a problem, because the error of this kind of information may cause a serious confusion. It is enough that the accurate information is delivered within one or two minutes after the event. Alarm must be released rationally and EEI may play an important role as one of the useful tools for this. It is necessary to grasp the distribution of earthquake motion at the early stage. It is recommended to progress the earthquake disaster prevention with the combination of the public information such as EEI by JMA rather late and local dense and quick information by the people.

5. CONCLUSION

The concluding remarks are as follows: 1) Network alarm is effective for middle distance area, but risky because of the data interruption caused by the network error, 2) On-site alarm by FREQL or AcCo is useful for anywhere, even epicentral area, and 3) Early Earthquake Information distributed by JMA is full of error and useless for damage area because of too late warning.

Accurate and quick earthquake information just after shaking is more useful than the late early warning. I hope JMA to make best effort that they can announce the earthquake information not only for main shock but also aftershocks, because these information is quite important for the quick response after the earthquake.

REFERENCES

Cooper, J. D., Earthquake Indicator, San Francisco Daily Evening Bulletin, 3rd November 1868.

Nakamura, Y., Earthquake Warning System of Japanese National Railways (in Japanese), Railway Technology, Vol. 42, No. 10, pp. 371–376, 1985.

Nakamura, Y., ON THE URGENT EARTHQUAKE DETECTION AND ALARM SYSTEM (UrEDAS), Proceedings of 9th WCEE, JAPAN, Vol. VII, pp. 673–678, 1988.8.

Nakamura, Y., A New Concept for the Earthquake Vulnerability Estimation and its Application to the Early Warning System, Early Warning Conference 98 in Potsdam, Germany, 1998.9.

Nakamura, Y., UrEDAS, Urgent Earthquake Detection and Alarm System, now and future, 13th WCEE, paper #908, 2004.

Nakamura, Y., On a Rational Strong Motion Index Compared with Other Various Indices, 13th WCEE, paper #910, 2004.

Nakamura, Y., Earthquake Early Warning and Derailment of Shinkansen at the 2004 Niigataken-Chuetsu Earthquake (in Japanese), Jishin Journal, No. 41, pp. 25–37, Association for the Development of Earthquake Prediction, June 2006.

Nakamura, Y. and Saita, J., UrEDAS, the Earthquake Warning System: Today and Tomorrow, Earthquake Early Warning Systems, Springer, pp. 249–281, 2007.

Nakamura, Y. and Saita, J., FREQL and AcCo for a Quick Response to Earthquake, Earthquake Early Warning Systems, Springer, pp. 249–281, 2007.

Istanbul Earthquake Rapid Response and the Early Warning System

Erdik M., Alcik H., Ozel O., Mert A., Kafadar N., Tahtasıoğlu B., Korkmaz A.

Department of Earthquake Engineering

Kandilli Observatory and Earthquake Research Institute

Bogazici University, Istanbul, Turkey

1. BACKGROUND AND INTRODUCTION

Management of earthquake risks is a process that involves pre-, co- and post-seismic phases. Earthquake Early Warning (EEW) systems are involved in the co-seismic phase. These involve the generation of pre-shakemaps as products of real-time seismology and/or generation of alarm signals directly from on-line instrumental data. The Rapid Response Systems take part immediately after the earthquake and provide assessment of the distribution of ground shaking intensity (Shake Maps) or physical damage and casualties (Loss Maps). These maps can serve to direct the search and rescue teams to the areas most needed and assist civil protection authorities in the emergency action.

As urbanization progresses worldwide Earthquake Early Warning (EEW) and Earthquake Rapid Response Systems (ERR) can be a useful tool for reducing earthquake risks by forewarning of forthcoming strong ground shaking. The implementation of urban earthquake early warning systems are proposed by United Nations – International Strategy for Disaster Reduction (UN-ISDR) (www.unisdr.org/) and by USGS-ANSS-Advanced National Seismic System (www.anss.org/) and by a series of international conferences (e.g. www.ew3.org, http://www.eqh.dpri.kyoto-u.ac.jp/src/eew/).

EEW systems must recognize the severity of expected ground motions within several seconds. Based on this information, suitable actions for the damage reduction can be triggered and executed. The major challenge in the development of earthquake early warning (EEW) systems is the achievement of a robust performance at largest possible warning time. Even several seconds of forewarning time will be useful for automated (servo) emergency stopping measures to avoid potential derailment of for rapid-transit vehicles, high-speed trains, it will be also useful for orderly shutoff of gas and oil pipelines to minimize fire hazards, safe-guarding of computer facilities to avoid loss of vital databases and safe shutdown of high-technological manufacturing operations to reduce potential losses. These objectives requite that the EEW systems have to be very fast and, at the same time, highly reliable. Reliability can be achieved through redundancies built in the system to make it robust.

The two main types of EEW systems can be distinguished: regional and onsite warning systems. The regional warning systems, such as the one installed in Taiwan and Japan (Wu et al., 1999; Gasparini et al., 2007), use networks of seismic sensors with real-time capability to determine the source parameters of an earthquake (i.e. real time seismology). The source parameters need to be interpreted to yield the ground motion parameters to initiate specific warning levels. On the other end, the onsite warning systems, such as the Japanese UrEDAS (Nakamura, 1988 and 1989), the Californian ElarmS (Allen and Kanamori, 2003), or the Romanian EEW system (Wenzel et al., 1999), are based on seismic observations at single (or collection of single) sensors. Currently EEW systems are either implemented on in construction or planning stage in Mexico City , Bucharest-Romania, Southern California-USA, Naples- Italy, Japan, Taiwan, Istanbul-Turkey and Greece (Espinosa-Aranda et al., 1995; Nakamura, 1988; Wenzel et al., 1999; Wu et al., 1999; Allen and Kanamori, 2003; Gasparini et al., 2007; Olivieri et al., 2008; Allen et al., 2009; Zollo et al., 2009).

The reduction of casualties in urban areas immediately following an earthquake can be improved if the location and severity of damages can be rapidly assessed by the information from Rapid Response Systems. Emergency management centers of both public and private sector with functions in the immediate post-earthquake period can allocate and prioritize resources to minimize the loss of life. The rapid response systems currently used in the United States rely on the »ShakeMap« systems that provide maps of ground motion and shaking intensity following significant earthquakes (http://earthquake.usgs.gov/eqcenter/shakemap/) in near-real-time. ShakeCast (http://earthquake.usgs.gov/shakecast/), short for ShakeMap Broadcast, is a fully automated system for delivering specific ShakeMap products to critical users and for triggering established post-earthquake response protocols. Among others, the Taiwan Earthquake Rapid Reporting System, the Real-time Earthquake Assessment Disaster System in Yokohama (READY), The Real Time Earthquake Disaster Mitigation System of the Tokyo Gas Co. (SUPREME) and the Istanbul Earthquake Rapid Response System provide near-real time damage estimation after major earthquakes (Erdik and Fahjan, 2006).

2. ISTANBUL EARTHQUAKE RAPID RESPONSE AND EEW SYSTEM

Istanbul faces a significant earthquake hazard with a 70% chance for an event of moment magnitude above 7.2 in the next 30 years (Erdik et al., 2004). To assist in the reduction of losses in a disastrous earthquake in Istanbul 160 strong motion recorders were stationed in free field stations in the Metropolitan area, on critical structures and at closest locations to the Main Marmara Fault, where the damaging earthquake is expected to originate (Figure 1). All together this network and its functions is called Istanbul Earthquake Rapid Response and Early Warning System (IERREWS). The system is designed and operated by Bogazici University with the logistical support of the Governorate of Istanbul, First Army Headquarters and Istanbul Metropolitan Municipality (Erdik et al., 2003; Erdik and Fahjan, 2006).

Ten (10) of the strong motion stations are sited in the Marmara region at locations as close as possible to the Great Marmara Fault in on-line data transmission mode to enable Earthquake

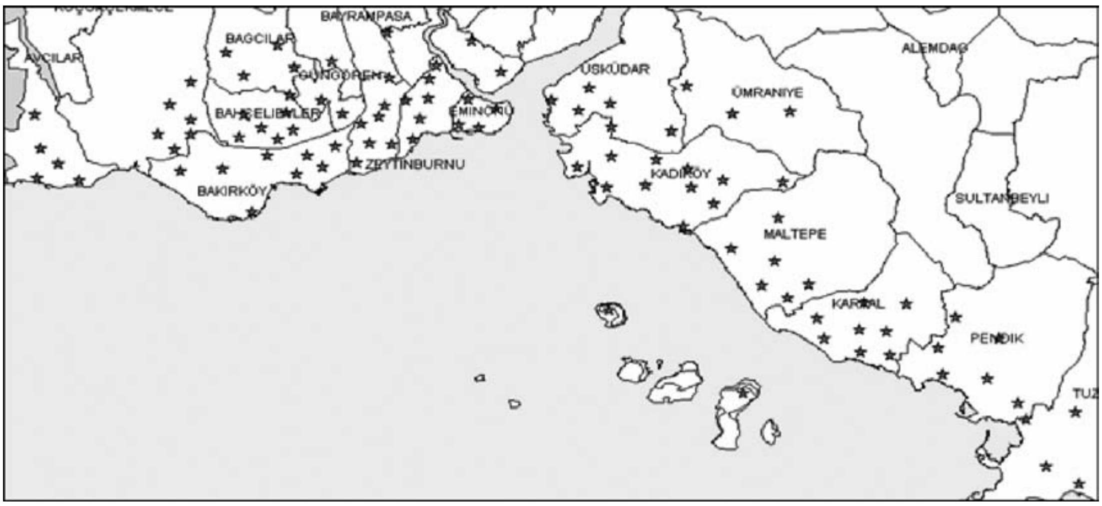

Figure 1: Earthquake Rapid Response Stations in Istanbul

Early Warning (Figure 11). Other strong motion recorder units were placed on critical engineering structures in addition to the already instrumented structures in Istanbul (Bosphorus and Fatih Sultan Mehmet Suspension Bridges, Hagia Sophia Museum, Suleymaniye, Fatih and Mihrimah Sultan Mosques. (http://www.koeri.boun.edu.tr/depremmuh/stronmotion.htm).

2.1 Istanbul Earthquake Rapid Response System

In Istanbul the post-earthquake rapid response information is be achieved through very fast acquisition, analysis and elaboration of data obtained from the 100 stations of the IERREWS network. The relative instrument spacing is about 2–3 km which corresponds to about 3 wavelengths in firm ground conditions and more than 10 wavelengths for soft soils for horizontally propagating 1 s shear waves. For communication of data from the rapid response stations to the data processing center and for instrument monitoring a reliable and redundant GSM communication system (backed up by dedicated landlines and a microwave system) is used.

In normal times the rapid response stations can be interrogated (for health monitoring and instrument monitoring) on regular basis. After triggered by an earthquake, each station processes the streaming three-channel strong motion data to yield the spectral displacements at specific periods, 12 Hz filtered PGA and PGV and sends these parameters in the form of SMS messages at every 20s directly to the main data center located at Kandilli Observatory and Earthquake Research Institute of Bogazici University (KOERI-BU). Ground shaking, damage and casualty distribution are automatically generated after the earthquake and communicated to the end users within 5 minutes after an earthquake (Figure 2).

The spectral displacements obtained from the SMS messages are interpolated to using two-dimensional splines and the earthquake demand at the center of each geo-cell is com-

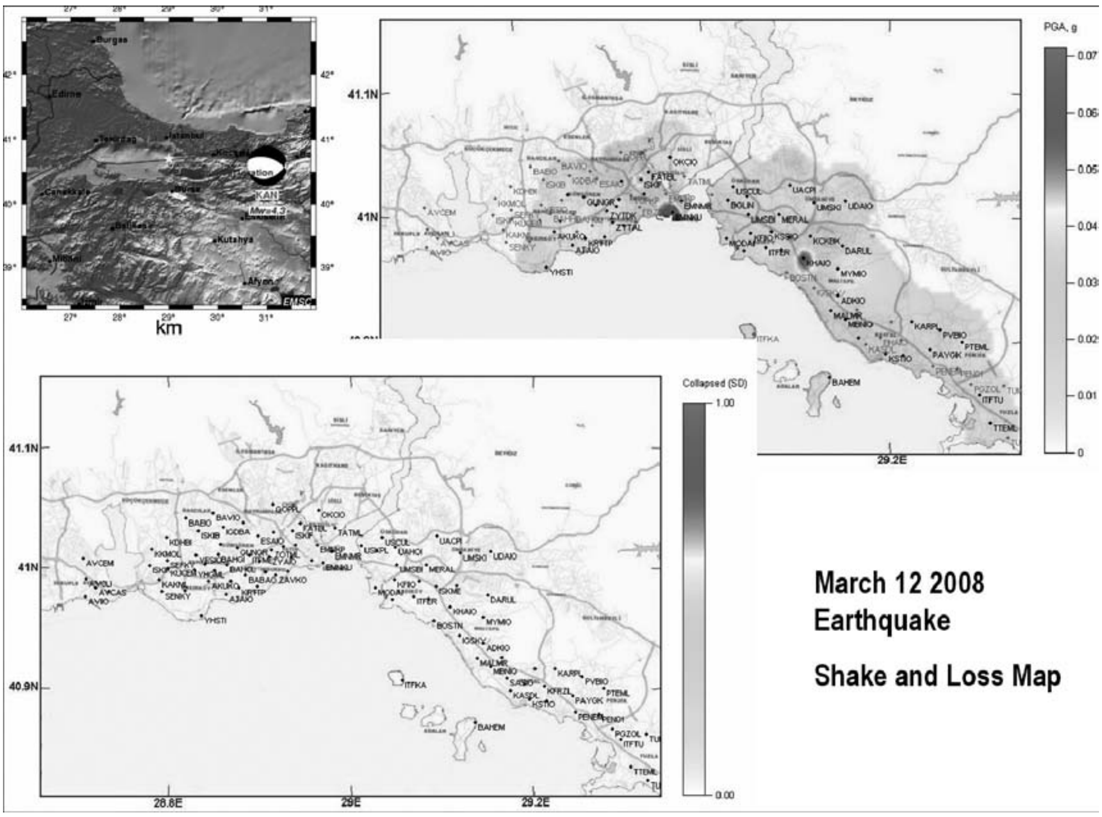

Figure 2: Shake and Loss Maps Generated by the IERRS after March 12, 2008 M4.3 Earthquake

puted. For the generation of Rapid Response information (Loss Maps) two methodologies based on spectral displacements and instrumental intensities are used. These methodologies are coded into specific computer program called ELER (Erdik et al., 2008), developed under the EU FP6 NERIES Project (http://www.neries-eu.org/). The loss estimation relies on the building inventory database, fragility curves and the direct physical damage and casualty assessment techniques. The computations are conducted at the centers of a 0.01° × 0.01° grid system comprised of geocells (1120 m × 830 m) size. The building inventories (in 24 groups) for each geocell together with their spectral displacement and intensity based fragility curves are incorporated in the database.

Everyday at 10:00 the field instruments send random (simulated) data to the data center where a simulated Loss Map is generated (Figure 3) and transmitted to the end users (Istanbul Governorate, Istanbul Municipality and First Army Headquarters, Figure 4).

Allen et al. (2009) has developed the »ElarmS« technique as a network-based methodology for rapid earthquake detection, location and hazard assessment. ElarmS uses the arrival time of the P-wave at the surface and the frequency content recorded on velocity and acceleration sensors to detect, locate and estimate the magnitude of an earthquake. The losses can then be estimated for known inventory and fragilities. An application of the ElarmS methodology using earthquakes recorded by the Istanbul Earthquake Rapid Response System is provided in Allen (2008) and also on the Internet address http://www.elarms.org/turkey/index.php. A result obtained for M5.2 October 24, 2006 indicates that 1s after the location and the magnitude was satisfactorily estimated.

2.2 Istanbul Earthquake Early Warning System
Within the Istanbul Earthquake Rapid Response and Early Warning System (IERREWS) the Kandilli Observatory of the Bogazici University in Istanbul operates 10 strong-motion sensors with realtime communication links to two datacenters in Istanbul (Erdik et al., 2003, Erdik and Fahjan, 2006). As illustrated in Figure 5, The Early Warning part of the IERREW ten (24 bit resolution) strong motion stations were located as close as possible to the Great Marmara Fault zone (Prince's Islands and specific coastal areas around the Marmara Sea) in

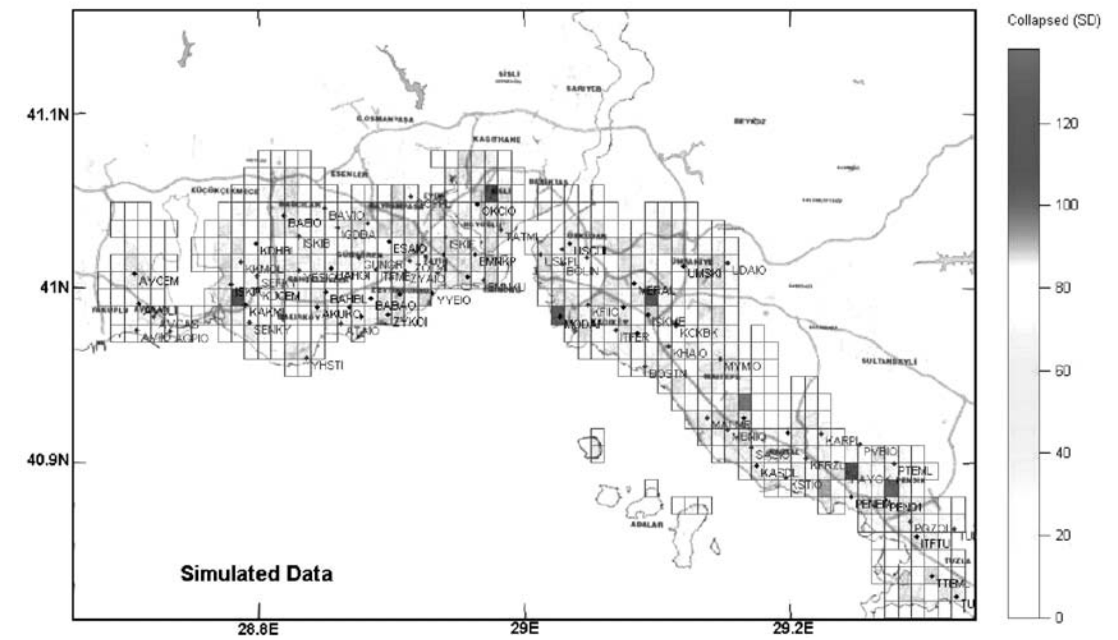

Figure 3: Building Damage Distribution (from Simulated Data)

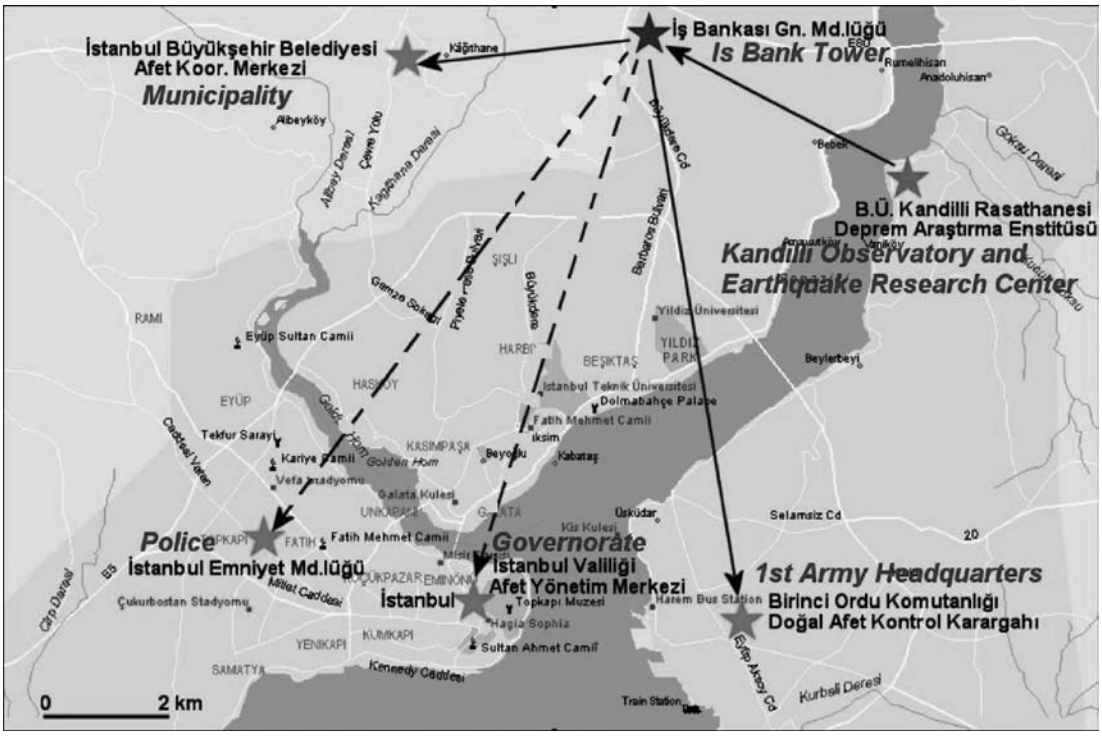

Figure 4: Rapid Response Information Sent to Emergency Response Centers

»on-line« mode. Two additional stations are kept as hot spares. Continuous transmission of data from these stations to the main data center is realized with digital spread spectrum radio modem system involving repeater stations and satellite telemetry.

Considering the complexity of fault rupture and the short fault distances involved, a simple and robust early warning algorithm, based on the exceedance of specified threshold time domain amplitude levels needs to be implemented. The band-pass filtered peak ground accelerations (PGA) and (alternatively) the cumulative absolute velocity (CAV-time integral of the absolute acceleration) compared with the specified threshold levels constitute the basis of this algorithm. When any acceleration or CAV (on any channel) in a given station exceeds specific threshold values it is considered a vote. Whenever we have 2 or 3 (selectable) station votes within selectable time interval, after the first vote, the first alarm is declared. After the first alarm, whenever we have 2 or 3 (selectable) votes for the second threshold values within a specified time interval of the second alarm, and similarly, the third alarm is declared.

In this approach, the definition and setting of the triggering thresholds levels of PGA and/or CAV (Figure 7) play major role. PGA vector within the time domain can be defined as,

$$\mathrm{PGA} = \max |a(t)|$$
$$\text{where} \quad |a(t)| = \sqrt{a_x^2(t) + a_y^2(t) + a_z^2(t)} \qquad (1)$$

CAV, given in Eqn. (2), was originally proposed by Kennedy and Reed in a study sponsored by the Electric Power Research Institute (EPRI NP-5930, 1988) as a parameter for determining the damage threshold for engineered structures.

$$\mathrm{CAV} = \int_0^{t_{max}} |a(t)|\,\mathrm{d}t = \sum_0^{t_{max}} |a(t)|\,\mathrm{d}t \qquad (2)$$

Where, $a(t)$ is acceleration time history, and t_{max} = duration of record.

A modified method of calculating CAV (Bracketed Cumulative Average Velocity, BCAV) was proposed by (EPRI TR-100082, 1991) in order

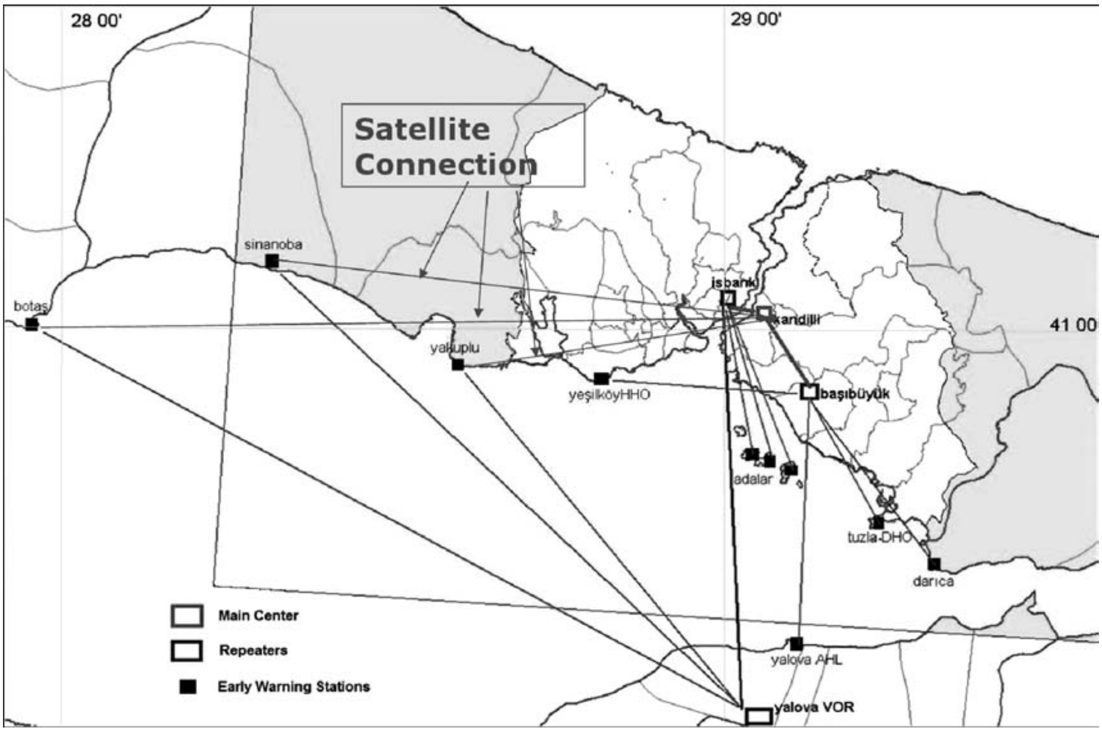

Figure 5: Station and Communication Layout of the Istanbul EEW System

to remove the dependence on records of long duration containing low (non-damaging) accelerations. The method of computing BCAV based on summation of average velocity within a time domain where the max acceleration is greater than a specific value minimum acceleration (typically 0.025 g) in a specific bracketed time Δt

$$\mathrm{BCAV} = \sum \int_{t_i}^{t_i+\Delta t} |a(t)|\,\mathrm{d}t$$

$$\text{where} \quad \Delta t = 1\,\text{sec}, \quad \max|a(t)| > 0.025\,\text{g} \qquad (3)$$

where $a(t)$ are acceleration values in a 1 second bracket window, where at least one value of the acceleration exceeds a predetermined minimum acceleration level. The use of CAV has further been studied on the basis of regional strong motion data (Alcik et al., 2009). Cabanas et al. (1997) and Böse (2006) expressed the potential structural damage by relating CAV with the Intensity. The optimum length of this window and bracket time and their effects on the BCAV values for different earthquake time histories records will be examined in further studies. Alcik et al. (2009) have further investigated the variation of BCAV for magnitude, distance and site classes.

The steps associated with each early warning algorithm used in the Istanbul Earthquake Early Warning System are as follows:

Algorithm Based on Exceedance of Filtered PGA Threshold

– All online acceleration data from all stations will be low-pass filtered at selectable frequencies of 12 and 25 Hz.
– When any acceleration (on any channel) in a given station exceeds a selectable first threshold value (20 mg) it will be considered a vote
– Whenever we have 3 (selectable) station votes within a selectable time interval of (5 s) after the first vote it will be declared the first alarm.
– After the first alarm, whenever we have 3 (selectable) votes for the second acceleration threshold value (50 mg) within selectable time interval of (5 s) after the first vote it will be declared the second alarm.

– After the second alarm, whenever we have 3 (selectable) votes for the third acceleration threshold value (100 mg) within selectable time intervals of (5 s) after the second vote it will be declared the third alarm.

Algorithm Based on Cumulative Absolute Velocity (BCAV)

– The CAV from acceleration data will be computed for only those 1 s intervals where PGA is greater than 3 mg. When any CAV (on any channel) in a given station exceeds a selectable first threshold CAV value (20 mg · s) it will be considered a vote.
– Whenever we have 3 (selectable) votes for the first threshold CAV value within selectable time interval of (5 s) after the first vote it will be declared the first alarm.
– After the first alarm, whenever we have 3 (selectable) votes for the second threshold CAV value (40 mg · s) within selectable time intervals of (5 s) after the first vote it will be declared the second alarm.
– After the second alarm, whenever we have 3 (selectable) votes for the third CAV threshold value (70 mg · s) within selectable time intervals of (5 s) after the second vote it will be declared the third alarm.

Studies are underway for the possible utilization of the Earthquake Early Warning algorithm developed by Wu and Kanamori (2005a, 2008) that uses the real-time strong motion signals. Same type of signals is also used in the IEWS. Wu and Kanamori (2008) has relied on the finding that the initial portion of the P wave carries the information of the earthquake size and thereby can provide the information on the strength of shaking to be brought by the following *S* wave. They explored a practical approach to EEW with the use of a ground-motion period parameter τ_c and a high-pass filtered vertical displacement amplitude parameter P_d from the initial 3 s of the *P* waveforms (Wu and Kanamori, 2005a, 2005b, 2008; Wu et al., 2007). At a given site, an earthquake magnitude could be determined from τ_c and the peak ground-motion velocity (PGV) could be estimated from. In this method, incoming strong motion acceleration signals are recursively converted to ground velocity and displacement. A *P*-wave trigger is constantly monitored. When a trigger occurs, τ_c and P_d are computed. When $P_d > 0.5$ cm, the event is most likely damaging as PGV at the site most likely exceeds the damaging level, i.e., 20 cm/s. This type of early warning approach will become effective especially for close-in sites where warnings are most needed.

Böse et al. (2008) have developed a novel Early Warning algorithms based on Pattern Recognition (Neural Network) in connection with her PhD studies on the Istanbul Earthquake Early warning System (Böse et al., 2003; Böse, 2006). This new method – called PreSEIS (Pre-SEISmic) – is as fast as methods based on single station observations and, at the same time, shows a higher robustness than most other approaches. In this methodology the seismic patterns are defined by the shape and frequency content of the parts of accelerograms that are available at each time step. From these, parameters relevant to seismic damage, such as peak ground acceleration (PGA), peak ground velocity (PGV) and response spectral amplitudes at certain periods are estimated using Artificial Neural Networks (ANN). At regular time-steps after the triggering of the first EEW sensor, PreSEIS estimates the most likely source parameters of an earthquake using the available information on ground motions at different sensors in a seismic network. The approach is based on two-layer feed-forward neural networks to estimate the earthquake hypocenter location, its moment magnitude, and the expansion of the evolving seismic rupture. The pattern recognition technique used is further combined with an additional rule-based system in order to detect inconsistencies between ground motion estimations and measurements. This combination provides a reliable and accurate system for early-warning that is demanded by its huge social and economic impact. As illustrated in Figure 17, Böse et al. (2008) has estimated median EEW times, for two sites in Istanbul, in the vicinity of about 8 s.

Wenzel et al. (2009) have investigated the efficiency of the Istanbul Earthquake Early Warning System and the optimization of the station layout on the consideration that (1). The system has to recognize whether an event will be such that the ground motion at the site of interest will be exceeded or not (which means that there will be no false or miss-alarms) and (2) The warning times should be as best as possible. Specifically the investigation has searched the optimal station locations, the optimal warning thresholds and also the minimum necessary number of stations and the benefit of a given number of ocean bottom stations. The results indicate that the current Istanbul EEW system is designed under optimal conditions and performs quite well. However the Level III thresholds may need to be increased to avoid Level III false alarms. Furthermore using three OBS stations located on the fault will serve to increase the currently available warning times by 2–3 s on the average (especially noticeable for class III events).

The earthquake early warning signals will be transmitted to the end uses by employing several communication companies as »service providers«. The encrypted early warning signals (earthquake alarm) will be communicated to the respective end users by FM, UHF and satellite communication systems. The first application of the Istanbul Earthquake Early Warning System will be for emergency traffic stopping at the Tube tunnel crossing of the Marmaray rapid transit system. Other Possible end users include gas and electric power distribution network, metro system and critical and hazardous industrial facilities.

REFERENCES

Alcik, H. O. Ozel, N. Apaydin, and M. Erdik, (2009), A Study on Warning Algorithms for Istanbul Earthquake Early Warning System, GRL, 36, L00B05, doi:10.1029/2008GL036659.

Allen, R. M., and H. Kanamori (2003), The potential for earthquake early warning in Southern California, Science 300, 786–789.

Allen, R. M., P. Gasparini and O. Kamigaichi (Eds.), 2009, New Methods and Applications of Earthquake Early Warning, A Special section of Geophys. Res. Lett., 36, 2009.

Allen, R.M., H. Brown, M. Hellweg, O. Khainovski, P. Lombard, D. Neuhauser (2009) Realtime earthquake detection and hazard assessment by ElarmS across California Geophys. Res. Lett., 36 L00B08, doi:10.1029/2008GL036766.

Allen, R. (2008), ElarmS Alert Maps: An earthquake in California and another near Istanbul, Presentation given in EU FP6 SAFER 2nd Annual Meeting, 25–27 June 2008, Istanbul.

Böse, M., 2006: Earthquake Early Warning for Istanbul using Artificial Neural Networks. PhD thesis, University of Karlsruhe (TH), Germany.

Böse, M., Erdik, M., Wenzel, F. (2003), Artificial Neural Networks for Earthquake Early-Warning, Proceedings AGU2003 Abstracts, S42B-0155 1330h POSTER.

Böse, M., F. Wenzel, and M. Erdik (2008), PreSEIS: A Neural Network-Based Approach to Earthquake Early Warning for Finite Faults, Bull. Seismol. Soc. Am., 98, No.1, 366–382.

Cabanas, L., Benito, B., and Herraiz, M. (1997), An Approach to the Measurement of the Potential Structural Damage of Earthquake Ground Motions, Earthquake Engineering and Structural Dynamics, 26, 79–92.

EPRI NP-5930 (1988), A Criterion for Determining Exceedance of the Operating Basis Earthquake, Electric Power Research Institute, Palo Alto, CA, prepared by Jack R. Benjamin and Associates, Inc.

EPRI TR-100082 (1991), Standardization of the Cumulative Absolute Velocity, Electric Power Research Institute, Palo Alto, CA, prepared by Yankee Atomic Electric Company.

Erdik, M., M. Demircioğlu, K. Sesetyan, E. Durukal, B. Siyahi (2004), Earthquake Hazard in Marmara Region, Turkey, Soil Dynamics. and Earthquake Engineering., 24, 605-631.

Erdik, M. and Y. Fahjan (2006), Damage Scenarios and Damage Evaluation, in Assessing and Managing Earthquake Risk, Oliveira, C. S.; Roca, A.; Goula, X. (Eds.), Springer, 2006, XXV, 543 p, ISBN; 978-1-4020-3524-1

Erdik, M., Y. Fahjan, O. Ozel, H. Alcik, A. Mert, and M. Gul (2003), Istanbul Earthquake Rapid Response and the Early Warning System, Bull. of Earthquake Engineering, 1, 157–163.

Erdik, M., Z. Cagnan, C. Zulfikar, K. Sesetyan, M.B. Demircioglu, E. Durukal, C. Kariptas (2008), Development of Rapid Earthquake Loss Assessment Methodologies for Euro-MED Region, Proc., 14, World Conference on Earthquake Engrg., Paper ID: S04-004.

Espinosa-Aranda, J., Jimenez, A., Ibarrola, G., Alcantar, F., Aguilar, A., Inostroza, M., and Maldonado, S., 1995: Mexico City Seismic Alert System. Seismological Research Letters, 66, 6, 42–53

Gasparini, P., G.Manfredi and J.Zschau, Jochen (Eds.), 2007, Earthquake Early Warning Systems, Springer, ISBN: 978-3-540-72240-3

Lee, J. R and S. H. Lee (2001), An experimental study on seismic damage indicator considering CAV concept, Transactions, SMiRT 16, Paper # 1776, Washington DC, August 2001.

Nakamura, Y. (1988), On the Urgent Earthquake Detection and Alarm System (UrEDAS), Proc. of the 9th World Conference on Earthquake Engineering VII, Tokyo, Japan, 2–9 August 1988, 673–678.

Nakamura, Y., 1989: Earthquake alarm system for Japan Railways. Japanese Railway Engineering, 8, 4, 3–7.

Olivieri M, R. M. Allen, and G. Wurman (2008), The Potential for Earthquake Early Warning in Italy Using ElarmS, Bull. Seismol. Soc. Am., 98, 495–503.

Wenzel, F., M. C. Oncescu, M. Baur, and F. Fiedrich (1999), An Early Warning System for Bucharest, Seismol. Res. Lett., 70, 2, 161–169.

Wenzel, F., A. Oth**,** E. Gottschämmer, N. Köhler, M. Böse and M. Erdik (2009), Efficiency of Earthquake Early Warning Systems, 2nd International Workshop on Earthquake Early Warning, Kyoto, Japan.

Wu, Y. M., and H. Kanamori (2005a), Experiment on an onsite early warning method for the Taiwan early warning system. *Bull. Seismol. Soc. Am., 95*, 347–353.

Wu, Y. M., and H. Kanamori (2005b), Rapid Assessment of Damaging Potential of Earthquakes in Taiwan from the Beginning of P Waves, *Bull. Seismol. Soc. Am., 95*, 1181–1185.

Wu, Y. M. and H. Kanamori (2008), Development of an Earthquake Early Warning System Using Real-Time Strong Motion Signals, Sensors, 2008, 8, 1–9

Wu, Y. M., J. K. Chung, T. C. Shin, N. C. Hsiao, Y. B. Tsai, W. H. K. Lee, and T. L. Teng (1999), Development of an integrated seismic early warning system in Taiwan – case for Hualien earthquakes. Terrestrial, Atmospheric and Oceanic Sciences, 10, 719–736.

Zollo, A., G. Iannaccone, M. Lancieri, L. Cantore, V. Convertito, A. Emolo, G. Festa, F. Gallovic, M. Vassallo, C. Martino, C. Satriano, and P. Gasparini (2009), Earthquake Early Warning System in Southern Italy: Methodologies and Performance Evaluation, Geophys. Res. Lett., 36, L00B07, doi:10.1029/2008GL036689.

Monitoring of civil infrastructures by wireless sensor networks: an ambient vibration test on the Fatih Sultan Mehmet Suspension Bridge in Istanbul, Turkey

Picozzi M. (1), Stengel D. (2), Milkereit C. (1), Zulfikar C. (3), Fleming K. (1, 8), Ditommaso R. (4), Erdik M. (3), Zschau J. (1), Fischer J. (5), Şafak E. (3), Özel O. (6), Apaydin N. (7)

(1) Helmholtz Centre Potsdam GFZ German Research Centre for Geosciences, Germany,
(2) Department of Reinforced Concrete Structures, University of Karlsruhe, Germany
(3) Bogazici University, Kandilli Observatory and Earthquake Research Institute, Earthquake Engineering Department, Istanbul, Turkey,
(4) Department of Structures, Geotechnics, Applied Geology, University of Basilicata, Potenza, Italy,
(5) Department of Informatics, Humboldt University (HU) Berlin, Germany,
(6) I.U. Engineering Faculty, Geophysical Engineering Department, Turkey,
(7) General Directorate of Highways 17th Division, Istanbul, Turkey,
(8) Department of Spatial Sciences, Curtin University of Technology, Perth, Western Australia, Australia.

Abstract

The rapid improvements in telemetry and computer technology and a continuous decrease in communication costs are driving a revolution in earthquake engineering. This is especially the case for the monitoring of civil built infrastructures, which is a task of major importance in earthquake-prone areas, both to ensure their structural integrity, and to obtain an insight into their responses in the event of an earthquake. Such insight would assist in the mitigation of urban earthquake risk by new, effective seismic design provisions.

Advantages associated with the use of wireless sensing unit include a considerable decrease in installation costs, decentralization of data analysis, and the possibility of broadening the functional capabilities by exploiting the use, at the same time and place, of different sensors. For these reasons, such sensors are becoming a valuable alternative to conventional wired monitoring systems.

In this work, we present the results of an ambient vibration recording field test performed on the Fatih Sultan Mehmet Bridge in Istanbul, Turkey, employing innovative, low-cost wireless sensing units able to collect, analyze, store, and communicate data and estimated engineering and other parameters. We found that the results obtained using such low-cost sensors are comparable to those from more sophisticated (and expensive) instruments. This offers the possibility of installing dense structural monitoring networks made up of such instruments economically and technically viable, enhancing options for seismic mitigation.

1. Introduction

Real-time structural health monitoring is a task of major importance, especially in earthquake-prone areas. In fact, after an earthquake, it is only by real-time structural health monitoring systems that it is possible to obtain the critical data necessary for a rapid assessment of any damage and structural degradation that may have occurred in the structure (Safak and Hudnut, 2006).

The earliest applications of wireless communication technology, which involved connecting together embedded personal computers and sensors for structural monitoring purposes, started in the late 90s (Straser and Kiremidjian,1998). These early experiments showed that real-time processing of data can be performed locally, and that wireless monitoring systems are feasible, reliable and cost-effective. Over the last few years, prototype structural wireless monitoring systems have been validated by tests performed on bridges and other structures (Lynch et al., 2006), where they have been found to be a highly cost-competitive, completely autonomous and very reliable alternative to traditional wired systems.

At the present time, a further significant step in the research fields of seismic early warning and the monitoring of strategic infrastructures has been the development of self-organizing wireless mesh information networks made up of low cost sensors (Fleming et al., 2009; Picozzi et al., 2009). In particular, an innovative system named the Self-Organizing Seismic Early Warning Information Network (SOSEWIN) is being developed by the *Helmholtz-Zentrum Potsdam GFZ German Research Centre for Geosciences* and *Humboldt University of Berlin* (HUB) within the framework of the European projects Seismic eArly warning For EuRope (SAFER, http://www.saferproject.net) and Earthquake Disaster Information systems for the Marmara Sea region, Turkey (EDIM, http://www.cedim.de/EDIM.php).

Istanbul, the largest and economically most important city of Turkey, is a mega-city (population about 14 million) that is under significant risk from earthquakes, being located at its nearest point only a few kilometers from the North Anatolian Fault, along which there have been a number of large earthquakes over the past century, the most recent being the 1999 Izmit (August 17th, Mw = 7.4) and 1999 Dûzce (November 12th Mw = 7.2) earthquakes (Milkereit et al., 2000; Erdik, 2003). For these reasons, a test version of SOSEWIN has been deployed since July, 2008 in Istanbul with the aim of eventually setting up a new, much denser people-centered earthquake early warning system (Fleming et al., 2009). Furthermore, we considered it worthwhile to explore the possibility of using these instruments for the structural monitoring of strategic civil infrastructures. Thus, we decided to undertake an experimental monitoring of the gravity-anchored Fatih Sultan Mehmet Suspension Bridge spanning the Bosporus Strait (Picozzi et al., 2009).

In the first part of this work we describe the hardware that make up the individual SOSEWIN wireless sensing units (hereafter WSU), and we introduce the main characteristics of the software adopted for the routing protocols and the data archiving.

In the following section is described the execution of the ambient vibration field test in Istanbul. In particular, the SOSEWIN system's versatility allowed the performance of contemporary recordings of the ambient vibrations at the different structural elements of the Fatih Sultan Mehmet Suspension Bridge using a network of 24 WSUs (i.e. with instruments installed along the two side of the deck, on top of the four towers, and at the base of the two vertical cables in the middle of the bridge).

Finally, from the analysis of the data-set collected, it is shown that the WSUs provide robust and reliable estimates concerning the main modal properties of the bridge, and that these latter are in remarkable agreement with the results of other workers who employed more sophisticate (as well as expensive and complex) instrumentation (Brownjohn et al., 1992; Erdik and Apaydin, 2005; and Stengel, 2009).

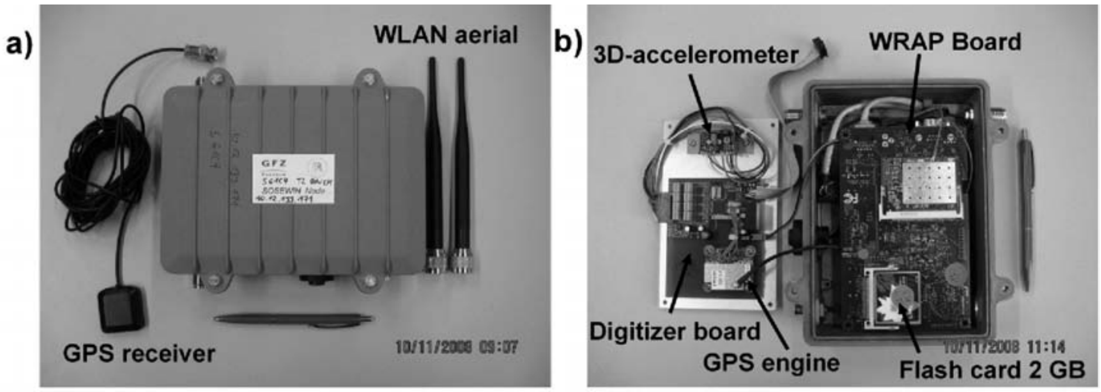

Figure 1: The prototype Wireless Sensing Unit (WSU): (*a*) the complete unit and (*b*) an internal view

2. The SOSEWIN wireless sensing units (WSU)

2.1 Hardware and Software

The SOSEWIN system employs advances in various technologies to incorporate off-the-shelf sensor, processing and communications components into low-cost accelerometric seismic sensing units that are linked by advanced, robust and rapid communications routing and network organizational protocols appropriate for wireless mesh networks (Fleming et al., 2009). The reduced sensitivity of these sensors, arising from the use of low-cost components, is compensated by the possibility of deploying high-density self-organizing networks performing real-time data acquisition and analysis. Such characteristics make systems of WSU of great interest for the monitoring of strategic civil infrastructure.

Each WSU consists of three main parts: the sensors, the digitizer board, and the wireless router applications platform (WRAP-board). Figure (1) provides a view of the main components of a WSU, while technical details can be found in Fleming et al. (2009).

All components are bought off-the-shelf, with the exception of the digitizer board's Analogue-Digital Converters (ADC), which have been developed within GFZ, leading to each unit being much less expensive than standard seismometers (about 600,00 Euro per unit).

The sensors incorporated into the WSU are comprised of accelerometers arranged to provide three component data, and an additional sensor to measure some environmental parameter, such as anemometers, humidity, strain gauges, temperature etc. The accelerometers used in the WSUs are based on MEMS (Micro Electro Mechanical Systems), and have a measurement range of +/− 1.7 g, with a bandwidth of 25 Hz and a noise-level of 0.5 mg.

The digitizer board consists of four ADCs, a GPS unit that provides time and geographical coordinates, and a USB interface (Figure 1). The ADCs have a resolution of 24 bits (effectively 19 bits), with sampling variable between 50 to 400 samples per second (sps), although at present 100 sps is being used.

The WRAP board (PC Engines, 2008) is responsible for carrying out the analysis, the communications, and data storage (Figure 1). It is made up of an embedded PC (i.e. a 233 MHz AMD Geode x86 CPU, 128 MB RAM) that uses a Compact Flash card (currently 2 GBytes but easily increased) as a hard disk. The communication of data is made possible through two WLAN Mini PCI cards (i.e. Routerboard R52 wireless 802.11a/b/g, 2.4 and 5GHz combo cards), a power supply plug, a serial port and 100 MBit/s Ethernet.

All boards were installed in waterproof outdoor metal cases. Omni-directional dual-band antennas with a gain of 5 dB were mounted with opposite vertical polarization.

The amount of power required by a WSU when all operational activities are fulfilled (recording and real-time communication of data) has been experimentally measured to be about 4 W.

The main software operating on the WSU currently consists of the following:

– OpenWRT: This is the operating system for the WRAP boards (OpenWrt, 2007) with Linux kernel 2.6.22 (Torvalds, 2007). It is an open-source freely available and highly configurable distribution.
– Data-provider: The program that handles the data streams from the digitizer board, and then archives them via SeisComP/SeedLink.
– SeisComP/SeedLink: A software package and concept for near real-time seismic data distribution, (http://geofon.gfz-potsdam.de/geofon//seiscomp/seedlink.html) developed by the GFZ. The SeedLink protocol is based on TCP (Heinloo, 2000) and data are sent in the form of 512-byte Mini-SEED packets with a 8-byte SeedLink header.

In the WSU, the SeedLink server of SeisComP stores the data in a ring buffer of configurable size on the Compact Flash card. With the current flash cards, the data in the ring buffer will be kept for the order of 20 days. If more storage is found to be necessary, then it is simply a case of using a larger card.

– Optimized Link State Routing (OLSR, 2004): OLSR is a table-driven pro-active routing protocol currently chosen for the wireless mesh network (http://www.olsr.org). Its role is to periodically assess and maintain the network topology by flooding information about its direct neighborhood throughout the whole network.

2.2 Real-time processing and communication

The general scheme of the WSU's real-time processing designed for structural monitoring

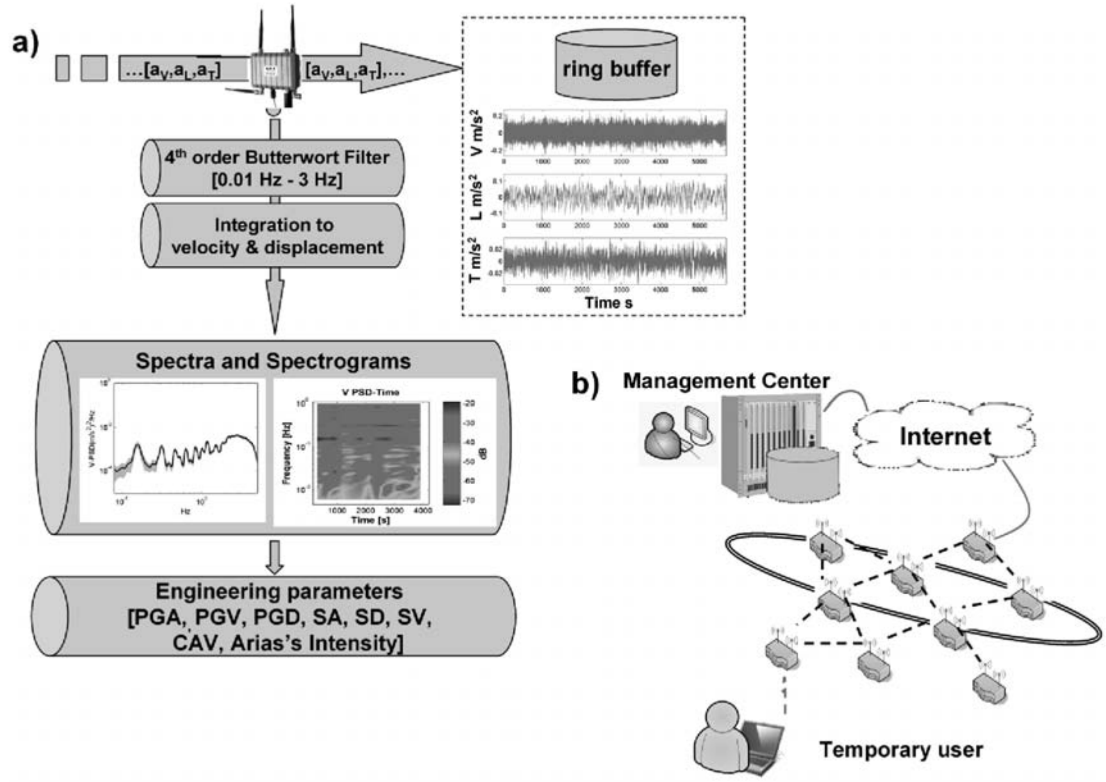

Figure 2: (a) The general scheme followed for the seismological processing and analysis that is being incorporated into the wireless sensing units. (b) General organization of a network made up of WSUs (e.g. SOSEWIN, Fleming et al., 2009). The WSUs are capable of creating a decentralized network that can communicate data and parameters towards a management center and temporary users

involves a local, relatively simple, rapid, and robust analysis of data (Figure 2a).

Accelerometer data are first filtered by a 4th order band-pass (i.e. selected for the bridge experiment to be 0.01–3 Hz) IIR Butterworth filter. Then, they are integrated to obtain velocity and displacement using the recursive formulation of Kanamori et al. (1999). In the meantime, raw accelerometric data are continuously stored in the ring buffer. For the long-term monitoring of structural modal properties, the Cooley-Tukey version of the FFT (Press et al., 1992) is applied to the signals, allowing the continuously extraction of the main frequency peaks for the three components of motion by an approach based on pattern recognition. In addition, other parameters of engineering interest, such as the cumulative absolute velocity (CAV, Böse, 2006), Arias Intensity (Arias, 1970), and maximum ground motion parameters (PGA, PGV, and PGD), as well as the acceleration, velocity, and displacement response spectra for some representative periods (e.g. those of the main modes of vibration estimated by modeling), are calculated.

Importantly, the engineering parameters are continuously updated and can be communicated through the other WSUs towards a final target by way of a gateway, or can be sent to a user's laptop temporarily connected to any node that belongs to the network (Figure 2b). WSUs are designed to form a self-organizing ad-hoc wireless mesh network (WMN), and rely on the OLSR (Optimized Link State Routing) as the routing strategy. The use of WMN protocols allows a network of WSUs to continuously adapt to changing circumstances (addition or removal of nodes, interference in

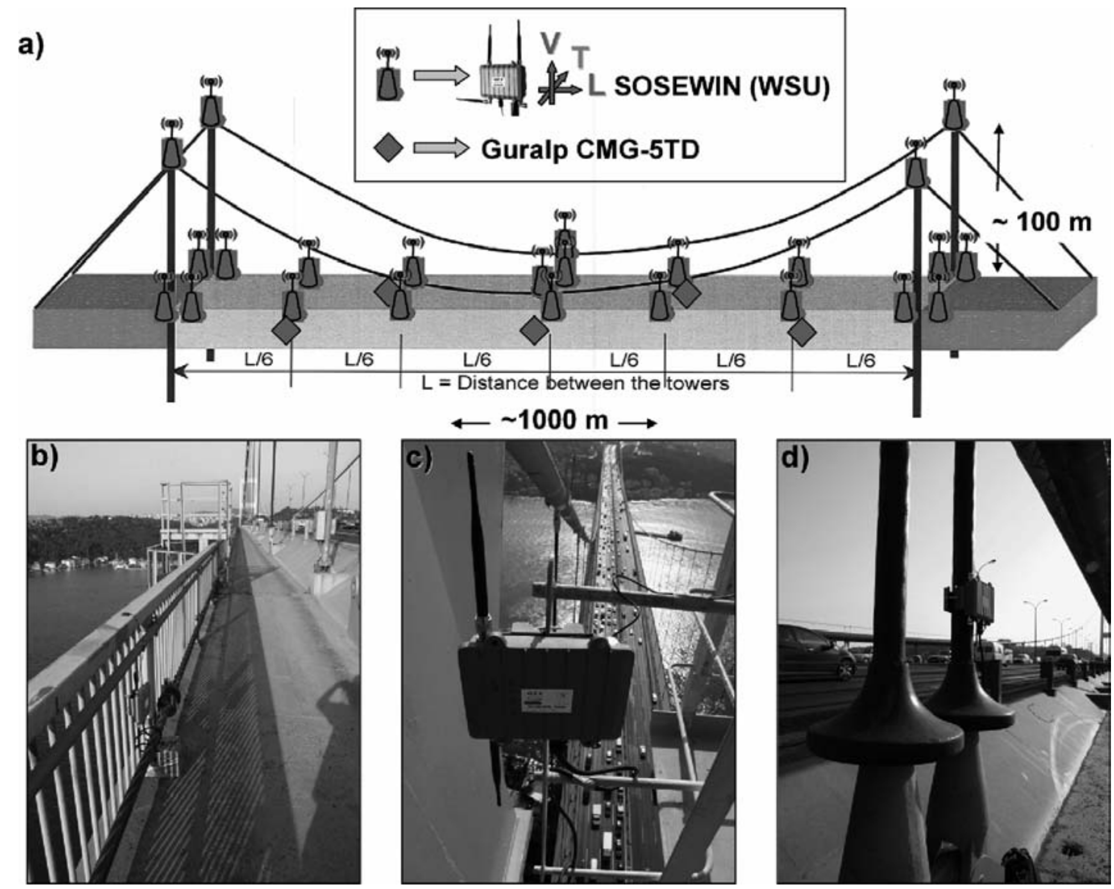

Figure 3: (a) Measurement positions with SOSEWIN WSU and Guralp instruments, and the WSU motion convention: vertical (V), longitudinal (L), and transversal (T) components. (b), (c), and (d) show examples of the sensor installation during the test measurements in June 2008

Table 1: First five inferred frequencies of the vertical, lateral and torsional, symmetrical and asymmetrical, deck modes, respectively (from Brownjohn et al., 1992)

Vertical	[Hz]	Lateral	[Hz]	Torsional	[Hz]
1 asym.	0.125	1	0.77	1 sym.	0.296
2 sym.	0.155	2	0.239	2 asym.	0.352
3 sym.	0.208	3	0.25	3 sym.	0.529
4 asym.	0.244	4	0.287	4 asym.	0.692
5 sym.	0.317	5	0.315	5 sym.	0.867

communications, loss of part of the network following an earthquake etc.) in order to maintain optimal communications.

The accelerometric data and estimated structural modal parameters are transferred following the above mentioned SeedLink protocol (i.e. by 512-byte Mini-SEED packets) at rates of up to 54 Mbps in both the 2.4 GHz and 5 GHz unlicensed bands. In the case of a low signal-to-noise ratio in the communication, the WLAN cards driver can automatically decrease the rate of transmission.

3. The Fatih Sultan Mehmet Suspension Bridge

The Fatih Mehmet Sultan Bridge is the second suspension bridge across the Bosporus strait in Istanbul, spanning the strait between Hisarüstü (European Side) and Kavacık (Asian Side). From a structural point of view, it is a gravity-anchored suspension bridge with steel pylons and double vertical hangers and no side spans. It is characterized by a box girder deck 39 · 4 m wide, 1090 m long, and steel towers rising 110 m above ground level (Figure 3). Among other theoretical studies of the bridge that have been carried out, Dumanoglu et al. (1992) and Apaydin (2002) provide details of the structural characteristics and a comprehensive assessment of the response of the Fatih Sultan Mehmet Bridge.

Suspension bridges are often critical nodes of major transportation systems; hence their failure during a strong earthquake is a major threat for both the potentially high number of fatalities and the substantial interruption of emergency activities (Erdik and Apaydin, 2005). For these reasons, monitoring the bridge's design parameters, vibration characteristics and dynamic properties represents a primary task for assessing their wind and earthquake safety.

One of the best methods utilized to assess the dynamic characteristics of such massive structures is the measurement of the structural response to ambient excitations, such as wind and traffic (e.g. Erdik and Uckan,1988). The structural vibrations caused by such excitations are termed the ›Ambient Vibrations‹. Full-scale dynamic analysis of a suspension bridge by ambient vibration recordings represents a reliable approach for the assessment of the free vibration characteristics (i.e. vibration mode shapes, frequencies and the associated damping ratios), the calibration of the analytical and finite element models, and the detection of changes in these vibration characteristics over time.

Ambient vibration tests have been conducted on the Fatih Sultan Mehmet Bridge (e.g. Brownjohn et al.,1992; Apaydin and Erdik, 2001; Apaydin, 2002; Kaya and Harmandar, 2004; Erdik and Apaydin, 2005). The experimental modal frequencies of vibration provided by Brownjohn et al. (1992) (e.g. the first five deck vertical, torsional and lateral modes are listed in Table 1), were recently confirmed by Apaydin (2002), Erdik and Apaydin (2005), and Stengel (2009).

This wealth of information makes the Fatih Sultan Mehmet bridge a test subject particularly suitable for testing the reliability of our innovative WSU instruments.

4. Ambient vibration monitoring test at the Fatih Sultan Mehmet Suspension Bridge

On the 27th June 2008, 24 WSU were used to perform ambient vibration measurements at the Fatih Sultan Mehmet suspension bridge (Picozzi et al., 2009). The acquisition scheme (Figure 3a) consisted of the installation of 4 reference sensors placed outside of the bridge's deck, 8 sensors along each side, 2 sensors on the lowest part of the vertical cable at the midpoint of the bridge, and 4 sensors on top of the bridge's towers. All sensors were installed following the same spatial convention, in order to detect the bridge vibrations on the vertical (V), the longitudinal (L), and the transversal (T) components. With a crew of 4 workers, both the installation and removal of all station required about 1 hour. Figure (3b, c, and d) shows examples of these installations. The test was performed for a few hours, and about 1-$^1/_2$ hours of contemporary recordings by all sensors are available. The sampling rate was fixed to 100 Hz, and the energy required by the WSU was provided by 17 Ah lithium-based batteries.

Furthermore, the bridge is also equipped by a traditional vibration monitoring system encompassing 5 Guralp Systems CMG-5TD instruments, which are installed on the bridge (Apaydin and Erdik, 2001; Apaydin, 2002; Stengel, 2009). These instruments are located inside at the edges of the deck and provide continuous data by transmission to the Kandilli Observatory and Earthquake Research Institute (KOERI).

Although each WSU is able to perform its own local signal analysis (as is the case when they are used for earthquake early warning purposes), the aim of this work is the evaluation of the WSU performance for structural monitoring. Hence, the results discussed in the following refer to post-survey analysis.

First, we compared the signals recorded by the WSU and Guralp sensors. Figure (4) shows the corresponding Power Spectrum Density (PSD) functions computed for the vertical components of motion at the sensors located approximately in the middle and one-third of the bridge's deck. All PSDs were computed using non-consecutive signal windows 200 s wide, which is suitable for the frequency range of interest and guarantee a sufficient frequency resolution. Before computing the spectra, the linear trend was removed from each window

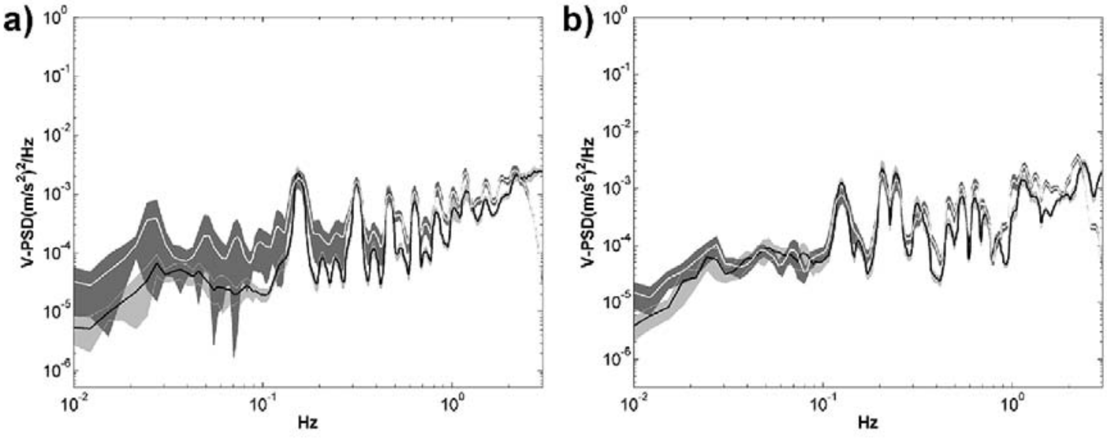

Figure 4: Power Spectrum Density (PSD) functions for the vertical components of motion. Average PSD plus +/–95% confidence interval for SOSEWIN (*white and dark gray, respectively*) and Guralp (*black and grey, respectively*). (*a*) Sensors located on the middle of the bridge's deck (i.e. WSUs over the deck, and Guralp within the deck). (b) Similar to (a), but with nodes located at about 1/3 of the way along the bridge's deck

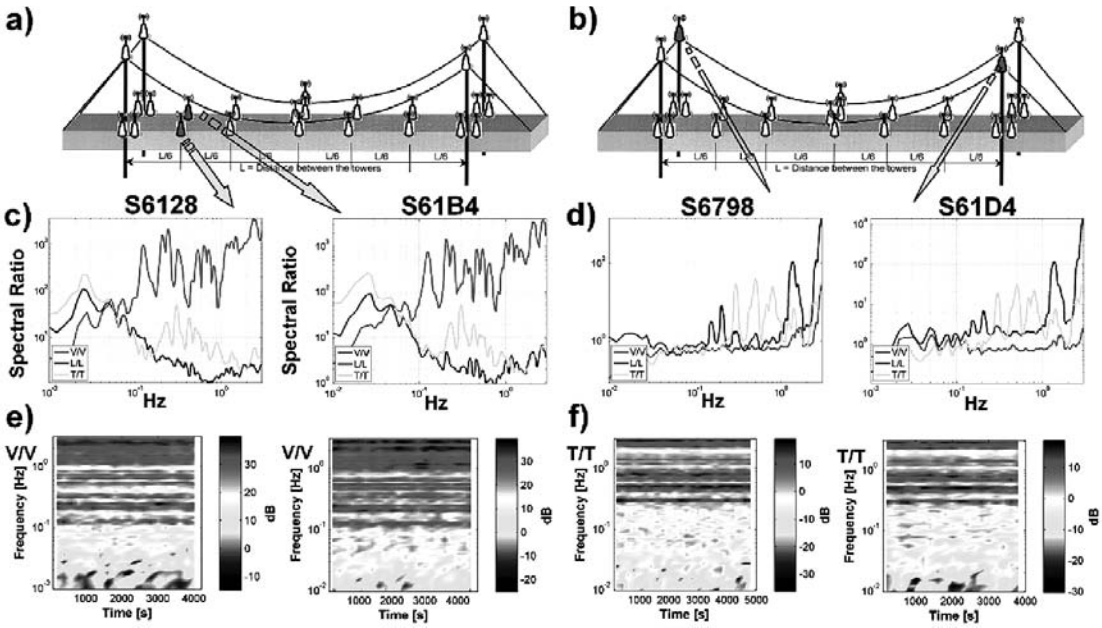

Figure 5: Results for pairs of WSUs. *(a)* Selected sensors (*red symbols*) placed at the bridge's deck. *(b)* similar to *(a)* but of sensors placed on top of the bridge's towers. *(c)* and *(d)* Spectral Ratio (SR) functions for the vertical (*red*), longitudinal (*blue*), and transversal (*green*) components of motion. (*e* and *f*) SR spectrograms for the different components of motion

Table 2: First five inferred SR peaks selected for the vertical (V/V), transversal (T/T), and longitudinal (L/L) directions

	V/V peaks [Hz]	T/T peaks [Hz]	L/L peaks [Hz]
A	0.122	0.076	0.204
B	0.152	0.22	0.247
C	0.207	0.302	0.311
D	0.241	0.43	0.387
E	0.314	0.5	0.467

and a 5% cosine-taper was applied at both ends. This scheme of analysis for the computation of PSDs was also adopted for all the other WSUs. Despite the WSUs lying over the bridge's deck while the Guralp sensors are installed inside the deck, the agreement between their PSDs is still strong (Figure 4).

PSD computed for the 4 reference sensors located outside of the bridge's deck were used for the computation of the Spectral Ratio (SR) functions for the vertical, transversal and longitudinal directions with respect to all the other 20 monitored points inside the bridge.

Figure (5) provides an overview of the SR results for a pairs of WSUs installed at characteristic locations on the bridge (i.e. the deck, and the towers, respectively). When comparing the average SR curves (Figures 5c, and 5d) for pairs of sensors installed at different points, it is clear that WSUs provide consistent and robust results, with a clear image of how the diverse parts of the bridge react differently to the ambient vibrations. Moreover, SR spectrograms (Figures 5e, and 5f) show that ambient vibrations have a stationary character, and indicate that the WSUs provide stable estimates.

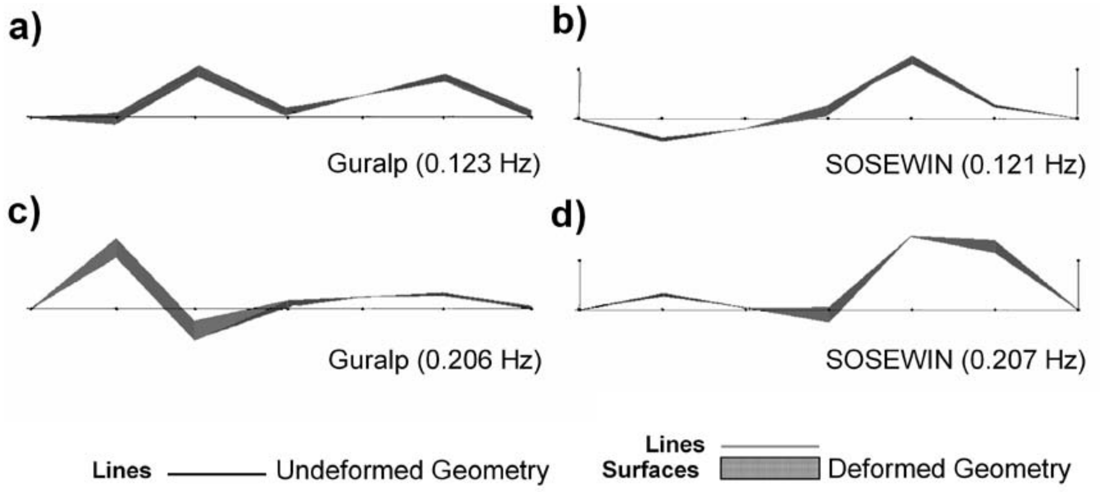

Figure 6: Mode shapes estimated by frequency-domain decomposition techniques from the vertical channels of the Guralp and WSU stations for the bridge's first (*a* and *b*) and third modes (*c* and *d*)

Results for the WSUs located on the deck (Figure 5a, c, e, and Table 2) indicate that the highest amplitude vibrations occur in the vertical component, and the SRs provide experimental vertical modes of vibration estimates (e.g. 0.122 Hz, 0.207 Hz) that match very well those (Table 1) obtained by Brownjohn et al. (1992). On the other hand, WSUs located on top of the towers (Figure 5b, d, f) indicate that, again in agreement with Brownjohn et al. (1992), the first two longitudinal vibration modes are at 0.155 Hz and 0.2 Hz, while the lateral modes are at 0.3 Hz, 0.5 Hz, and 0.8 Hz.

The first five experimental modes of vibration, which have been selected by the comparison of SR curves computed for WSUs placed at different locations on the deck, are listed for each direction in Table 2 (see also Picozzi et al., 2009). It is worth noting that these results (e.g. in Table 1) are in an excellent agreement with those obtained by previous studies (e.g. Brownjohn et al., 1992, and Apaydin 2002).

Stengel (2009) analyzed the dynamic behavior of the bridge through the commercial software ARTeMIS Extractor by Structural Vibration Solutions (ARTeMIS Pro, 2009) using first a dataset from 7 WSU instruments, and then an ambient vibration set of 4 of the permanently installed Guralp instruments. In both data sets, which are independently obtained, the instruments essentially on 1 side of the bridge deck (i.e. 4 Guralp, 7 SOSEWIN), while the data set's length was 3 hours for the Guralp sensors, and about 1 hour for the WSUs.

Figure (6) shows the mode shapes of the first and third vertical modes for the two data sets. The data set's length is a fundamental parameter, since it affects the reliability of the estimated modes and shapes using the software integrated frequency domain decomposition technique. However, although the length of this WSU data set is not optimal for this method, the 7 WSU nodes allowed a satisfactorily estimation of the bridge's modal shapes, which are in agreement with those retrieved from Guralp sensors and also with the numerical found modes determined by Brownjohn et al. (1992).

The results of the modal analysis conducted with using the WSU recordings are only preliminary, due to the limited time span of the data-set. However, is it remarkable that the mode shapes are nonetheless still well estimated. Therefore, future modal analysis, obtained by recording for a longer time period, would benefit from the installation of a denser mesh of monitoring instruments, which could be easily realized using the WSUs employed here.

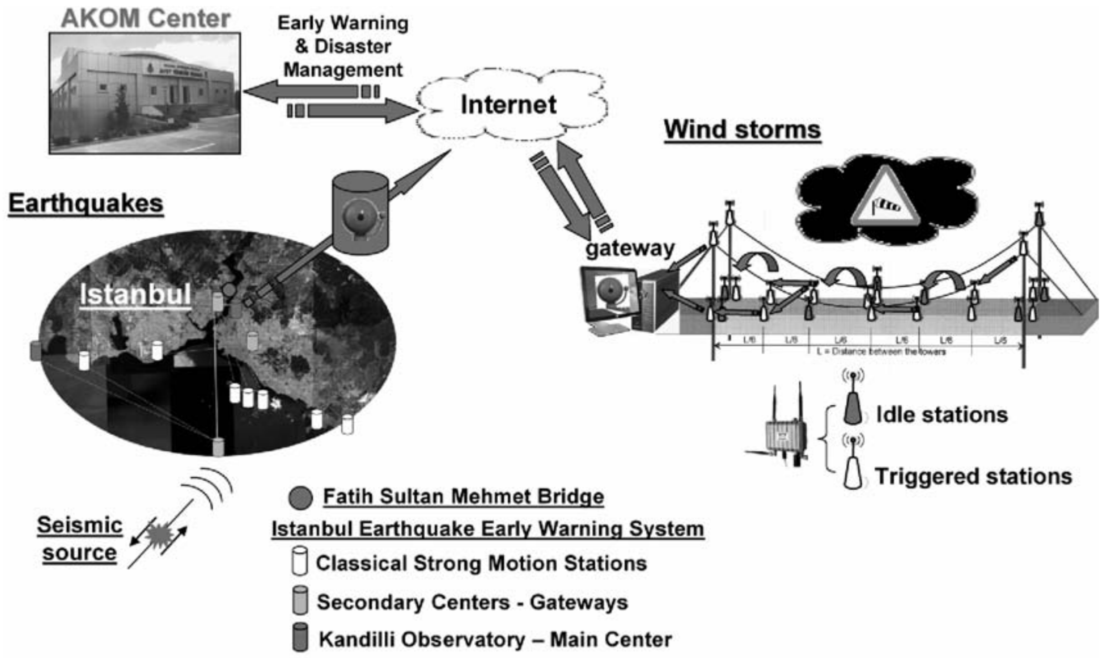

Figure 7: The possible »double way« early warning system for the Fatih Sultan Mehmet bridge. The warning can be issued by a gateway from the bridge in the event the WSUs detect anomalous bridge behavior (*e.g.* wind storms). The wireless network can also receive earthquake early warnings from the IERREWS operated by KOERI

5. Conclusion

In this work we have presented a new low-cost wireless sensing unit that has been designed to form dense wireless mesh networks, and that can be used for the structural health monitoring. Wireless sensing units offer the advantage that the analysis and data storage can be decentralized, while only the most significant information and estimated parameters be communicated through the whole network towards dedicated targets. The reduced cost of the instruments (less than one tenth of a standard instrument) and the possibility of creating dense, self-organizing and decentralized seismic monitoring networks are key aspects from which the standard approaches followed for structural engineering monitoring might have a considerable benefit. In particular, the decentralized, self-organizing character guarantees the functionality of the network during a disastrous event, even when some of the sensing units are damaged.

We conducted an experiment to determine the suitability of such a system for structural monitoring, involving ad-hoc ambient vibration recordings performed on the Fatih Sultan Mehmet bridge in Istanbul (Turkey). Comparisons with standard instrumentation and results obtained in terms of modal properties of the bridge indicate an excellent performance of the low-cost WSU. The results were found to be consistent with those from the studies of Brownjohn et al. (1992), Apaydin (2002), Stengel (2009). On the base of these results, the current, traditional structural health monitoring system operating on the Fatih Sultan Mehmet Suspension Bridge (Apaydin and Erdik, 2001; Apaydin 2002) might be profitably and economically extended by additional low-cost WSU instruments.

In particular, a dense wireless network of WSUs for a long-term, full scale, ambient vibration monitoring program of the Fatih Sultan Mehmet Suspension Bridge might allow the main modal properties of the bridge to be regularly re-evaluated in great detail and accuracy. Furthermore, thanks to the availability in the instrument of an additional channel, extra functionality to the WSU network could be explored, allowing, for example, the long-term monitoring of the wind load on the structure, or measuring temperature and air humidity, which are important factors when evaluating the estimations of the damping ratios.

In future, a dense wireless network of WSUs on the bridge could provide an early warning capacity for the bridge itself (Figure 7). In fact, the system might deliver independent warning through a gateway to some target (e.g. the Disaster Coordination Center of the Istanbul Metropolitan Municipality) in the event that anomalous bridge behavior were detected (e.g. during wind storms). In the meantime, the wireless network could receive warnings from the Istanbul Earthquake Rapid Response Early Warning System (IERREWS) operated by KOERI (Erdik *et al.* 2003b) in the event of an earthquake. Thus, it could be used to coordinate mitigation actions (e.g. stopping traffic access to the bridge) and to perform real time condition assessment and damage detection of the structure.

Acknowledgements.
The work undertaken was supported by the SAFER (Seismic eArly warning For EuRope, European Commission proposal no. 036935) and EDIM (Earthquake Data Information system for the Marmara Sea, Turkey, German Federal Ministry of Education and Research) projects.

The SAFER and EDIM working groups developing the WSU are J. Zschau, C. Milkereit, M. Picozzi, K. Fleming, I. Veit, K.-H. Jäckel, J. Nachtigall, and H. Woith (Helmholtz-Zentrum Potsdam Deutsches GeoForschungsZentrum, Germany); J. Fischer, J.P. Redlich, B. Lichtblau, F. Kühnlenz, K. Ahrens, I. Eveslage, and S. Heglmeier (Department of Informatics, Humboldt University (HU) Berlin, Germany).

K.-H. Jäckel and Mike Hönig have developed the Analogue-Digital Converter (ADC) board.

References

Apaydin, N. and M. Erdik (2001). Structural Vibration Monitoring System for the Bosphorus Suspension Bridges in Strong Motion Instrumentation for Civil Engineering Structures (NATO Science Series), Vol. 373, Ed. By. M. Erdik et al., Springer-Verlag New York, LLC.

Apaydin, N (2002). Seismic Analysis of Fatih Sultan Mehmet Suspension Bridge, Ph.D Thesis, Department of Earthquake Engineering, Bogazici University, Istanbul, Turkey.

Arias, A. (1970). A measure of earthquake intensity, Seismic Design for Nuclear Power Plants, ed. R.J. Hansen, MIT Press, 438–483.

ARTeMIS Extractor Pro (2009). Release 4.2, Structural Vibrations Solutions A/S, Denmark.

Böse, M. (2006). Earthquake early warning for Istanbul using artificial neural networks, Doctor of Natural Sciences thesis, Faculty of Physics, University of Karlsruhe, Karlsruhe.

Brownjohn, J. M. W., Dumanoglu, A. A., and Severn, R. T. (1992). Ambient vibration survey of the Fatih Sultan Mehmet (Second Bosphorus) Suspension Bridge, Earthquake Engineering and Structural Dynamic, Vol. 21, 907–924.

Dumanoglu, A. A., Brownjohn J. M. W., and Severn, R. T. (1992). Seismic analysis of the Fatih Sultan Mehmet (Second Bosphorus) Suspension Bridge, Earthquake Engineering and Structural Dynamic, Vol. 21, 881–906.

Erdik, M and E. Uckan (1988). Ambient Vibration survey of the Bogazici Suspension Bridge, Report No: 89-5, Department of Earthquake Engineering, Bogazici University, Istanbul, Turkey.

Erdik, M., Aydinoglu, N., Fahjan, Y., Sesetyan, K., Demircioglu, M., Siyahi, B., Durukal, E., Ozbey, C., Biro, Y., Akman, H., & Yuzugullu, O. (2003). Earthquake Risk Assessment for Istanbul Metropolitan Area, *Earthquake Engineering and Engineering Vibration*, vol. 2, No. 1, 1–27.

Erdik, M., and Apaydin, N. (2005). Earthquake Response of Suspension Bridges, Vibration

Problems ICOVP, Ed. By E. Inan and A. Kiris, Springer, pp. 181–195.

Fleming, K., Picozzi, M., Milkereit, C., Kuehnlenz, F., Lichtblau, B., Fischer, J., Zulfikar, C., Ozel, O., and the SAFER and EDIM working groups. The Self-Organising Seismic Early Warning Information Network (SOSEWIN), accepted to be published by *Seismological Research Letters*.

Heinloo, A. (2000). SeedLink design notes and configuration tips. http://geofon.gfz-potsdam.de/geofon/seiscomp/seedlink.html. Accessed December 09, 2008.

Kanamori, H., Maechling, P. and Hauksson, E. (1999). Continuous monitoring of ground-motion parameters, *Bulletin of the Seismological Society of America*, vol. 89(1), 331–316.

Kaya, Y., and Harmandar, E. (2004). Analysis of Wind Induced Vibrations on Bogazici and Fatih Sultan Mehmet suspension Bridges, Internal Report, Department of Earthquake Engineering, Bogazici University, Istanbul, Turkey.

Lynch, J. P., Wang, Y., Loh, K. J., Yi, J.-H. and Yun, C.-B. (2006). Performance monitoring of the Geumdang Bridge using a dense network of high-resolution wireless sensors, Smart Materials and Structures, 15(6): 1561–1575. Accessed December 09, 2008.

Milkereit, C., Zünbül, S., Karakisa, S., Iravul, Y., Zschau, J., Baumbach, M., Grosser, H., Günther, E., Umutlu, N., Kuru, T., Erkul, E., Klinge, K., Ibs von Seht, M., Karahan, A. (2000). Preliminary aftershock analysis of the Mw=7.4 Izmit and Mw=7.1 Düzce earthquake in Western Turkey – In: Kozaci, Ö.; Barka, A. (Eds.), The 1999 Izmit and Düzce Earthquakes: preliminary results, Istanbul Technical University, 179–187.

OLSR project (2004). http://www.olsr.org/docs/README-Link-Quality.html. Accessed December 09, 2008.

OpenWRT (2007). http://www.openwrt.org. Accessed December 09, 2008.

PC Engines (2008). WRAP.2E boards. http://www.pcengines.ch/wrap2e3.htm. Accessed December 09, 2008.

Picozzi, M., Milkereit, C., Zulfikar, C., Fleming, K., Ditommaso, R., Erdik, M., Zschau, J., Fischer, J., Safak, E., Özel, O., and Apaydin N., (2009). Wireless technologies for the monitoring of strategic civil infrastructures: an ambient vibration test on the Fatih Sultan Mehmet Suspension Bridge in Istanbul, Turkey. In press on Bulletin of Earthquake Engineering, DOI 10.1007/s10518-009-9132-7.

Press, W. H., Teukolsky, S. A., Vetterlin, W. T., and Flannery, B. P. (1992). Numerical Recepies in C: The Art of Scientific Computing, Cambridge: Cambridge University Press.

Safak, E., and Hudnut, K. (2006). Real-time structural monitoring and damage detection by acceleration and GPS sensors, 8th US National Conference on Earthquake Engineering, San Francisco, California.

Stengel, D. (2009). System Identification for 4 Types of Structures in Istanbul by Frequency Domain Decomposition and Stochastic Subspace Identification Methods. Diploma Thesis, University of Karlsruhe, Karlsruhe, Germany.

Straser, E. G., and Kiremidjian, A. S. (1998). A Modular, Wireless Damage Monitoring System for Structures, Report No 128, John A. Blume Earthquake Engineering Center, Stanford University, Stanford, CA.

Torvalds, L. (2007). The Linux kernel. http://www.kernel.org. Accessed December 09, 2008.

Sensor fusion in an ad-hoc Multi-Hop Sensor network for real-time monitoring of landslides endangering human infrastructures

Arnhardt C., Fernández-Steeger T. M., Azzam R.
Department of Engineering Geology and Hydrogeology, RWTH Aachen University

Abstract
Existing monitoring systems for early warning are often monolithic systems that are very cost-intensive, considering installation as well as operational expenses. The joint project ***»Sensorbased Landslide Early Warning System« (SLEWS)*** deals with the development of a monitoring and early warning system for mass movements using low-cost sensors from industry in a wireless Ad-hoc, Multi-Hop sensor network. The self-organizing and self-administrating structure of such a system allows the setup of a very flexible sensor network, with independently working nodes due to their own energy supply. This allows the monitoring of larger areas, even in regions with low accessibility. Mikrosensors (MEMS) are used for tilt-, acceleration-, height- and elongation-measurements to observe surface deformation and gap opening. Due to fast data transfer, processing and visualization processes, it is possible to monitor and also to send warning-messages in real-time. The combination of sensor data (sensor fusion) allows to cross-check and to evaluate the sensor signals according to decision theory. This contributes essentially to the enhancement of data quality but also to the reduction false alarm rates.

Keywords: mass movement, landslide, Early Warning System, wireless sensor network, SLEWS

1. Introduction
In the most mountainous regions of the world, landslides represent one of the major threats to human life, properties and infrastructures. The combination of anthropogenic activities and increasing urbanization, but also the uncontrolled land use in many countries, together with climatic changes leads to a vulnerability rise to population and infrastructures (Kalsnes et al., 2008). This development is not only a specific problem of the high mountain areas, but also the low mountain ranges in Germany and Europe. For example landslides and rockfalls along the German railway track in the Rhine and Moselle valleys cause intensified stabilization and monitoring programs in this area since 2001, with costs more than 100 million Euros (Krauter, 2004). Apart form the high costs for the constructive measures and for the slope control, the landslides had (and have) also a high impact on the infrastructures in this region. Trains had to be stopped, streets were closed, what also meant that some villages in the river valley could only be reached by other ways (what often needed more time). In the last years early warning systems developed to one of the main pillars of disaster prevention in natural hazards especially where mitigation strategies are not realizable. Therefore, the call for multi-hazard early warning systems and improvement of monitoring capabilities is steadily growing. The joint project ***»Sensor based Landslide Early Warning Systems« (SLEWS)*** that is part of the DFG/BMBF special program »Early Warning in Earth Management«, deals with the develop-

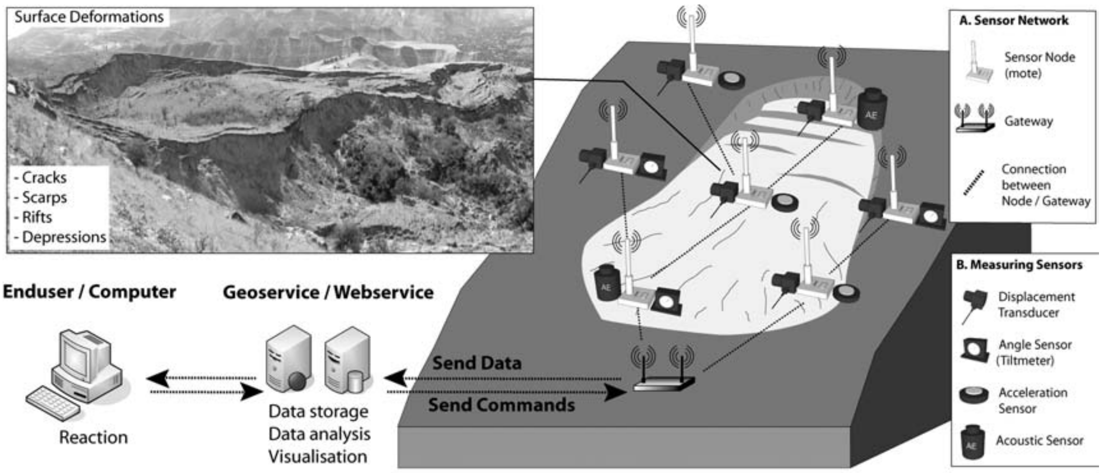

Figure 1: Scheme, showing the main components of the monitoring and warning structure developed in the frame of the SLEWS-project. The basic technical components are the wireless sensor network and the spatial data infrastructure using geo-/webservices for standardized information handling and retrieval

ment of a prototypic alarm- and early warning system (EWS) for different types of landslides, using wireless sensor networks and low cost but precise microsensors (MEMS). Different setups are developed for the monitoring of surface changes and deformation (like opening of cracks, tilting of blocks and so on) but also on buildings, constructions and infrastructures (like walls, cable lines etc.) in the landslide area (Fig. 1). The measured data from the sensor network is stored, processed, and visualized in a new developed spatial data infrastructure (SDI) using open interfaces according to the Open Geospatial Consortium (OGC) standards. As there is no typical enduser for an early warning or alarm system in Germany but many groups (scientists, consultants, administration, enforcement authorities, or emergency service) with specific requirements on warning and alarm messages (Fernández-Steeger et al, 2009), different cases and warning structures are examined. Due to the investigation of the complete information chain, from data gathering via information processing up to the user centered information distribution, it becomes possible to define the needs and challenges of a people centred monitoring and warning system. As reliable real-time data are necessary for the detection of hazards, fast warning and response, the potentials of wireless sensor networks for rapid data transfer and retrieval are investigated during this project.

The following descriptions focus mainly on the technical aspects of a monitoring system, like sensor networks and microsensors, and the validation of sensor signals using sensor fusion.

2. Wireless ad-hoc Multi-Hop sensor network

The progressive technical developments, miniaturization and emerging computational power allow the integration of microsensors, CPU´s, wireless communication units and independent energy sources in very small and low priced so called Sensor nodes (or motes). The wireless connection of numerous Sensor nodes using standard technologies allows to establish a wireless sensor network (WSN), which enables the monitoring of different phenomena in a wide area (Sohraby et al., 2007). Modern, so called Ad-Hoc wireless sensor networks (WSN) are characterized by a self organization and self-healing capacity of the system (autonomous systems), without predefined infrastructures (Arnhardt, 2008). It permits a non hierarchic data exchange and thus allows a very simple adaption of the network to changed conditions. The use of a wireless system eliminates the need of extensive cabling outside in the monitored area and so reduces

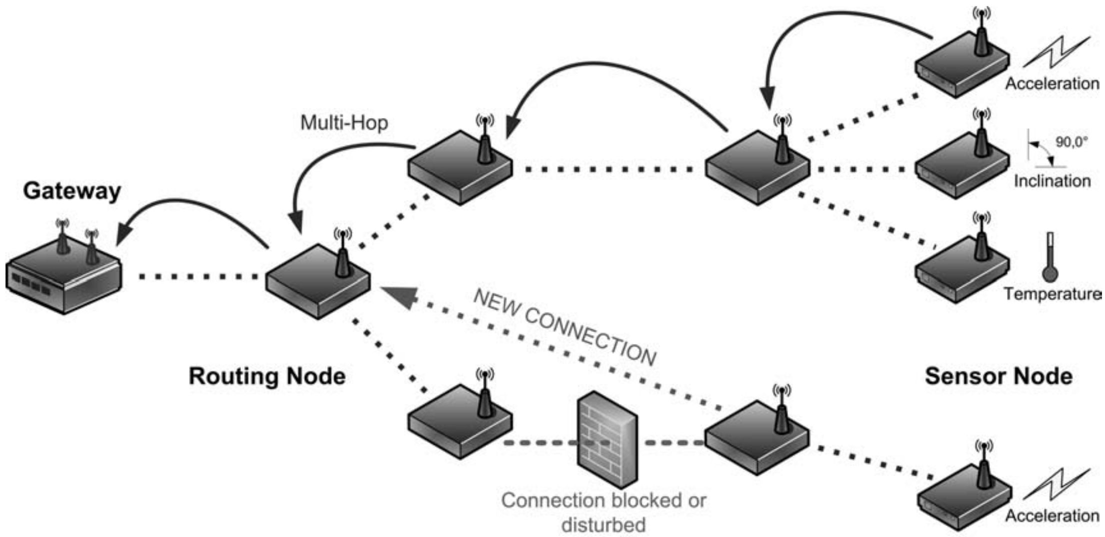

Figure 2: Structure of a non-hierarchic wireless ad-hoc, multi-hop sensor network as it is used in the SLEWS project. The routing is self organized and modifies automatically if connections weaken or break down

material costs and increases system reliability (as cable breaks are not possible anymore) (Garich, 2007). The sensor network used in this project uses the 868 MHz frequency band for sending radio signals. The frequency band is divided in further 30 sub-bands to avoid noisy channels. Data rates range from 4,8–115 kbits/s at transmission distances from 10 m to 1,2 km (ScatterWeb, 2007). The network consists of numerous sensor nodes that can communicate with their neighboring nodes (Fig. 2) and perform simple processing tasks. Each node has its own voltage supply, transmission and a receiving unit (Transceiver), microprocessor, and internal memory. The independent energy supply of each node allows an autonomous operation in the WSN and thus, avoids the collapse of the whole system because of single node failures. This permits a stable runtime of the WSN and enables a permanent monitoring. Data packages from each node are sent via radio directly or over other nodes (Multi-Hop) to a collection point (gateway). The Multi-Hop function reduces the requirement for long-range transmission and allows the buildup of a transmission chain of nodes. The nodes have different energy-saving modes that range from approximately 100 µA in sleeping modus to 250 µA in a precise transmission mode. Based on the RSSI value (received signal strength indication) the minimum transmission energy between communicating nodes is chosen automatically. Data transfer is performed by time-synchronized communication and depending on connection and connection strength. Each sensor node in the network is able to search individually the best link to other points of the network. This helps also to avoid the failure of the system even if some of the nodes break down. The bidirectional structure of the system enables data transfer from each node over the gateway-interfaces to the main computing unit (PC, Laptop, Server), but also allows to transmit commands like data requests as well as software-updates to specific nodes or a group of nodes. Additionally, the modular setup of the hardware and the use of standardized interfaces allows an easy adaption or integration in existing solutions.

2.1 Test-Network and Data Transfer

In order to investigate the communication stability, data stream and to provide real-time data for the development of the SDI a small wireless sensor network was set up (Fig. 3). It consists of 4 sensor nodes with up to 7 different measuring sensors (light, vibration, motion, battery status, connectivity and two internal control sensors) on each node.

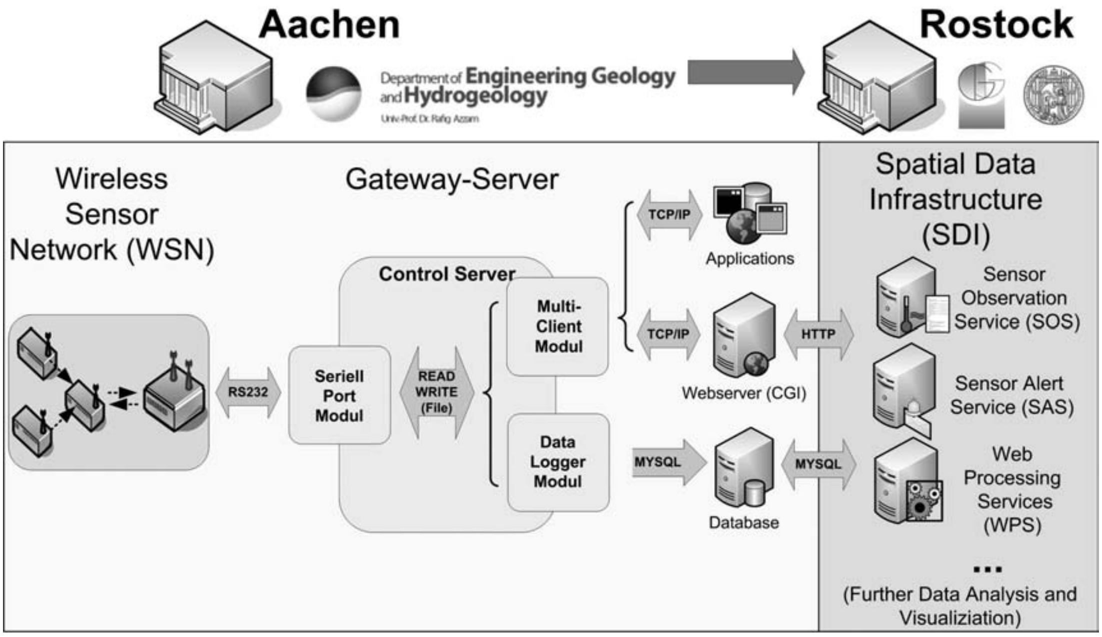

Figure 3: The network environment and its spatial distribution. While the sensor network and the gateway infrastructure are located in Aachen, the spatial data infrastructure and databases are sited and operated in Rostock. The special feature of the established structure is the multi channel data provisioning of the gateway server (Fernandez-Steeger et. al., 2008)

The signals are sent via radio to the gateway and from there to a gateway server for data retrieval and processing. The development of a modular gateway- or control-server allows the communication of different client applications with the gateway of the WSN. The multi client module enables the communication between client and gateway with TCP/IP socket, while the data logger module writes the data in a SQL-database. The TCP/IP sockets and the database provide an interface for the project partners to this evaluation network. Bidirectional communication with the network was implemented recently and tested locally. Furthermore, local software allows access to the network and database environment for sensor tests and calibration of sensor nodes. As the local data environment works now stable and fits the basic requirements, all new sensors nodes are integrated directly into the network, even for short experiments.

3. Measuring devices for landslide monitoring

The general term »landslide« comprises different movement processes like flowing, sliding, falling, lateral spreading and topples (Varnes, 1978; Cruden, 1996), with combination of different processes (complex and compound landslides). Sensors that are used for direct movement detection and measurement (i.e. movement yes/no) must have the accuracy and the sensitivity to register one or some of these movement patterns or the effects of this displacement very precisely. As most landslides do not show continuous deformations but are rather sporadically active (Terzaghi, 1950; Leroueil, 1996) with stronger acceleration before slope failure, a permanent landslide monitoring is important, so changes can be detected at the moment they occur (USGS, 2005). Therefore all or at least some sensors have to be active all the time. This requires on the one hand a stable energy-supply but on the other hand also a low energy-consumption of the sensors (Fig. 4) besides the quality of the sensors. To guarantee not only a permanent but also longtime (more than one year) monitoring of a landside area the sensor must be able to operate stable and without calibrations over a long time (Fig. 4). To work under the changing and sometimes inhospitable weather conditions outside, the sensors have to be also very robust and unsusceptible. Besides this requirements arising from the operation tasks and environments, further sensor requirements result from the integration of sensors in a WSN. In order to achieve an efficient and stable communication between measuring sensor and sensor node, it is important that both devices have compatible digital interfaces.

Another important point in the frame of the SLEWS project is the development of a low-cost, but still precise landslide monitoring system. To accomplish this, low-cost and small-sized measuring sensors with standardized industrial interfaces are chosen. These sensors are used for example in the automotive industry (airbags), for consumer electronics (mobile phones, GPS enhancement), for technical instruments (electronic levels) or medical equipments. Based on the technology of Micro-Electro-Mechanical-Sensors – (MEMS), they combine very small mechanical and electronic units, sensing elements and transducers on a microchip.

The selected first sensor set up consist of MEMS silicon capacitive sensors made of single crystal silicon and glass to measure acceleration tilting and barometric pressure (Fig. 4). The 3 axis *acceleration sensor* has an digital SPI interface, with a sensitivity of 1333 counts/g, acceleration range of ±2 g, Operating temperature from –40° to 125 °C, bandwidth of 45 Hz and a low current consumption of 480 μA by 2,5 V. It includes an internal temperature module and a small internal memory. Typical applications of this sensor are inertial navigation, inclination sensing in digital inclinometers and tilt compensation in electronic compass. The *inclination sensors* or *tilt sensor* (inclinometer or tiltmeter) are 2-axis measuring sensors and have a digital SPI interface, with a bandwidth of 8–28 Hz, an operating temperature of also −40° to +125 °C and a current consumption of about 4 mA by 5 V. Two different inclination sensors are tested in this project. The first one is a dual axis inclinometer with a measuring range of ±30°, a sensitivity of 1638 counts/g while the other one has a measuring range of 90° and a sensitivity of 819 counts/g. The sensors also have an internal temperature device. Typical applications are platform leveling/stabilization and 360° vertical orientation measurement. The digital absolute *barometric pressure sensor* has a resolution of 1,5 Pa with a low <10 μA current consumption and is used for measuring sub-meter hight changes (*altimeter*). The measuring range goes from 30 kPa to 120 kPa, with a operating temperature from –20° to +70 °C. The relative pressure accuracy is specified with ±50 Pa. It also has a standard SPI digital interface and an internal temperature device (accuracy ±1 °C). The pressure and temperature output is compensated and calibrated inter-

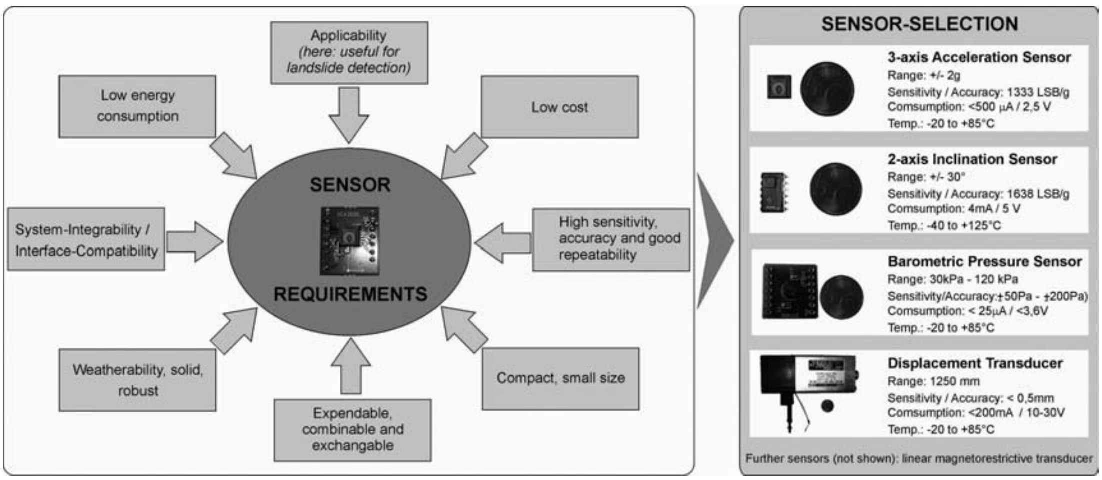

Figure 4: Sensor-Requirements and overview of selected sensors

nally. The sensor has 4 measuring modes that combine high 17-bit resolution (8 cm of air column) with either 2 Hz or 1 Hz (low power consumption with 10 µA) data read, or alternatively 15-bit resolution (20 cm of air column) with high speed data read (9 Hz) or ultra low power consumption (<10 µA). Typical applications of this sensor are Barometric pressure measurement and altimeter applications, usage for home weather stations, medical applications and level gauging.They are assembled on a so called sensor board providing all necessary interfaces for energy supply and the node. For the measurement of extensions, elongations and compressions potentiometric *displacement transducers* and linear *magnetorestrictive position transducers* are used. Both have an SSI Interface with an analogue digital converter. The measuring range of the displacement transducer used has a length of up to 1250 mm with a given linearity of ±0,05% of the effective range. It has a high-grade steel cable that is protected by a small box made of aluminium, high-grade steel and synthetic material (protection class: IP 54). The operating temperature is –20 °C to +85 °C. The linear position transducer used in this project has a measuring range of 1000 mm, with a given linearity of < ±0,01% of the effective range. The operating temperature is –40 °C to +75 °C. While these two types of transducers are very precise, they have a quite high high current consumption (100 to 200 mA) by voltage of 12 to 24 V. First tests were done under stable conditions to get information about data spreading and thus the accuracy of the different sensors in the setup (Fig. 5).

Even considering the accuracy limitations of the used test environments, the deviation of measuring data is quiet low, with minor variance. All tests were performed using sensors integrated in the sensor network environment to prove the operational accuracies. and The tested accuracies of the tilt sensor was +/–0,06°, +/–0,008g for the acceleration sensor and +/–0,1 mm for the displacement transducer. To improve the test environment more accurate and sensitive test stations with very precise computer control are developed now. Further tests were performed to get information about the measuring resolution of the sensors in the WSN environment. The results are also quite good. For example tilt changes of up to 0,1° and displacements of 0,1 mm can be detected very reliable. In the near future field tests for the sensors in suitable landslide environments will follow.

To integrate the sensors in the sensor network a new sensor board was developed that

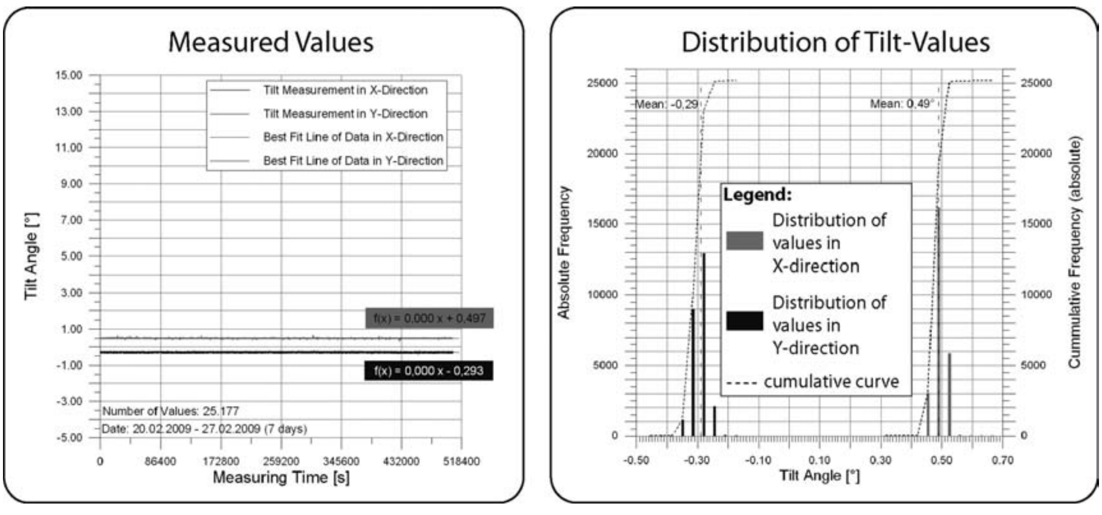

Figure 5: Example of tilt-measurement tests under stable conditions to prove accuracy and shift of measurements. The kurtosis and distribution of measuring data indicate that now shifts were observed

includes the measuring sensors (acceleration, inclination temperature and barometric pressure sensor) and the sensor node for data transfer in the WSN (Fig. 6). The inclination sensor is placed on a separate small board that is connected via ribbon cable with the sensor board. This allows to adjust the orientation of the 2-axis inclination sensor. At the moment a second sensor board set up for the displacement and linear transducers is under preparation for laboratory tests. Two energy sources are available for the nodes (Fig. 6). One is a solar powered energy module with solar panel, solar battery and charge control and the other is a long live battery module for situations where the solar panels cannot cover the energy demand. Antenna, sensor-node (sensorboard and node) and energy pack are separate units of the system that can be assembled or replaced individually. Each of them is protected against external influence like weather by a robust box. The units are connected by weather-resistant cables and connectors. This modular setup makes it easier to install the system in the field as the setup allows an easy adjustment to different environmental conditions. In addition the maintenance and support of the monitoring system is much easier (damaged parts can be replaced very quickly). Because of the higher energy consumption and the bigger size of the displacement transducer, it is it connected with a small sensorboard that consists only of the sensor node but no other sensors. There are also two different versions of the gateway. One is more for the indoor or close to infrastructure use, with energy supply from an external source (e.g. power adapter) but also robust casing. A second very robust solar powered gateway with GSM/GPRS modem was developed for field use where no suitable infrastructures are available. It has a solid metal frame and a waterproof box for gateway, modem, solar battery and charge controller.

A last very important aspect for the operation of the WSN is the measuring interval of each sensor and subsequently the data management. The frequency of measuring and sending of data has a large impact on the energy

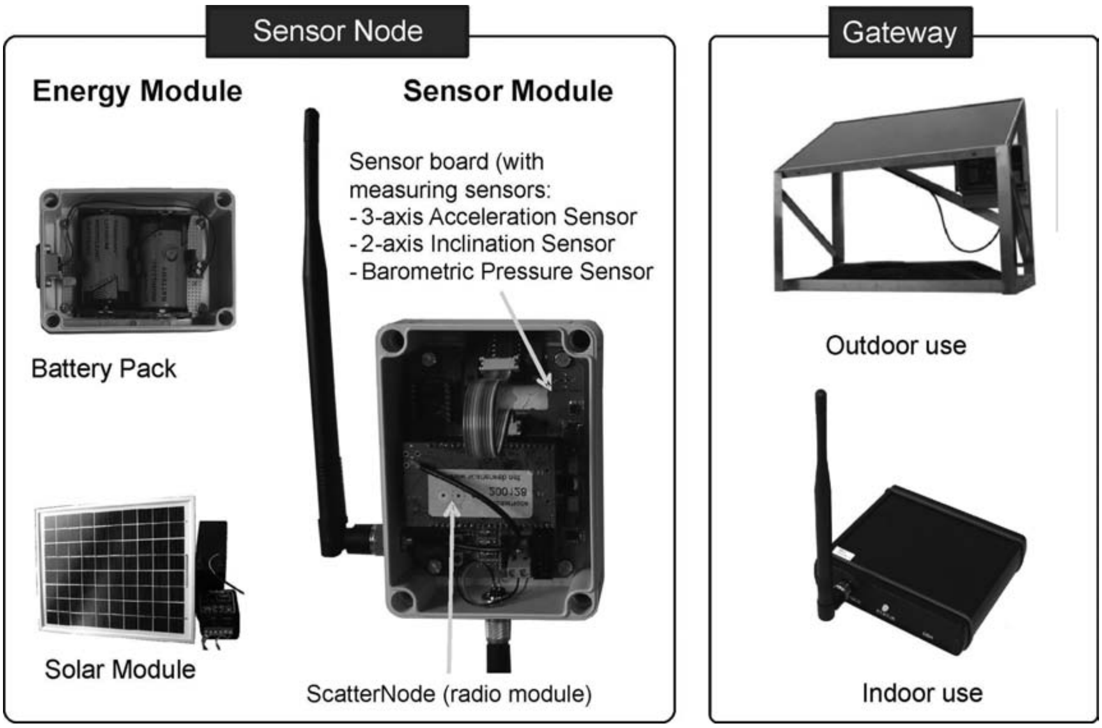

Figure 6: Technical components of the sensor network. Left side: battery-powered and solar-powered energy module and sensor node with measuring sensors. Right side: gateway systems (data sinks) with solar powered energy (top) and external energy source

consumption and the sensitivity of the system but also on the data volume and the data management. Therefore the optimization of the sensor measuring interval is an important task in the course of sensor network development. First simple algorithms for activation and regulation of sensor processes are developed now. In first tests a set up is under investigation using the precise and energy efficient acceleration sensor as a lead sensor, measuring and sending data more than once per second, while the others remain in standby or sleeping mode. If this sensor detects changes of the measuring values (acceleration) that are higher than a defined threshold value the other sensors will be activated automatically. To prove the functionality of the network and its components, every sensor is sending at least one measuring value every minute irrespective of movement or not. Further more sophisticated algorithms will be developed and programmed in the future keep the amount of data in a efficiently manageable range.

4. Sensor fusion

Mass movements, e.g. slope failure or rock fall, may be described as complex deformation processes, leading to a down-slope movement of the affected masses and result in a surface modification. The monitoring of such movements needs a large number of observations and information. Only the combination of such information permits an appropriate interpretation of the mechanism and attitude of the affected area (moving body) resulting in early warning or alarm. The Fusion (i.e. combination and comparison) of all sensor data from the sensor network contributes to the decision making of alarm and early warning systems and allows a better interpretation of data (Arnhardt, 2009). The comparison of data from different (complementary sensor fusion) but also same sensor-types (redundant sensor fusion) permits a verification of the data (Fig. 7). The development of special algorithms allows in a further analyzing and evaluation step the combination of data from all nodes of the network (sensor node fusion).

Figure 8 shows an exemplary case for sensor fusion applied for a block rotation. To monitor the movement, several sensor nodes are attached directly or near the moving block, but also on the stable not moving rock face. If the

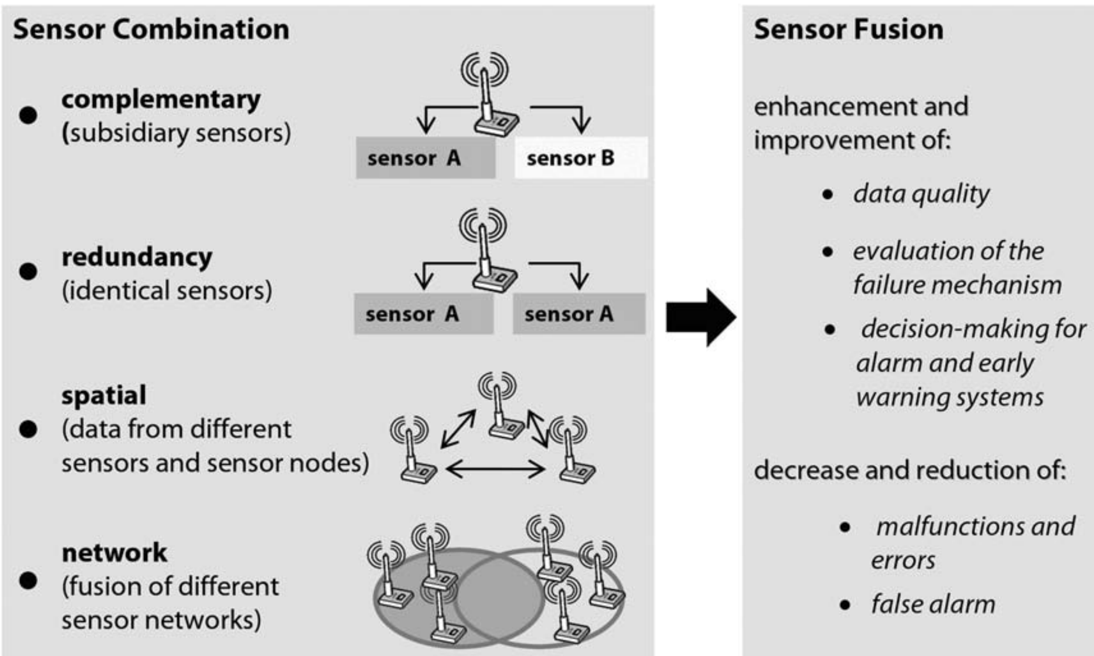

Figure 7: Different concepts for sensor combination und sensor fusion which can be used to evaluate and verify sensor signals in critical infrastructures like alarm or warning systems (Fernández-Steeger et al, 2008)

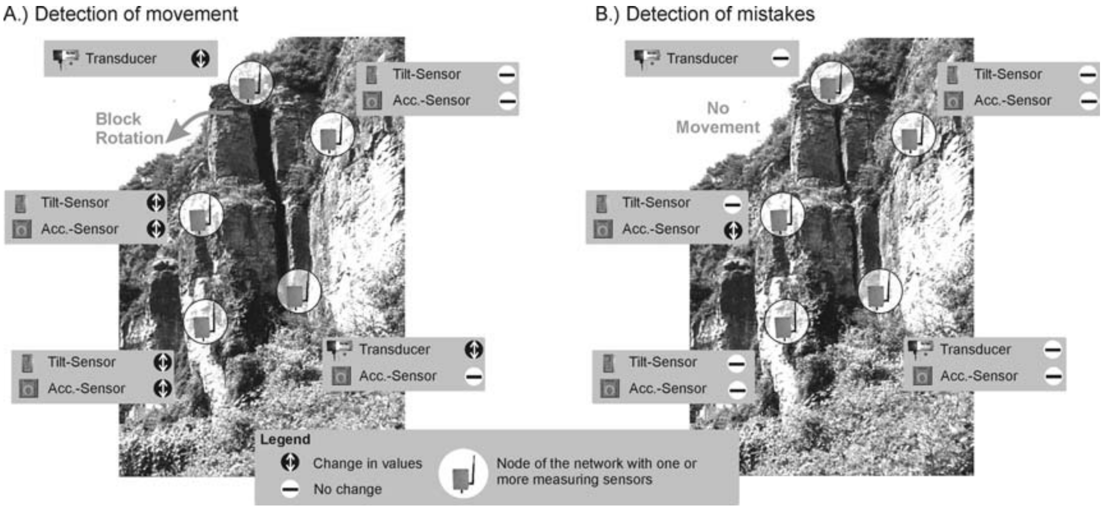

Figure 8: Sensorfusion applied to a tilting rock tower at a large rock face. Sensor fusion might be used as shown at the left side (A.) for movement-detection, but also for the verification and error detection as shown at the right side (B.)

block moves, the sensors are affected by this and show changes in their measuring values (presuming that the movement exceeds the sensor resolution). The rotation causes at the head of the block the opening of cracks, which leads to an elongation of the measuring cable of the displacement transducer mounted at these gaps. As the opening at the top is larger than close to the rotation point at the bottom, displacement transducers mounted on top should show higher changes than the ones close to the rotation point. Thus the combination of identical sensor types mounted at different positions of the moving block provides already information about movement intensity, but also the type and direction of movements (foot rotation or head rotation). Further knowledge may be gained from other sensors. Tilt sensor at the toppling block should show changes in tilt angle and thus give information about the amount of movement. Acceleration sensors can either be used for the detection of jerky movements or peak accelerations (dynamic accelerations) but also to measure the change of position (static acceleration). Sensors at the stable not moving rock face should normally indicate no changes. The comparison and interlacing of all sensor data allow a better interpretation of the deformation, intensity in different movement areas but also the validation of sensor information.

Furthermore the sensorfusion provides the option to detect errors and malfunctions of sensors and therefore helps to prevent false alarms. Especially the malfunction and error detection is of special interest because it is important for the suitability and acceptance of a monitoring system. A system with a lot of false alarms is not taken seriously anymore even if there is a real event. One option to face this problem is to verify the observations of single sensors by other sensors at the same or near location. If the measured values show no coherent motion picture, the probability of an error or malfunction is very high. In the illustration on the right side of figure 8 an acceleration sensor shows movement, while the sensors nearby show no changes. Also the tilt sensor on the same sensor node shows no changes. Thus the data from the acceleration sensor must be an error. To prove this concept experiments for sensor combination and sensor fusion were accomplished under defined laboratory conditions. First tests showed a good correlation and verification between signals from different sensors is possible (Fig. 9). Additionally outliers and errors can be recognized very well.

In the future a robust decision algorithm has to be developed and tested to evaluate the data from all nodes of the network (sensor

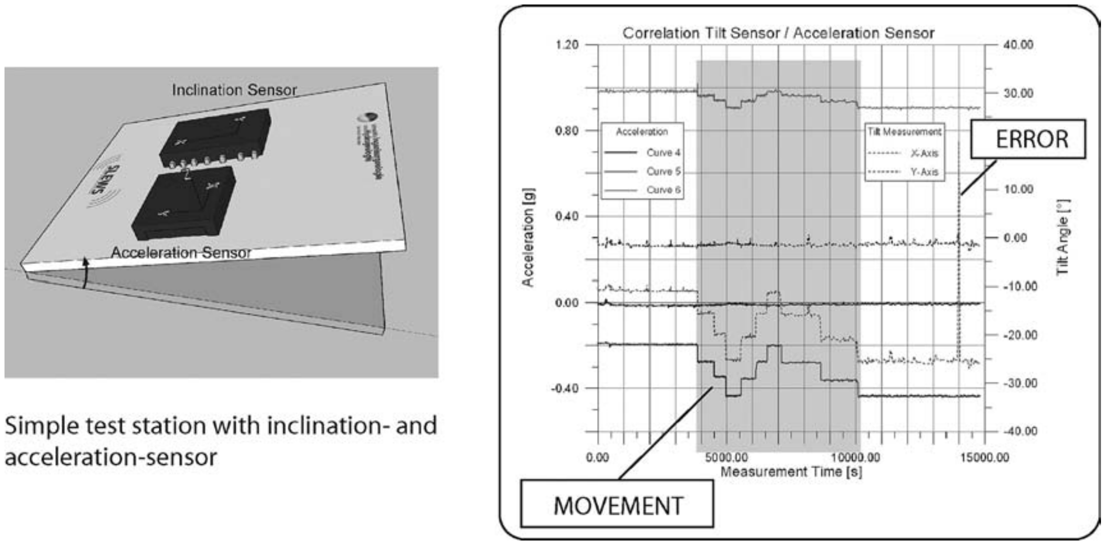

Figure 9: Evaluation of an experiment using a sensor node with an acceleration and tilt sensor. The sensor signals from both sensors show very well the changes of the position of the node (tilting). Anyhow close to the end of the experiment an error occurs at one axis of the tilt sensor. Because the acceleration sensor does not show any changes (and because it is known from the experimental procedure that there was no movement at that time) the peak can be classified as an error

node fusion). Anyhow some aspects have to be taken in consideration in the course of sensor fusion. As different sensors have different accuracies and different resolutions, the sensors are unequal sensitive for the detection of movement. More sensitive sensors (like the displacement transducer) must have a higher priority if they indicate changes. In addition some sensors are more adequate for the detection of specific processes than others (e.g. tilt sensors for toppling). Also the position of the sensors has to be taken into account as sensors in the center of a landslide show usually stronger movements than the ones at the boundaries. This shows that not only the sensor signals but also some other information like the sensor type, accuracy, position, motion rate and type of movement process have to be taken in consideration in the process of sensor fusion for data enhancement and validation. Anyhow this shows that there are large potentials in the concept of sensor fusion for sensor networks, not only regarding the data quality but also to derive additional information about the movement process.

Conclusion

The Monitoring system described here is characterized by a very, flexible structure, cost efficiency and high fail-safe level. The usage of a modern so called multi-hop wireless sensor network allows a longer data transfer via radio signal from node to gateway whereby the length of the transmission can be expanded. Through this large areas can be monitored. The self-organizing, so called ad-hoc structure of the system enables a very rapid and flexible adjustment to changed boundary conditions. New and/or more stable lines of communications between nodes and gateway are found autonomous, if some routes are blocked or disturbed. This prevents the breakdown of the whole system when some nodes are not working anymore. Through this the functionality of the system (or at least parts of it) are guaranteed and thus a monitoring is still possible. The application of wireless sensor networks in combination with low-cost, but precise microsensors (MEMS) provides an inexpensive and easy to set up intelligent monitoring system for spatial data gathering in large areas. Because of the small size, weatherability, low energy consumption of these MEMS they are suitable for outside applications. First laboratory tests with different MEMS showed that these sensors have a quite good accuracy and resolution to detect movements like tilting, spreading but also acceleration. Therefore it is possible to use them for the monitoring of different deformations on the surface of mass movements. The standardized interface of the sensors allows an easy integration in the wireless sensor network. The sensor fusion (correlation of data from same or different sensor types) is a substantial improvement in comparison to today existing early warning systems and permit a simple linkage also with other data sources (e.g. climate data) or other sensor networks (network fusion). It allows the verification of sensor data and thus enables a better interpretation of mechanism and dynamic of the affected area. Active (moving) parts of the area can be identified and enable well-directed reactions (expansion of the system in these parts, safeguard measures etc.). Furthermore it helps to detect errors and malfunctions and thus prevents the triggering of false alarms, what is important for the acceptance and attention of such kind of system. All these aspects are necessary in the context of environmental monitoring and observation of endangered infrastructures where fast, precise and reliable information are the requirement for an adequate and user-specific warning structure.

Literature

Arnhardt, C. (2009): Anwendung drahtloser Ad-Hoc Multi-Hop Sensornetzwerke im Bereich Umwelt-Monitoring zur Echtzeitüberwachung von Massenbewegungen, In: Tagungsband der 17. Tagung für Ingenieurgeologie, 6–9 Mai 2009, Zittau, Deutschland, 369–372.

Arnhardt, C., Nakaten, B., Fernandez-Steeger, T. M., Azzam, R. (2008): Data-Fusion of MEMS-Sensors in a wireless Ad-Hoc Multi-Hop Sensor Network for Landslide Monitoring and Real-time Early Warning, In: Schriftenreihe der Deutschen Gesellschaft für Geowissenschaften, International Conference and 160th annual meeting of the Deutsche Geologische Gesellschaft für Geowissenschaften e. V. and 98 annual meeting of the Geologische Vereiningung e. V., Geo 2008 Aachen, 176.

Arnhardt, C.; Asch, K.; Azzam, R; Bill, R.; Fernandez-Steeger, T. M.; Homfeld, S. D.; Kallash, A.; Niemeyer, F; Ritter, H.; Toloczyki, M.; Walter, K. (2007): Sensor based Landslide Early Warning System – SLEWS. Development of a geoservice infrastructure as basis for early warning systems for landslides by integration of real-time sensors. In: GEOTECHNOLOGIEN Science Report 10. Early Warning Systems in Earth Management, p. 75–88.

Barry K. Myers, M. Asce, L. Radley Squier, F. Asce, Mark P. Biever, and Rex K. H. Wong, M. Asce (2007): Performance monitoring for a critical structure built within a landslide. – S. 91–108, Asce Publication.

BILL, R., NIEMEYER, F., WALTER, K. (2008): Konzeption einer Geodaten- und Geodiensteinfrastruktur als Frühwarnsystem für Hangrutschungen unter Einbeziehung von Echtzeit-Sensorik. In: GIS – Zeitschrift für Geoinformatik. 2008, Nr. 1, S. 26–35.

Fernandez-Steeger, T. M., Haß, S., Niemeyer, F., Walter, K., Arnhardt, C., Nakaten, B., Homfeld, S. D., Asch, K., Azzam, R., Bill, R., Ritter, H. (2009): SLEWS – Ein prototypisches Beispiel für flexible Echtzeitüberwachung von Massenbewegungen mit offenen Geodateninfrastrukturen und Sensornetzwerken. 17. Tagung Ingenieurgeologie. 6–9 May 2009, Zittau, Germany.

Fernandez-Steeger, T. M., Arnhardt, C., Niemeyer, F., Haß, S., Walter, K., Homfeld, S. D., Nakaten, B., Post, C., Asch, K., Azzam, R., Bill, R., Ritter, H., Toloczyki, M. (2008): Current Status of SLEWS – a Sensor Based Landslide Early Warning System, In: R & D Programme GEOTECHNOLOGIEN – Early Warning Systems in Earth Management, Status-Seminar, 8–9 October, Osnabrück.

Kalsnes, B., Nadim, F., Glade, T. (2008): Effects of Global Change on Landslide Risk. In: International Consortium on Landslides (ICL) – The First World Landslide Forum 2008, 18.–21. Nov. 2007, Tokyo (USA), Abstract.

Krauter, E., Feuerbach, J., Lauterbach, M. (2004): Risikoabschätzung von Hangbewegungen und Schutzkonzepte. – In.: 10. Internationales Symposium Interpraevent 2004, Riva del Garda/Trient.

Leroueil, S., Vaunat, J., Picarelli, L., Locat, J., Lee, H., and Faure, R., (1996): Geotechnical characterization of slope movements. In: Proceedings of the International Symposium on Landslides, Trondheim, 22 pp.

ScatterWeb GmbH (2007): Company presentation. http//www.scatterweb.com (Time: 04/2008).

Sohraby, K., Minoli, D., Znati, T. (2007): Wireless Sensor Networks – Technology, Protocols, Application. – Wiley & Sons, Canada.

Terzaghi, K. (1950): Mechanism of Landslides. In Engineering Geology (Berkel) Volume. Ed. da The Geological Society of America, New York, 1950.

U.S. GEOLOGICAL SURVEY (2005): Real-Time Monitoring of active Landslides – Reducing Landslide Hazards in the United States. In: Fact Sheet 091-99

Varnes, D. J. (1978): Slope movement types and processes, – In: Landslides – Analyses and control, S. 11–33, National Research Council, Washington D.C.

Preliminary investigation on integration of semi-active structural control and earthquake early warning

Iervolino I., Galasso C., Manfredi G.

Dipartimento di Ingegneria Strutturale, Università degli Studi di Napoli Federico II

via Claudio 21, 80125 Naples, Italy

eMail: Iunio.iervolino@unina.it, carmine.galasso@unina.it, gaetano.manfredi@unina.it

1. Introduction

Earthquake Early Warning Systems (EEWS) are tools for real-time seismic risk management. EEWS potentially enable different possible risk mitigation actions, to be carried out when an alarm is issued, depending on the amount of lead-time available (defined as the warning time between the alarm and the strike at the site of interest). Examples of such actions, classified according to the lead-time required to be undertaken, are reported in Figure 1 for the Campania region (southern Italy) which is provided with a regional EEWS, the Irpinia Seismic Network (ISNet) comprised of 29 seismic stations with real-time capabilities (Weber et al., 2007).

In epicentral areas, only a few seconds of warning time is available, and an EEWS can only be used to trigger automated decision and risk mitigation procedures (i.e., the lead-time is too short to allow for manned operations). This is the case, for example, of the Campania region where the most hazardous seismogenetic sources zone is close to densely urbanized areas and time-consuming security actions, as evacuation, may be unfeasible.

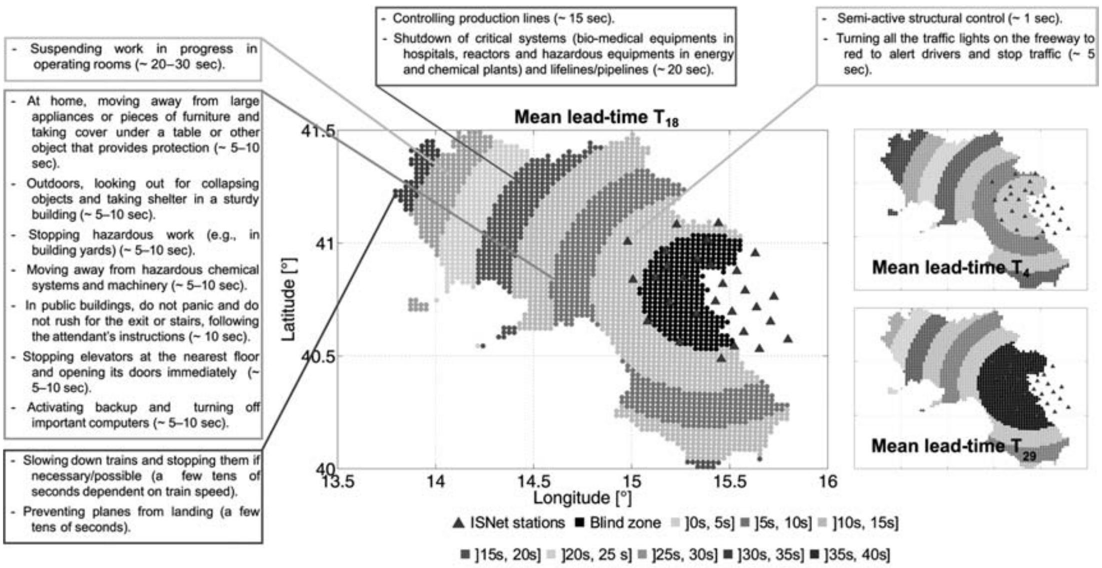

Figure 1: Information-dependent lead-time maps for the Campania (southern Italy) region and possible risk reduction actions (Iervolino et al., 2009)

Some studies discuss, as an engineering application of EEW, especially in areas where the available lead-time is low, the semi-active control of structures; i.e., the building can change its dynamic properties within a few seconds (or milliseconds) to better withstand the impending ground motion (Pnevmatikos et al., 2004; Occhiuzzi et al., 2008). The combined use of EEWS and structural control may reduce the structural vulnerability of specific systems, for example, critical buildings which have to be operable for emergency management purposes right after the event; e.g., hospitals, fire stations, or lifelines.

Currently, integration of structural control and EEWS relies substantially on semi-active devices. However, the key issue in the application of early warning to structural control is to account for the uncertainty in the estimation of the event's features the EEW is based on, because the efficiency of such systems depends on the quality of pre-arrival ground motion information provided.

In this paper, some very preliminary results related to a feasibility study about structural control integrated with *hybrid* EEWS (Iervolino et al., 2006), are presented and discussed. Although, interaction between earthquake early warning and structural control is a subject which still requires substantial investigation to be addressed.

2. Background

Recent efforts of real-time seismology on rapid assessment of earthquake magnitude and location enable to provide an estimate of the event's features from a few seconds to a few tens of seconds before the ground motion arrives at a specific site. Then, when an event is occurring, probabilistic distributions of magnitude and source-to-site distance are available. Consequently the prediction of the peak ground motion at the site (or spectral ordinates), conditional on the seismic network measures, may be performed in analogy with the well known probabilistic seismic hazard analysis (PSHA); e.g., Iervolino et al. (2006) and Convertito et al. (2008). This results in time-dependent hazard curves which may be used as a support tool for automated decision making in order to reduce the expected loss of specific structures/infrastructures in the framework of performance-based earthquake engineering (PBEE), even in those cases where limited lead-time renders evacuation unfeasible. However, real-time peak ground motion predictions are performed in very uncertain conditions which both refer to the real-time estimation of source parameters and traditional uncertainties involved in PSHA.

2.1 RTPSHA

Seismologists have recently developed several methods to estimate the magnitude (M) of an event given limited information of the P-waves for real-time applications. Similarly, the source-to-site distance (R) may be rapidly determined by analyzing the time and order of the seismic stations detecting the developing earthquake. Therefore, it is possible to assume that, while the event is still propagating, estimates of M and R are available, and the peak ground motion at the site can be predicted via the probabilistic seismic hazard analysis conditional to the real-time information given by the seismic sensors network. In fact, assuming that at a given time t from the earthquake's origin, the seismic network can provide a vector of measures informative for the magnitude, $\underline{\tau} = \{\tau_1, \tau_2, \ldots, \tau_n\}$, the posterior probability density function (PDF) of M conditional to the measures, $f(m\,|\,\underline{\tau})$, may be obtained via the Bayes theorem, as in Eq. (1):

$$f(m\,|\,\underline{\tau}) = \frac{f(m\,|\,\underline{\tau})\,f(m)}{\int_{M_{\min}}^{M_{\max}} f(m\,|\,\underline{\tau})\,f(m)\,\mathrm{d}m} \qquad (1)$$

In the Bayesian framework $f(m)$, the *a priori* distribution, is used to incorporate the information available before the seismic network performs the measurements. Then, in this application, a natural candidate for $f(m)$ is the truncated exponential, derived by the Gutenberg-Richter relationship typically used in the classic hazard analysis. The parameters $\{\beta, M_{min}, M_{max}\}$ of Gutenberg-Richter relationship are dependent on the seismic features of the region under study and will be assumed for the Campania region equal to {1.69, 4, 7}.

The joint PDF $f(\underline{\tau} \mid m)$ is the *likelihood* function. It is used to incorporate into the analysis all information on M contained into the real-time data. Under the hypothesis that the τ-measurements are s-independent and identically distributed lognormal random variables it may be formulated as in Eq. (2).

$$f(\underline{\tau} \mid m) = \left(\frac{1}{\sqrt{2\pi}\sigma_{\ln(\tau)}} \right) \left(\prod_{i=1}^{n} \frac{1}{\tau_i} \right) e^{\left(-\frac{1}{2} \frac{\sum_{i=1}^{n} (\ln(\tau_i))^2}{\sigma^2_{\ln(\tau)}} \right)} e^{\left(\frac{2\mu_{\ln(\tau)} \sum_{i=1}^{n} \ln(\tau_i) - n\mu^2_{\ln(\tau)}}{2\sigma^2_{\ln(\tau)}} \right)} \quad (2)$$

The parameters in Eq. (2) may be, for example, the mean, $\mu_{\ln(\tau)}$, and the standard deviation, $\sigma_{\ln(\tau)}$, of the log of the predominant period of the first four seconds of the P-waves retrieved from the study of Allen and Kanamori (2003), Eq (3). Combining Eq. (2) into Eq. 1, the posterior PDF of the magnitude results that of Eq. 4, which depends on the measures only via the summation of the logs, $\hat{\tau} = \sum_{i=1}^{n} \ln(\tau_i)$ and n.

$$\begin{cases} \mu_{\ln(\tau)} = \dfrac{M - 5.9}{7 \log(e)} \\ \sigma_{\ln(\tau)} = \dfrac{0.16}{\log(e)} \end{cases} \quad (3)$$

$$f(m \mid \underline{\tau}) = \frac{e^{\left(2\mu_{\ln(\tau)} \left(\sum_{i=1}^{n} \ln(\tau_i) \right) - n\mu^2_{\ln(\tau)} \right) / 2\sigma^2_{\ln(\tau)}} e^{-\beta m}}{\int_{M_{min}}^{M_{max}} e^{\left(2\mu_{\ln(\tau)} \left(\sum_{i=1}^{n} \ln(\tau_i) \right) - n\mu^2_{\ln(\tau)} \right) / 2\sigma^2_{\ln(\tau)}} e^{-\beta m} \, dm} \quad (4)$$

Regarding the source-to-site distance, because of rapid earthquake localization procedures, a probabilistic estimate of the epicenter may also be available. For example, during an earthquake, the algorithm developed by Satriano et al. (2008) allows to assign to each point of a grid, defined in the region where the network operates, the probability that the hypocenter is coincident with that point based on the sequence according to which the stations trigger, $\underline{s} = \{s_1, s_2, \ldots, s_n\}$. Consequently, also the PDF of R, $f(r \mid \underline{s})$, may be retrieved in real-time. Thus, it is possible to compute the probabilistic distribution (or hazard curve) of a ground motion intensity measure at a site of interest as in Eq. (5), which also requires an attenuation relationship, $f(im \mid m, r)$, available for the chosen IM. This procedure will be referred to as RTPSHA and may be used to predict, for example, of peak ground acceleration (PGA), Eq. (5), or spectral ordinates. The subscript (n) in the left-hand side of Eq. (5) means that the computed hazard curve refers to a particular set of triggered stations and, therefore, evolves with time.

$$f_n(pga \mid \underline{\tau}, \underline{s}) = \int_M \int_R f(pga \mid m, r) \, f(m \mid \underline{\tau}) \, f(r \mid \underline{s}) \, dm \, dr \quad (5)$$

When the hazard integral of Eq. (5) is computed (i.e., the prediction of the IM at the target site is obtained) the decision whether to issue an alarm or not is taken. The alarm issuance implies a decisional rule. For example, assuming that the predicted IM is the PGA, a simple one consists of issuing the alarm if the risk that the critical peak ground motion value (PGA_c) will be exceeded in the strike, is larger than a probability threshold (P_c), Eq. (6).

Allarm if

$$1 - \int_0^{PGA_c} f_n(pga) \, dpga = P[PGA > PGA_c] > P_c \quad (6)$$

For structural application of EEWS, the prediction of structural response in terms of an Engineering Demand Parameter (EDP), rather than in terms of a ground motion IM, may be of larger concern. This requires a further integration to get the PDF of EDP:

$$f_n(edp \mid \underline{\tau}, \underline{s}) = \int_{IM} f(edp \mid im) \, f_n(im \mid \underline{\tau}, \underline{s}) \, dim \quad (7)$$

where the PDF, $f(edp \mid im)$, is the probabilistic relationship between IM and EDP, and may be obtained, for example, via non-linear incremental dynamic analysis which was also developed for controlled structures (Barroso and Wintersein, 2002). Obviously, this approach can be extended further to predict the expected loss in a structure conditional on the measures of the seismic instruments, and this contains the highest level of information for alarm issuance decision (Iervolino et al., 2007).

2.2 ERGO: a prototypal EEW terminal.
RTPSHA above was implemented, in a simplified form, in ERGO (EaRly warninG demO) which is a visual terminal developed to test the potential of hybrid EEWS (Festa et al., 2009). The system was developed by staff of the RISSC lab (www.rissclab.unina.it) and of the Department of Structural Engineering of the University of Naples Federico II (www.dist.unina.it) under the umbrella of AMRA scarl (www.amracenter.com). It was installed in the school of engineering of the University of Naples Federico II on July 25 2008 and continuously operates since then.

ERGO processes in real-time the accelerometric data provided by a part of the sensors of ISNet and it is able to perform the RTPSHA and eventually to issue an alarm in the case of events occurring with magnitude larger than 3 in the southern Appennines region. ERGO is composed of four panels (Figure 2):

1. *Real-time monitoring and event detection.*
   In this panel two kind of data are given: (a) the real-time accelerometric signals of the stations associated to the EEW terminal, shown on a two minutes time window; and (b) the portion of signal that, based on a signal-to-noise ratio determined the last trigger (i.e., event detection) for a specific station (on the left). Because it may be the case that local noise (e.g., traffic or wind) determines a station to trigger, the system declares an event (M larger than 3) only if at least three station trigger within the same two seconds time interval;

2. *Estimation of earthquake parameters.*
   This panel activates when the first panel declares an event. If this condition occurs the magnitude and location are estimated in real-time as a function of evolving information from the first panel. Here the expected value of the magnitude as a function of time from the origin of the detected event and the associated standard error are given. Moreover, on a map where also the stations are located, it shows the estimated epicenter, its geographical coordinates and the origin time;

3. *Lead-time and peak-shaking map.*
   This panel shows the lead-time associated to S-waves for the propagating event in the whole region. As a further information, on this panel the expected PGA on rock soil is given on the same map. As per the second panel, this one activates only if an event is declared from panel 1 and its input information come from panel 2.

4. *RTPSHA and alarm issuance decision.*
   This panel performs RTPSHA for the site where the system is installed based on information on magnitude and distance from panel 2. In particular, it computes and shows real-time evolving PDFs of PGA at the site. Because a critical PGA value has been established for the site (arbitrarily set equal to 0.01 g) the system is able to compute the risk this PGA is exceeded conditional to the estimates for the ongoing event as a function of time. If such a risk exceeds 20% (i.e., the decisional rule of Eq. (6)) the alarm is issued and a otherwise green light turns into red. This panel also gives, as summary information, the actual risk that the critical PGA value is exceeded along with the lead-time available from the site and the false alarm probability.

Figure 2 refers to a real event detected and processed in real-time by ERGO on November

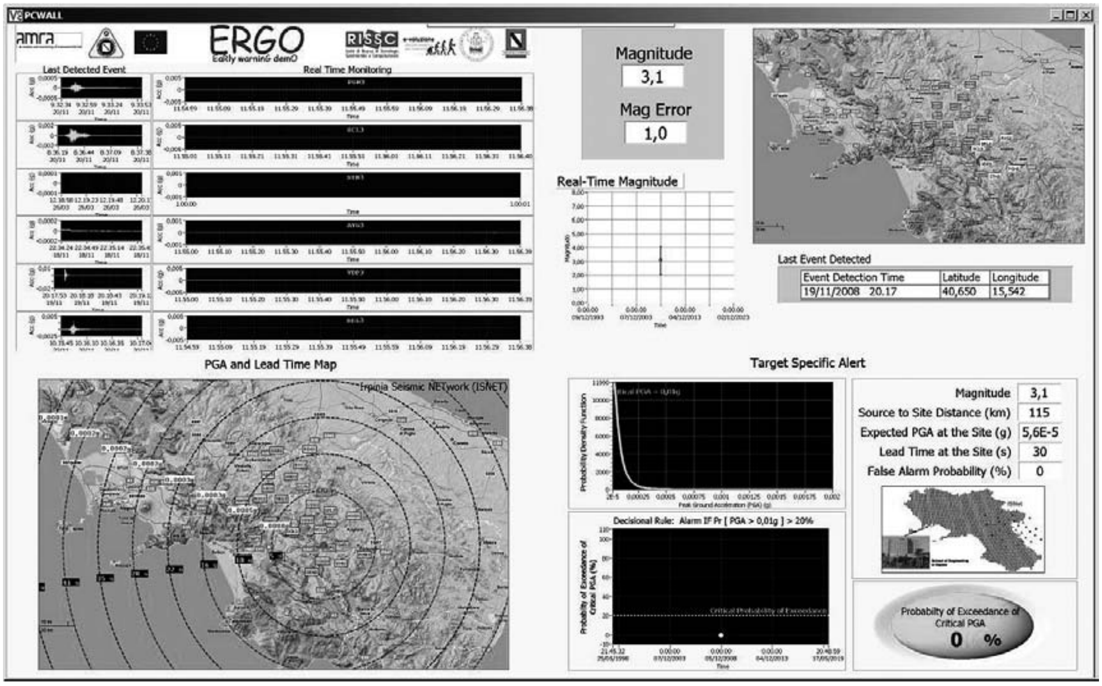

Figure 2: The ERGO EEW terminal

19 2008. The system estimated the event as a M 3.1 earthquake located close to Potenza (a town capital of the Basilicata region), with an epicenter 115 km far from the site. Because the event was a low-magnitude large-distance one, the risk the PGA_C could be exceeded was negligible and the alarm was, correctly, not issued. Finally, note that ERGO is a visual panel only for demonstration and testing purposes, but it may be virtually ready be connected to devices for real-time automated risk reduction actions.

3. EEWS and control systems for seismic protection of structures

The three major classes of control systems for protecting structures subjected to ground motion are: (1) *passive*, (2) *active*, and (3) *semi-active* (e.g., Symas and Constantinou, 1999; Soong and Spencer, 2002).

1. A passive control system is based on the motion of the structure (e.g., the relative motion within the passive device) to develop the control force, and does not require an external power source to operate. Such systems basically reduce the seismic demand on the structure either increasing the energy dissipation potential and/or changing its fundamental oscillation period moving it away from the most energetic frequency content of ground motion (i.e., seismic base isolation). Note that when dealing with passive control, design usually means fixing a set of boundary conditions and choosing a device optimized for that set of conditions (in other words passive systems need to be designed according to an expected scenario of the seismic action). Then, it is hard to integrate EEWS with passive control systems.

2. An active control system supplies control forces based on feedback from sensors (located on the structure) that measure the excitation and/or the actual response. The recorded measurements from the response and/or excitation are monitored by a controller (a computer) which, based on an algorithm, operates the actuators producing the forces. The generation of control forces by electro-hydraulic actuators requires power sources on the order of tens ok kilowatts for small structures and may

reach several megawatts for large structures. Active control strategies are based on information about the full waveform or structural response which can't be predicted by an EEWS, although *site-specific* EEWS (see Kanamori, 2005) may be potentially used to prepare the system when the earthquake is about to strike at the site of the structure.

3. A semi-active (SA) system develops control forces based on the feedback from sensors that measure the excitation and/or the response of the structure (Figure 3). However, the control forces are not realized, as in the active case, by actuators, but rather by modifying, in real-time and according to a preselected decisional rule, the mechanical characteristics of special devices (SA links). The energy required for the modification of the basic parameters of the devices is minimal, generally on the order of tens of watts, and may be furnished even by a simple battery (e.g., to open/close of a valve). Control strategies based on SA control combine the best features of both passive and active control systems offering the adaptability of active systems (without requiring the associated large power sources) and the reliability of passive systems. For these reasons, SA control strategies, seem to have a potential in seismic protection of structures and infrastructure in combination with an EEWS. In fact, as shown in the following, for ON-OFF SA systems (i.e. SA system which can assume only two states of operation) the decisional rule (i.e. the decision of activating the control system) may be formulated on the basis of a single parameter representative of earthquake potential rather than the full waveform.

3.1 Fluid viscous dampers for EEW-based semi-active structural control

One means of achieving a semi-active damping device is to use a controllable valve to alter the resistance to flow of a conventional hydraulic fluid damper. Semi-active fluid viscous dampers typically consist of a hydraulic cylinder containing a piston head which separates the two sides of the cylinder. As the piston is cycled, the fluid within the damper (usually oil) is forced to pass through small orifices at high speeds. The pressure differential across the piston head, and thus the output force, is modulated by an external control valve which connects the two sides of the cylinder.

If the device is characterized by only two states (e.g., the valve can only be open or closed) the system is referred to as an ON-OFF SA system, otherwise if the mechanical parameter of the device can assume any value in a certain range (e.g. the valve opens and closes gradually) the system is referred to as a continuous SA system.

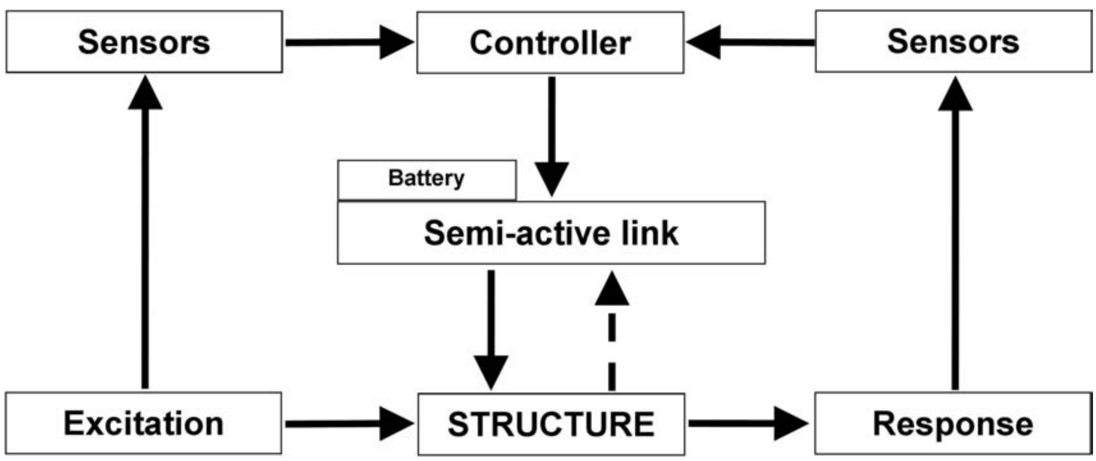

Figure 3: Block diagram of semi-active control systems (adapted from Soong and Spencer, 2002)

Although more complex models are available, the dynamic behavior of the fluid dampers over the frequency range of interest for structural control applications, may be described based on a simple phenomenological model consisting of a linear viscous dashpot with a voltage-dependent damping coefficient, $C_{SA}(u)$. The force output, F, is thus described by:

$$F = C_{SA}(u) \cdot \hat{x} \tag{8}$$

where $\hat{x}$ is the relative velocity of the piston head with respect to the damper housing and u is the command voltage. The damping coefficient of Eq. (8) increases if the command voltage decreases and it is bounded by minimum and maximum values corresponding to the open and closed valve positions respectively, Eq. (9). The response time for modifying the variable damper from higher-to-low or low-to-high damping is generally less than 30 ms.

$$\begin{aligned} &\text{valve closed} \Leftrightarrow C_{SA}(u) = c_{\max} \\ &\text{valve open} \Leftrightarrow C_{SA}(u) = c_{\min} \end{aligned} \tag{9}$$

In the EEW prospective, once a prediction of a seismic demand parameter for a structure of interest is available, a decisional condition has to occur to issue the alarm (i.e. to activate the device). For example, the device may be activated if the expected value, $E[EDP_{uncontrolled} \mid \underline{\tau}, \underline{s}]$, of the structural response variable exceeds a critical threshold EDPc, Eq. 10. The expected value of the chosen EDP may be computed as in Eq. (11) extending the RTPSHA concept.

$$\begin{aligned} C_{SA}(u) &= c_{\max} \text{ (i.e. Device ON)} \\ &\quad \text{if} \quad E[EDP_{uncontrolled} \mid \underline{\tau}, \underline{s}] \geq EDP_c \\ C_{SA}(u) &= c_{\min} \text{ (i.e. Device OFF)} \\ &\quad \text{if} \quad E[EDP_{uncontrolled} \mid \underline{\tau}, \underline{s}] < EDP_c \end{aligned} \tag{10}$$

$$E_n[EDP_{uncontrolled} \mid \underline{\tau}, \underline{s}] = \int_{EDP}\int_{IM} edp_{uncontrolled}\, f(edp_{uncontrolled} \mid im)\, f_n(im \mid \underline{\tau}, \underline{s})\, dEDP\, dIM \tag{11}$$

4. Example of basic interaction of EEWS and SA structural control

Let's consider a reference structure modeled as a $T = 0.6$ s single degree of freedom (SDOF) system with an elastic-perfectly-plastic behavior and a yielding moment of 200 kNm. The structure may be representative of the simple one storey/bay frame in Figure 4a equipped with a bracing system including variable viscous dampers operating in ON-OFF SA mode. Similarly, the SDOF can describe a simple bridge with a deck free to move via rolling bearings at one side and constrained to the pier by additional devices in the other one (Figure 4b). In the uncontrolled configuration, the semi-active damper has the control valve fully open, and thus the damper produces no control force. In the controlled configuration, the control valve is held fixed in the closed position (i.e., in a high damping configuration).

The considered EDP related to structural damage is the interstorey drift ratio (IDR) as a function of the PGA. To get a relationship between IDR and PGA for the case-study structure incremental dynamic analysis (IDA) was carried

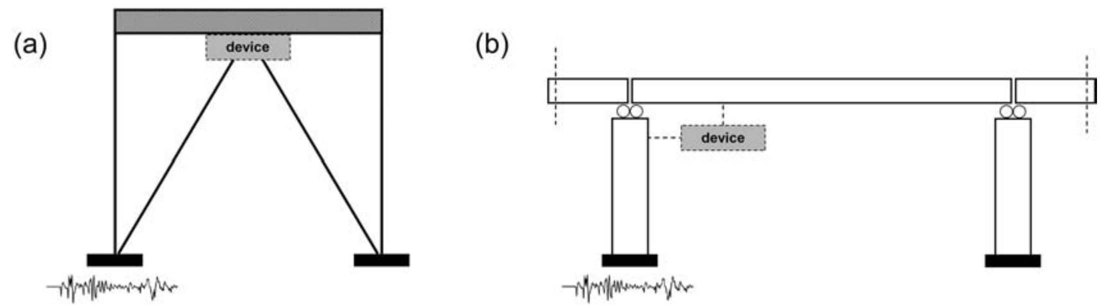

Figure 4: Examples of controlled structures which may be modeled as controlled SDOF systems

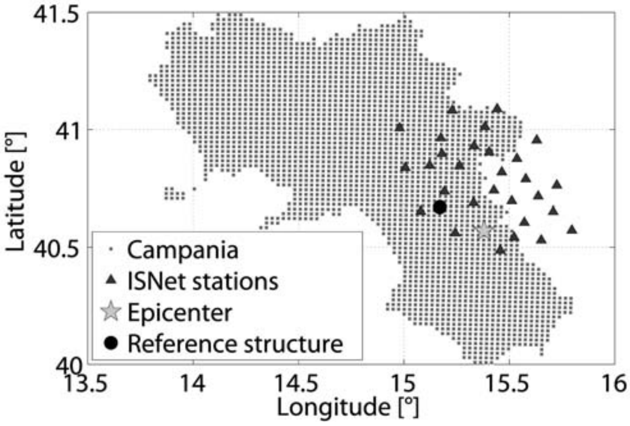

Figure 5: Scheme of the ISNet network and possible location of the reference structure

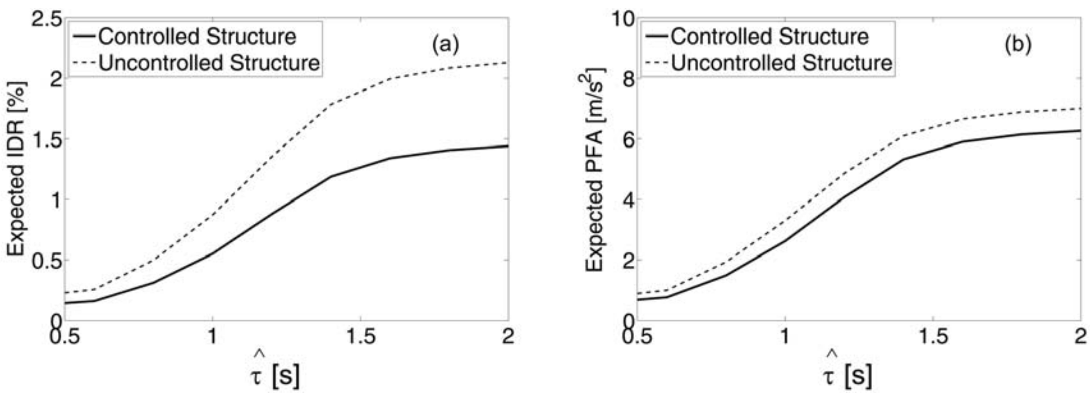

Figure 6: Comparison between the expected (a) IDR and the expected (b) PFA of controlled and uncontrolled structure as a function of the statistics of the network measurements

out (Vamvatsikos and Cornell, 2002). As an additional EDP, which may be of concern in the case one is interested in the response of non-structural elements, the peak floor acceleration (PFA) was also considered. Then, the (IDA) was also retrieved for the PFA as a function of the PGA[1]. Results in terms of IDR and PFA obtained by these simulations have been used to get a probabilistic representation of the seismic demand conditioned to the PGA, i.e. the PDF of Eq. (7) and Eq. (11).

The expected values of the chosen EDPs were computed via Eq. (11), as a function of the information provided in real-time by the EEWS ($f_n(im \mid \underline{\tau}, \underline{s})$ was obtained by applying the methodology described in section 2.1). To this aim it was supposed that the structure is in the Irpinia region at 10 km (in terms of epicentral distance) with respect to the location of an hypothetical earthquake occurring within the ISNet (Figure 5).

Note that Eq. (5) and consequently Eq. (11) depend on n (i.e., number of instruments of the seismic network have triggered and collected data). All the analyses are conditional to the fact that the level of information provided by the EEWS corresponds to 18 triggered stations out of 29 (i.e., n = 18); e.g., 18 measures of τ are available. This is because, as shown in Iervolino et al. (2009), the information on the impending ground motion stabilizes when about 18 stations have provided τ (i.e., the

1 In order to obtain the relationship between the predicted PGA and the chosen EDPs in both controlled (damping ratio ξ = 15%) and uncontrolled case (damping ratio ξ = 5%), the non-linear structural model has been subjected to a set of 21 European ground motion records, each of those scaled to multiple levels of intensity between 0.1 g and 1 g.

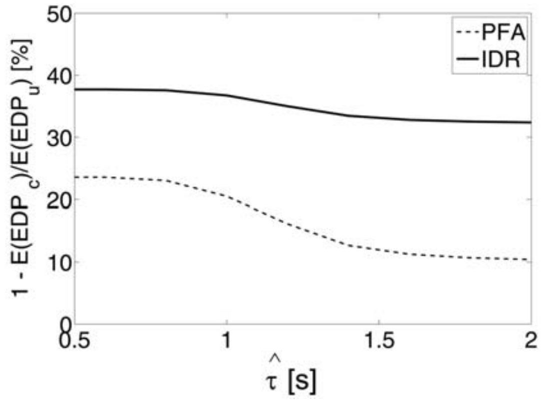

Figure 7: Response comparisons between the uncontrolled and controlled structure in terms of EDPs reduction as a function of the statistics of the network measurements

estimation of the PGA, and then of the EDP, does not benefit much from further information provided by additional ISNet stations). Moreover, since the localization method gives an about deterministic value of distance after 4 s for an event within the network, which is shorter than the time to trigger 18 stations, then the R value has been deterministically fixed to 10 km and, therefore, the relationship of the structural response with the information of the EEWS depends on $\hat{\tau}$ only and does not depend on $\underline{s}$.

The expected values of both IDR and PFA were computed for 11 equally spaced values in the range between 0.5 s and 2 s as suggested by the relation between and the magnitude of an even in Allen and Kanamori, 2003. Results of the analyses are presented in Figure 6a and Figure 6b. The curves represent the trends of the EDPs for the specific structure at the given location. They provide the mitigation of structural response eventually given by the structural control (solid curves), with respect to the *as is* structure (dashed curves), in the case of different earthquakes represented by specific $\hat{\tau}$ values and may be used for design of integrated EEW and structural-control systems.

For the specific case-study, response comparisons between the uncontrolled and controlled structure shows that the peak acceleration and drift at the top floor may be reduced, on average, by about 15% and 35% respectively, if the EEWS triggers structural control[2] (Figure 7).

5. Conclusions

This paper presented a preliminary discussion about possible integration of state-of-the-art early warning systems (hybrid EEWS) and structural control. The issues associated to the real-time adaption of PSHA and PBEE for earthquake early warning purposes were given first. It was shown how the hazard integral can incorporate the information provided by a seismic network about a developing earthquake, and how it results in time-dependent hazard curves which may be used for automated decision making. A prototypal EEW terminal based on the seismic network (ISNet) installed in the Irpinia region in southern Italy was also presented.

Secondly, a procedure to compute the expected structural response in a EEW framework was discussed. The key element of the proposed procedure is the development, in real-time on the basis of the information provided by the EEWS, of probabilistic seismic demand curves for a structure equipped with semi-active control devices. These curve are a first attempt of tools aimed at the design of integration of structural control and earthquake early warning. Nevertheless, cost/benefit and loss analyses are still required to show the efficiency of such systems with respect to traditional control and seismic risk mitigation strategies for structures.

References

Allen R. M., Kanamori H. (2003) The potential for earthquake early warning in southern California. Science, 300: 786–789.

[2] Results may change with location of the specific structure with respect to the earthquake.

Barroso L. R., Winterstein S. (2002), Probabilistic seismic demand analysis of controlled steel moment-resisting frame structures, Earthquake Engineering and Structural Dynamics 31: 2049–2066.

Convertito V., Iervolino I., Giorgio M., Manfredi G., Zollo A. (2008) Prediction of response spectra via real-time earthquake measurements. Soil Dyn Earthquake Eng, 28: 492–505.

Festa G., Martino C., Lancieri M., Zollo A., Iervolino I., Elia L., Iannaccone G., Galasso C. (2009) ERGO: a visual tool for testing earthquake early warning systems. (in preparation).

Kanamori H. (2005) Real-time seismology and earthquake damage mitigation, *Annual Review of Earth and Planetary Science,* 33, 195–214.

Iervolino I., Convertito V., Giorgio M., Manfredi G., Zollo A. (2006) Real-time risk analysis for hybrid earthquake early warning systems. Journal of Earthquake Engineering, 10: 867–885.

Iervolino I., Giorgio M., Galasso G., Manfredi G. (2009) Uncertainty in early warning predictions of engineering ground motion parameters: what really matters? Geophysical research letters, 36, L00B06
doi:10.1029/2008GL0366449.

Iervolino I., Giorgio M., Manfredi G. (2007) Expected loss-based alarm threshold set for earthquake early warning systems. Earthquake Engn Struct Dyn, 36: 1151–1168.

Occhiuzzi A., Caterino N., Maddaloni G. (2008), Structural control strategies for seismic EWS, Proc. of 14th World Conference on Earthquake Engineering, Beijing, China, October 12–17 2008.

Pnevmatikos N. G., Kallivokas L. F., Gantes C. J. (2002), Feed-forward control of active variable stiffness systems for mitigatin hazard in structures, Engineering Structures 26: 471–483.

Satriano C., Lomax A., Zollo A. (2008). Real-time evolutionary earthquake location for seismic early warning, Bull Seism Soc Am, 98: 1482–1494.

Soong T. T., Spencer B. F. Jr (2002), Supplemental energy dissipation: state-of-the-art and state-of-the-practice, Engineering Structures 24: 243–259.

Symas M. D., Constantinou M. C. (1999), Semi-active control systems for seismic protection of structures: a state-of-the-art review, Engineering Structures 21: 469–487.

Vamvatsikos, D., and C.A. Cornell (2002). Incremental Dynamic Analysis, Earthquake Engineering and Structural Dynamics 31, 491–514.

Weber E., Convertito V., Iannaccone G., Zollo A., Bobbio A., Cantore L., Corciulo M., Di Crosta M., Elia, L. Martino, C. Romeo A., Satriano C. (2007) An advanced seismic network in the southern Apennines (Italy) for seismicity investigations and experimentation with earthquake early warning. Seism Res Lett, 78: 622–634.

Earthquake Early Warning Demonstrator for Transport Lines

Titzschkau T. (1), Wenzel F. (1), Buchmann A. (2), Hohnecker E. (2), Hilbring D. (3), Bonn G. (3)

(1) Geophysical Institute, University of Karlsruhe, Germany

(2) Institute for Road- and Railway Systems, Department of Railway Systems, University of Karlsruhe, Germany

(3) Fraunhofer Institute for Information and Data Processing, Karlsruhe, Germany

1. Introduction

The project EWS Transport (Early Warning System for Transportation Lines) analyses the potential of earthquake early warning for railway systems. The study focuses on rapidly producing an alert map during an ongoing earthquake as well as providing a shake map immediately after the strong-motion phase. On the basis of the alert map and pertinent risk parameters for railways (e.g. acceleration thresholds), risk reduction measures, such as the stopping or braking of affected trains, are devised. Furthermore, a vulnerability analysis for various railway infrastructure components using the shake map data is performed and a map showing potential infrastructure damage is generated. A flexible standard-based architecture is specified in EWS Transport to ensure future reusability of the design principles. Based on these characteristics, EWS Transport is exploring early warning possibilities beyond the Japanese railway earthquake early warning system (UrEDAS), so far the only existing system with a focus on the special requirements of transport lines. In this paper, the functional principles of EWS Transport – from extracting earthquake parameters to visualizing estimated infrastructure damage – as well as their realization in an online demonstrator are described. The demonstrator is an end-user oriented prototypical information system which is used to test, visualize, and optimize the various EWS Transport components and the interaction between them.

2. Realtime Seismology for EWS Transport

2.1 Synthetic Database

The federal state of Baden-Württemberg (BW), located in the south-west of Germany, was chosen as test area for EWS Transport because of e.g. the availability of GIS railway data, knowledge of the railway operational system and information on the local geology. BW is the state in Germany with the highest seismic activity which, however, from a global viewpoint is low but not negligible. The maximum magnitudes range between 6.0 and 6.5 and in terms of European Macroseismic Scale intensities, the non-exceedence probability of 90% in 50 years ranges between V and VIII (Grünthal and Bosse, 1996; Grünthal et al. 1998). Due to the rare occurrence of earthquakes and the lack of large magnitude events, there is a shortage of observed data that are suitable for this study. Synthetic seismograms of earthquakes in and around BW thus have been generated and provide the basis for the analysis of EWS Transport options.

Within the scope of this study, Sokolov and Wenzel (2008) developed the first stochastic ground motion model customized to BW. It is based on regional earthquake ground motion data and site amplification parameters. With this model, ground motion records can be created at any point in the test area and for any given hypocenter and magnitude. In order to generate scenarios that are as realistic as possible and as hazardous as necessary for EWS

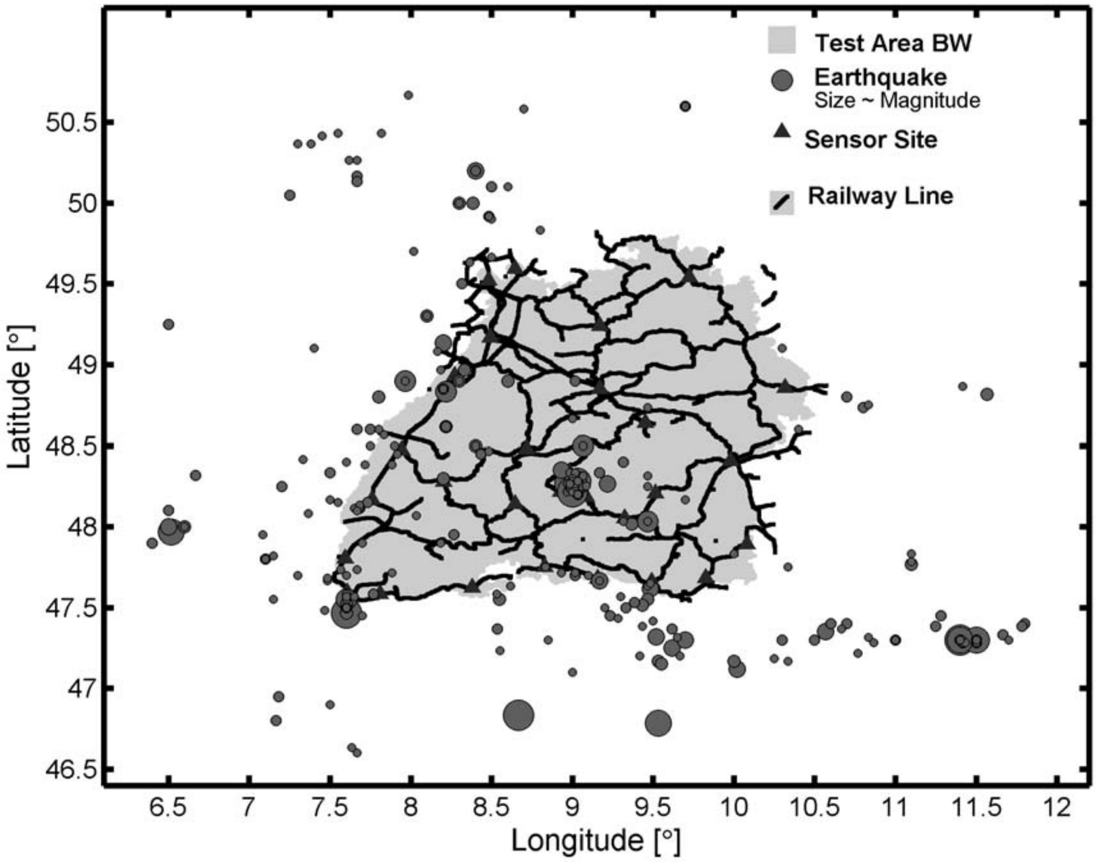

Figure 1: Earthquake Magnitude and Hypocenter Distribution

Transport testing purposes, the historic earthquake catalog of Germany was consulted (Leydecker, 2008). The distribution of earthquakes was obtained from hypocenter coordinates of historic events with an intensity ≥5 in a radius of 250 km around the center of BW. A Gutenberg-Richter relationship of $\log_{10} N = 4.9 - 0.72M_L$, where N is the number of earthquakes with a local magnitude M_L or greater, was determined from all earthquakes in the catalog with $M_L \geq 2.5$. As input for the generation of synthetic ground motion, 290 earthquakes with a magnitude distribution between 4.5 and 6.5 following the Gutenberg-Richter relationship were randomly distributed over the hypocenters. For the sake of testing the system, 11 additional earthquakes with magnitudes between 6.6 and 8.0, which are considered as impossible in this area, were added at the locations of historically greatest earthquake intensity. The distribution of all 301 earthquakes is shown in Figure 1.

The use of synthetically generated ground motion makes it possible to test different earthquake and sensor network scenarios. EWS Transport's innovative idea of implementing a large number of low cost sensors in or near railway tracks can thus be simulated. Such a network could make use of the given infrastructure, power lines and communication options and would provide comprehensive information directly for and directly at the object of interest.

For the first version of the online demonstrator, synthetic ground motion was generated at 30 virtual stations that are randomly distributed along railway lines in the test area (Figure 1, blue triangles). P and S waves were simulated separately with different input parameters for the average radiation pattern, the wave velocity and the attenuation model. The waveforms were then combined to obtain a complete seismogram, using travel times

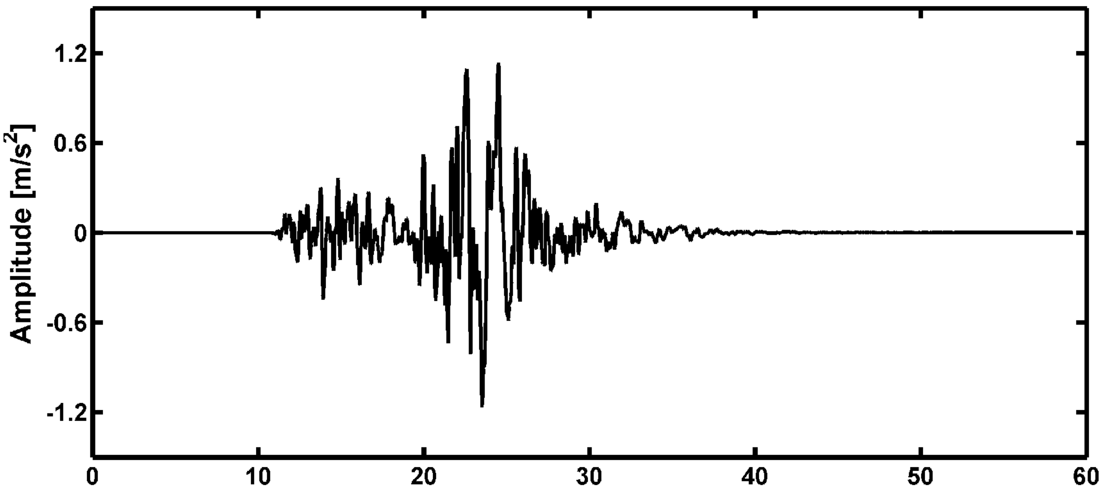

Figure 2: Synthetic Waveform Example of a magnitude 6.5 earthquake in a hypocenter to station distance of 63.3 km

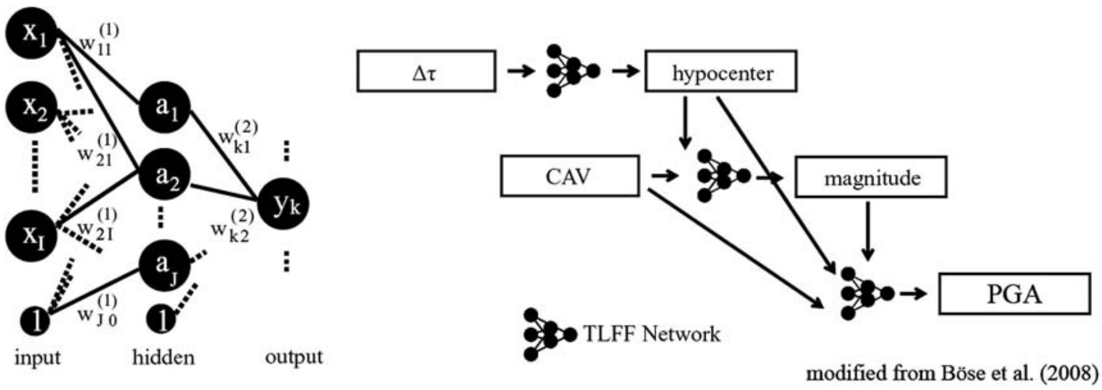

Figure 3: Parameter Estimation in PreSEIS

respective to an average P wave velocity $v_P = 6$ km/s (Stange and Brüstle, 2005) and an S wave velocity $v_S = 3{,}5$ km/s ($v_S = \frac{1}{\sqrt{3}} v_P$; Lay and Wallace, 1995). A waveform example is given in Figure 2.

2.2 Earthquake Early Warning with PreSEIS

EWS Transport implements a modified version of the earthquake early warning method PreSEIS (Böse et al., 2008) for earthquake detection and analysis. In PreSEIS, earthquake parameters are extracted from the sensor network via artificial neural net technology. Two layer feed forward (TLFF) neural networks are trained with a subset of the synthetic dataset to recognize P waves and issue parameter estimations. Our networks are trained to estimate hypocenter coordinates magnitude and horizontal peak ground acceleration (PGA) at each of the 30 sites from the onset time differences between the stations, from the cumulative absolute velocity (CAV) of each waveform and from previous parameter estimates, see Figure 3.

The performance of the trained neural network is tested with the remainder of the dataset. This early warning method combines the advantages of regional and on-site early warning approaches (Böse et al., 2008; Köhler et al., 2009): PreSEIS is quick and reliable because it is not required that seismic waves have arrived at all stations before parameter estimations can be issued and the parameters are continuously updated using the incoming information from all triggered and not yet triggered stations.

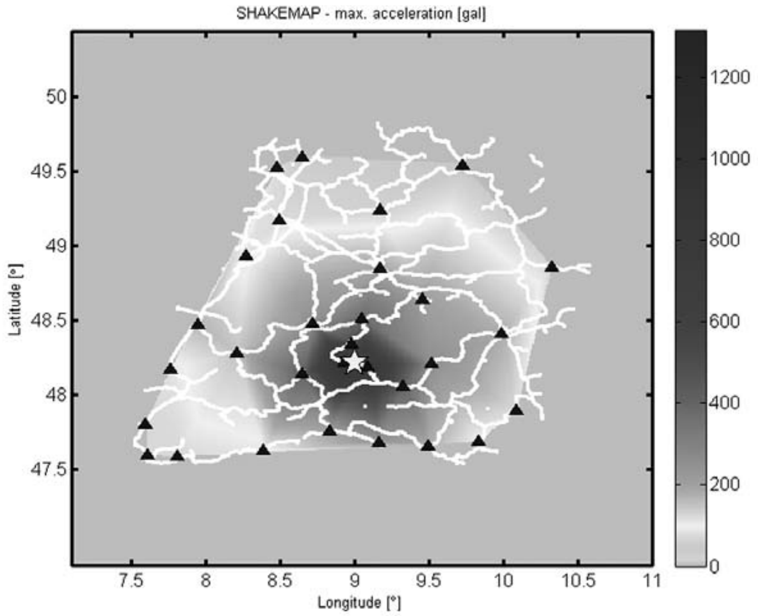

Figure 4: Shakemap of a Magnitude 7.4 Earthquake near Albstadt (yellow star)

In the demonstrator, any one of the 301 earthquakes can be selected to begin a simulation of real-time processing of the respective sensor data. Once the earthquake has been detected by PreSEIS, alert maps for BW with a resolution of 1 km^2 are rapidly calculated by interpolating the estimated PGA values at the 30 stations and can be updated in regular time intervals. Alert maps are a crucial component of EWS Transport as they provide the basis for hazard assessment along the railway lines in the test area.

Immediately after an event, a shake map is calculated using the true PGA values obtained from the seismograms of each station (Figure 4). Shake maps allow the identification of areas with very high ground shaking and the assessment of potential damage to the railway infrastructure.

3. Risk reduction for transport lines

Commonly, risk is defined as the product of three factors, hazard, vulnerability, and value (Meskouris et al., 2007). Here, »hazard« refers to the probability of occurrence (frequency) of a seismic event of given ground acceleration within a fixed period of time. The factor »vulnerability« describes the degree of expected infrastructure damage for a given seismic hazard. Finally, the factor »value« indicates the severity of the consequences, e.g. number of casualties, in case of system failure.

In order to reduce the risk for railbound transportation systems during and after an earthquake, it is necessary to identify the relevant hazard and damage parameters and to make reliable predictions for the expected damage on various infrastructure elements for given earthquake parameters. As discussed in the following, we distinguish two main applications of EWS Transport: (i) early warning phase right before and during strong motion and (ii) the subsequent damage analysis.

3.1 Hazard parameters, thresholds, and emergency measures

The horizontal peak ground acceleration a_{PGA} at the site of the track has been identified as the crucial parameter that characterizes the hazard in train operation. In particular, the acceleration threshold above which train derailment may occur has been defined.

Current practice for high speed trains (Shinkansen) identifies the local acceleration threshold $a_{PGA} = 0.4$ m/s^2 above which the local power supply at the train position is switched off and an emergency braking of the train is initiated (Nakamura, 1996). These measures are applied directly without the intermediary of a train control center. As a first step, EWS Transport adopts the local horizontal peak ground acceleration a_{PGA} at the track site as the relevant hazard parameter, and $a_{PGA} = 0.4$ m/s^2 as the critical threshold above which train operation must be considered unsafe and emergency train control measures are initiated.

Concrete measures depend on the actual ground acceleration along the track and the type of railway system, e.g. high speed or low speed lines. For the early warning phase we currently employ two measures in the EWS Transport demonstrator:

(a) for high speed lines with v > 80 km/h trains are stopped and the corresponding lines are blocked if the horizontal ground acceleration is above 0.4 m/s^2

(b) for low speed lines with v < 80 km/h train speed is reduced to v < 20 km/h if the horizontal ground acceleration exceeds 0.4 m/s^2 but is below a second threshold usually taken as 1 m/s^2 (Nakamura, 2008). For $a_{PGA} > 1$ m/s^2 trains are stopped and the track infrastructure is inspected on foot, before it is decided where and in which form train operation is resumed.

This classification is based on the fact that high speed trains are more vulnerable to derailment than low speed trains. Derailment takes place when horizontal track forces Y, which increase quadratically with train speed, become larger than the vertical axle load Q. Track stability and safety against derailment requires that the ratio of horizontal to vertical track forces Y/Q be below the critical value $Y/Q < 0.8$ (Prud'homme, 1978, Lichtberger 2004). Ground shaking and seismically induced track irregularities cause additional train velocity dependent horizontal forces so that fast trains reach the critical value $Y/Q = 0.8$ earlier than slow trains.

3.2 Development of infrastructure damage catalogues and damage maps

For fast damage map generation immediately after the earthquake, the expected damage to the railway infrastructure for a given set of earthquake parameters is calculated in advance and the results are stored in a data base (damage catalogues).

The development of damage catalogues will first be carried out for a specific railway network and geographical region. The »Deutsche Bahn AG« has supplied the EWS Transport research partners with data of its infrastructure in BW. These data (GIS ArcView shape files) contain the entire railway network including information on the geographic location of stations, bridges, tunnels, as well as route number, electrification, etc. In the case of railway bridges there is a coarse distinction of (i) bridges with a length of up to 150 m and (ii) bridges with a length >150 m. The data base does not yet contain information on the construction type, material properties, etc.

The GIS infrastructure data of the Deutsche Bahn AG for BW and the shake map (sect. 2.2) form the basis for the construction of a prototypical damage map (see Figure 8). The damage map will be generated with the help of a damage catalogue, which contains information on the expected infrastructure damage for a given seismic event. The damage catalogue is organized in the form of a matrix where the rows contain the various infrastructure elements (e.g. free track, bridges, tunnels, buildings) and their main attributes, and the columns describe various damage classes (e.g., none, minor, moderate, major, and complete) together with the ground acceleration thresholds underlying the definition of these damage classes. In the first version of the demonstrator, we concentrate on assessing the seismic vulnerability of railway bridges, for which the following structure attributes are relevant: construction type, construction year, length, number of spans, width, abutment technique, foundation, eigenfrequencies, etc.

A reliable damage classification for a given structure and seismic loading will be possible if the design loads for this structure and the local soil classes are known. For buildings in

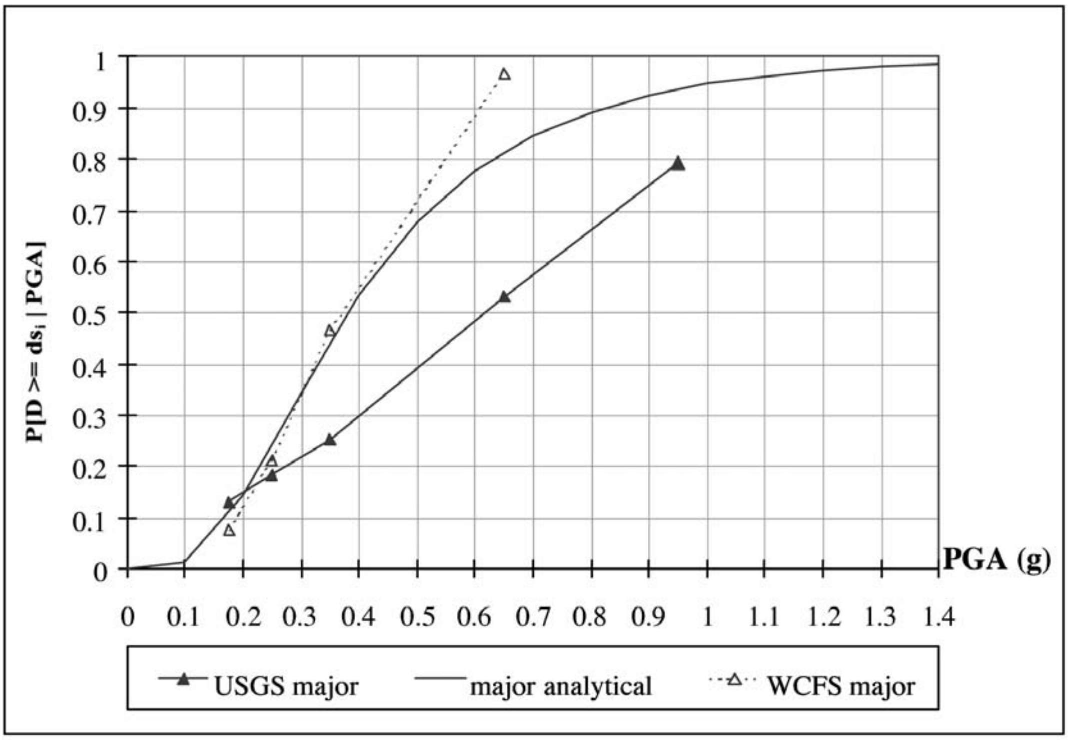

Figure 5: Analytical and Empirical (USGS and WCFS) Fragility Curves (Basöz and Mander, 1999)

Germany design loads and soil classes are defined by DIN standards (DIN 4149, 2005). For highway bridges a seismic damage analysis is available (Meskouris, 2007; Basöz and Mander, 1999), where five bridge damage states (none, minor, moderate, major, complete) and the corresponding peak ground acceleration thresholds are defined for various generic bridge construction types. For assessing the seismic vulnerability of a bridge so called fragility curves (see Figure 5) are used. The latter describe the probability P as a function of PGA that the actual bridge damage D exceeds a certain damage state ds_i, where the subscript i indicates one of the five damage states. These classifications and the corresponding fragility curves may after some adjustments also be used for estimating railway bridge damage in EWS Transport.

A comparison of analytical and empirical (USGS and WCFS) fragility curves for discontinuous multiple span bridges with single column bents and non-monolithic abutments for the damage class »major damage« is shown in Fig. 5.

Presently, the EWS Transport demonstrator includes only two bridge classes, short bridges with a length $l < 150$ m and long bridges with $l > 150$ m, and employs step functions at the corresponding median accelerations of the fragility curves.

Although railway bridges are generally recognized as the most vulnerable infrastructure elements of a railway system, there are various other and more frequently occurring causes for system failure. Examples are seismically induced liquefaction and landslides, which render a railway line unserviceable. The seismic vulnerability of a free straight track segment has recently been discussed (Pitilakis, 2009). It appears to be closely linked to the lateral track resistance w [N/m] and will be the subject of a forthcoming publication.

3.3 Track network as an earthquake detector and infrastructure monitor

An interesting aspect of railbound systems is the principal possibility to employ the existing rail network for early detection and for information transmission. The earthquake early warning system would then become part of the standard train control and protection system. The train control and protection infrastructure is currently redesigned with the aim of achieving technical interoperability between different EU member states (Berger, 2004). Therefore, we also investigate how the existing train control track infrastructure must be modified so that it can be used for early detection purposes, fast damage map generation, as well as for continuous track state monitoring.

4. Information System for EWS Transport

Early detection of an earthquake in combination with alert creation and finally the manipulation of rail traffic is a complex task. Therefore, EWS Transport requires an information system that addresses aspects like the visualization of spatial data and the decision creation of appropriate actions. Such an information system should be based on a well specified system architecture, which has been developed by EWS Transport. The architecture is tested in an end-user oriented prototypical information system (demonstrator). The latter is used to test, visualize, and optimize the various EWS Transport components and the interaction between them.

4.1 Design of the System Architecture

The Information System of EWS Transport is designed according to the principles of an open architecture with standard-based interfaces of system components. These interfaces ensure the flexible and easy exchange of components and are especially advantageous for the joint use of system components between cooperating institutions. The architecture document is set-up according to the ISO »Reference Model for Open Distributed Processing« (RM-ODP), which uses several architectural views to characterize the system. The first views defining user requirements, the information model and the service components are described on an abstract basis before the decision for specific implementation architecture is taken. The abstract parts of the architecture can be reused if new information technologies are developed or the implementation needs to be changed. Furthermore the Sensor Service Architecture of the SANY Project based on RM-ODP is taken into account. Inside the service view the standards of the Open Geospatial Consortium (OGC), especially those of the Sensor Web Enablement Group (e.g. Sensor Observation Service (Nah, Priest 2007)) are considered.

The Information System of EWS Transport is designed according to several functional blocks (see Figure 6) concentrating semantically related parts of the system. Block A »Sensor System and Early Detection« realizes the early detection of the earthquake with PreSEIS (see section 2.2). This block encapsulates the sensor network from the information system. Block B »Assessment and Decision« combines the earthquake information delivered by Block A with the railway infrastructure to identify potential hazards and damages. Block C »Action Execution« is responsible for the execution of the actions proposed by Block B. Block D visualizes the results and provides analysis functionality. The Client realizes the user interface of the information system and manages the workflows.

The functional blocks define the main structure of the system. They have been combined

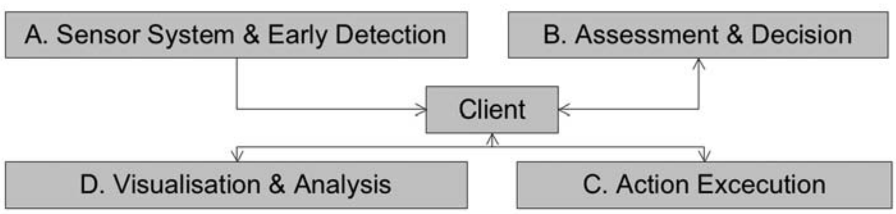

Figure 6: Functional Blocks of EWS Architecture

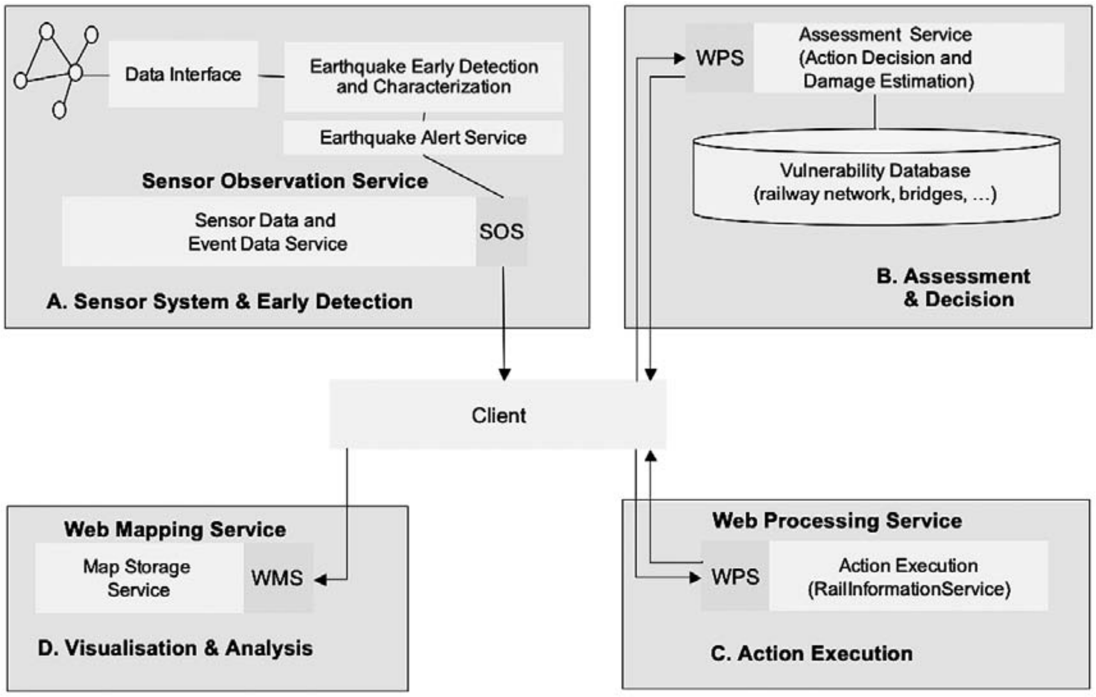

Figure 7: Service Architecture of EWS

with the use cases specified in the user requirement view. The goal was to fill each block with appropriate services, which were qualified to realize the main workflow. Wherever possible, open geospatial standards defining service interfaces were used. This ensures on the one hand that system components can be easily exchanged and on the other hand that information produced by the system can be accessed from outside the system. Figure 7 shows the filled functional blocks with the necessary services used for the realization of the main use case of the system: the workflow from the detection of an earthquake via the creation of alert and shake maps, the analysis of potential hazards and damages to the execution of proposed actions and the visualization of the results. The following OGC services could be identified for defining standard based interfaces in the Information System of EWS Transport: the Sensor Alert Service (SAS), the Sensor Observation Service (SOS), the Web Processing Service (WPS (Schut, 2007)) and the Web Map Service (WMS (Beaujardiere, 2006)).

Up to this point the architecture described in the EWS Transport project is independent of technical implementation decisions. They were made for the realization of a first demonstrator.

4.2 Realization of Demonstrator

To test the project results a first demonstrator has been implemented. One goal is the use of artificial neural networks to demonstrate rapid and robust early warning possibilities for railway lines. The demonstrator can simulate any one of 301 synthetic earthquakes for which ground motion records have been generated at 30 virtual stations along railway lines in the test area. Another important goal of the demonstrator was to test the applicability of the service architecture for an early warning system. Via realizing the system as open service architecture the interoperability between standard based components can be tested in collaboration with other projects.

Web Services were chosen for the implementation architecture. The advantages are, firstly that available open source components could be tested and used for the implementation and secondly that the demonstrator is online accessible for demos. It is possible to use Web Services for real time applications. However the performance was not in focus for the realization of the first demonstrator. Quantitative measurements will be performed in future versions.

The demonstrator simulates the important parts of the scenario: occurrence of an earthquake, triggering of the sensors, estimation of earthquake parameters, production of an alert map, estimation of hazards, train alert, production of a shake map and estimation of damages. Since the goal for the first realization of the demonstrator was to test the applicability of the architectural concepts existing OGC standards and available open source components were used to realize the workflow:

– Currently the further development of the Sensor Alert Service is unclear in the OGC. Therefore in EWS Transport the decision was taken to realize a Sensor Observation Service in the first version of the demonstrator. The SOS provides detected earthquake event data. The earthquake observation type of the SOS combines a field of peak ground acceleration values with main the parameters of an earthquake: Hypocenter and magnitude. For the realization of this SOS the SOS developed by the FP6 SANY project was reused (Kunz et al., 2009).
– The 52North Web Processing Service was used as basis for the analysis and decision algorithms (52North 2009). New algorithms were integrated into the WPS, which realize the combination of the earthquake event data with the infrastructure elements of the railway system (railway tracks and railway bridges) to identify infrastructure elements in danger of damage.
– The Web Feature Service of GeoServer was used to realize the damage catalogue (see section 3.2), which contains the vulnerability information of the infrastructure elements (GeoServer 2009).
– Two different Web Mapping Services were used for the visualization of the results. The WMS of the GeoServer visualizes the sensor stations and the railway infrastructure elements. The Map and Diagram Service visualizes the alert and shake maps, because it provides functionality for the quick visualization of online created coverage data, which is accessible via the Sensor Observation Service (QGIS Mapserver 2009).

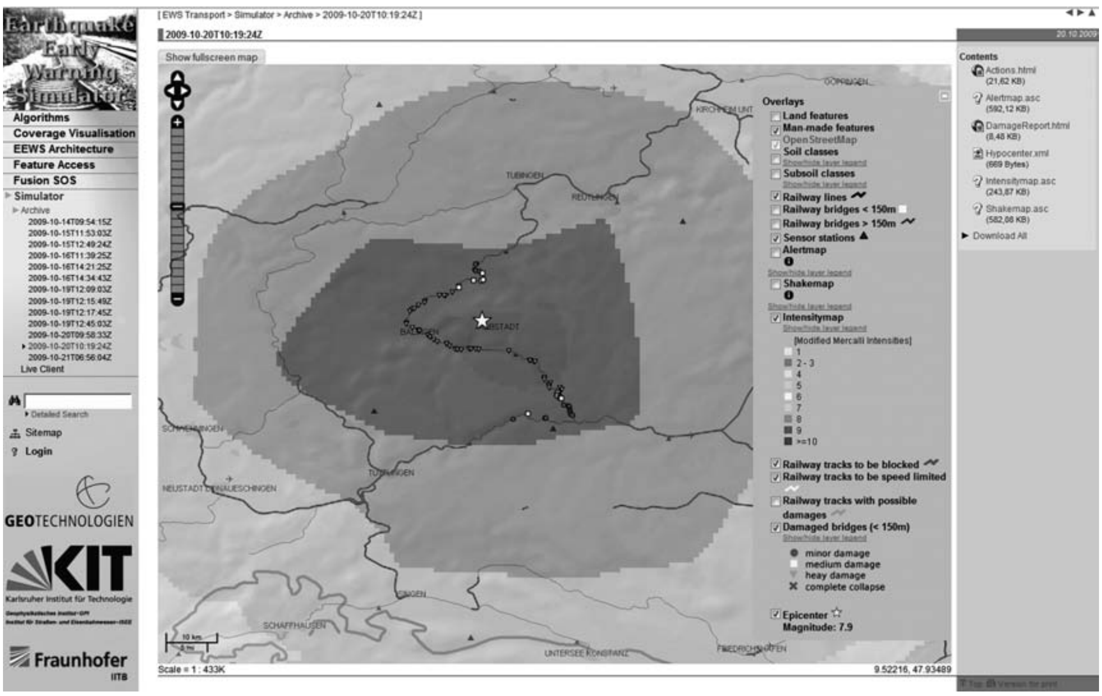

Figure 8: Client of Earthquake Early Warning Simulator

Furthermore, a client has been implemented. It realizes the workflow of the scenario and visualizes the results in a Web Mapping Client. The Mapping Client shows different result layers (alert map, shake map, damage map) together with base layers (sensor stations, railway tracks, topography). Figure 8 shows a screenshot of an earthquake simulation with magnitude 7.4 in the developed client. In this case the stopping of trains on red railway tracks is advised and a potential damage for several bridges has been estimated.

Results of just simulated earthquake events are visualized in the so called »Live Client«. They are moved to an event archive once the simulated earthquake has finished. The event archive contains different earthquake events for comparative analysis. The services and clients are online accessible on the following server: http://ews-transport.iitb.fraunhofer.de.

5. Conclusion

The project's main innovations are (i) the use of a dense station network that detects earthquakes based on a neural network method, (ii) a risk analysis that identifies and warns endangered parts of the railway network as well as estimates potential damages to the railway infrastructure, and (iii) the specification of an open service architecture providing access to information and results created by the early warning workflow.

On the basis of these results, the entire early warning chain ranging from earthquake detection and risk reduction measures for railway transportation to damage map generation is modeled in an online demonstrator. The demonstrator is a useful tool for optimizing the various subtasks of the early warning chain as well as their interrelations. Furthermore, it facilitates communication with end users and reveals most clearly strengths and weaknesses of the current implementation. Thus, it represents an important step in the development of early warning system for transport lines. Experiences gained herewith will lead to an improvement of the Early Warning System Architecture specified by EWS Transport.

References

Basöz, N. and Mander, J. (1999), Enhancement of Highway Transportation Lifeline Module in HAZUS, Draft 7, Federal Emergency Management Agency (FEMA) and National Institute for Building Sciences, 1999.

Beaujardiere (ed.) (2006), OpenGIS Web Map Server Implementation Specification, Open Geospatial Consortium Inc., OGC 06-042.

Berger, R. et al. (2005), The way to coordinated deployment of ERTMS/ETCS throughout the European Network, Railway Technical Review 4, 21, 2005.

Böse, M., Wenzel, F. and Erdik, M. (2008), PreSEIS: A Neural Network-Based Approach to Earthquake Early Warning for Finite Faults, Bulletin of the Seismological Society of America, 98, 366–382.

DIN 4149-2005-04 (2005), Bauten in deutschen Erdbebengebieten – Lastannahmen, Bemessung und Ausführung üblicher Hochbauten, 2005.

Esveld, C. (1989), Modern Railway Track, MRT Productions, Duisburg,1989.

GeoServer (visited in June 2009), GeoServer, http://geoserver.org

Grünthal, G. and Bosse, Ch. (1996) Probabilistische Karte der Erbebengefährdung der Bundesrepublik Deutschland – Erdbebenzonierungskarte für das Nationale Anwendungsdokument zum Eurocode 8, GeoForschungsZentrum Potsdam, STR 96/10, 24 pp.

Grünthal, G., Mayer-Rosa, D., and Lenhardt, W. A. (1998) Abschätzung der Erdbebengefährdung für die D-A-CH-Staaten – Deutschland, Österreich, Schweiz, Bautechnik, 10, 753–767.

Köhler, N., Cua, G., Wenzel, F., and M. Böse (accepted: June 2009) Rapid source parameter estimations of southern California earthquakes using PreSEIS. Seismological Research Letters, in press.

Kunz, Usländer, Watson (2009): A Testbed for Sensor Service Networks and the Fusion SOS: towards plug & measure in sensor networks for environmental monitoring with OGC standards, submitted to 18th World IMAC /MODSIM Congress, Cairns, Australia.

Lay, T. and Wallace, T. C. (1995), Modern Global Seismology, International Geophysics Series, Vol.58, Academic Press, San Diego, California.

Leydecker, G. (2008) Erdbebenkatalog für die Bundesrepublik Deutschland mit Randgebieten ab dem Jahre 800; Datafile: http://www.bgr.de/quakecat; Bundesanstalt für Geowissenschaften und Rohstoffe (BGR); Version 22.05.2008.

Lichtberger, B. (2004), Handbuch Gleis, Tetzlaff Verlag, Hamburg 2004.

Meskouris, K. et al. (2007), Gefährdungsabschätzung von Brücken in Deutschland unter Erdbebenbelastung, Forschung Straßenbau und Straßenverkehrstechnik 952, Bundesministerium für Verkehr, Bau und Stadtentwicklung, 2007.

Nah, A., Priest, M. (eds.) (2007), Sensor Observation Service, Open Geospatial Consortium, OGC 06-009r6.

Nakamura, Y. (1996), Real-time information systems for seismic hazards mitigation UrEDAS, HERAS and PIC, Quaterly Review of RTRI, Vol. 37, No. 3, 1996.

Nakamura, Y. (2008), private communication.

Pitilakis, K., these proceedings.

Prud'homme, A., Forces and behaviour of railroad tracks at very high train speeds, Railroad Track Mechanics and Technology, ed. A. D. Kerr, Pergamon Press, Oxford, 1978.

QGIS Mapserver (visited in June 2009), Implementing an easy to use and cartographically rich Web Map Server, http://karlinapp.ethz.ch/qgis_wms/index.html

Schut P (ed.) (2007), OpenGIS Web Processing Service, Open Geospatial Inc., OGC 05-007r7

Sokolov V. and Wenzel F. (2008) Toward realistic ground motion prediction models for Baden-Württemberg, Germany, Proceedings of the 31 General Assembly of European Seismological Commission, 7–12 September 2008, Crete, Greece, CD ROM.

Stange, S. and Brüstle, W. (2005) The Albstadt/Swabian Jura seismic source zone reviewed through the study of the earthquake of March 22 2003, Jahresberichte und Mitteilungen Oberrheinscher Geologischer Verein, Neue Folge 87, 391–414.

Usländer, T. (ed.) (2008): SANY D2.3.2 Specification of the Sensor Service Architecture V1, http://sany-ip.eu/publications/2420

52North, (visited in June 2009), WPS, http://52north.org/maven/project-sites/wps/52n-wps-webapp/

Railway Infrastructure and Seismic Early Warning Systems: 1 – Type and Viability of Integrated Measurements and 2 – Appropriate Features of EDILON Corkelast® Embedded Rail System

Quante F. (1), Schnellbögl G. (2)

(1) Fachhochschule Bielefeld, Wilhelm-Bertelsmann-Str. 10, 33602 Bielefeld
e-mail: franz.quante@fh-bielefeld.de

(2) edilon)(sedra GmbH, Kistlerhofstraße 168, 81379 München
e-mail: g.schnellboegl@edilonsedra.com

1. Type and Viability of Integrated Measurements

1.1 Introduction

The combined project »Early Warning System Transport«, funded by Bundesministerium für Bildung und Forschung (BMBF) and Deutsche Forschungsgemeinschaft (DFG), is looking for realizing the architecture of a warning system for earthquakes using different functional blocks.

In one block sensors and their connection to the transport infrastructure play a major role which is described in this contribution.

The following section 1.2 gives an overview about the amplitude of sensor signals which may be excited through earthquakes and which will be contrasted in section 1.3 to the comparatively high magnitude of such signals which are to be expected adjacent to the track during train operations and due to temperature.

1.2 Earthquakes and important sensors

For the following considerations three classes including five sensors were taken into consideration:

– Vibration sensors for the capture of seismic waves (acceleration, velocity, displacement)
– Strainmeters for the capture of tensions due to displacements of the surface
– Tiltmeters for the capture of inclinations of the surface

These sensors were chosen because they are widely used in earthquake investigations.

1.2.1 Earthquakes and vibrations

Earthquakes cause vibrations of quite different amplitudes. Best documentations are available for the amplitude of accelerations (abbreviation a). Their values were used for the calculation of corresponding amplitudes for velocities (v) and displacements (s) [Quante, F. (2008)].

Tab. 1 contains such values which may (see below) partly be regarded as astonishingly low by railway experts. Please observe that in Japan at values for the maximum acceleration

Tabelle 1: Some consequences of earthquakes depending on Mercalli-grade together with rough estimates for the occurring amplitudes of the vibration signals *a*, *v* und *s*. The values for *a* are taken from literature ([X1] and [Meskouris, K. et al. (2007), S. 139]) or calculated for *v* and *s* using dominant frequencies of $f = 5$ Hz and $f = 0.5$ Hz

Mercalli-grade	Consequences	Richter-scale	a_{max} [g]	v_{max} 5Hz [m/s]	s_{max} 5Hz [m]	s_{max} 0.5Hz [m]
I	Imperceptible, can only be verified by measurements	1	< 0.001	< 0.0003	< 0.00005	< 0.005
VI	Furniture may be displaced, slight damages	5.3–5.9	0.03–0.1	0.009–0.03	0.0003–0.001	0.03–0.1
XII	Large-area devastating catastrophy	> 9	> 2	> 0.6	> 0.02	> 2

a_{max} of above 0.04 g all high speed trains are stopped immediately for safety reasons.

1.2.2 Earthquakes and strain

In California a lot of research is conducted, see [Agnew, D. C. (2007)], to find out the suitability of strain and inclination for the early detection and prediction of earthquakes. This work is done at Piñon Flat Observatory (PFO) near the San Andreas fault, where many earthquakes can be observed in their pre-, co- and post-seismic phase. One of the applied strain meters had a rather long measurement basis (Laser strainmeter, length 732 m) to suppress local disturbances and to achieve the necessary resolution of 10^{-9} (equivalent to 1 mm upon 1000 km), to be able to differentiate effects in the order of 10^{-8}. The equipment is very complicated and has to be kept at constant temperature.

Some important results: The increase in strain, although predicted in a model, could not be observed reliably during the pre-seismic phase. During co- and post-seismic phases contradictory trends could be observed being characterized by simultaneous increases and decreases depending on the direction. The amplitude of changes probably induced by an earthquake with a magnitude of about 7 was of the order of $0{,}2 \cdot 10^{-6}$ to $1 \cdot 10^{-6}$ and could only be isolated by careful suppression of noise caused by the oceanic tides. Tidal effects as such had the same amplitude as co- and post-seismic changes.

At this point already a clear statement can be made that the complexity of the measuring apparatus and the small size of strains (10^{-6} for earthquakes with magnitude 7) to be detected don't give any hope for making successful measurements utilizing the rail itself (with its noise by trains and climatic influences) with regard to early warning or prediction.

1.2.3 Earthquakes and inclinations

The team from PFO also observed a manifold of signal changes when measuring inclinations. During co-seismic phases distinct changes due to earthquakes can occur. But they are again contradictory. The tiltmeters operated on a basis of more than 500 m showing co-seismic changes up to about 0.3 µrad; in single cases there was no reaction and during pre-seimic phases there was no clear tendency that could have been exploited for early warning or prediction.

The final statement to be made resembles that of the preceding section: Tiltmeters offer no advantages for early warning or prediction.

1.3 Vibrations and their frequency during railway operation

1.3.1 Rail cars

Under all operational conditions the car ride has to be stable and rocking on the suspensions is not allowed. Coaches are dimensioned for vertical eigenfrequencies of 1 Hz and the vertical eigenfrequency of the bogies is about 10 Hz [Knothe, K. (2001)]. Therefore the dynamics of rail cars mainly happen in a frequency range up to 30 Hz and fully overlap with the range of earthquake vibrations.

In curves the outer rails are super elevated to compensate the influence of centrifugal forces. The difference between resulting centrifugal and downhill-slope accelerations may be up to 0,5 m/s² [Fiedler, J. (2005), S. 59 ff], a value that is bigger than the allowed value for earthquake accelerations used in Japan for the immediate stop of the Shinkansen.

Even on straight tracks horizontal accelerations will be excited as a consequence of the natural sinusoidal side motion of rail cars. This horizontal movement of the cars is a consequence of the conicity of the wheels and can reach amplitudes that touch the rail at its shoulder. According to [Quante, F. (2008)] the velocity dependent frequency of these side motions lies for velocities of trains between 36 km/h and 360 km/h (i.e. 10 m/s to 100 m/s) between 5 Hz und 5 Hz, overlapping with the range for earthquake detection.

1.3.2 Bogie and wheel-rail contacts
Different causes of vibrations and wear produce wheels out of roundness and wear induced structures (like corrugation) in the rail surface. Then wheel-rail contacts give rise to velocity dependent vertical vibrations of bogie, rail car and track. Together with an assumed diameter of 1 m for a wheel the exciting length of the circumference is about 3 m. This means that for velocities of trains between 36 km/h and 360 km/h consequently frequencies between 3 Hz and 30 Hz will be excited which also severely interfere with the range of earthquakes.

1.3.3 Track components
Non-uniform settlements of the track, hollow spots, stiffness changes of the subsoil (e.g. bridges, earthworks) are permanent structural changes with a length in the order

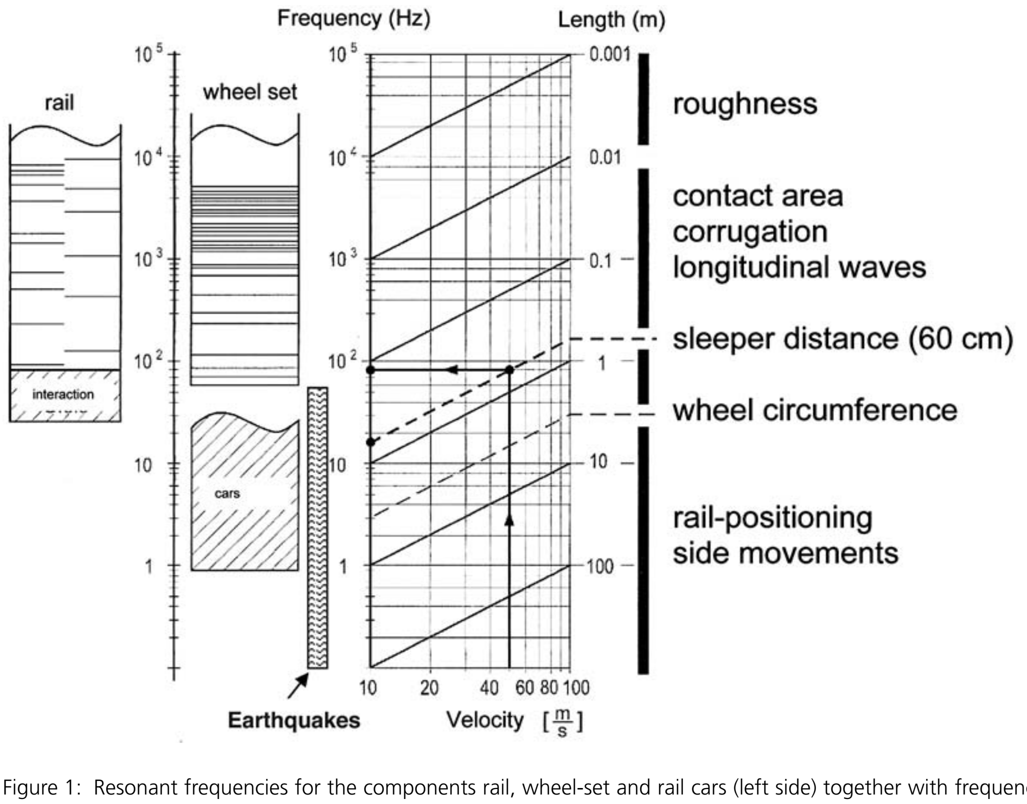

Figure 1: Resonant frequencies for the components rail, wheel-set and rail cars (left side) together with frequency range of earthquakes, and operationally induced frequencies depending on train velocity and structural length (right side) [Knothe, K. (2001), S. 61]

of a meter that will contribute to the excitation of vibrations.

In addition to such unpredictable effects, the rail support system (slab track and ballasted track) is dimensioned in such a way that under each wheelset the rail sinks about 1 mm down to guarantee a broader distribution of loads. This is again the cause of vibrations which for a sleeper distance of 60 cm occur in the range between 16 and 160 Hz for the relevant train velocities between 36 km/h and 360 km/h.

The different vibrations described above will of course also interfere with measurements of strain and tilt which will be given a short consideration in section 1.4 after summarizing the different vibrations and their frequency ranges in the following section.

1.3.4 Vibrations due to rail operation

The dashed line for the sleepers corresponds to a distance of 0.6 m. Sleepers cause frequencies at the upper rim of the frequency range for earthquakes. The wheel circumference and especially rail positioning faults and side movements cause disturbances amidst the critical frequency range.

This summarizing figure stresses again that a detection of weak p-waves as a precursor for bigger vibrations in an earthquake will be very problematic near the track.

1.4 Strain and inclination under railway operation

1.4.1 Strain

The sinking of the rail under the load of an axle results in strains which can easily be calculated [Quante, F. (2008)]. An estimation for a sleeper distance of 60 cm and a sinking of 1 mm yields a strain ε of $1.4 \cdot 10^{-6}$. This value exceeds those of post-seismic measurements performed at PFO.

Temperature also causes strain that can be estimated utilizing the temperature-coefficient of steel with a magnitude of $13 \cdot 10^{-6}$/°C. This means that a change in temperature of only 10 °C results in a change of α of $1{,}3 \cdot 10^{-4}$, being much more than measured for earthquakes at PFO.

1.4.2 Inclination

The sinking of the rail under axle loads can also be employed to derive an estimate for the inclination angle α. The result of $\alpha = 1.7$ mrad is an angle showing a thousandfold value of inclinations under the influence of earthquakes.

The previous statements are confirmed: the measurement of strain and inclination in the track itself is not suited for the purpose of prediction or early warning.

1.5 Summary: Applicability of integrated measurements

The intention of employing the rail itself as a decisive part of a sensor for the purpose of early detection or even for the prediction of earthquakes does not look promising. This conclusion was gained by literature analyses evaluating vibration signals and the magnitudes of occurring strains and inclinations.

But the rail infrastructure could well be equipped with sensors for the purpose of continuous condition monitoring that would also allow an immediate and area wide analysis of earthquake induced damages as basis for a detailed planning of rescue activities where needed most urgently (see chapter 2).

2. EDILON Corkelast® Embedded Rail System – a promising offer for Early Warning Systems

2.1 Introduction

The company **edilon)(sedra**, with its EDILON Corkelast® Embedded Rail System (ERS), has changed the traditional concept of discretely supported rails (by means of sleepers or blocks), into continuously supported rails. This homogeneous elastic support is providing the same dynamic spring and damping behaviour as e.g. ballasted track under traffic load, but completely eliminates the influences of individual rail seats or sleepers. Track loads become more evenly spread and dynamic load amplification is getting lower.

By virtue of the position-stable integration of the rails into a concrete or steel channel structure, track loads have a negligible effect on track gauge, position and buckling. The primary characteristics of the EDILON Corkelast® Embedded Rail System (ERS) are based on EDILON Corkelast®. This provides elastic bonding to the rail and the supporting rail channels. The unique, proven, reliable two component embedding compound assures outstanding position stability over decades – along with simple installation, reduced construction height, low system costs, and minimum maintenance.

As such ERS also offers unique advantages for the stable integration of sensors for continuous condition monitoring of the rail infrastructure that could even be utilised in case of wide-area damages induced by an earthquake to analyse where rescue activities are most urgently needed.

2.2 System Characteristics

The ERS rail fastening was developed in the beginning of the 1970s jointly with the Netherlands State Railways for use on bridges (since 1973) and level-crossings (since 1976) as well as ballastless track (also since 1976).

Introduced in Germany since 1996, the ERS rail fastening is approved by the German railway approval agency (EBA) for $v_{max} \geq 300$ km/h in combination with the INFUNDO® ballastless track system and for $v_{max} = 160$ km/h on level-crossings type STELFUNDO®.

It is also used on many Light Rail Systems throughout the world.

Main characteristic of ERS rail fastening is the continuous rail support in vertical and lateral direction with the two-component compound EDILON Corkelast®. This compound guarantees homogeneously embedded rails with defined static rail deflection (e.g. limited horizontal rail head deflection) corresponding to the various performance requirements. EDILON Corkelast® is a polyurethan-compound which can be provided in specific elasticity, as required.

The EDILON Resilient Strip regulates the static spring constant of the EDILON Corkelast® Embedded Rail System. Thickness and hardness of the EDILON Resilient Strip vary according to the system stiffness required.

Filler profiles are used to reduce the use of EDILON Corkelast®, they can be used for (signalling) cables over short distances, however.

Summary of Advantages of ERS–tracks

– Small effect of loads on track gauge, position and buckling – inherent safety

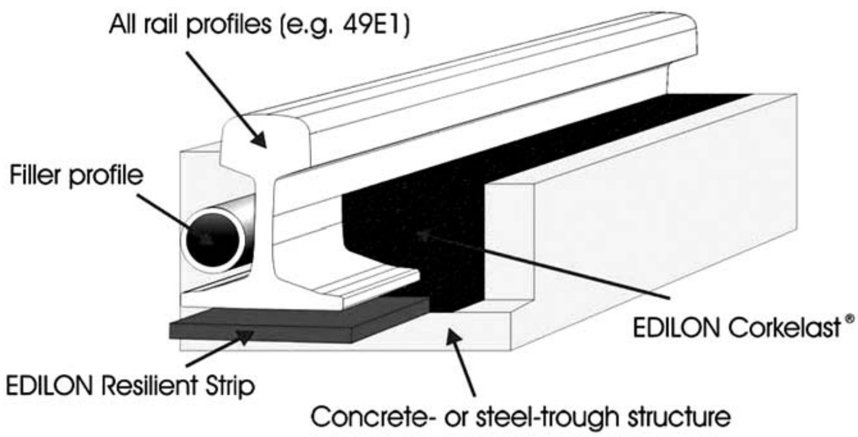

Figure 2: The principle of EDILON Corkelast® Embedded Rail system

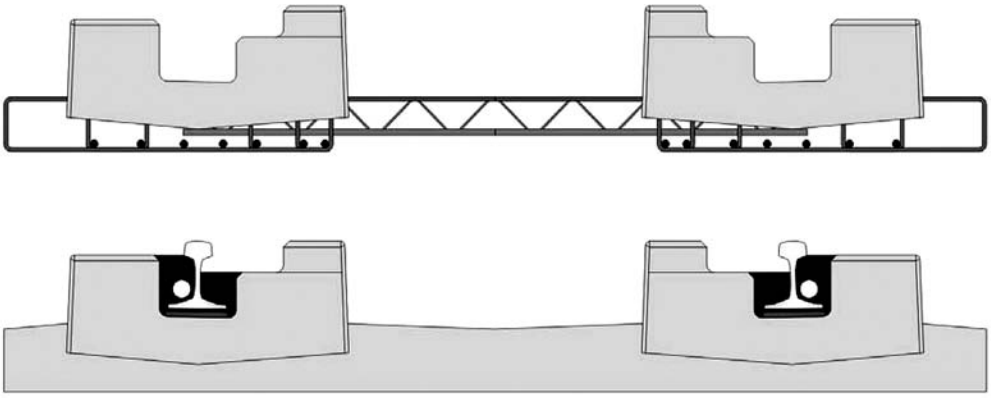

Figure 3: Example for semi-prefabricated slabs, here: Donau Bridge at Tulln, Austrian Railways 2009

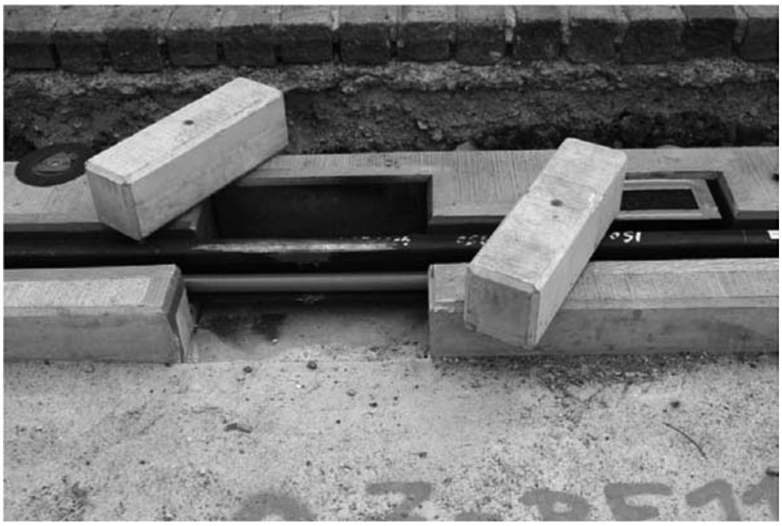

Figure 4: Rail joint cut-out (left) and axle counter (right) recesses in semi-prefabricated slabs at Guntramsdorf, Austria; street running section of Wiener Lokalbahnen AG. This section caters for light rail passenger transit as well as heavy goods traffic

- Lower wear of rails – use of smaller rail profiles possible
- Reduction of noise and vibration emissions
- Minimisation of components necessary for the support and fixing of rails
- Shorter construction time – economical solution for renewals
- Reduced height of track bed – smaller cross sections of tunnels
- Filler profiles embedded in the corkelast sealing usable as ducts for protected sensor and cable laying
- Considerable reduction of life cycle costs

2.3 Various Constructive Options

Trough structures can be prefabricated or constructed in situ. In recent years, edilon)(sedra developed semi-prefabricated slabs, e.g. only the rail troughs itself are prefabricated and are completed through the use of in-situ concrete. Apart from the rail itself, the rail trough structure needs to have recesses for the various rail installations. The grounding of cables, switch controls, axle counters, drainage, rail joint cut-out, door controls can all be placed in recesses of the rail trough and fixed with EDILON Corkelast®.

2.4 Summary of possible Early Warning System Applications

Thus, due to the continuous and durable rail support in vertical and lateral direction, together with its defined system stiffness, the EDILON Embedded Rail System offers ideal conditions for the use of sensors and their application. Attached sensors might perhaps even be used to detect approaching waves of an earthquake. But the most promising application is the permanent surveillance of the tracks themselves.

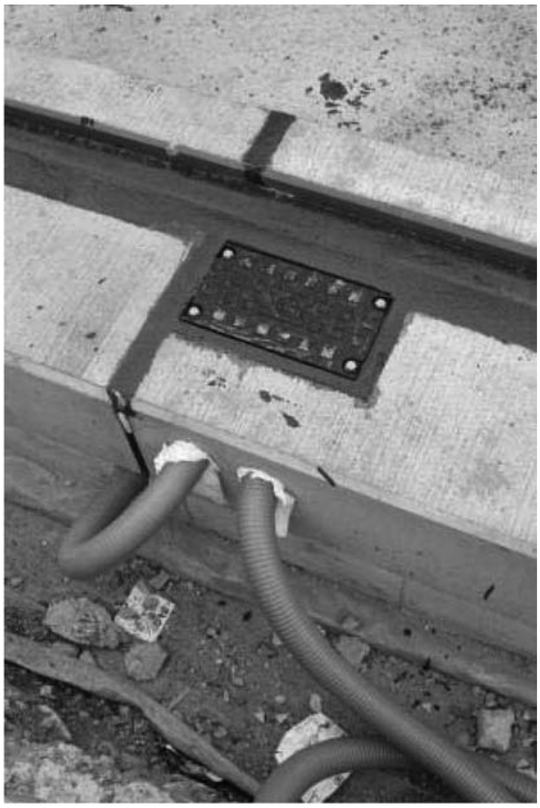

Figure 5: Electric Installation of an axle counter at Guntramsdorf

Figure 6: Drainage in prefabricated slabs for Verkehrsbetriebe Karlsruhe, Germany

Figure 7: Switch control and heating at Toyama Portram route, Japan

Figure 8: Model of a sensor rod

This system therefore also offers a big potential for the assessment of damages caused by an earthquake. For this purpose, railway lines could be equipped with sensor stations being about one kilometre apart, integrated into the ERS structure and aiming at the detection of different faults:

– Sensors inside the trough, also directly connected to the rail:
  Strain meters for the detection of excessive strains, buckling, and breakage of rails and of supportive layers

– Embedded in the supporting concrete layer, e. g. amidst the two rails, employing a sensor head guarding the sensitive equipment mounted on a structured rod for a good coupling to signals in the material surrounding it:

Inclinometers and/or distance meters
for the permanent control of the safe geometrical rail position, i.e. controlof rail track parameters like longitudinal height, cant, twist, track gauge and curvature.

Accelerometers for the detection of excessive movements of the track outside
train passing.

– Placed near the rail employing the sensor rod which may be fixed in a bore hole:
  Accelerometers and/or geophones for the early detection of seismic waves

References

Agnew, D. C. (2007), Before PBO: An Overview of Continuous Tilt and Strain Measurements in the United States. Journal of the Geodetic Society of Japan, 53, S 157–182, 2007.

Fiedler, J. (2005), Bahnwesen, Werner Verlag, München, 2005.

Knothe, K. (2001), Gleisdynamik. Ernst & Sohn. Berlin, 2001.

Meskouris, K., Hinzen, K.-G., Butenweg, C., Mistler, M. (2007), Bauwerke und Erdbeben. Vieweg, Wiesbaden, 2007.

Quante, F. (2008), EWS-Sensorik, Research Report, Fraunhofer- IITB, Karlsruhe, 2008.

X1, Erdbeben und auftretende Beschleunigungen, visited Dec. 30, 2008: http://geol43.uni-graz.at/05W/650136/erdbeben.html.

Fiber Optical Sensing with Fiber Bragg Gratings

Eisenmann Th.
INFAP GmbH, Fürstenrieder Straße 279a, 81377 München
thomas.eisenmann@infap.de

Summary
A new measurement method is presented utilizing glass fibers with inscribed Fiber Bragg Gratings (FBG). Strain and temperature changes have direct effects on these gratings. With this technology and suitable transducers, however, also parameters like pressure, dislocation, vibration, acceleration, humidity and even chemicals can be monitored. A broadband or sweeping laser light source is used and light with wavelengths corresponding to the FBGs is reflected back to a data acquisition unit (interrogator). Depending on variations of the parameter to be measured, the grating is stretched or compressed and as a result the reflected (Bragg) wavelength is shifted to longer or shorter wavelength respectively. This shift is proportional to the change of the parameters value. The fiber sensor or the transducers can be fixed, welded, glued onto or even embedded in the media, which shall be monitored. The biggest advantages of the technique are

- A single fiber can carry a multitude of sensors, sensing is done simultaneously parallel (multiplexing).
- The optically encoded signals of the measured parameters are transmitted in the fiber to the data acquisition unit. Thus, no additional data line is necessary.
- The sensors have minimum volume with low weight, are flexible and easy to install.
- Measuring with light does not require power for the sensors or the fibers, sensing is immune against electro-magnetic interference (EMI) and intrinsically safe. Consequently, measurement can be done in places that are explosion-proof zones, exhibit strong magnetic fields or are not accessible anymore after the sensors have been installed.
- Attenuation 0.1 dB/km only. Thus a measurement length of some 100 km can be realized.

1. Introduction

Initially conceived as a medium to carry light and images for medical endoscopic applications, optical fibers were later proposed in the mid 1960's as an adequate information carrying medium for telecommunication applications. At the heart of this technology is the optical fiber itself – a hair-thin cylindrical filament made of glass that is able to guide light through itself by confining it within regions having different optical indices of refraction. Ever since, optical fiber technology has been the subject of considerable research and development. For measurements, optical fibers eventually found numerous applications in areas, as different as pharmacy and structural health monitoring.

In principle, a fiber optic sensor contains an optical element, whose material properties are changed by the measured parameter. Light is influenced in its intensity, phase or polarity. Consequently, a characteristic spectrum results from the measured value. Many physical and chemical parameters can be determined by this. Temperature, pressure and strain can be measured as wells as humidity and appearance of gases. FBG sensing is a so-called intrinsic technique, i.e. the fiber properties are changed by external effects and hence, the fiber itself is the senor. Temperature or strain has a direct impact on the glass fiber, as the properties of light travelling through the fiber will be altered locally (Krug, 2007).

2. Principle

Fiber Bragg Gratings are optical interference filters inscribed into the core of single-mode glass fibers. For generating fiber gratings, the core of a single-mode fiber is exposed to the perpendicular impact of a periodic pattern of ultraviolet light coming from e.g. an Excimer laser (UV 248 nm). This impact produces a permanent increase of the refractive index corresponding to the periodic pattern with fixed spacing, called grating. As a result, a periodic modulation of the refractive index takes place with areas of high and low refractive indices, reflecting back light of a certain wavelength. The grating strength or amplitude is a function of how long the fiber has been exposed to the ultraviolet illumination. A portion of light is reflected back at each change of the refractive index (Fig. 1). All these reflection signals together result in a coherent large back-scatter of a specific wavelength. Thereby, the spacing of the FBG is half the reflected wave length. This is denoted as Bragg condition and Bragg wave length. For all wavelengths not fulfilling this condition, the grating is transparent (Fig. 1). Consequently, incident light travels through the grating structure with negligible signal variation or attenuation, as the reflected light signal will be very narrow. Thus, an important property of a Fiber Bragg Grating is the precise wavelength.

The reflected wavelength is centered at the Bragg wavelength fulfilling the Bragg equation $\lambda_{\mathrm{refl}} = 2n\Lambda$, with n being the refractive index and Λ the distance between the gratings. Due to the temperature and strain dependence of n and Λ, also the reflected wavelength is dependent and varies as a function of temperature and/or strain (Fig. 1). This dependence is known and enables the unambiguous determination of temperature and strain from the reflected Bragg wavelength. Hereby the detected signal is spectrally encoded so that transmission losses are of no concern. Nevertheless, if strain and temperature alterations are expected to occur simultaneously, it becomes necessary to use a grating decoupled from strain for temperature compensation. With appropriate transducers many parameters like pressure, deformation, dislocation, vibration etc. can be inferred from the basic strain or temperature changes.

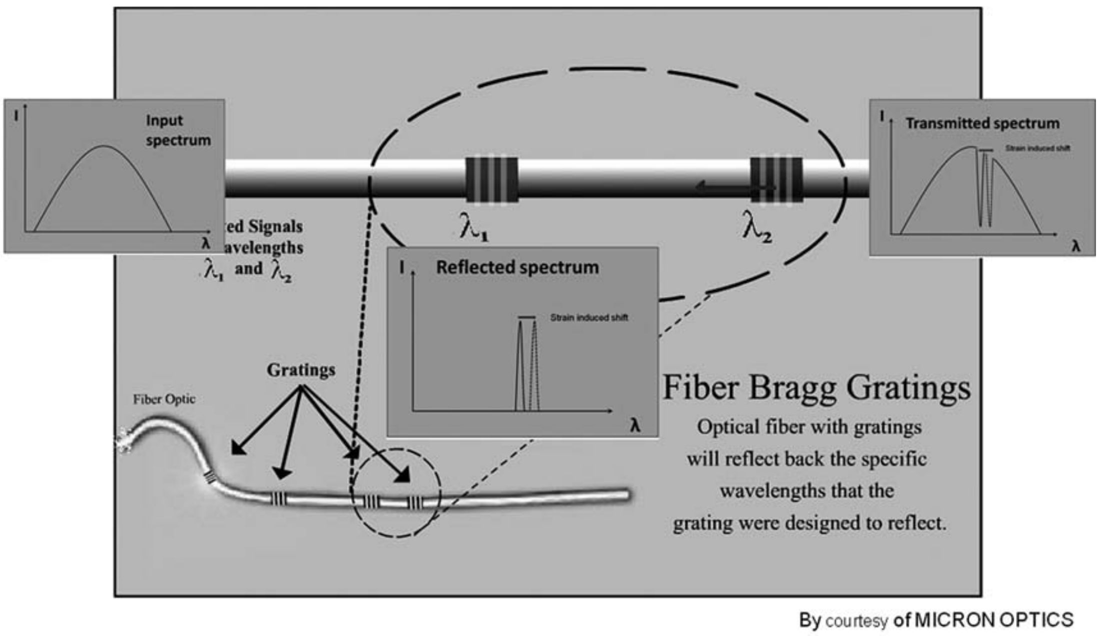

Figure 1: Principle of Fiber Bragg Gratings

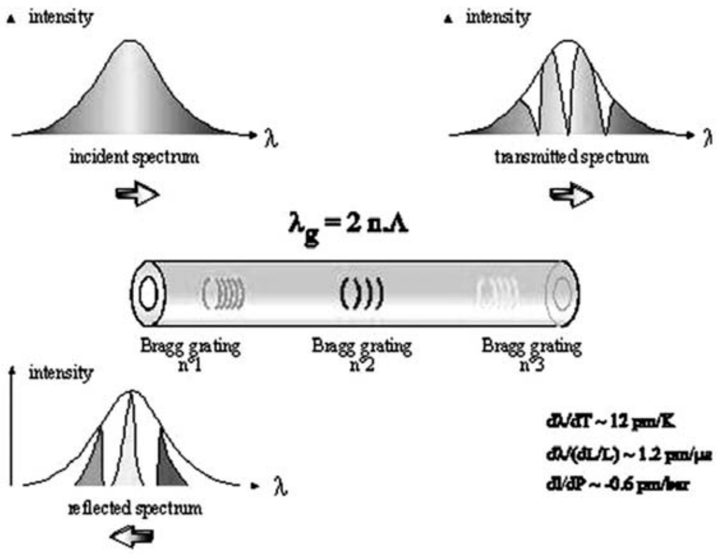

Figure 2: Wavelength Division Multiplexing (WDM)

Typically, the fractional wavelength change in the peak Bragg wavelength is in the order of 10^{-12} pm/°C. Strain shifts the Bragg wavelength by physically increasing or decreasing the grating spacing by mechanical strain and by changes in the refractive index due to the strain optic effect. For axial loads, the wavelength change is typically 1.2 pm per micro strain ($\mu\varepsilon$) or 12 nm for 1% strain. Assuming such performance, an accuracy and resolution of 1 µs, 0.1 °C or 1 µm in case of deformation measurements can be achieved.

One of the key characteristics and biggest advantages of this measurement method is multiplexing, i.e. the answer of numerous different FBGs can be achieved with one fiber only by inscribing various FBGs with different spacing and wavelengths in a serial configuration. Each reflected wavelength corresponds to a distinct FBG. This is called wavelength division multiplexing (WDM). In this configuration each FBG is assigned a given »slice« of the input broad-band light spectrum. Caution has to be exercised, however, to avoid overlapping of distinct FBG's spectra.

Today, most popular WDM interrogators (spectrum analyzer and data acquisition units) use fast sweeping lasers as light source instead of a broadband source. The advantages are longer range (due to higher source power) and greater sensor capacity (due to the wider wavelength windows of 50 to 100 or even 160 nm) and the ability to simultaneously interrogate many fibers, each with dozens of sensors.

A further increase in the number of sensors per fiber that can be interrogated is possible using time division multiplexing techniques (TDM) in combination with WDM. In this approach, the spectrum of the source is used multiple times to scan separate groups of FBGs in time. If a short duration pulse of light from the source is launched into this system, the reflections from the FBGs at every point in the array will return at the detector at increasingly later times depending on how farther away they are to the detector itself. If the detector is synchronized and time-gated, it is possible to selectively interrogate a given FBG array in time for a given wavelength window. Drawback of this way to interrogate sensors is the limited scanning frequency, which would limit the response of the system to dynamic signals and transients. FBGs can be spaced no closer than 1 meter for the even the best TDM systems (MICRON OPTICS, 2005).

Another drawback of the TDM technique, when combined with Bragg gratings, is that of cross-talk (Morey, et al., 1991). There are two sources for cross-talk: multiple reflections and spectral shadowing. Multiple reflection cross-talks arise from the delay introduced into a reflected light signal upstream that has undergone multiple reflections during its travel and has effectively overlapped in time with the reflected signal of a grating downstream. The effect is proportional to the grating's reflectivity and can be minimized using low reflectivity gratings (<5%). In fact, the number of grating elements that can be interrogated under a given signal-to-noise ratio will depend on the amount of cross talk. Hence, the pairing of low-reflectivity gratings with high sensitivity detection will be essential to interrogate large arrays of gratings. The spectral shadowing cross-talk is the distortion introduced in the reflected spectrum of a downstream grating resulting from the double pass of the incoming light through an upstream grating. The above deleterious effect can be eliminated by staggering the grating arrays to avoid spectrum overlaps by having arrays branching off instead of serially connected. To reduce time overlaps and cross-talk the time interval between gratings can be increased by adding passive delay lines. These measures can be implemented at the expense of additional components such as fiber couplers, delay lines and stronger reflectivity FBGs. If more than one sensor fiber is used with one data acquisition unit, an optical switch triggers the relative fiber.

3. System components

An FBG optical fiber sensing system usually consists of the following components (see also Fig. 3 & 4):

a. Interrogator: Light source and data acquisition unit – spectrum analyzer (mono-static arrangement, i.e. light source and detector are arranged adjacent in one case) for light transmission and reception of the optical signals and conversion into digital data.
b. Fiber Sensor: The Fiber Sensor is a glass fiber with inscribed sensors (Fiber Bragg Grating) and fiber plug (FC/APC). These fibers are usually coated with polyimide, acrylate or preferably with ORMOCER®, an

Figure 3: Interrogator (model si730 from MICRON OPTICS)

Figure 4: Different types of transducers: Spot welded strain sensor, screw-in temperature sensor, embedded concrete strain sensor

inorganic-organic hybrid polymer (trademark of the Fraunhofer-Gesellschaft zur Foerderung der angewandten Forschung e.V. Munich/Germany). ORMOCER offers a more durable and homogenous coating than the so called recoated fibers.

c. Transducer (some examples are depicted in Fig. 4) for the parameter to be measured, e.g. weldable or embedded strain or temperature sensors, screw-in temperature sensor, accelerometer etc.
d. Extension fibers: Commercially available glass fiber cables for realizing large distances between sensors and data acquisition units (up to several km).
e. Data evaluation software: e.g. LabVIEW (National Instruments) based software for read-out and analyzing data as well as specific adaptation for applications and of the graphic user interface (GUI).

Usually application-oriented systems including commissioning are configured with above components. This guarantees that measurements can be done exactly adapted to fit the requirements for laboratory or field purposes.

4. Applications

Fiber Bragg gratings are often used for either strain or temperature sensing, especially where environments are harsh (e.g. high-EMI, high-temperature or highly corrosive conditions). As mentioned, it is also possible to use fiber Bragg gratings to sense other parameters such as pressure, vibration, acceleration, dislocation by using an additional transducer instead of using the Fiber Bragg grating itself.

Once the sensor is attached by e.g. sticking, welding or embedding it to the place or into/onto the structure in the field, it is very important to protect the fiber from damage. This can be challenging if the point, where the measurement is taken will be quite distant from the interrogator. Fortunately, a number of excellent cabling methods for optical fibers exist, such as Kevlar wrap or metallic shrouds for optical fiber.

As strain measurement is of high significance for applying FBG sensing in rail tracks and rail networks and also for earthquake prone regions and structures, more generally for structural health monitoring, emphasis shall be put on static and dynamic strain sensing in the following applications chapter.

Long-term Static Strain Sensing

Long term static strain testing is very easy to accomplish with fiber Bragg gratings due to their inherent self-referencing (MICRON OPTICS, 2005). Self-referencing is the ability to determine a starting point. Each Bragg grating has an associated zero strain wavelength. Initially the unstressed fiber Bragg grating has a specific center wavelength. However, when it is attached to a structure, this process will alter the shape of the FBG. Therefore, the zero strain point must be reevaluated after mounting. The internal forces in the glue used for mounting will cause strain within the grating. Hence, after the fiber Bragg grating is attached to the structure, it needs to come to a steady state and then the zero point before the measurements is determined. With the grating mounted to the structure in question, the initial wavelength is determined. With a set amount of time passed, one can return to the structure, reattach and refer back to the initial wavelength. That would give the determination of the strain compared to the initial condition at that time.

This is in contrast with electrical strain gauges and other types of instruments were changes in the sensor itself would have to be constantly monitored, whether it is a resistance change, a capacitance change or other electrical change. With an electrical strain gauge, the ability to disconnect your monitoring instrumentation does not exist as is with a fiber Bragg measurement arrangement. The reason for this is that with electrical strain gauges you have to balance out the gauge each time you connect your resistance strain gauge to it. This ability to return to the fiber Bragg grating after long time such as months or even years constitutes another big advantage of the method (MICRON OPTICS, 2005).

An example is strain testing over time in number of bridges. If sufficient budget exists, one set of instrumentation per bridge could be installed. However, if 100 bridges need supervision, it is not economical to purchase 100 times the equipment. Instead one set of instrumentation would be adequate to test each of these 100 bridges on an e.g. monthly cycle. It would be much more efficient to attach numerous fiber Bragg grating sensors throughout those bridges, attach the instrumentation to them on a periodic basis and conduct all the testing within very reasonable time. Besides bridges, other examples of using fiber Bragg gratings for long-term static strain monitoring would be rails, buildings, tunnels and structures in high earthquake prone areas. Most earthquakes and other earth tremors are low frequency events. Fiber Bragg gratings can be attached to structures and monitor the vibrations during such events. Other applications to monitor low frequency events would be the connection of fiber Bragg gratings to piers and other shore structures to determine their vibration during the ebb and flow of tides or the reaction of high-rise buildings to wind.

Dynamic Strain Sensing

In addition to the very low frequency modes that structures may have, they may also have higher frequency modes due to the effects of wind and tide. Dynamic strain testing appropriate to the 25 Hz region can also be performed on transportation vehicles such as automobiles, trains, and airplanes. Such measurements can also be used to diminish fatigue effects on vehicle structures. Fatigue is an example of how fiber Bragg gratings can be used for Dynamic Strain Testing in addition to long-term Static Strain Testing. Here not only the momentary vibrations undergone by the structures are of significance, but also the effects of these vibrations on the long-term strain of the metallic surfaces. Fiber Bragg gratings can similarly be attached to industrial machinery to determine the frequency and amplitude of stress vibrations. The vibration signature of either piece can then be used in a feedback loop to be sure that the correct amount of load is applied at all times during the machining process (MICRON OPTICS, 2005).

For static and dynamic strain as well as temperature measurements, many application areas can be found like

- Structural health monitoring (SHM)
  - Construction/plant construction
  - Geotechnical engineering, e.g. landslides, slopes, pipeline, dam and tunnel monitoring, building inventory in earthquake threatened areas
  - Infrastructure, e.g. roads and rails
- Aerospace
- Renewable energies like blade supervision for wind turbines
- Composite or metallic structures
- Transformers and power grids
- Pharmacy
- General research

5. Features and Benefits

Due to its nature measurements generally with fiber sensors and in particular also with fiber Bragg gratings exhibit a number of benefits, when used for appropriate applications. The most prominent of these are:

- The technique is fast, accurate and reliable in challenging environments.
- A single fiber can carry a multitude of sensors, sensing is done parallel (multiplexing).
- The optically encoded signals from the measured parameters are transmitted in the fiber to the data acquisition unit. Thus, no additional separate data line becomes necessary.
- Temperature range can be from –270 °C up to +600 °C.
- The sensors have minimum volume with low weight, are flexible, easy to install and do typically not require any maintenance.
- Measuring with light does not require power for the sensors or the fibers, is immune against electro-magnetic interference (EMI) and intrinsically safe. Consequently, measurement can be done in places that are explosion-proof zones, exhibit strong magnetic and electric fields or are not accessible anymore after the sensors have been installed (e.g. if they are embedded in concrete or in material structures like in carbon or glass fiber reinforced plastic).
- Attenuation typically totals up to 0.1 dB/km only. Thus a measurement length of some 100 km can be realized.
- A resulting additional value can be lower overall lifetime cost of the measurement set-up.

6. Using FBG for Rail Track Application

For rail network monitoring, especially the benefits

- measurement lengths in the kilometer range
- discontinuous interrogation of multiple sensors or continuous monitoring
  and
- easy mounting with simple cabling

are advantageous. The fiber sensors with suitable transducers can easily be attached by spot welding to the rails. For static strain monitoring the technique is superior due to the fact that multiple locations, where strain sensors are attached to rails can be interrogated with one measurement unit. This interrogator just needs to be connected to the fiber sensors in an e.g. monthly or bi-monthly schedule. Sensors can be placed in rail networks at distances of 500 or 1000 m. With dynamic measurements of 100 Hz or above, strain from trains riding above a sensor location can be tracked and compared in long-term monitoring campaigns. Here both strain and accelera-

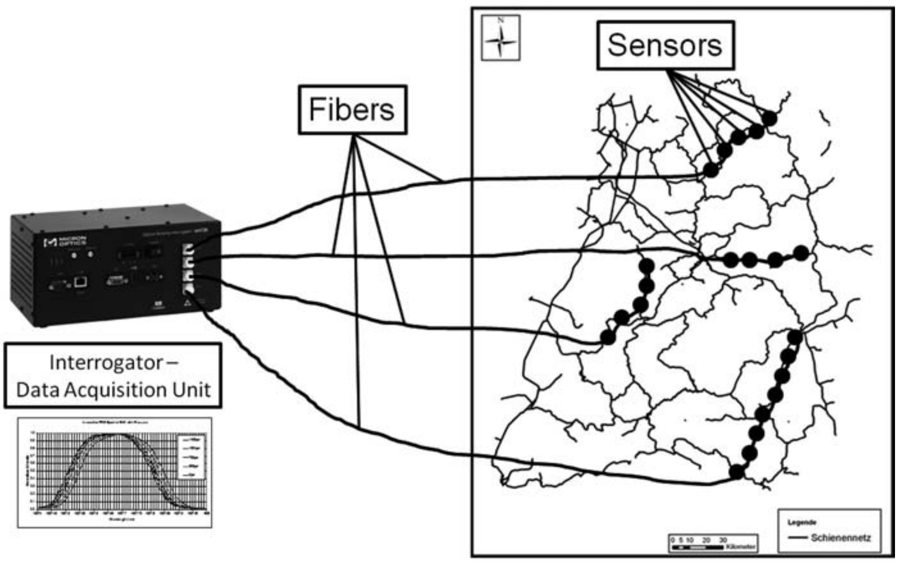

Figure 5: Integrating FBGs in a track network (schematic)

tion can be measured. With these results life time monitoring with early detection of arising damages as well as tracking of damage perpetrators seems feasible. Assessment of damages resulting from catastrophic dislocations due to e.g. earthquakes or landslides (track buckling) would be another application, where measurements can be done remotely and in real-time utilizing continuous monitoring of multiple sensors. Generally, from the perspective of safe rail traffic, the determination of parameters like track gauge, longitudinal height, superelevation, curvature and twist are to the fore. All these values are in principle ascertainable with FBG sensors (personal communication Prof. Quante).

A totally different, yet railway related application is temperature monitoring of bogies like it has been done for the Mass Rapid Transit in Hongkong (personal communication MICRON OPTICS).

7. Conclusion

Fiber-optical sensing for measuring physical parameters like strain and temperature, but also pressure, dislocation, vibration and acceleration is rapidly developing, especially into applications, where conventional electrical gauging finds its limits. Accordingly, measurements based on fiber Bragg gratings (FBG) can successfully be utilized in areas as different as construction and geotechnical engineering or material science, power grids/transformers and pharmaceutical production. Static and dynamic processes can be monitored in harsh environments exhibiting strong electro-magnetic fields, corrosive atmospheres or explosion risks.

For structural health monitoring, fiber-optical sensing is already proven in a large number of installations worldwide, mainly to investigate bridges, dams, dikes, slopes or tunnels. Due to the versatility of FBG sensors by integrating a large number of them in one fiber cable and multiplexing as well as the very low signal attenuation, even extended rail networks can easily be monitored with respect to stress coming from operational influences or damages due to natural disasters. Especially with embedded rail systems, sensors can easily be mounted. Consequently, measurements and monitoring with bespoke fiber-optical systems can contribute to protect vulnerable infrastructures.

References

Krug, F (2007): Messen mit faseroptischen Sensoren, Elektronik messen + testen 2.2007, pp. 54–58.

MICRON OPTICS (2005): Optical Fiber Sensors Guide Fundamentals & Applications, 21 pp.

MICRON OPTICS: Personal communication.

Morey, W. W., Dumphy, J. R., and Meltz, G. (1991): Multiplexing Fiber Bragg Grating Sensors, SPIE Proc. Vol. 1586, pp. 216–224.

Quante, F: Personal communication.

Seismic Risk Assessment of Lifeline Systems with Emphasis to Transportation Systems

Pitilakis K. (1), Argyroudis S. (2)

(1) Professor, Lab. of Soil Mechanics, Foundations & Geotechnical Earthq. Eng., Aristotle University of Thessaloniki, POB 424, 54124, Thessaloniki, Greece, kpitilak@civil.auth.gr

(2) Civil Engineer, Lab. of Soil Mechanics, Foundations & Geotechnical Earthq. Eng., Aristotle University of Thessaloniki, POB 424, 54124, Thessaloniki, Greece, sarg@civil.auth.gr

1. Introduction

Transportation systems include roadway, railway and subway networks, port and airport systems and infrastructures. Each system is actually a complex system of various components like bridges, roads, tunnels, embankments, retaining walls in case of highway system; wharfs, cranes, buildings, utility systems, tanks, etc in case of port facilities. Experience from past earthquakes reveals that lifelines are quite vulnerable, while their damage could be greatly disruptive due to the lack of redundancy, the lengthy repair time or the rerouting difficulties. For example, the disruption to the road network can strongly affect the emergency efforts immediately after the earthquake or the rebuild and other business activities in the following period. A typical paradigm is the port of Kobe after the strong Great Hansin earthquake (M7.1, 1995) that has lost almost the 50% of its annual income, despite the enormous retrofitting works (Fig. 1).

The complexity of elements at risk, their variability from one place and one country to another, and till recently, the lack of well validated damage and loss data from strong earthquakes and the spatial variability of ground motion, make the vulnerability assessment of each particular component and of the network as a whole, a quite complicated problem. Adding to that the spatial extend of transportation networks, the synergies with other systems and the inherent uncertainties in seismic hazard estimates, it is obvious that the risk assessment of transportation networks is indeed an extremely complex and challenging issue.

Figure 1: Extended damages to port facilities (left) and collapse of Hanshin Expressway during the Kobe (1995) earthquake

2. Short review of loss estimation studies for transportation systems

Several methodologies have been developed and applied worldwide, which can be assigned to the following three levels:

- **Level I** is focused on the functioning of the network in terms of pure connectivity (Franchin et al., 2006; Nuti and Vanzi, 1998). The considered vulnerable elements are those internal to the network itself, which generally consists of bridges, viaducts, tunnels, retaining structures, etc, and other elements of the surrounding environment, such as residential buildings and hospitals. This type of studies focuses on just one of the services provided by the network, most typically the rescue function immediately after the earthquake, and may be of interest in identifying portions of the network which are critical with respect to the continued connectivity of the network and allows the determination of direct economic loss.

- **Level II** is further considering the network capacity to accommodate traffic flows (Kiremidjian et al, 2006; Werner et al., 2000; Shinozuka et al., 2003a). In the latter study, the damage to the network, (determined based on Monte Carlo simulation of probabilistically defined seismic scenarios and fragility curves of the bridges), causes traffic congestion, resulting in increased travel time which is in turn translated into monetary terms. The latter is a first approximation of the indirect loss caused by the earthquake. The analysis is repeated at fixed interval of times after the event taking into account the repair process to evaluate the distribution of increased travel time (driver's delay) with time elapsed from the event.

- **Level III** is the most general approach, which aims at obtaining a realistic estimate of total loss, inclusive of direct physical damage to the built environment (residential and industrial buildings as well as network com-

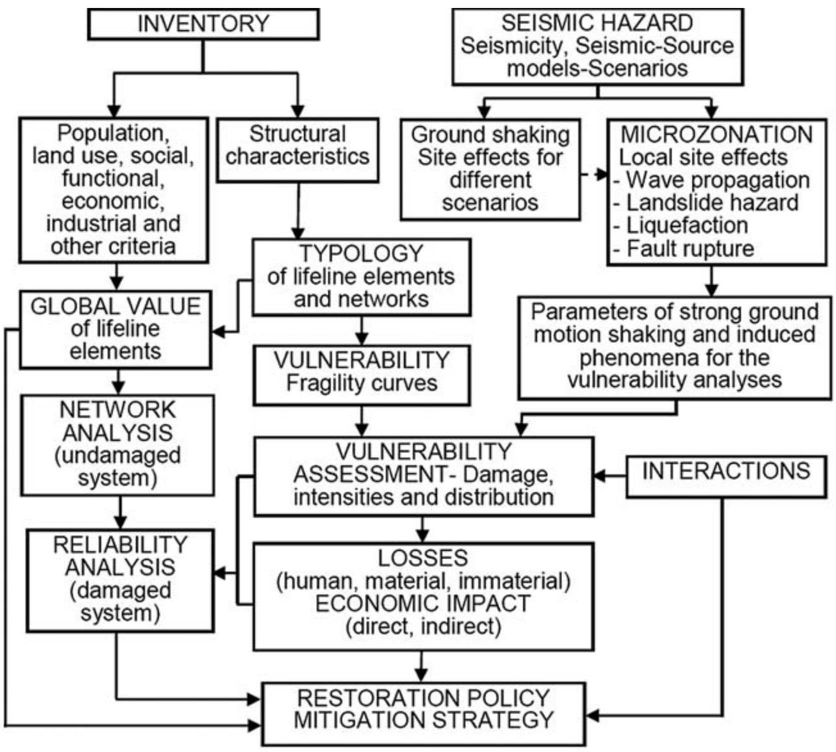

Figure 2: Flowchart of the methodology for the vulnerability and risk assessment of lifelines (Pitilakis et al, 2006)

ponents), network-related loss (increased travel time) and loss due to reduced activity in the economic sectors (industry, services) (Karaca, 2005; Veneziano et al., 2002). Economic interdependencies are accounted for, such as the reduction in demand and supply of commodities (due to damaged factories, etc.), hence in the demand for travel, and due to the increased travel costs. At this level the relevance and the complexity of the economic models become dominant over that of the transportation network.

The global vulnerability is expressed in terms of physical vulnerability of the elements at risk and the economic-societal vulnerability which is much more complicated and less studied so far. Advanced research and multilevel applications have been performed in Europe during the last years concerning the seismic risk assessment and mitigation of buildings and lifelines (see RISKUE, 2001–2004; LessLoss, 2004–2007; SRMLIFE, 2003–2007). Similar studies for the earthquake impact assessment have been carried out in the USA (e.g. Elnashai et al, 2008). The physical vulnerability and risk assessment of lifeline systems and in particular of the transportation systems are usually performed with the general scheme. The main points of this general flow methodology are summarized in the following paragraphs with few representative examples of application in a city scale (Thessaloniki, Greece).

3. Inventory-Typology

Inventory is an essential step to identify, characterize and classify all types of transportation elements according to their specific typology and their distinctive geometric, structural and functional features. GIS offers the perfect and indispensable platform to implement any inventory inquires; however, several difficulties arise in the collection and archiving of the data. Besides the great inherent uncertainties the key assumption in the vulnerability assessment of transportation systems is that structures having similar structural characteristics, being in similar geotechnical conditions, are expected to perform in the same way for a given seismic loading (source and path effects are excluded). Within this context, the damage is directly related to structural properties of the transportation elements. Typology is thus a fundamental descriptor of a system, derived from the inventory of each element at risk.

4. Vulnerability Assessment

4.1 Damage Levels

The most common way to define earthquake physical consequences (damages) in transportation components is a classification in terms of the following damage states: No damage – Slight / minor – Moderate – Extensive – Complete. This qualitative approach requires an agreement about the meaning and the content of each damage state; in general the definition of damage states is rather sub-

Table 1: Description of damage states for roads

Damage state	Description	Serviceability level
No	/	Fully open.
Minor	Slight settlement (<30cm) or offset of the ground.	Open to traffic. Reduced speed during repairs.
Moderate	Moderate settlement or offset of the ground (30 to 60cm).	Fully closed due to temporary repairs for few days. Partially closed to traffic due to permanent repairs for few weeks. The duration of closure depends on the length and width of damaged roadway.
Extensive/ Complete	Major settlement or offset of the ground (>60 cm).	Fully closed due to temporary repairs for few days to few weeks. Partially closed to traffic due to permanent repairs for few weeks to few months. The duration of closure depends on the length and width of damaged roadway.

jective. Damage states are usually related to functionality capacity and restoration time of each component. As an example the damage states for roads are described in Table 1.

4.2 Fragility Approaches

Approaches using the *vulnerability index* are mainly used for the ranking of bridges, based on a rating system that combines the main factors affecting the seismic behaviour of the structure. The year of design, the type and geometry/morphology of superstructure, the pier and abutment detailing, the seat length, and the skewness are considered as main factors of vulnerability. Such methods have been proposed by Kawashima & Unjoh (1990), Kim (1993), Pezeshk et al. (1993), Buckle & Friedland, (1995), Basöz (1996) among others.

Approaches based on *fragility curves*, which describe the probability of an element at risk, to be in or to exceed different damage states for a given seismic intensity, are widely used. They are usually described as two parameter cumulative probability density functions, characterized by a median value of ground shaking or failure and an associated dispersion factor (lognormal standard deviation) for each damage state. A representative example is given in Figure 3. These curves could be derived:

– Empirically, based on statistical analysis of damage data from past earthquakes. (Basöz and Kiremidjian, 1998, Yamazaki et al., 2000, Shinozuka et al., 2003b for bridges; Nariyuki et al. 2004, for road embankments; ALA, 2001 for tunnels).
– Analytically, based on numerical simulations (Shinozuka et al. 2000, 2003b, Choi et al. 2004, NIBS, 2004, for bridges; Argyroudis et al., 2007, for tunnels).
– Based on expert judgement, using questionnaires, by which the experts are queried on the probability of a component being in a certain damage state for a given intensity (ATC, 1985, 1991).

In general it is not always realistic to compare the empirical and analytical fragility curves as they are constructed using two different methods and input data. However, the comparison between the empirical (NIBS, 2004; ALA 2002) and analytically derived curves (Argyroudis et al., 2007) in case of tunnels, shows that the empirical curves are rather describing an average response. These curves are based on PGA values which have been back-calculated at the tunnel location using attenuation models, (presenting the well known inherent uncertainties), while the uncertainties in the ground motion and in the tunnel performance are also considered. Analytical fragility curves are able to take into account specific features such as the local soil conditions, which are proved to be important for the seismic response of underground structures (Figure 4).

5. Seismic Hazard Analysis

Seismic hazard in case of vulnerability analysis and risk assessment of transportation systems must be specified according to the precise needs for the particular components, networks as well as the models used to describe vulnerability fragility curves or relationships.

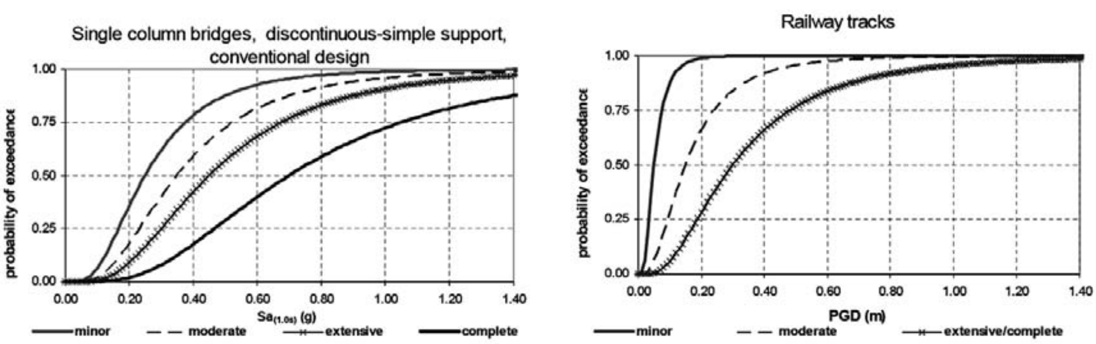

Figure 3: Example of fragility curves for concrete bridges and railway tracks (NIBS, 2004)

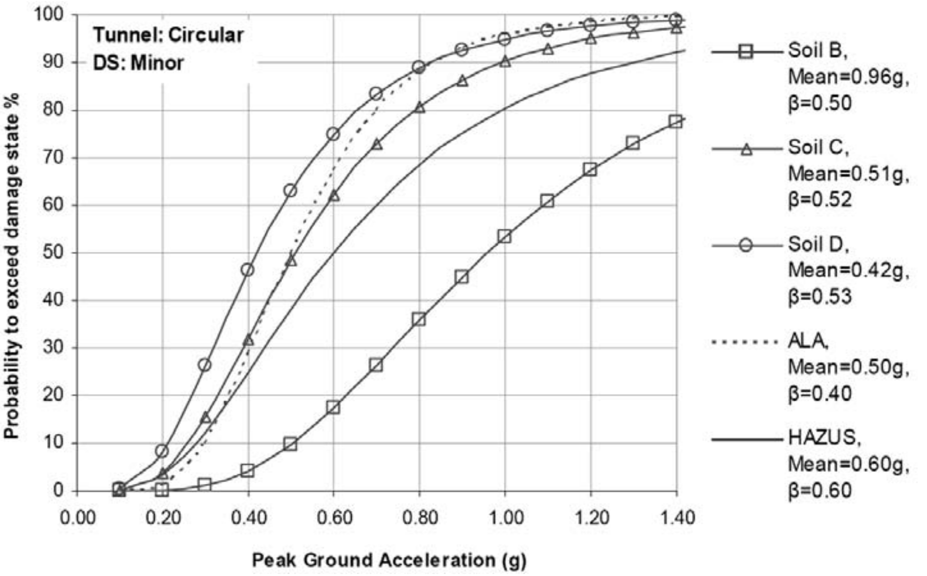

Figure 4: Comparison of empirical and analytical fragility curves for circular tunnel section in minor damage state (Argyroudis et al, 2007)

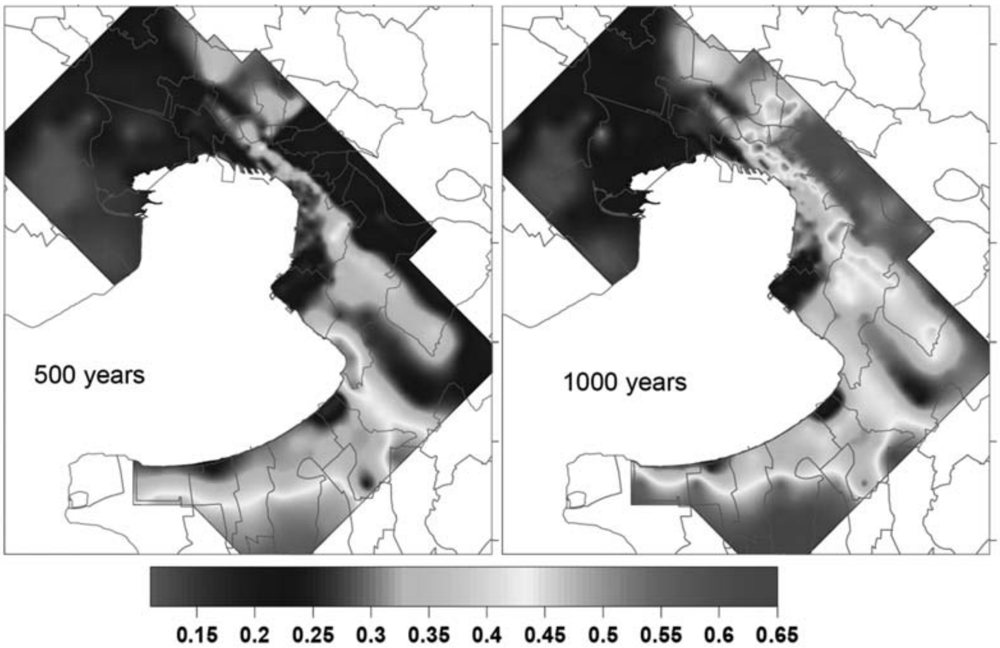

Figure 5: Distribution of mean »peak« acceleration values at surface (g) in Thessaloniki, based on seismic response analysis for two scenarios (Pitilakis et al, 2007)

Moreover due to the large extent of transportation systems, it should describe the spatial variability of ground motion considering local soil conditions, topographic effects etc. For bridges the best descriptor is a response spectral value at a specific period (i.e. T = 1.0 sec). For other components it may be peak ground acceleration (i. e. waterfront structures) or even the permanent ground deformations (i.e. embankments, roadways, railways). So, it is absolutely necessary to perform site specific seismic hazard analyses. The seismic hazard analysis may be probabilistic or scenario based; the later being usually applied in practice.

6. Losses Estimation

The losses from a destructive earthquake are distinguished as direct and indirect. Direct losses are estimated in terms of physical damages (i.e. failure of a bridge pier). Indirect losses are in many cases more important, as after the main event and the aftershocks a chain of induced losses are generated. For example, a damaged roadway network can cause losses not only due to the structural damages of the individual components, but mainly because the potential inability of transportation facility, which is affecting seriously all production, economic and social sectors. The estimation of direct losses is usually based on the repair or replacement cost of the damaged elements according to the vulnerability assessment and the definition of damage states. The estimation of indirect losses is a more complicated issue, where time is an important factor due to the restoration process. In any case the result of loss estimation is a valuable tool for decision-makers in order to develop appropriate seismic risk mitigation strategies.

Losses due to interactions between systems and elements may be also very important and exceed direct consequences, (for example losses of port system due to damages in electric power facilities). Another important threat for road network in urban areas, with high building density, is the collapse of buildings that can partially or fully block the adjacent streets and consequently the rescue and restoration activities could be prevented.

7. Seismic Risk Management

An advanced seismic risk study of a transportation system should include the functional and social vulnerability, taking into account the functional relations between the different elements, urban activities (production, consumption, exchanges) and relations of the network with its surrounding urban or rural environment. In that way each network will be analyzed as an integrated part of the seismic risk scenario and as a part of the urban system, with human, material and immaterial elements. The main issues of the system will be identified through ranking of the value of the exposed elements, based on various factors that describe the importance and role of each element in the urban system. As an example, such factors for road bridges could be the traffic volume (on and under the bridge), the type of crossed element (river, railway, and motorway), the emergency importance (ex. access to hospital), the historical value, the monetary value and others. This kind of analysis is useful for the definition of priorities for efficient risk mitigation strategies, such as the retrofitting actions or the restoration works (Figure 6).

8. Application

The above methodology to estimate physical damages and to perform seismic risk analysis has been applied in the city of Thessaloniki in Greece. Appropriate fragility curves have been used for the transportation elements at risk (bridges, tunnels, waterfront structures etc).

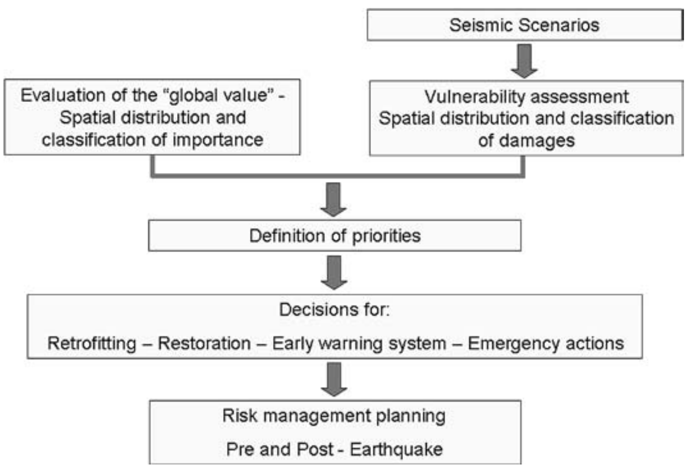

Figure 6: Risk management layout

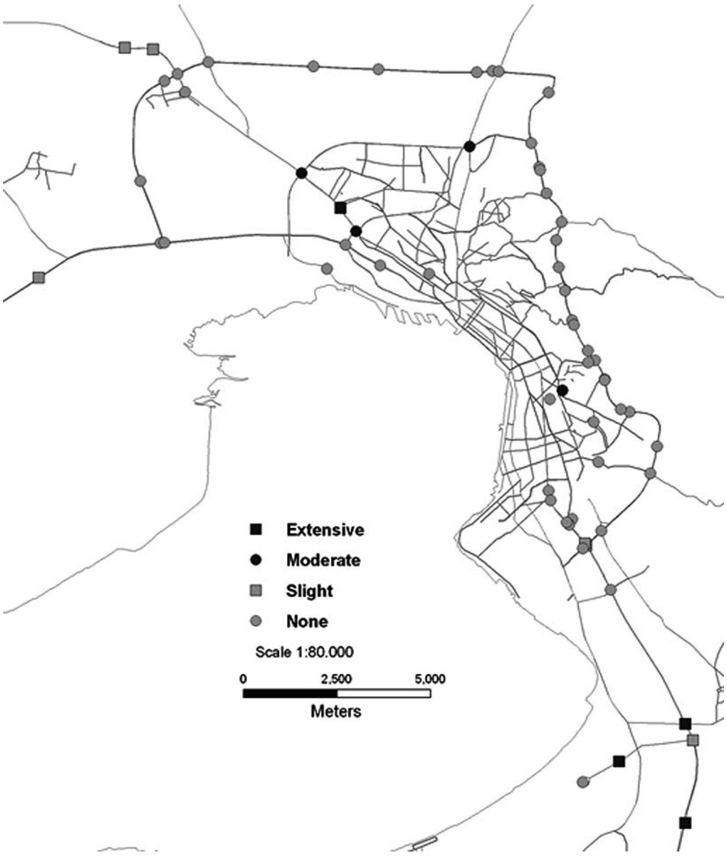

Figure 7: Vulnerability assessment of Thessaloniki roadway bridges for the scenario with T = 1000 yrs.

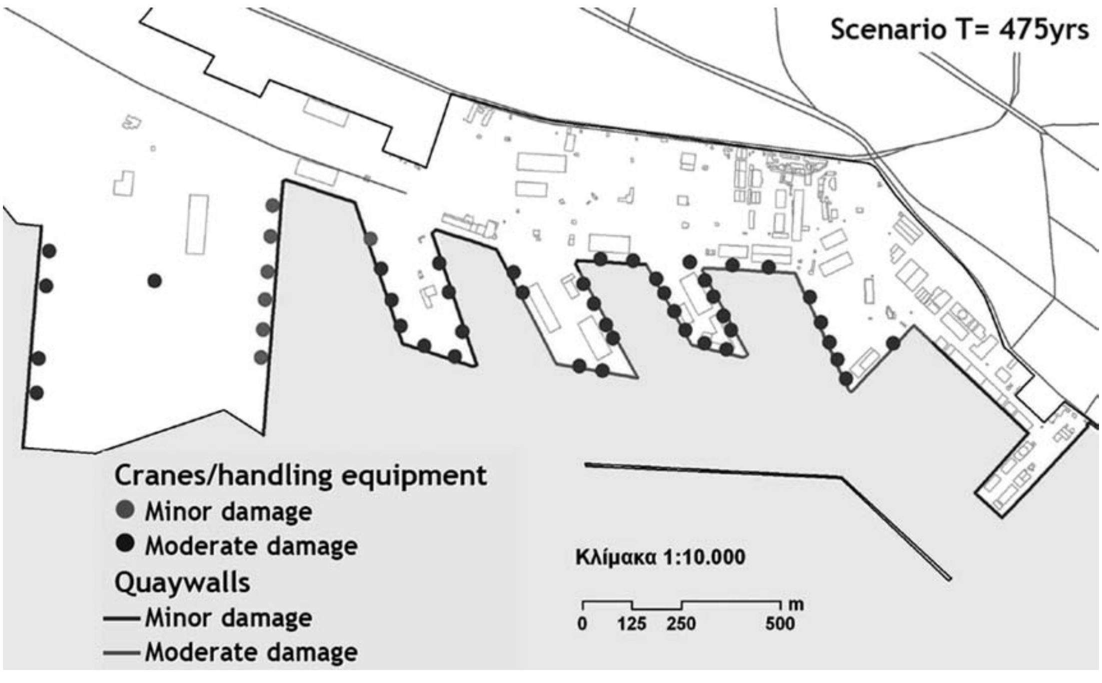

Figure 8: Vulnerability assessment of Thessaloniki port (cranes and quaywalls) for the scenario with T = 475 yrs.

They were derived either from existing ones (e.g. NIBS, 2004), or they have been constructed based on analytical approaches (e.g. for metro tunnels).

The risk assessment is performed for three seismic hazard scenarios with mean return period equal to 100, 475 and 1000 years. Site effects due to local soil conditions, are taken into account through analytical and very detailed seismic response analyses (see Fig. 5). Indicative examples are illustrated in Fig. 7 and 8 for roadway bridges and port facilities. The risk management priorities for the transportation systems in Thessaloniki are defined based on the combination of vulnerability assessment and the classification of importance. The later is estimated using value indicators and appropriate criteria.

9. Conclusions

The scope of the seismic risk assessment is:

– to define the vulnerable elements of the system;
– to estimate the direct and indirect losses;
– to assess the weak points and areas of the network in order to define the priorities for efficient pre earthquake (retrofitting) and post earthquake (restoration) actions;
– to design the configuration and the deployment of the appropriate early warning system;
– to design and support the emergency interventions (e.g. define appropriate routes for emergency vehicles) based on the early warning system information and the estimation of expected damages.

Nowadays, the advanced seismic risk assessment of lifeline systems, and in particular of the transportation systems, is possible using modern technologies and know-how. The existing methodologies are rather robust and powerful. However, further improvements are necessary, especially in the field of physical and non-physical vulnerability estimation methods. A reliable and realistic vulnerability assessment of elements and systems is the basis for any seismic risk management policy and strategy scheme. Regarding in particular the early warning systems, the results of a specific vulnerability analysis and the consequent global loss assessment, are essential factors for the design of these systems, which properly designed and maintained, may be an important parameter for an efficient seismic risk management.

References

American Lifelines Alliance (2001): Seismic Fragility Formulations for Water Systems. Part 1 – Guideline. ASCE-FEMA, 104 pp.

Applied Technology Council (1985): ATC-13-Earthquake Damage Evaluation Data for California, Redwood City, California.

Applied Technology Council (1991): ATC-25-Seismic Vulnerability and Impact of Disruption on Conterminous United States, Redwood City, California.

Argyroudis S., Pitilakis K., Boussoulas N., Nakou, F. (2007): Vulnerability Assessment of Shallow Metro Tunnels in Greece, In proceedings of the 4th International Conference on Geotechnical Earthquake Engineering, June 25–28, Thessaloniki, Greece, paper ID: 1693.

Basöz, N. (1996): Risk Assessment for Highway Transportation Systems, Ph.D. Thesis, Department of Civil Engineering, Stanford University, July.

Basöz, N., Kiremidjian, A.S. (1998): Evaluation of Bridge Damage Data from the Loma Prieta and Northridge, California Earthquake. Technical Report MCEER-98-0004, State University of New York, Buffalo.

Buckle I. G. & Friedland I. M., (ed), (1995): Seismic Retrofitting Manual for Highway Bridges, Report FHWA-RD-94-052, Grant DTFH61-92-C-00106, Sponsored by the Office of Engineering and Highway Operations R&D, Federal Highway Administration, Washington, DC.

Choi, E., DesRoches, R., and Nielson, B. (2004): Seismic Fragility of Typical Bridges in Moderate Seismic Zones, Engineering Structures, vol. 26., no. 2, pp. 187–199.

Elnashai Á.S., Cleveland L.J., Jefferson T., Harald J., (2008): Impact of Earthquakes on the Central USA. Mid-America Earthquake Center Report 08-02, September.

Franchin, P., Lupoi, A., Pinto, P.E. (2006): On the Role of Road Networks in Reducing Human Losses after Earthquakes, Journal of Earthquake Engineering, Vol 10(2), pp. 195–206.

Karaca, E. (2005): Regional Earthquake Loss Estimation: Role of Transportation Network, Sensitivity and Uncertainty, and Risk Mitigation. PhD thesis, MIT, Cambridge, MA.

Kawashima K., & Unjoh S., (1990): An Inspection Method of Seismic Vulnerability of Existing Highway Bridges, Structural Eng./Earthquake Eng., 7 (1): 143–150.

Kim, S. H. (1993): A GIS-based regional risk analysis approach for bridges against earthquakes, Dissertation, State University of New York at Buffalo, Department of Civil Engineeing.

Kiremidjian A., Moore J., Fan Y. Y., Basöz N., Yazali O., Williams M., (2006): Highway Demonstration Project, PEER Report 2006/02, Pacific Earthquake Engineering Research Center, College of Engineering University of California, Berkeley.

LessLoss (2004–2007): Risk Mitigation for Earthquakes and Landslides. Research Project European Commission, DG XI, Contract: GOCE-CT-2003-505448 (URL:http://www.lessloss.org).

Nariyuki, Y., Hirao, K., Fukui, Y., (2004): Discriminant Analysis of Street-Blockades in Kobe City due to the 1995 Hyogoken-Nanbu Earthquake, in: Proceedings of 13th World Conference on Earthquake Engineering, Vancouver, B.C., Canada, August 1–6, Paper No. 1296.

National Institute of Building Sciences (NIBS), (2004): HAZUS-MH: Users's Manual and Technical Manuals. Report prepared for the Federal Emergency Management Agency, Washington, D.C.

Nuti, C. and Vanzi, I. (1998): Assessment of Post-Earthquake Availability of Hospital System and Upgrading Strategies, Earthquake Engineering & Structural Dynamics, 27, pp. 1403–1423.

Pezeshk, S., Chang, T. S., Yiak K. C. & Kung H. T. (1993): Seismic vulnerability evaluation of bridges in Memphis and Shelby County, Tennessee, Earthquake Spectra, 9(4): 803–816.

Pitilakis K., Alexoudi A., Argyroudis S., Monge O., Martin C., (2006): Chapter 9: Vulnerability and risk assessment of lifelines, in: Goula X., Oliveira C. S. & A. Roca (ed): Assessing and Managing Earthquake Risk, Geo-scientific and Engineering Knowledge for Earthquake Risk Mitigation: developments, tools, techniques, Springer: 185–211.

Pitilakis K., Anastasiadis A., Kakderi K., Argyroudis S., and Alexoudi M., (2007): Vulnerability assessment and risk management of lifelines, infrastructures and critical facilities. The case of Thessaloniki's Metropolitan area, in: Proceedings of the 4th International Conference on Geotechnical Earthquake Engineering, June 25–28, Thessaloniki, Greece, paper ID: 1774.

RISK-UE (2001–2004): An Advanced Approach to Earthquake Risk Scenarios with Applications to Different European Towns. Research Project, European Commission, DG ◊I, Contract: EVK4-CT-2000-00014 (URL:http://www.risk-ue.net).

Shinozuka M., Murachi Y., Dong X., Zhou Y., Orlikowski M. J., (2003a): Seismic performance of highway transportation networks, in: Proceedings of the China-US Workshop on

Protection of Urban Infrastructure and Public Buildings against Earthquakes and Manmade Disasters, Beijing, China, 21–22 February.

Shinozuka, M., Feng, M. Q., Kim, H.-K., and Kim, S.-H. (2000). Nonlinear Static Procedure for Fragility Curve Development. Journal of Engineering Mechanics, 126 (12), 1287–1296.

Shinozuka, M., M. Q. Feng, H.-K. Kim, T. Uzawa, T. Ueda (2003b). Statistical Analysis of Fragility Curves, Technical Report MCEER-03-0002, State University of New York, Buffalo.

SRMLIFE (2003-2007): Development of a Global Methodology for the Vulnerability Assessment and Risk Management of Lifelines, Infrastructures and Critical Facilities. Application to the Metropolitan Area of Thessaloniki. Research Project, General Secretariat for Research and Technology, Greece.

Veneziano, D., Sussman, J., Gupta, U., Kunnumkal, S.M. (2002): Earthquake Loss under Limited Trasnsportation Capacity: Assessment, Sensitivity and Remediation, in: Proceedings of the 7th USNCEE, Boston, MA, USA.

Werner S. D, Taylor C. E., Moore J. E., Walton J.S., Cho S., (2000): A risk-based methodology for assessing the seismic performance of highway systems, Technical Report MCEER-00-0014, State University of New York, Buffalo.

Yamazaki F., Motomura H., Hamada T., (2000): Damage assessment of expressway networks in Japan based on seismic monitoring, in: Proceedings of 12th World Conference on Earthquake Engineering, CD-ROM, Paper No. 0551.

Railway System and Seismic Load

Hennecke M.
Zilch + Müller Ingenieure GmbH, Munich

1. Introduction

Railway systems can be heavily affected by earthquakes. Damages can cause direct loss of life, breakdown of the railway net and disruption of the economic activity in a region. The railway system consists of tracks, structures as bridges, tunnels and buildings, electric power supply and a complex control system with signals, communications equipment and central control units.

Due to the high speed of modern trains (up to 300 km/h), the permitted deflections of the tracks are very low. Damage at a single element of the railway system can cause a total disruption of the entire system. A normal train transports several hundred passengers. Due to these points the railway system is more vulnerable than the road system.

In this paper impacts of seismic loads on railway systems will be discussed. The focus will be on the train stability, but first a survey of pertinent railway system damages will be given.

2. Types of Damages

Geology and Ground

Earthquakes are sudden motions of the ground. So it is easy to see, that the ground is primarily affected. The effects are surface faulting, rockfall, landsides or soil liquefaction.

Tracks

The tracks are the essential element of the railway system. There are two construction types. The common one consists of ballast, sleepers and the rails. For high speed trains the slab track system has been developed. A slab track consists of reinforced concrete plates, on which the rails are fixed. Due to earthquake motions tracks be can demolished by deflection and acceleration. Characteristic damages are embankment failure and track misalignment.

Structures

Bridges and tunnels can be destroyed by earthquakes. Due to the defection of the ground a failure of the tunnel lining can occur. Bridges can be affected by dislocations, deformations and destruction of structure elements.

Buildings

To the railway system belong a lot of buildings as stations and control centers. The buildings have an import function for the system. The use of a train without a station is not possible.

Trains

Due to the ground acceleration the stability of the train can be disturbed. The trains can be overturned or derailed. This can cause injury or loss of life of the passengers.

Passengers

The access of the passengers to the trains in stations can be disturbed, if stations are evacuated or even destroyed. A railway system without passengers is not a functioning railway system.

In Table 1 damages are allocated in two groups.
– infrastructure
– service

Finally, both groups will affect the service, but the strategy to avoid damages is different. The service will be affected directly.

Table 1: Matrix of damages

	Service		Infrastructure				
	trains	passengers	soil	track	tunnel	bridges	buildings
Overturned trains	X						
Rockfalls			X				
Soil liquidation			X				
Embankment failure				X			
Track misalignment				X			
Damage of the Construction		X			X	X	X
Hazard due to destroyed structures	X	X					

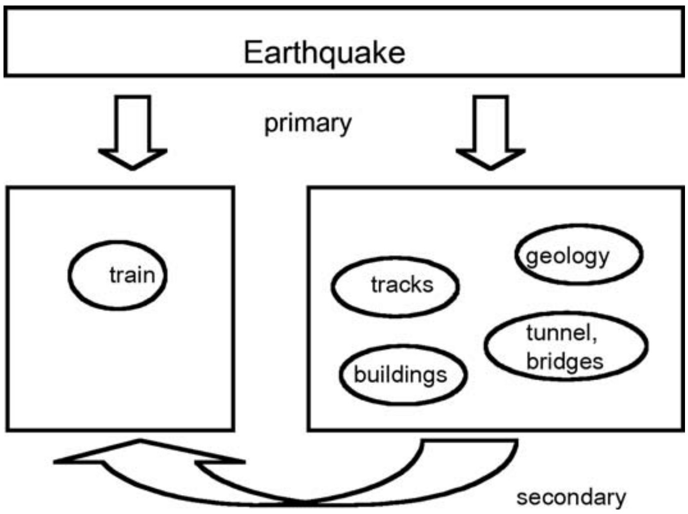

Figure 1: Damages to the railway system

In Fig. 1 a structure of the effects of an earthquake on the railway system is shown. The service can be primarily affected by perturbing the stability of running trains and secondarily by destroyed infrastructure.

The only way to reduce or avoid earthquake damages at the infrastructure is appropriate planning and construction. This process starts with a site investigation including the issue of potential earthquake risks. For buildings, bridges and other physical structures the design must take into account the action of an earthquake to the structure, and finally the construction work must be accurate. The achievement of good construction work can be seen in the comparison of the degree of damage in countries with different levels of structural engineering. The degree of damages in a country with a high state of the art is much reduced in comparison to countries with a lower level of civil engineering skills.

In the field of service the degree of damage can be reduced by risk managing. This could be for example the evacuation of a station or stopping of a train. By reducing the speed of a train the safety can be increased in a case of an earthquake. For this way of risk management early information is essential.

3. Train stability under seismic loads

In this section , the special topic of derailed and overturned trains will be discussed.

In Fig. 3 the forces, accelerations, and characteristic distances of the train on the tracks are shown.

Due to the centrifugal forces the forces on both tracks are different. To reduce the difference between the both tracks, there is a cant. This cant is estimated for a specific speed of the train and is called u_0. If a train is running faster, there is a cant deficiency. This cant deficiency $\Delta u = u_0 - u$ must not exceed a certain value and thus limits the maximum speed of the trains.

In the following equations the forces on the tracks are shown as a function of the cant deficiency. For the definition of symbols see Fig. 3.

Train stability requires that the sum of torques with respect to the centre of mass vanish. With, $P = P_1$ the equilibrium condition reads

$$P \cdot e = -Q_t \cdot h + Q_v \cdot \left(\frac{e}{2} + \frac{u \cdot h}{e} \right)$$

$$P = -\frac{v^2 \cdot Q_v}{g \cdot r} \cdot \frac{h}{e} + Q_v \cdot \left(\frac{1}{2} + \frac{u \cdot h}{e^2} \right)$$

$$P = Q_v \cdot \left(\frac{1}{2} + \frac{u \cdot h}{e^2} - \frac{v^2 \cdot h}{g \cdot r \cdot e} \right)$$

$$P = Q_t \cdot \left(\frac{1}{2} + \frac{(u_0 - \Delta u)h}{e^2} - \frac{v^2 \cdot h}{g \cdot r \cdot e} \right)$$

$$P = Q_t \cdot \left(\frac{1}{2} + \frac{u_0 \cdot h}{e^2} - \frac{v^2 \cdot h}{g \cdot r \cdot e} - \frac{\Delta u \cdot h}{e^2} \right)$$

$$P = Q_t \cdot \left(\frac{1}{2} + \frac{v^2 \cdot e}{g \cdot r \cdot e^2} - \frac{v^2 \cdot h}{g \cdot r \cdot e} - \frac{\Delta u \cdot h}{e^2} \right)$$

$$P = Q_t \cdot \left(\frac{1}{2} - \frac{\Delta u \cdot h}{e^2} \right) = Q_{t,k} \cdot \left(\frac{1}{2} - \frac{\Delta u \cdot 1{,}8}{1{,}5^2} \right)$$
$$= Q_t \cdot \left(\frac{1}{2} - 0{,}8 \Delta u \right)$$

$$P = \frac{1}{2} Q_v \cdot (1 - 2 \cdot 0{,}8 \Delta u)$$
$$= Q_{\text{wheel}} \cdot (1 - 2 \cdot 0{,}8 \Delta u)$$

Figure 2: Overturned train

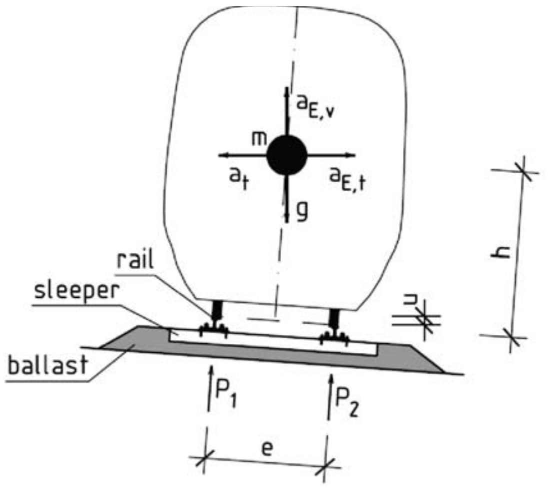

Figure 3: Train on the track

Cant deficiency causes unequal loads on the both rails of the track. They are:

$$P_{\min} = Q_{\text{wheel}} \cdot (1 - 1{,}6 \cdot \Delta u)$$
$$P_{\max} = Q_{\text{wheel}} \cdot (1 + 1{,}6 \cdot \Delta u)$$

This function is based on the centrifugal forces and the corresponding acceleration in an arc. But there are additional horizontal accelerations, because of horizontal track irregularities and of the sinusoidal train motion. All these dynamics effects result in an unequal load on both rails, which can be calculated by the empirical formulae

$$Q_{\text{dyn}} = Q_{\text{stat.}} + \Delta Q_{\text{stat.}} = Q_{\text{stat}} \cdot (1{,}1 \ldots 1{,}2)$$
$$\Delta Q_{\text{stat}} = (0{,}1..0{,}2)\, Q_{\text{stat}}$$
$$\Delta Q_{\text{stat}} = 2 \cdot 0{,}8 \cdot \Delta u \cdot Q_{\text{stat}} = 0{,}2 \cdot Q_{\text{stat}}$$
$$\Delta u = \frac{0{,}2}{2 \cdot 0{,}8} = 0{,}125 [\text{m}]$$

$$a_T = g \frac{\Delta u}{e} = 9{,}81 \cdot \frac{0{,}125}{1{,}5} = 0{,}82\, [\text{m}/\text{s}^2]$$

Due to vertical track irregularities there is dynamic behaviour in the train run. The dynamic vertical forces depend on the quality of the track and the speed of the train. These effects can be estimated by the empirical functions:

$$Q_{v\,\text{dyn.}} = s \cdot Q_{\text{stat.}}$$
$$s = n \cdot \phi$$

where n is a factor characterizing the track condition and ϕ is factor that depends on the train speed.

track in very good condition	$n = 0{,}1$
track in good condition	$n = 0{,}2$
track in poor condition	$n = 0{,}3$

In the following equations the influence of the vertical $a_{v,E}$ and horizontal $a_{t,E}$ ground acceleration to the train stability can be shown.

$$P \cdot e = m \cdot (g - a_{E,v}) \cdot \left(\frac{e}{2} - \frac{u \cdot h}{e} \right) - m \cdot a_{E,t} \cdot h$$
$$P = m \cdot g \cdot \left(\frac{1}{2} - \frac{u \cdot h}{e^2} \right) - m \cdot a_{E,v}$$
$$\times \left(\frac{1}{2} - \frac{u \cdot h}{e^2} \right) - m \cdot a_{E,t} \cdot \frac{h}{e}$$
$$P = g \cdot \left(\frac{1}{2} - 0{,}8 \cdot u \right) - a_{E,v}$$
$$\times \left(\frac{1}{2} - 0{,}8 \cdot u \right) - a_{E,t} \cdot \frac{h}{e}$$

Critical limit state

$$P = 0$$
$$m \cdot g \cdot \left(\frac{1}{2} - 0{,}8\, \Delta u \right) - m \cdot a_{E,v}$$
$$\times \left(\frac{1}{2} + \frac{u \cdot h}{e^2} \right) - m \cdot a_{E,t} \cdot \frac{h}{e} = 0$$
$$\left(\frac{1}{2} - 0{,}8\, \Delta u \right) - \frac{a_{E,v}}{g}$$
$$\times \left(\frac{1}{2} + \frac{u \cdot h}{e^2} \right) - \frac{a_{E,t}}{g} \cdot \frac{h}{e} = 0$$
$$\frac{a_{E,v}}{g} \cdot \left(\frac{1}{2} + \frac{u \cdot h}{e^2} \right) + \frac{a_{E,t}}{g} \cdot \frac{h}{e} = \left(\frac{1}{2} - 0{,}8\, \Delta u \right)$$
$$a_{E,v} (0{,}051 + 0{,}8u) + 0{,}1223 a_{E,t} =$$
$$\left(\frac{1}{2} - 0{,}8\, \Delta u \right)$$
$$a_{E,v}$$
$$= \frac{1}{(0{,}051 + 0{,}8u)} \cdot \left(\frac{1}{2} - 0{,}8\, \Delta u - 0{,}1223 a_{E,t} \right)$$

The critical limit state depends on the horizontal und vertical ground acceleration and the cant deficiency of the track. The train is more vulnerable to horizontal than to vertical accelerations. The straight lines in Fig. 4 sepa-

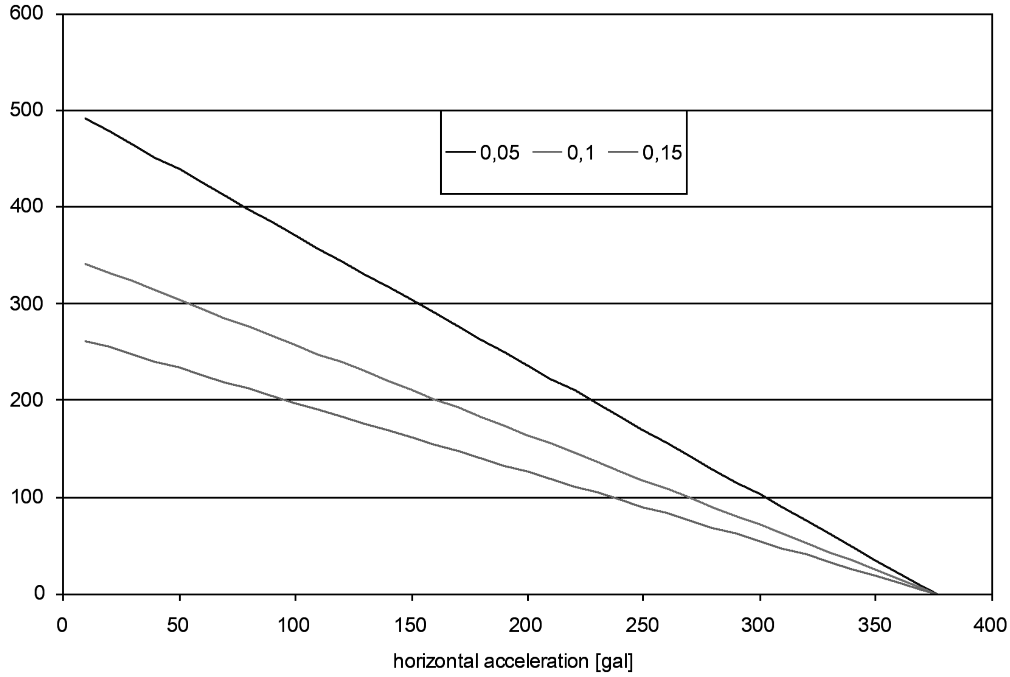

Figure 4: Critical limit state for different cant deficiencies

rate potentially safe from unsafe regions of ground accelerations for the considered failure mode of train overturning.

4. Summary

In this paper, I have discussed some effects of seismic loads on railway systems. As an example, the vulnerability of moving trains with respect to the failure mode of overturning has been considered in more detail and a relationship between horizontal and vertical ground accelerations has been derived. The latter separates potentially safe and unsafe regions of ground accelerations.

Seismic vulnerability assessment of motorway bridges

Meskouris K. (1), Renault P. (2)

(1) Baustatik und Baudynamik, RWTH Aachen University, Mies-van-der-Rohe-Str. 1, 52074 Aachen
e-mail: meskouris@lbb.rwth-aachen.de

(2) swissnuclear, P.O. Box 1663, CH-4601 Ofden
e-mail: philippe.renault@swissnuclear.ch

Abstract

The paper presents a general Seismic Vulnerability Benchmark System (SVBS) for bridges, developed within the framework of the research project »Seismic vulnerability assessment of bridges in Germany« funded by the German Federal Highway Research Institute. For each bridge type, a three-level vulnerability assessment procedure is provided and the system is linked to the national database which contains detailed information of all important motorway bridges in Germany. The level of assessment and the corresponding effort can be chosen depending on the importance of the bridge and the required scope and accuracy of the results. The practical use of the method is demonstrated by an example dealing with the Rhine bridge Emmerich, the longest suspension bridge in Germany.

Key words: Earthquake engineering, vulnerability assessment, bridges, dynamic analysis, fragility curves, Rhine bridge Emmerich.

1. Introduction

During and after a strong earthquake many casualties may occur due to the blocking of road arteries because of bridge failures. In the context of a seismic evaluation it is therefore important to assess the seismic vulnerability of existing bridges in order to be able to judge their functionality in the case of a strong earthquake. The assessment procedures should take current standards into account and must be easy to use by engineering professionals. The pending introduction of the Eurocode 8, part 2 [1] has been instrumental in motivating this project.

In the following, a general seismic vulnerability assessment system for bridges is presented, developed in the research project »Seismic vulnerability assessment of bridges in Germany« funded by the German Federal Highway Research Institute. The main feature of the system is a classification of bridges according to typology and the provision, for each bridge type, of a three-level comprehensive vulnerability assessment procedure. The system is linked to the national bridge database »SIB-Bauwerke« [2], which contains authoritative information for all strategically important motorway bridges in Germany. The assessment level (1, 2 or 3, in ascending order of required effort and degree of accuracy of the obtained results) is chosen depending on the importance of the bridge in question and the findings of the assessments carried out at a lower level (e.g. a Level 1 investigation may be complemented by a Level 2 investigation, the latter with a Level 3 investigation if deemed necessary).

2. Description of the approach

As already mentioned, the vulnerability assessment procedure contains three investigation levels with increasing expenditure of time and higher demands for information about the bridge structure. The implementation has been carried out in form of a management system linked to the existing national motorway bridge database. In the following the management system and the procedures in the three investigation levels are described.

2.1 Management system

The system offers engineering professionals a tool for the efficient execution of the investigation. It supports the bridge data acquisition, the determination of the seismic site hazard, the generation of the computer models, the evaluation and interpretation of the investigation results and finally the structured storage of the data on the central database server. Furthermore, the system incorporates a hierarchical user management with different levels of data access authorizations.

For obtaining the pertinent bridge data, the management system is connected to the national bridge database »SIB-Bauwerke« [2]. Data update is carried out via a secure connection over the intranet or the internet. In order to simplify data exchange, the bridge classification implemented in the national database was adopted. In accordance with this typology, the management system includes the following bridge types (Fig. 1):

– Beam girder bridges: slab, girder, tee-beam, box girder
– Frame bridges: opened, closed
– Arched bridges: spandrel-braced arch, arched trough
– Suspension bridges: one pylon, two pylons
– Cable-stayed bridges: one pylon, more than one pylon
– Cantilever-truss bridges

Each of these bridge classes is subdivided into various subclasses with respect to the type of deck continuity and the details of the supporting piers.

The site seismic hazard is described by a design spectrum, which is produced automatically according to the DIN 4149 or the EC 8 specifications depending on the earthquake zone and the ground type (Fig. 2). Optionally, there exists the possibility of introducing other spectra instead of using the ones provided by the codes. Synthetic accelerograms to be used in the third investigation level are normally generated as spectrum compatible records, but the system also supports the use of measured or otherwise obtained site-specific accelerograms.

The generation of the finite element simulation model for the second investigation level is aided by providing generalized templates for the different bridge types. These templates allow the automatic generation of the simulation models using geometry, material and cross-sectional parameters gleaned from the database.

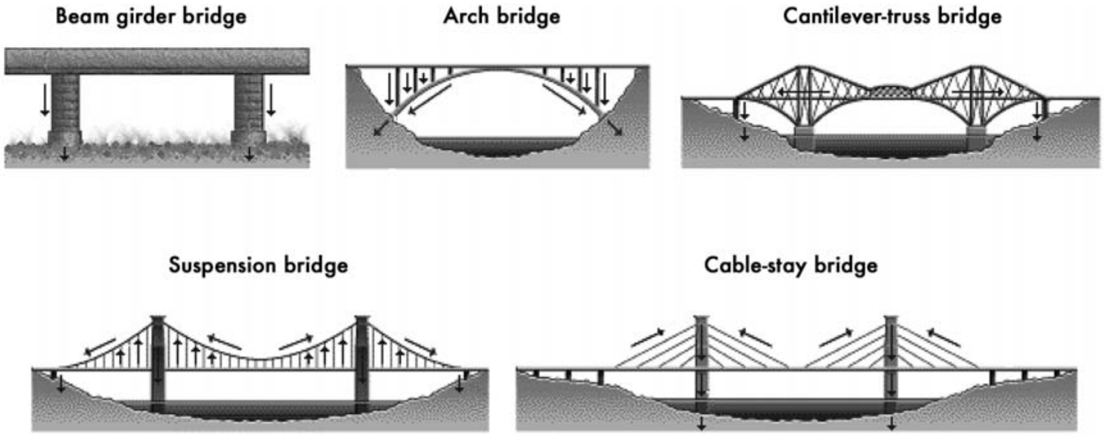

Figure 1: Bridge types included in the system

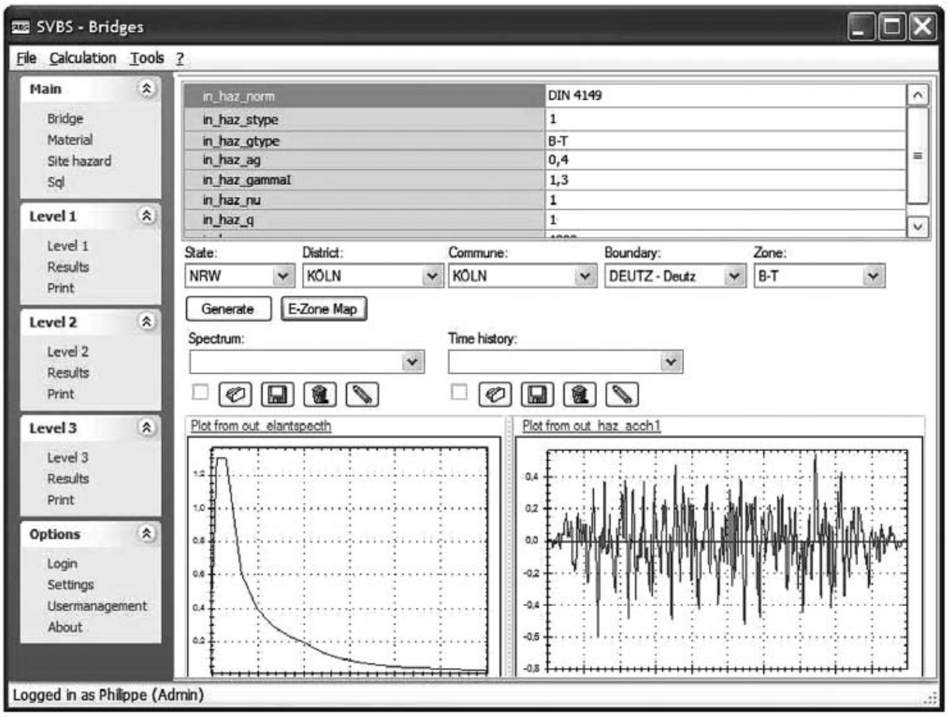

Figure 2: Management system: Definition of the seismic site hazard

The interpretation of the results is facilitated by the detailed presentation of input and output data complete with statistical evaluations and result visualizations. As the geographic position has to be entered in the management system, it offers an interface for the visualization of the results through a Geographical Information System (GIS). Finally, all bridge data and results are stored on the central database server, so that future events like long-term deterioration or rehabilitation measures can be considered. An advantage of the central database is also the continuous updating of the bridge data.

2.2 Investigation level I

In the first investigation level, the seismic behavior of the bridge is described by fragility curves which define the relation between spectral acceleration and the probability of occurrence of certain damage states. The curves are obtained using the procedure described in HAZUS-MH [4], with the bridge type, the response spectrum for the specific location and the bridge geometry required as main input parameters. The curves included in HAZUS-MH are based on a comprehensive statistical evaluation of the seismic damages on bridge structures [5] due to the Northridge and Loma Prieta earthquakes. The bridge data necessary for the calculation of the fragility curves are extracted from the national bridge database [2].

Additionally, for each bridge type an extensive evaluation system is incorporated in the management system, based on the inclusion of structural details. Bridge foundation and possible risks of base failure and soil liquefaction are also considered. The results of the evaluation system provide additional information for pinpointing the individual bridge's deficiencies. For this, more detailed bridge data stemming from bridge inspections, static calculations and construction plans are necessary. The result of the first investigation level is a first estimation involving a relatively small expenditure of time and effort. It serves as decision basis for the necessity for further investigation steps.

A priority index *P* for the bridge is evaluated by the system according to Eq. (1), with I as an importance factor based on the socio-economic importance of the bridge, V for vulnerability and S for the seismic site hazard.

$$P = V \times S \times I. \tag{1}$$

2.3 Evaluation of the importance factor

In EC 8, part 2, bridges are grouped into three different importance classes corresponding to a »less than average«, »average« and »greater than average« bridge importance. According to EC 8, national road motorway bridges and rail bridges typically fall into the »average« group. The highest importance class contains bridges with crucial co- and post-seismic functioning, further bridges the failure of which is associated with a large number of possible casualties and major bridges for which a design life greater than normal is required.

For the engineer, this description might not be readily useful or precise enough, as many parameters describing the situation might not be available. In the evaluation system, the following expression for the importance factor I of a bridge is proposed [6]:

$$I = 0.7 \cdot \left[\mathrm{ST}_{\mathrm{over}} \cdot \left(\frac{\mathrm{DTV}_{\mathrm{over}}}{\mathrm{DTV}_{\mathrm{max,\,over}}} \right)^{0{,}25} \cdot \mathrm{UL}_{\mathrm{over}} \cdot \mathrm{ESU}_{\mathrm{over}} \right] + 0.3 \cdot \left[\mathrm{ST}_{\mathrm{under}} \cdot \left(\frac{\mathrm{DTV}_{under}}{\mathrm{DTV}_{\mathrm{max},\, under}} \right)^{0{,}25} \cdot \mathrm{UL}_{\mathrm{under}} \cdot \mathrm{ESU}_{\mathrm{under}} \right]_n \tag{2}$$

Eq. (2) is in agreement with a MCEER technical report [7] and the work of Basöz and Kiremidjian [8]. The equation contains two terms, with the first one describing the importance of the road and traffic on the bridge itself (index »over«) and the second one the importance and traffic of the crossed road (index »under«). Both terms are evaluated separately and added, assuming there is no interaction. The following variables appear in (2):

- ST: Road type (e.g. 1 for Autobahn, 0.8 for Bundesstraße, 0.6 for Landesstraße)
- DTV: Average daily traffic of the road
- DTV_{max}: Maximum average daily traffic of the road
- UL: Detour of x km yields a value of $\left(0.6 + 0.4\frac{x}{150}\right)$
- ESU: Influence of the road type over/under the bridge on the road type of the detour

Values of the importance factor are between 0 and 1, from the lowest to the highest importance. Considering the three importance classes defined in EC 8, the following classification is proposed: For an importance factor $I \leq 0.2$ »less than average«, for $0.2 < I \leq 0.6$ »average« and for $0.6 < I \leq 1.0$ »greater than average«, this being in agreement with the stipulation that highway and railway bridges belong to the »average« importance class.

2.4 Investigation level II

The second investigation level includes a numerical simulation of the bridge based on an equivalent simplified linear model of the overall system consisting of linear beams connected by (in the case of suspension bridges) simple tension-only elements. Structural details are not taken into account in the simplified model. For the determination of the internal forces the modal response spectrum analysis is used. Soil-structure interaction is considered by the use of the truncated cone model of Wolf [9]. This model idealizes the soil as an homogeneous, linear elastic, half-infinite medium and can be used for foundations on homogeneous as well as on layered soils. The time spent at this investigation level essentially depends on the availability of geometrical, material and cross-section parameters. This information is entered into the template provided by the management system and by using input from the external database, the simplified numerical model is generated mostly automatically. The result of the second investigation level is the evaluation and verification of the earthquake resistance on the basis of simple design checks using the calculated internal forces and deformations. This investigation level is normally sufficient for making a reliable statement about the existing earthquake resistance.

2.5 Investigation Level III

The third investigation level is based on a detailed evaluation of the construction documents, on bridge inspections in combination with measurements of its natural frequencies and mode shapes and also on nonlinear time-history analyses using a detailed numerical model. The latter must include all critical structural details identified in the preceding investigation levels, in order to be able to take into account all possible failure mechanisms.

The measured natural frequencies are used for the calibration of the numerical model by varying the assumed stiffness distribution. Time-history analyses of the calibrated model are carried out mostly using synthetic target-compatible accelerograms generated from the elastic response spectra, if site-specific motions records (based e.g. on 1D- or 2D wave propagation models) are not available. Soil-structure interaction is considered in the same way as in the second investigation level. On this accuracy level there is no provision of general templates, so that the expenditure of time is always high. Accordingly, a third-level investigation should be limited to critical bridge structures, the seismic resistance of which can only be verified considering their nonlinear capacity reserves.

3. Investigation of the Rhine bridge Emmerich

The described approach is demonstrated by the Rhine bridge Emmerich, situated near the German border to the Netherlands. With a span length of 500 m in the main span and a total length of 800 m, the bridge is the largest suspension bridge in Germany. In case of a bridge failure, traffic would have to be rerouted under considerable difficulties over roads involving a detour of approximately 35 km. Because of the infrastructural importance of the bridge, a comprehensive investigation was carried out on all three levels.

3.1 Description of the bridge

The Rhine bridge Emmerich is a suspension bridge with two pylons and ground-anchored main cables, completed in 1965. The four-lane federal road B220 crosses the bridge with a pedestrian and bicycle lane on each side of the 22.50 m wide deck. The deck is supported by roller bearings, which allow displacements in the longitudinal direction. The 74.15 m high

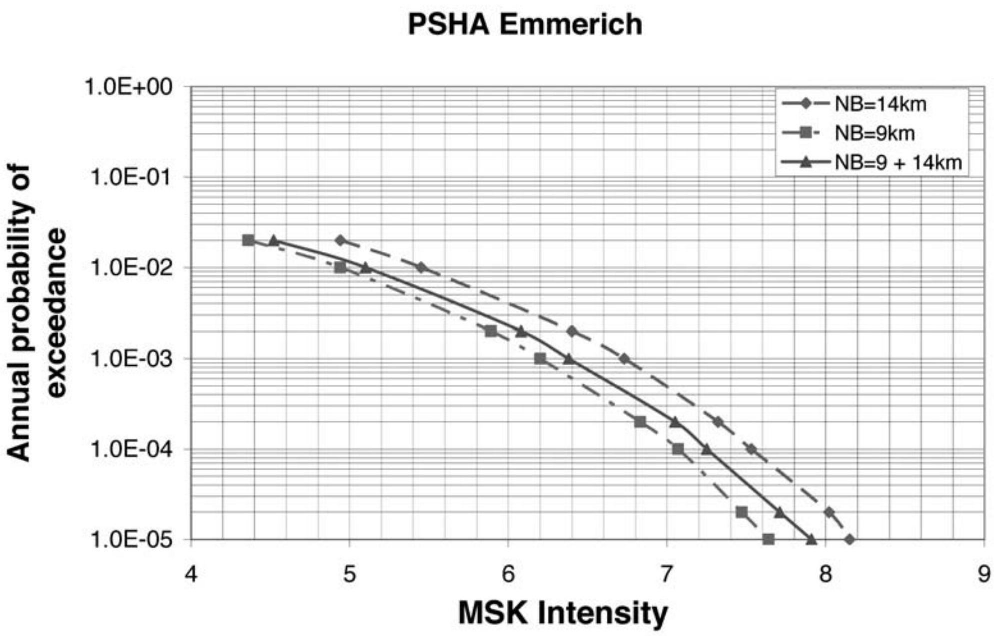

Figure 3: Seismic hazard curves for the Rhine bridge Emmerich [10]

pylons with rectangular steel box cross-sections are connected by a tie bar, thus forming a frame. The main construction material is steel S355, and the bridge has a total weight of 10200 t.

3.2 Seismic site hazard

Due to the infrastructural importance and the size of the Rhine bridge Emmerich, the site-specific seismic hazard was determined by the Federal Institute for Geosciences and Natural Resources [10] using probabilistic seismic hazard assessment (PSHA) methods. As a result, the highest possible intensity in the Lower Rhine region was determined to 8.5 MSK, while the maximum historically observed intensity amounted to 8.0 MSK. The resulting seismic hazard curves are shown in Fig. 3, with a standard deviation of 0.5 MSK.

The two exterior curves represent events with characteristic focal depths of 9 and 14 km for the Lower Rhine bay (NB). The curve used here corresponds to a weighing of the two curves by factors of $^1/_4$ for the depth of 14 km and of $^3/_4$ for the depth of 9 km. Following the conversion of intensity into soil acceleration according to the relationship of Murphy and O'Brien [11], a relationship between annual probability of exceedance and soil acceleration can be determined. Using this relationship, response spectra can be set up for deep geology class T and ground type C according to the revised version of the DIN 4149 for different exceedance probabilities.

3.3 Computer models for investigation levels II and III

In the simplified linear finite element model, the pylons, the deck and the foundations were modeled by beam elements with equivalent stiffness properties. The roller bearings were modeled by linear spring-damper elements and tension-only elements were used for the idealization of the cables. The interaction between soil and structure was considered by truncated cone models after Wolf for a homogeneous soil. The entire model consists of approximately 3500 degrees of freedom. In the detailed nonlinear model the bridge deck was modeled by shell elements. The bracing truss which accounts for the torsional rigidity in the main span was modeled with bars. The rectangular hollow cross-section of the pylon with internal stiffening by IPE profiles was modeled by a thin-walled beam element with equivalent rectangular cross-sectional shape. The detailed model has approximately 6000 degrees of freedom. To take into account physical nonlinearities, a bilinear material law for steel according to EC 3 [12] was assumed.

3.4 Seismic action

The seismic action for the simplified model of investigation level II is described by a response spectrum according to the revised version of the DIN 4149 for importance class III and a behavior factor q = 1.0. This is in agreement with EC 8, part 2, which recommends this conservative value for cable systems due to the participation of higher oscillation modes. The seismic action for the detailed model in investigation level III is an uncorrelated base excitation for the two abutments and the pier foundation. Since no measured acceleration time-history records are available for the given location, they were generated synthetically for the elastic response spectrum provided in the investigation level II for different return periods.

In EC 8, part 2, the combination of the seismic loads with other load cases is described. Here, the seismic actions were combined with the permanent dead loads, pre-stress and 20% of the live load. Live loads were determined according to DIN Technical Report 101 [13] for load model 1, containing both point loads and uniformly distributed loads. It covers the effects from truck and passenger car traffic as well as from pedestrian and bicycle traffic. The additional loads of the prescribed load case combination are considered as distributed masses in the bridge deck of the numerical models.

3.5 Model calibration

The calibration was carried out by varying the stiffness distribution and comparing the computed and the measured fundamental natural

Table 1: Measured and computed natural frequencies

Measured and computed natural frequencies [Hz]					
Torsion		Transversal		Vertical	
Measurement	Calculation	Measurement	Calculation	Measurement	Calculation
0.527	0.525	0.254	0.251	0.234	0.247
0.547	0.553	0.430	0.389	0.273	0.273
0.781	0.635	0.742	-	0.410	0.419
0.898	0.753	1.445	1.147	0.508	0.544
1.269	1.163	1.482	1.305	0.645	0.654

frequencies, while the mass distribution was assumed to be constant. Only a slight modification of the stiffness distribution became necessary, which was implemented by adjusting the cable pre-stress.

Table 1 shows a comparison of the measured and the calculated natural frequencies of the detailed model. Only natural frequencies with significant effective modal masses are listed. The sum of the effective modal masses of all mode shapes in Table 1 was higher than 90% of the total structural mass, so that the requirements in DIN 4149 and EC 8 were met. The comparison of the measured and the computed natural frequencies shows a good agreement throughout.

4. Investigation results

4.1 Level I

In investigation level I, the fragility curves of the suspension bridge were first determined by the procedure given in HAZUS-MH (Fig. 4). The probability of a defined damage state can be obtained for a given spectral acceleration.

Here, »slight« damage essentially means that only cosmetic repairs are necessary. »Moderate« damage involves some movements of the abutments (<5 cm) and the possibility of a failure of the roller bearings or moderate settlement of the bridge approach ramps. »Extensive« damage is characterized by column damage without complete failure, by significant residual deformations at connections or by major settlement of the bridge approach ramps. »Complete« damage occurs in the case of complete column or support failures, which lead to an imminent deck collapse. Tilting due to foundation failure is also possible in this damage state. An evaluation of the fragility curves with the maximum spectral acceleration of 0.5 m/s^2, determined according to the design spectrum of the newest version of DIN 4149, suggests only slight damage might occur. In addition to the fragility curves, the evaluation system for suspension bridges provided a more detailed picture taking into account critical structural details. The priority index *P* for the Rhine bridge Emmerich obtained from the evaluation system was 0.32, so that only uncritical damages were expected. The validity of this first assumption was borne out by the results in the other investigation levels.

4.2 Level II

In investigation level II the structural response was evaluated by means of the damage indicators suggested by Dicleli and Bruneau [14]. Additionally, the seismic internal forces and moments were computed with a partial safety factor of γ_M = 1.1 for material uncertainties and a weighting factor of γ_I = 1.0 for the seismic action. Stability analysis and stress verifications were carried out according to EC 3 [12] at the critical points of the structure. Some results for the impact of the bridge deck

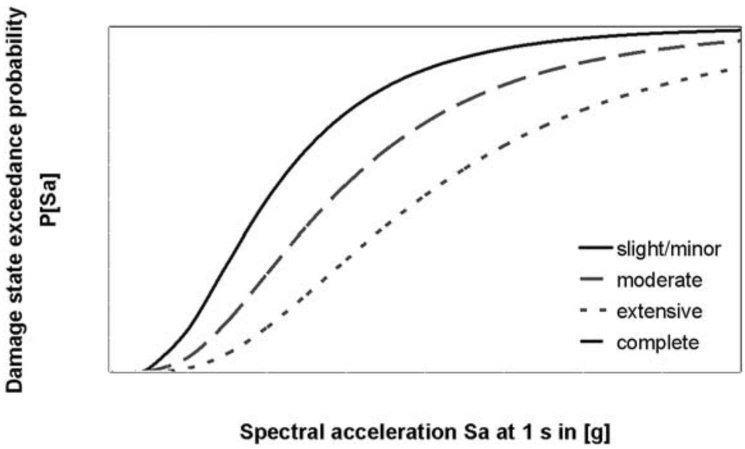

Figure 4: Fragility curves for the Rhine bridge Emmerich

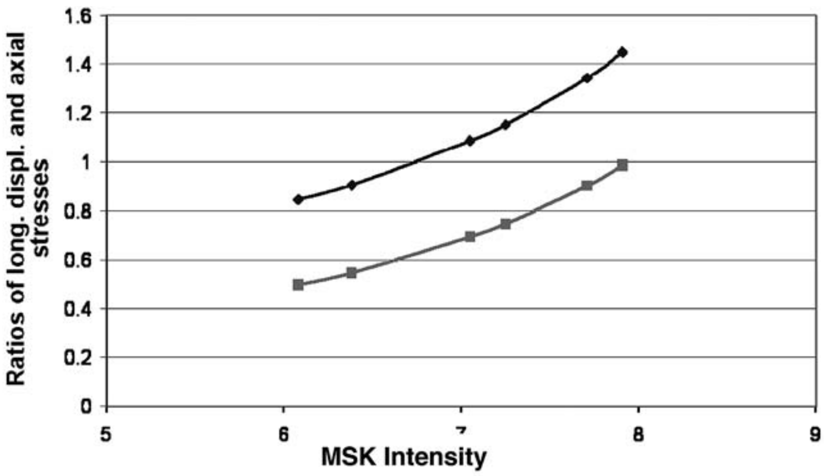

Figure 5: Level II results: Top curve shows the index for the longitudinal displacement of the deck, bottom curve the index for axial stresses at the pylon base

on the abutments as well as the verification of the axial stresses at the pylon base are presented here. These are the criteria that proved to be relevant, shown in Fig. 5 for different seismic intensities. It depicts ratios of the calculated longitudinal displacement of the bridge deck to the width of the expansion joint and of the actual to the permissible axial stresses. The analysis naturally also took the effects of a temperature expansion of the bridge deck into account.

Results show that exceeding the permissible axial stresses of the pylon is to be expected only for seismic intensities higher than VIII, with an annual exceedance probability of 10^{-5} for the specific location. Deck impact on the abutments is possible for intensities higher than VI–VII, corresponding to an annual exceedance probability of $5 \cdot 10^{-4}$. These probabilities are below the ones specified in the Codes ($2 \cdot 10^{-2}$), so the safety level for this bridge can be regarded as sufficient.

4.3 Investigation level III results

The same indicators concerning bridge deck impact on the abutments and axial stresses in the pylon base were used. The results were computed for earthquakes of the intensity VII–VIII, corresponding to a soil acceleration of 1.5 m/s^2 according to the relationship of Murphy and O'Brien. Results essentially confirmed the ones of Level II. Due to frame action axial stresses at the pylon base were not critical but an impact of the deck against the abutments is possible.

5. Conclusions

A three-step procedure for the evaluation of the earthquake resistance of existing bridge structures is presented and illustrated by the example of the suspension bridge Emmerich. The approach is supported by a management system with database functionality linked to the national bridge database »SIB-Bauwerke« [2].

References

[1] Comité Européen de Normalisation. EN 1998-1: 2004, *Eurocode 8 – Design of structures for earthquake resistance, Part 1–6*. Brussels, 2004.

[2] Programsystem SIB-Bauwerke. URL: http://www.sib-bauwerke.bast.de.

[3] B. Nielson. *Bridge Seismic Fragility-Functionality Relationships: A Requirement for Loss Estimation in Mid-America*. CBE Institute, Texas A&M University, Jan 5–11, 2003.

[4] FEMA. *Multi-hazard Loss Estimation Methodology*. (USSAS), USA, Jessup, Maryland, 2004.

[5] National Institute of Building Sciences. *Enhancement of the Highway Transportation Lifeline Module in HAZUS*. Prepared by Nesrin Basöz and John Mander, January, 1999.

[6] N. Rizo Osuna-Moyano. *Vulnerability assessment of a cable-stay bridge – Severins bridge*. Diploma thesis, Chair of Structural Statics and Dynamics, RWTH Aachen University, 2005.

[7] A. Thomas, E. Eschenaur and S. Kulicki. *Methodologies for Evaluating the Importance of Highway Bridges*. Technical report MCEER-98-0002, Multidisciplinary Center for Earthquake Engineering Research, 1998.

[8] N. Basöz and A. Kiremidjian. *Prioritization of bridges for seismic retrofitting*. Technical report, The John A. Blume Earthquake Engineering Center, 1995.

[9] J. P. Wolf. *Foundation Vibration Analysis Using Simple Physical Models*. Englewood Cliffs, Prentice Hall, 1994.

[10] T. Schmidt. *PSHA for the site of Emmerich.* Internal communication, Federal Institute for Geosciences and Natural Resources, 2005.

[11] H. Bachmann. *Erdbebensicherung von Bauwerken*. Zürich, Birkhäuser, 1995.

[12] Deutsches Institut für Normung e.V. DIN V ENV 1993, *Eurocode 3 – Design of steel structures*. Berlin, 1994.

[13] Deutsches Institut für Normung e.V. DIN-Fachbericht 101, *Einwirkungen auf Brücken*. Berlin, 2003.

[14] M. Dicleli and M. Bruneau. Quantitative approach to rapid seismic evaluation of slab-on-girder steel highway bridges. *Journal of Structural Engineering*, 122 (10), 1160–1168, 1996.

Integration of Sensors into Early Warning Systems based upon Open Geospatial Service Platforms

Usländer T., Watson K.
Fraunhofer IITB, Fraunhoferstraße 1, 76131 Karlsruhe, Germany
eMail: thomas.uslaender | kym.watson@iitb.fraunhofer.de

1. Introduction

One of the key issues for early warning systems is the integration of environmental information from various sources, being in-situ, airborne or space borne sensors or environmental data bases. Observations from these sensors are required to protect humans, natural resources or human-made artefacts from environmental hazards, either being subtle effects or sudden environmental events such as earthquakes, storms or forest fires. Public safety from environmental dangers, one of the five key elements in Environmental Security, has to be considered »within and across national borders« (Landholm (ed.), 1998). As a consequence, environmental risk management applications shall enable an efficient and flexible exchange of information as well as the remote call and eventually the reuse of their embedded functional components across system boundaries. Thus, there must be an agreement on information models and service interfaces – in the best case based on international standards.

Such applications usually contain Environmental Information Systems (EIS) as kernel components for the gathering, processing and rendering of environmental information (see Figure 1). EIS play a key role in the human's understanding of the past, current and future status of the environment. Usually based on large databases that are indirectly (offline) or directly (online) coupled to environmental sensors they allow the user to query and process environmental information and visualize it in thematic maps, diagrams and reports. More advanced functions cover, for instance, the estimation of future values of environmental parameters based on simulation or stochastic models as a basis for decision-support or early warning. Resulting actions are performed either by human activities outside of the EIS or through actuators triggered by the EIS.

Three major trends resulting from the demands of the stakeholders have determined the EIS design in the last years (Usländer, 2008):

1. Domain Integration: demand of enabling the correlation of EIS information and services across various thematic domains, mainly driven by the needs to understand the complex inter-domain relationships in ecological systems.
2. Wider Distribution: demand to open an EIS up to a wider spectrum of users (from employees in environmental agencies, over politicians in ministries up to the citizen) as well as to design the functions of an EIS as callable units from other applications. Environmental information has to be offered in a variety of formats and aggregation levels to a multitude of users.
3. Functional Enrichment: Demand to make sophisticated functions such as environmental simulations or geo-processing capabilities directly available within an EIS in order to lower the purchase, development, user training and maintenance costs.

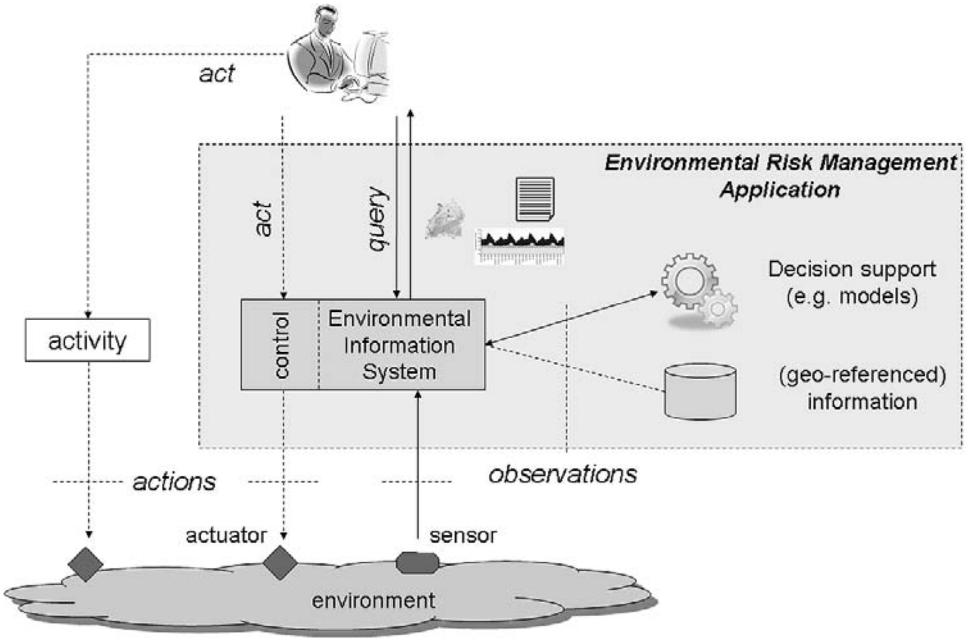

Figure 1: Structure of Environmental Risk Management Applications

An architectural answer to these demands is a service-oriented approach. An open geospatial service platform may provide generic Web services with a varying degree of functional richness (e.g. data access, cartographic mapping or geo-statistical interpolations). These services may be composed in a loosely-coupled way and coupled to one or more EIS applications. This approach is much more flexible than highly-sophisticated functions embedded in standalone systems, e.g. as a Geographic Information System (GIS).

2. Sensors and Geospatial Service Platforms

2.1 Reference Model

An »open geospatial service platform« provides seamless access to resources (information, services and applications) across organisational, technical, cultural and political borders, thus overcoming real-world heterogeneity and assuring a sustainable investment for the support of future, yet unknown requirements. »Open« hereby means that service specifications are published and made freely available to interested vendors and users with a view to widespread adoption. Furthermore, an open service platform makes use of existing standards (e.g. from the Open Geospatial Consortium OGC) where appropriate and otherwise contributes to the evolution of relevant new standards.

Based on a systematic analysis of user and system requirements, the European research project ORCHESTRA (Open Architecture and Spatial Data Infrastructure for Risk management) has specified and implemented a reference model and a series of architecture services that provide the generic and platform-neutral functional grounding of such open geospatial service platforms. This Reference Model for the ORCHESTRA Architecture (Usländer (ed.), 2007) has been accepted as a best-practices document for architectural design by the OGC.

2.2 Integration of Sensors

The European research project SANY (Sensors Anywhere) (Schimak et al, 2008) extends the ORCHESTRA architecture into a Sensor Service Architecture (SensorSA) by the inclusion of sensors and sensor networks (Usländer, 2009). This extension is based upon the services and information models of the OGC Sensor Web Enablement architecture (Simonis (ed.), 2008). Sensors provide the input data for environmental monitoring as well as for risk manage-

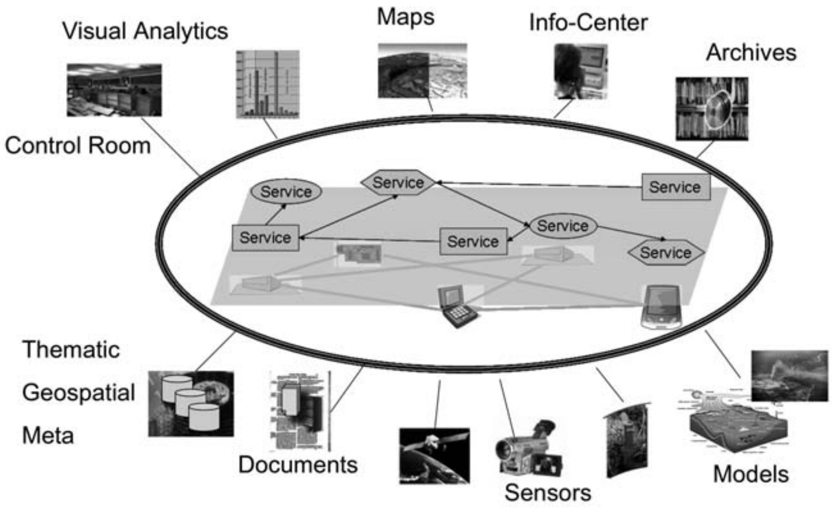

Figure 2: Open Geospatial Service Platform

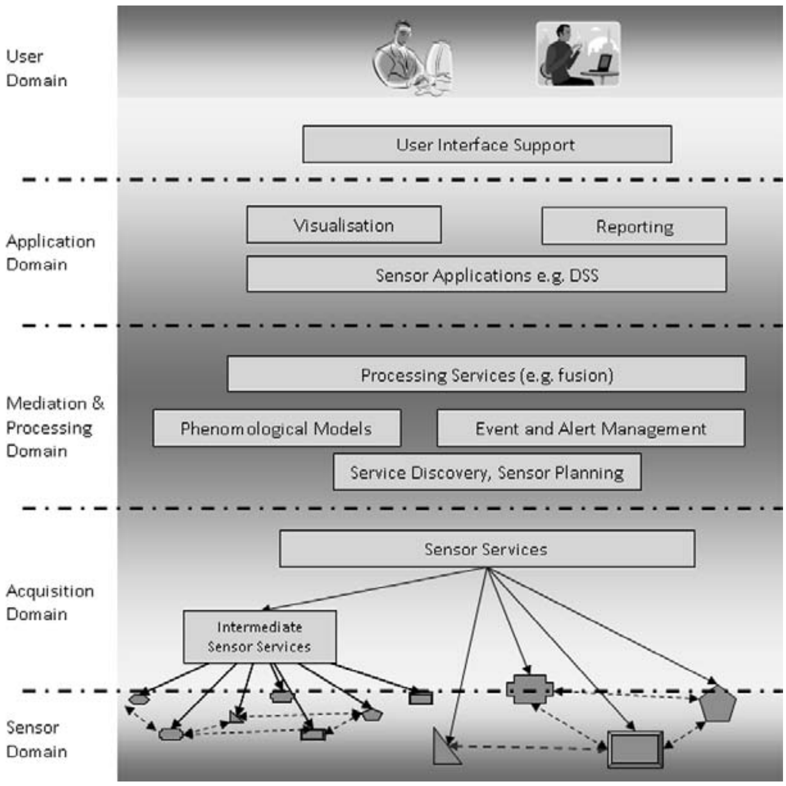

Figure 3: Functional Domains of the Sensor Service Architecture (SensorSA)

ment of natural, technical and man-made hazards (Watson and Usländer, 2008).

As a result, a high percentage of the required functionality of an environmental security application may already be covered by applying and tailoring the generic architecture services of both projects listed in Table 1 and Table 2. They are based upon international standards but extend them where necessary. For illustrative purposes, they are organised in the following functional domains (see Figure 4):

– Services in the *Sensor Domain* cope with the configuration and the management of individual sensors and their organization into

Table 1: List of Major Architecture Services and Interfaces required for an Open Geospatial Service Platform (Usländer, 2008)

Name of Service and Interface Type [functional domain]	**Application**
Basic Interface Types [all]	Enable a common architectural approach for all architecture services, e.g. for the capabilities of service instances
Annotation Service [MP]	Relates textual terms to elements of an ontology (e.g. concepts, properties, instances).
Authentication Service [MP]	Proves the genuineness of principals (i.e. the identity of a subject) using a set of given credentials.
Authorisation Service [MP]	Provides an authorisation decision for a given context.
Catalogue Service [MP]	Ability to publish, query and retrieve descriptive information (meta-information) for resources of any type. Extends the OGC Catalogue Service by additional interfaces for catalogue cascade management and ontology-based query expansion.
Coordinate Operation Service [MP]	Changes coordinates on features from one coordinate reference system to another.
Document Access Service [MP]	Access to documents of any type (e.g. text and images).
Feature Access Service [MP]	Selection, creation, update and deletion of features available in a service network. Corresponds to the OGC Web Feature Service but is extensible by schema mapping.
Map and Diagram Service [AP]	Enables geographic clients to interactively visualise geographic and statistical data in maps (such as the OGC Web Map Service) or diagrams.
Ontology Access Interface [MP]	Supports the storage, retrieval, and deletion of ontologies as well as providing a high-level view on ontologies.
Service Monitoring Service [MP]	Provides an overview about service instances currently registered within service network incl. status and load.
User Management Service [MP]	Creates and maintains subjects (users or software components) including groups (of principals) as a special kind of subjects.

sensor networks. Examples are services that support communication between the sensors themselves, e.g. a take-over service in case of an impending sensor battery failure. Services in this domain are abstractions from proprietary mechanisms and protocols of sensor networks. They are described in more detail in section 3

– Services in the *Acquisition Domain* (»AC« in table 1) deal with access to observations gathered by sensors. This includes other components in a sensor network (e.g. a database or a model) that may offer their information in the same way (as observations) as sensors do. They explicitly deal with the gathering and management of information coming from the source system of type »sensor«. The information acquisition process may be organized in a hierarchical fashion by means of intermediate sensor service instances (e.g. using data loggers).

– Services in the *Mediation and Processing Domain* (»MP« in table 1) are specified independently of the fact that the information may stem from a source system of type »sensor«. They mediate access from the application domain (see below) to the underlying information sources. They provide generic or thematic processing capabilities such as fusion of information, the management of models and the access to model results. In addition, support for resource discovery, naming resolution or service chaining are grouped in this domain.
– Services in the *Application Domain* (»AP« in Table 1) support the rendering of information in the form of maps, diagrams and reports directly to the end-user in the user domain.
– The functionality of the user domain is to provide the system interface to the end user. Usually, open generic architectures do not specify dedicated services for this domain. Both projects consider this functionality to be specified in a dedicated implementation architecture that also may take proprietary components and products into account.

3. Services and Information Models in OGC Sensor Web Enablement

The Sensor Web Enablement (SWE) services of the Open Geospatial Consortium (OGC) are used for the functions of the SensorSA Acquisition Domain as shown in Table 2.

The related information models are the XML-dialects SensorML (Sensor Model Language) (Botts, 2005) and the O&M (Observation & Measurements Model) (Cox, 2007). SensorML is for the description of sensors and other assets. Typical data in SensorML are manufacturer, operator, measurement quantities and their accuracy, measurement procedure and the sensor position (if fixed). O&M is used to describe sets of observations and related metadata. Measurements are simply scalar observations. Both models provide a framework for the definition of many model variants. As such application profiles are needed to ensure that interoperable applications can be realized without undue effort. The general modeling approach in SensorML and O&M is

Table 2: OGC Sensor Web Enablement Services

Name of Service [Acquisition Domain]	**Application**
Sensor Observation Service (SOS)	access to sensor observations
Sensor Planning Service (SPS)	configuring and tasking assets such as sensors, platforms (satellites, UAVs, …) and models (simulation, computations), persons (e.g. to take samples)
Sensor Alert Service (SAS)	publishing and receiving alert messages
Web Processing Service (WPS)	execution of processing functions
Web Notification Service (WNS)	dialogue with other services over communication protocols such as fax, text messages, e-mail, …

Table 3: SOS Operations, excerpt of (Nah and Priest (eds.), 2007)

Operation	Purpose
GetCapabilities	yields available sensors, observed features and groups of observations (offerings).
DescribeSensor	gives description of sensor in SensorML; this may include the procedure used to produce the result data from the input.
RegisterSensor	registers a sensor as described in SensorML with a SOS.
GetObservation	returns a collection of observations, whereby the following filters are allowed: time interval, region, observed property, sensor. The results is a self-describing XML file in the O&M Model incl. spatial, temporal and thematic references, a structural description and the actual data (as a reference to an external source or inline).
InsertObservation	Inserts a new observation into the SOS server

Table 4: SPS Operations, excerpt of (Schut (ed.), 2007)

SPS Operation	Purpose
GetCapabilities	returns meta-data of assets which may be tasked
DescribeTasking	returns description of asset parameters
GetFeasability	evaluates the feasibility of the asset tasking before the submit request. The extent of the evaluation lies in the responsibility of the SPS server, e.g. to check if the task can be scheduled with the available resources, and if the input parameters are valid.
Submit	submits asset for execution with given parameters; the request may be rejected if not or no longer feasible.
GetStatus	returns the current status of that task (e.g. degree of completion)
DescribeResultAccess	Applies to a successfully executed task, returns the SOS request needed to access the according fusion result (spatial coverage) stored in the Fusion SOS
Cancel	Cancels the execution of a running task as soon as possible

to provide sufficient meta-data to allow processing by client applications. For example, O&M includes the encoding and units of all observations as well as the coordinate system used for position information. The OGC services offer several operations at their interfaces as shown in Table 3 and Table 4. A very promising approach adopted in an example below is to combine services and operations in the same server instance to enhance the overall functionality.

4. A service oriented test bed for fusion services

A test bed has been developed for the fusion of sensor observations based upon OGC services (Kunz et al., 2009). The test bed implementation architecture has been designed for scalability and experiments in a wide range of scenarios, such as mobile sensors traversing several networks. At the sensor network level, an ad hoc ZigBee wireless network includes physical nodes that measure properties such as temperature, humidity, radiance and acceleration. Labview is used to configure the sensor nodes, to collect the measurement data and register sensors and insert observations on a SOS.

The objective of the test bed implementation architecture was to smoothly integrate fusion processes into the landscape of OGC compliant sensor-related services: Incoming data is provided by SOS instances as sensor observations, the configuration of the fusion service is performed through an SPS instance, and, the output data is offered through a special SOS instance in the test bed, called a Fusion SOS.

One SOS server contains data originating from real sensors, whereas two other SOS servers handle data generated by a sensor simulator. The simulation facility allows experiments with many sensors of different types including tests with sensor data that is not uniformly distributed in space or time. Such data can be expected e.g. from sensors with intermittent availability or from moving sensors. New sensors entering the system are registered automatically with a SOS. The fusion algorithms aim to fill the spatio-temporal gaps by computing intermediate values with an associated uncertainty depending on the quality of the input data.

This setup is complemented by simulated sensor nodes as illustrated in Figure 4. The sensor node simulation is realized as a Labview application. New observations are inserted into a selected SOS with the *InsertObservation* operation. The SOS may vary in the case of sensors moving between networks. The simulated sensor measurements follow a given spatial-temporal field with random noise added. The number of sensors and frequency of observations can be varied for scalability experiments.

The Fusion SOS Server generates its observations as spatio-temporal coverages using a fusion algorithm that is parameterized and tasked by an SPS instance. An instance of the Map and Diagram Service is used to display the fusion results as a layer on a map.

As a further component an instance of the catalogue service has been integrated to provide semantically-enhanced query support. The Semantic Catalogue stores meta-information about all available sensors, assets, services and observations and is used for the resource discovery in the test bed (Hilbring and Usländer, 2006).

The overall fusion process flow comprises the following sequence of service operations:

(1) A client application A wishes to create a new fusion result for observed property *P* in a time interval *T* and a set of sampling points *S*, e.g. a rectified grid, by using source data from available SOS servers. This algorithm takes several configuration parameters as additional arguments described in SensorML for submission to the SPS. A prior *GetFeasibility* operation can be executed to check if the arguments are correct and acceptable. The SPS launches the fusion task. Its execution can take up to several minutes depending on the amount of data to be processed and the computational cost of the algorithm. The client may inquire about the execution progress with a *GetStatus* operation.
(2) The fusion task queries the Semantic Catalogue for SOS servers with observations of property *P* in time interval *T* and in the area of a bounding box BBox{S} around the sampling point set. In addition, the Catalogue could have been queried in the previous step for suitable algorithms and SPS servers.

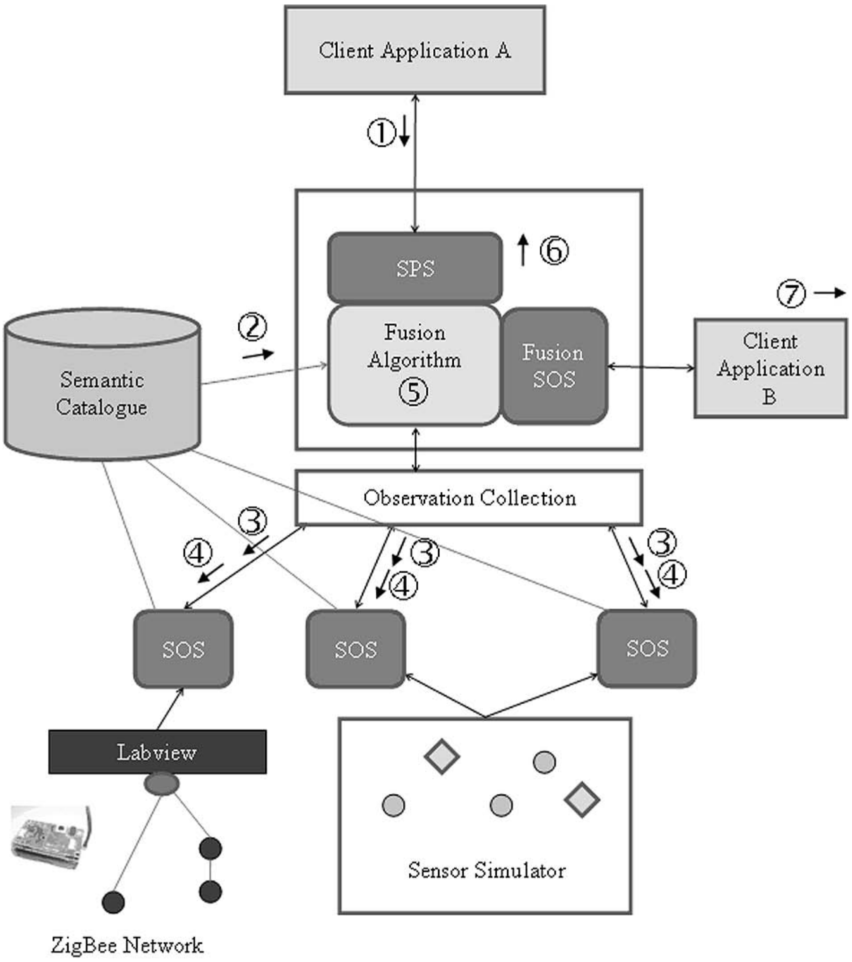

Figure 4: Service Oriented Architecture of the Fraunhofer test bed

(3) The fusion task has an observation collection as an input argument. The observation collection is formed by applying a *GetObservations* operation to each SOS server to obtain the available observations of property *P*. Duplicates are recognized as observations taken by the same procedure (sensor) at the same sampling time; duplicates are deleted from the observation collection.

(4) Accuracy information, either in the observation result or in the associated SensorML, is encoded into the observation collection. In the case of the test bed, this meta-information is in the SensorML of the related procedure. So the fusion task executes a *DescribeSensor* operation at the relevant SOS server to acquire this information. The descriptive model language UncertML developed by the INTAMAP project (INTAMAP, 2007) is used to encode the accuracy information into the XML file containing the result of the observation collection.

(5) Now the fusion algorithm itself can be executed with the arguments a) fusion parameters, b) the observation collection including (if available) the uncertainty of the observations, expressed as accuracy intervals, c) the sampling points at which the fusion is to estimate a value of the property. The result of the fusion algorithm is a coverage, i.e. a set of estimated property values for the sampling points together with a quantified description of their uncertainty. The uncertainty is described as a statistic such as variance or a probability distribution. The descriptive model language UncertML is used once again to encode the uncertainty information into the XML fusion result file.

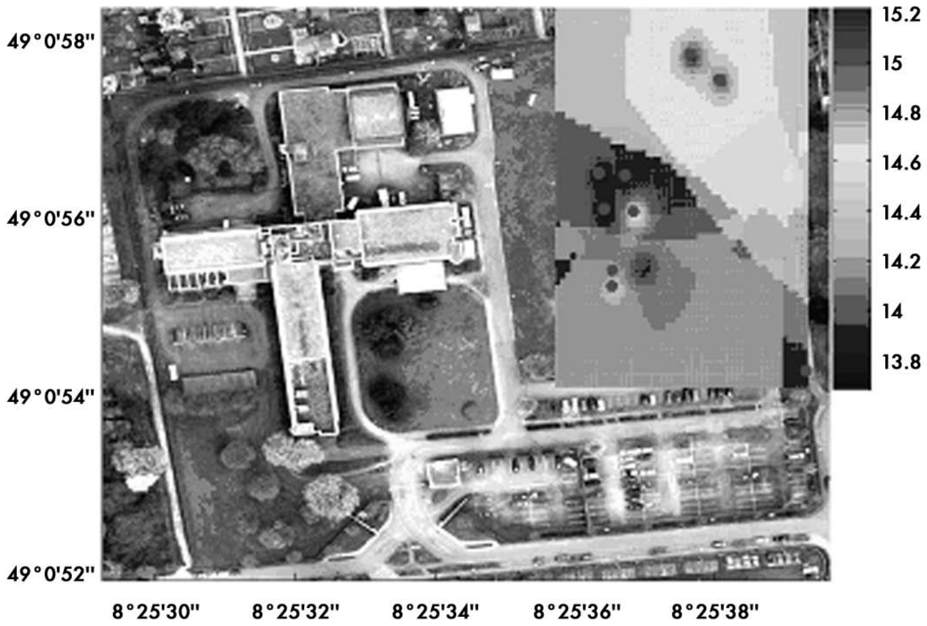

Figure 5: Fusion result as heat map (red circles show sensor locations)

(6) The completion of execution of the fusion task is recorded by the SPS which can issue a notification to the client (e.g. with the OGC Web Notification Service) or another notification broker (with the Web Services Notification of OASIS). The SPS responds to the operation *DescribeResultAccess* with the XML file argument required by a client when executing a *GetObservations* request to the Fusion SOS server to retrieve the fusion result.

(7) Application Client B can, for example, display the fusion results geo-referenced and visualized using the Map and Diagram service, in this case as a heat map as shown in Figure 5.

The fusion architecture based on OGC services as described above has also been applied to the design of the Information System of EWS Transport (Titzschkau et al, 2009).

The Fusion SOS/SPS has been realised on the basis of the information management system WebGenesis® of Fraunhofer IITB. Files produced during the fusion process may be stored and referenced on WebGenesis– for tracing and reproducibility of results (provenance).

5. Conclusion

Service-oriented architectures based on OGC standards are a promising approach to the design of environmental monitoring and risk management systems. Resulting open geospatial service platforms can handle the increasing need for data exchange across organizations and regions.

Information providers and consumers both benefit from the standardized interface operations and information models with metadata such as location, time, theme and quality. The metadata not only allows information sources and services to be discovered, but also supports the automated data processing. New services can be easily composed by chaining or combining existing services. The OGC Sensor Observation and Sensor Planning Services can be combined to achieve advanced tasks such as the fusion of sensor data from different sources with configurable fusion procedures. The source data as well as the fusion result are represented as observations in the O&M Model.

The high degree of flexibility of the information models O&M and SensorML implies that profiles are needed for full interoperability of applications. Studies and realization projects are under way in a number of areas in order to establish best practices.

6. Acknowledgment

Much of the research and development work presented in this paper was performed in the project SANY (Sensors Anywhere). SANY is an FP6 Integrated Project co-funded by the European Commission within the Thematic Priority »Information Society Technologies« in the area of ICT for environmental risk management. The SANY consortium is composed of 16 partners from eight countries. It includes the two research organisations Austrian Institute of Technology (coordinator of the consortium) and Fraunhofer, six companies, three universities, four public authorities and the Open Geospatial Consortium Europe. The primary objective of SANY during the project duration 2006–2009 is to specify an architecture for sensors that allows seamless »plug and measure« of sensors in applications, and sharing of information between sensor networks.

The SANY Sensor Service Architecture (SensorSA) and the service specifications have been made publicly available on the SANY project server (http://www.sany-ip.eu). The SANY specifications and best practice experience are contributed to the OGC standardisation work.

Information about the Open Geospatial Consortium (OGC) and its standards may be found at http://www.opengeospatial.org.

References

Botts, M. (2005). Sensor Model Language Version 1.0.0. OGC Document 07-000, http://portal.opengeospatial.org/files/?artifact_id=21273, 2007.

Cox, S. (Ed.): Observation & Measurements – Part 1: Observation Schema. OGC Document 07-022r1, approved as OpenGIS® specification, October 2007.

Hilbring, D. and Usländer, T. (2006): Catalogue Services Enabling Syntactical and Semantic Interoperability in Environmental Risk Management Architectures. Proceedings of the 20th International Conference on Informatics for Environmental Protection (EnviroInfo 2006), September 6-8, 2006, Graz, Austria, ISBN-10:3-8322-5321-1, (2006) S. 39–46.

INTAMAP (2007): UncertML – XML language for exchanging uncertainty, http://www.intamap.org/uncertml/uncertml.php, visited in July 2009.

Kunz, S., Usländer, T. and Watson, K (2009): A Testbed for Sensor Service Networks and the Fusion SOS: towards plug & measure in sensor networks for environmental monitoring with OGC standards. In Proceedings of 18th World IMACS / MODSIM Congress, Cairns, Australia 13–17 July 2009.

Landholm, M. (ed.), 1998, Defining Environmental Security: Implications for the U.S. Army, Army Environmental Policy Institute, AEPI-IFP-1298.

Nah, A., Priest, M. (eds.) (2007), Sensor Observation Service, Open Geospatial Consortium, OGC 06-009r6.

Schimak, G., Usländer, T., Havlik, D. and Argent, R. (2008): Creating robust sensor networks – architecture and infrastructure, in: Proceedings of the International Congress on Environmental Modelling and Software (iEMSs 2008), ISBN: 978-84-7653-074-0, Vol. 3, (2008) S. 1885–1897.

Schut, P. (ed.) (2007). OpenGIS Web Processing Service, OGC 05-007r7.

Simonis, I. (ed.) (2008). OGC® Sensor Web Enablement Architecture, OGC Best Practices Document 06-021r4 Version: 0.4.0, 2008.

Titzschkau, T., Wenzel, W., Buchmann, A., Hohnecker, E., Hilbring, D. and Bonn, G. (2009): Earthquake early warning demonstrator for transport lines. In these workshop proceedings.

Usländer, T. (Ed.) (2007): Reference Model for the ORCHESTRA Architecture Version 2 (Rev. 2.1). OGC Best Practices Document 07-097.

Usländer, T. (2008): The Growing Importance of Open Service Platforms for the Design of Environmental Information Systems, in: Proceedings of the International Congress on Environmental Modelling and Software (iEMSs 2008), ISBN: 978-84-7653-074-0, Vol. 3, (2008) S. 1628–1635.

Usländer, T. (Ed.) (2009): Specification of the Sensor Service Architecture, Version 3.0 (Rev. 3.1) OGC Discussion Paper 09-132r1. SANY Project Deliverable D2.3.4.

Watson, K. and Usländer, T. (2008): Integration of Sensors and Information Services to Protect Critical Infrastructures. In: Thoma, K.; Fraunhofer EMI; Fraunhofer Verbund Verteidigungs- und Sicherheitsforschung; Bundesministerium für Bildung und Forschung – BMBF –: Fraunhofer Symposium Future Security. 3rd Security Research Conference 2008: 10–11 September 2008, Congress Center Karlsruhe, Germany: Fraunhofer IRB Verlag, (2008) S. 221–225.

Spatial Data Infrastructure Components for Early Warning Systems

Kiehle Ch.
lat/lon GmbH, Aennchenstr. 19, 53177 Bonn, Germany,
eMail: kiehle@lat-lon.de

Abstract
The Earthquake Disaster Information System for the Marmara Region, Turkey (EDIM) is a current interdisciplinary research and development project in the context of Early Warning and Decision Support Systems. Within this project several components based on the concept of Spatial Data Infrastructures have been developed to support the relevant stakeholders in gathering concise information for early warning and disaster management purposes.

The components considered are based on the Open Source Spatial Data Infrastructure framework deegree. It is outlined which components comprise the system, how spatial information can be accessed by users and which technologies are relevant. Based on the concept of grid-computing, a proposal for ensuring fail-safe operation is laid out.

Keywords: Spatial Data Infrastructure, Early Warning System, Turkey, Sensor Observation Service, Web Processing Service

Introduction
Early warning systems should be based on a great variety of data and information sources, especially with a direct or indirect relation to space. Spatial data may include topological data sets, elevation models, satellite imagery and data collected through sensors. To provide accurate decision-supporting information, early warning systems should be capable of hiding the complexity of the underlying data sources and information models through well-known interfaces (component interfaces as well as user interfaces). Within the Earthquake Disaster Information System for the Marmara Region, Turkey (EDIM), the Open Source framework deegree (Fitzke et al. 2004; Müller & Fitzke 2008) provides an implementation of interfaces for data, services, and user interaction. Deegree provides an Open Geospatial Consortium (OGC) compliant set of server and client components to support the design and implementation of sustainable early warning systems. Besides classic service interfaces for raster-, vector-, and mapping data (i.e. Web Coverage Service, Web Feature Service, and Web Map Service). deegree also provides access to sensor data collections through a Sensor Observation Service (SOS, Na & Priest 2007) and accompanying user interfaces.

The user interfaces are based on portal technology to provide access to distributed information sources through a consistent interface. Maps can be overlaid with aerial imagery as well as just-in-time information from sensor data. A chart module is capable of visualisation of numerical datasets as charts (e.g. pie charts, line charts or scatter plots) within a map to support decision makers. For event-driven workflow (e.g. issuing early warnings after seismic events) a Web Processing Service (WPS, OGC 2007) is available to propagate alerts.

Being primarily developed for early warning systems related to seismic events, the components demand to be prepared for generic purposes. Focussing on the information technology aspects rather than the functional aspects of the EDIM application, the components presented are of vital interest to adjacent projects[1] with a focus on spatial data processing and visualisation.

The EDIM Project

Earthquake Disaster Information System for the Marmara Region[2] (EDIM) is a joint research and development project funded by the German Federal Ministry of Education and Research (Bundesministerium für Bildung und Forschung, BMBF) and the German Research Foundation (Deutsche Forschungsgemeinschaft, DFG) within the special programme Geotechnologien[3] (Stroink&Mossbrugger 2008). It is carried out by a project consortium consisting of geo- and computer scientists and practitioners in spatial information systems:

– University of Karlsruhe (TH), Geophysical Institute (project lead)
– GeoForschungsZentrum (GFZ) Potsdam
– Humboldt University Berlin, Computer Science Department
– lat/lon GmbH
– DelphiIMM GmbH
– Kandilli Observatory and Earthquake Research Institute of Bogazici University, Istanbul, Turkey

The project partners work jointly on three subprojects. The overall goal is to investigate the expansion of an already existing Istanbul Earthquake Rapid Response and Early Warning System (IERREWS) to the regional scale of the Marmara region as well as to enhance the quality of the provided information.

The Marmara region is Turkey's most densely inhabited area, inhabited by nearly 18.000.000 people. Since a large geologic fault crosses the Marmara Sea, Istanbul has been regularly shocked by earthquakes (up to magnitudes exceeding 7.0). This raises the need for improving early warning and rapid response systems in this area. The associated Kandilli Observatory ensures that the research and development undertaken in EDIM suits the needs of the stakeholders in Istanbul.

The EDIM approach to early warning and rapid response is comprised of three subprojects, each targeting a specific area of earthquake detection, analysis and visualisation utilizing information and communication technology:

– *Part A* enhances methodologies for improvement of real-time information of earthquake source parameters and shakemaps.
– *Part B* enhances sensor technology and software for self-organising networks of sensor units.
– *Part C* uses the data and methodologies collected from subproject A and B and integrates them into a consistent Spatial Data Infrastructure. The remainder of this paper will focus the developments of subproject C with an special emphasis on components to set up a Spatial Data Infrastructure for the EDIM project.

The EDIM Spatial Data Infrastructure

The relevant data sets are comprised out of different kinds of data formats.

– Raster data displaying satellite imagery, topographic data, shakemaps, and damage classification data
– Vector data representing geological formations, faults, socio-economic data, etc.
– Sensor data representing measurements of relevant base data for earthquake detection

Data sets are in various source formats like ESRI shape files, georeferenced Tagged Image File Format (tiff) images and databases containing geometries. In order to provide a vendor neutral access to all available data, the interfaces have to be based on internationally accepted standards. For EDIM the information system should be based on standards as pub-

[1] EDIM is carried out within the thread »Early Warning Systems Against Natural Hazards«. A complete project list can be found on http://www.geotechnologien.de/portal/-?$part=Geotechnologien&locale=en
[2] The project homepage is available through http://www.cedim.de/EDIM.php
[3] www.geotechnologien.de

lished by the Open Geospatial Consortium (OGC) to allow integration into a broad variety of information systems. The following subchapters describe the base services that make up the EDIM infrastructure.

Data Services

The infrastructure is comprised of several data services. Most importantly, a Sensor Observation Service is responsible for storage of and access to real-time-data. Other important services are a Web Coverage Services, Web Feature Services and Web Map Services which are described in the following sections.

A Sensor Observation Service (SOS) is part of the Sensor Web Enablement (SWE) family of specifications (Botts et al. 2007). It aims at standardizing the access to data from observations and measurements. It defines three obligatory interfaces:

– GetCapabilities describes the capabilities of the service and provides metadata about the service instance.
– Describe Sensor returns a sensor description which is encoded using the Sensor Model Language (SensorML, Botts 2007).
– GetObservation: returns the actual values of a sensor. Those values are encoded using the Observations & Measurements (O&M, Cox 2007) encoding.

Sensor data in the EDIM project are taken from a test site in Istanbul, comprised of 20 sensors measuring earthquake-relevant data (e.g. STA/LTA, PGA, PGV, PGD, CAV). The data is recorded in the proprietary format of the sensors, which hinders the exchange of data. A SOS is used to access the data and provide the data in a well-known format (O&M). This allows generic clients to access the sensors through a standardized layer.

Figure 1 illustrates EDIM's SOS architecture for storing and archiving data from sensor nodes. A shared database (prototypically based on ApacheDB, port to PostgreSQL/PostGIS is planned) is used to write raw measurements

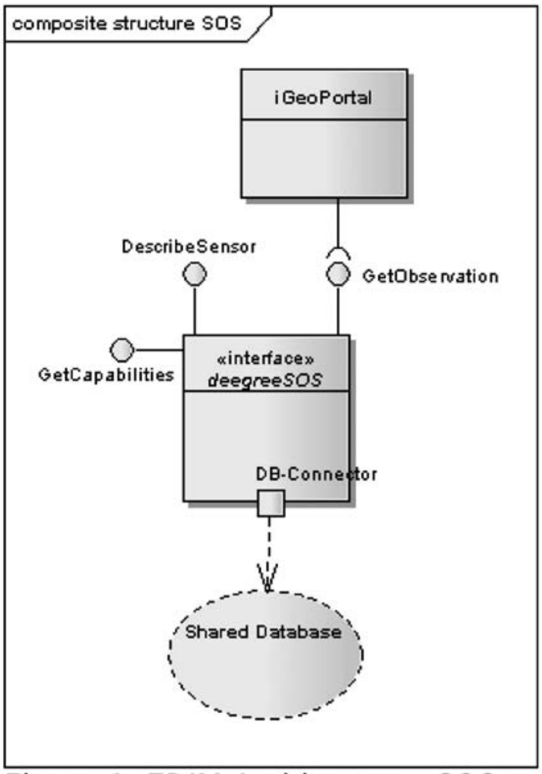

Figure 1: EDIM Architecture: SOS

data to. This database is more for long-term storage of sensor data than to access real-time data. The purpose of this database is to allow scientists to access the data after seismic events to analyse the data recorded by sensors. A seismic event has not necessarily to be an earthquake causing damage to buildings or people.

The database structure can be tailored to suit the needs of other potential applications. On top of the database an adapter layer (db-connector) provides object-relational mapping. This layer is responsible for accessing the database, retrieving data, and restructuring the data into encodings provided by an SOS (Observations & Measurements). All the functionality defined by the SOS specification is provided by the interface deegree SOS, namely the operations GetCapabilities, DescribeSensor and GetObservation. Since GetObservation is the operation to retrieve data from the SOS, this operation is accesses by the information system (iGeoPortal).

A Web Coverage Service (WCS) is used to access coverage data (e.g. topographic maps) through the obligatory interfaces:

- GetCapabilities
- DescribeCoverage to access detailed metadata about the served coverages.
- GetCoverage returns a coverage data stream.

A WCS is currently not actively used inside EDIM. It is planned to integrate a WCS to serve radar images for estimation of land cover.

A Web Feature Service (WFS) provides standardized access to vectorial data through the interfaces:

- GetCapabilities
- DescribeFeatureType returns an description of the served features of the service
- GetFeature returns the actual geodata

A Web Map Service (WMS) gives standardized access to map images, allowing to overlay different map images from local as well as remote service instances. It defines three interfaces:
- GetCapabilities
- GetMap retrieves an map image
- GetFeatureInfo: retrieves additional information for a user-defined location on the map.

While WFS, WCS and SOS allow access to spatial data for the more technically experienced user, inside an information portal, the Web Map Service is likely the service accessed most. Inside EDIM, WMS is used inside a portal environment as the central source of information.

The EDIM Client Infrastructure

The EDIM client infrastructure is comprised of a set of loosely coupled client components to access the services explained above. The most relevant part of the application from a user's perspective is the web mapping portal iGeoDesktop. iGeoDesktop is an integrated environment to access web maps and provide functionalities for interaction with maps (e.g. pan, zoom, measure, add or remove layers, etc.) (see Fig. 2). The portal is configured with

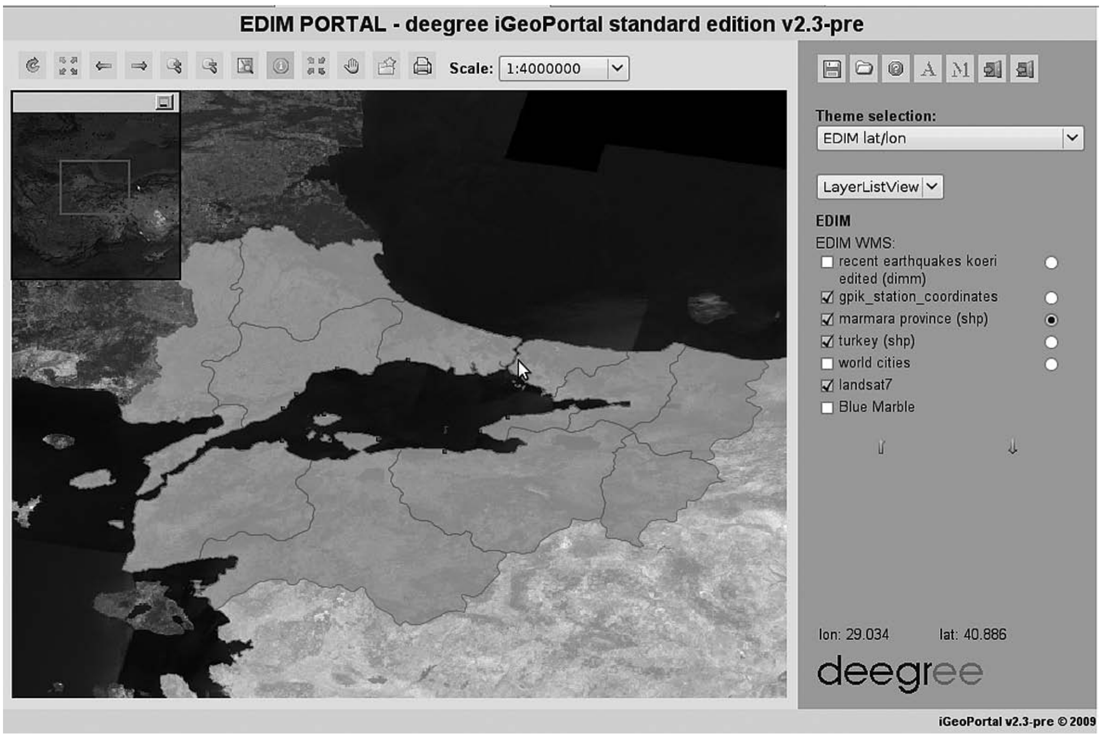

Figure 2: Screenshot of EDIM's iGeoPortal

a security component to allow access to different sources of information only to authenticated users.

iGeoPortal serves as a single-point-of-entry to all information gathered inside the EDIM project. The workflow is based on an interactive map. A user may explore the relevant area by navigating inside the map and requesting further information on selected spatial features. Without authentication, the information provided is rather coarsely grained. Only satellite imagery, county boundaries and other non-sensitive information are available. After authentication through the iGeoSecurity[4] component, a user may – depending on his rights – see more detailed information like sensor stations, status of sensors and other services. He is also capable of adding further map layers and to define a set of information layers (so called Web Map Contexts) based on his needs.

Figure 2 illustrates a layer containing sensor stations (gpik_station_coordinates). These stations, marked by red dots on top of the coastline can be queried for further information. Using iGeoPortal's getFeatureInfo functionality triggers an opaque workflow to actually assess a single sensor station. The workflow is as follows:

– user selects a sensor by clicking on a sensor station in the map (utilizing the getFeatureInfo function of iGeoPortal)

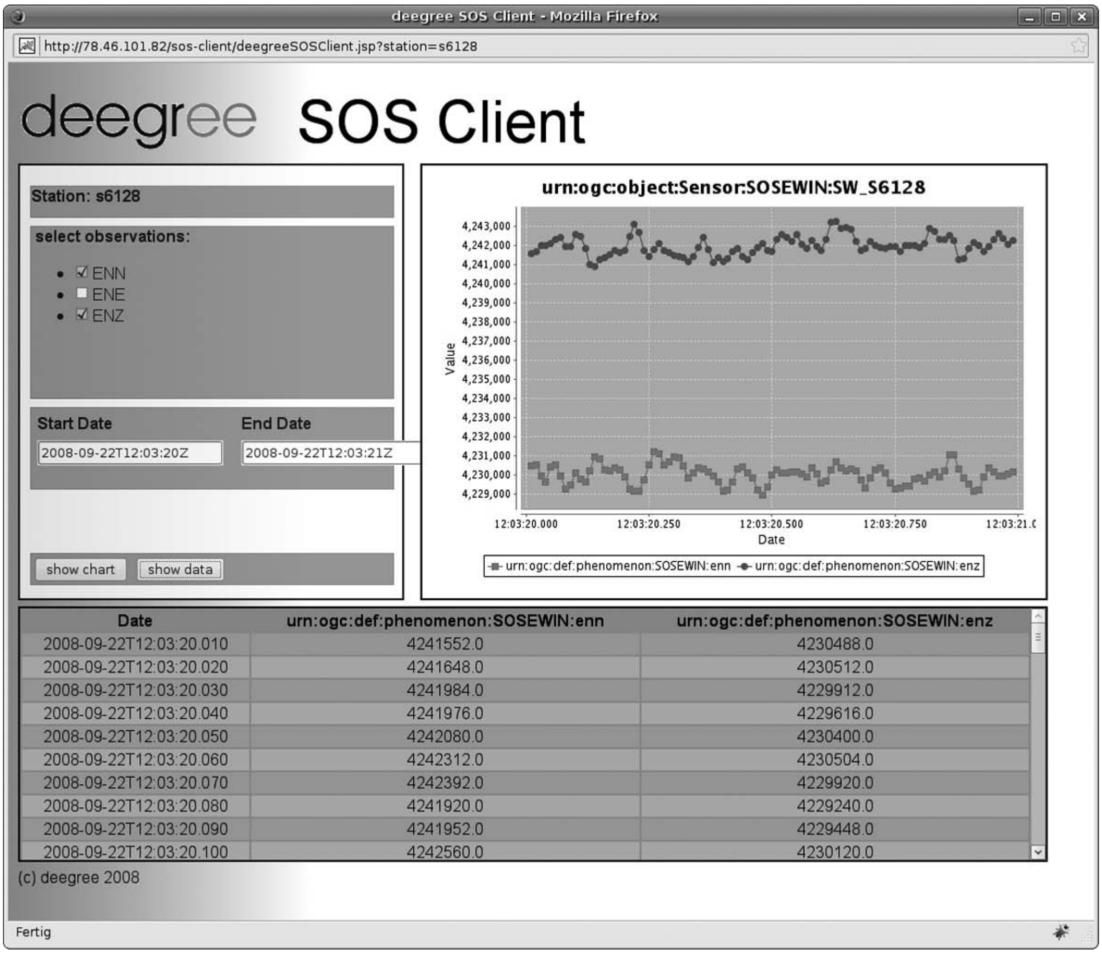

Figure 3: prototype of SOS client

[4] Futher details on iGeoSecurity, deegree's approach to security implementation, can be found on https://wiki.deegree.org/deegreeWiki/iGeoSecurity

- the system transmits an identifier (ID) of the sensor station to a prototypical Sensor Observation Client (see Fig. 3).
- The client allows the user to interactively request information from the sensor. Adjustable parameters contain the sensor information to be displayed and the requested time interval.
- The client displays the requested data in form of a table containing the relevant data. A charting module is responsible for integrating the measurements into a line chart diagram to better access the relevant information.

For more technical application, it is also possible to directly access the results as XML data.

The sensor station being operated by project partners from subproject B offer live data of seismic events. In fact, currently the access is only simulated, but the connection to the live sensor network will be realized within the final project phase.

System Stability through Grid Computing

Early Warning Systems require a high-grade of system stability. In case of an incident, the servers running the Early Warning System could be affected, too. It is indispensable that the system keeps running even under theses circumstances. All components comprising the system must have a back-up, which contain all the most recent information. A simple back-up mechanism (e.g. by nightly data backup) would not be sufficient. The system should be based on a distributed computing environment, which allows a transparent replacement of single computing and storage instances in real time.

The concept of grid computing (Foster & Kesselmann 1998; Foster et al. 2001) seems to suit these needs. A grid provides a network of storage and computing power, usually based on a distributed architecture. The distributed parts are accessed through a grid middleware, which encapsulates the distributed nature of the underlying computing and storage facilities. Grid computing offers immense computing and storage power, since it is comprised of several grid-nodes, working together through a standardized protocol layer.

For EDIM, the Globus Toolkit middleware (Foster 2006) has been evaluated to provide access to a computing and storage grid. Globus is, like deegree for OGC webservices, an Open Source framework to set up a grid infrastructure. Within the project GDI-Grid (Padberg & Kiehle 2009), first experiences in coupling grid computing with deegree have been gathered.

The EDIM infrastructure can benefit in several ways from grid computing:

- *System stability:* grid implements a distributed computing platform. In case a single grid node fails, another grid node is able to replace it. Since neither grid node is accessed directly but through an abstraction layer, the system will not even notice, that parts of the system are running on a different machine.
- *System scalability*: In case of huge computing and/or storage demands, additional grid nodes may be integrated without affecting the overall system during runtime. This offers a very flexible way to enhance computing and storage as required.
- *System performance:* grid computing systems usually offer computing and storage resources which exceed regular computers (servers, clusters, etc.) by far. The German D-grid for example currently offers about 20.000 Central Processing Units and more than 10 Petabyte of storage capacity. Similar grid infrastructures exist in many other countries (U.K., U.S.A., etc.)

In case of an incident, grid computing seems to be a good choice to avoid data loss, to ensure permanent uptime of the information system and to handle the increasing number of request to be expected.

Preliminary Results and Outlook

Within the EDIM subproject C, a couple of preliminary results have been achieved so far:

– *Spatial Data Infrastructure Components:* The deegree framework provides Open Source components for setting up custom tailored Spatial Data Infrastructures. Within EDIM, deegree has been enhance in ways to provide access to sensor data through a standards-compliant Sensor Observation Service (SOS). A Web Processing Service Components to access vector- and raster data have been configured to serve data sets for the EDIM infrastructure in a standards-compliant way.
– *Client Components:* Available client components have been enhanced to support stakeholders from the field of Early Warning Systems in data and information retrieval. This includes the set-up of a specific Geoportal (based on deegree's iGeoPortal software) as well as the integration of a Sensor Observation Client. In order to make the SOS data accessible more easily, the SOS client offers a variety of filter capabilities, basic statistics and graphical overview (i.e. chart functionalities). To support local authorities, the system can be configured to offer multi-language support.
– *User-Rights Management:* Since Early Warning Systems contain sensible information (e.g. building damage classification, land tenure, etc.) it has been necessary to restrict access to certain information layers for defined user-groups. Therefore a user-rights management system has been integrated, which only gives access to authorized users. Besides authorization based on roles, the authorization can be defined on spatial predicates. This can affect certain layers containing spatial data as well as certain features (i.e. vectors).
– *Concept for system stability:* In order to provide system stability even in case of an incident, a data and service backup system has been defined. The concept is based on grid computing paradigm in order to replicate data, services and computing tasks on a distributed computing platform.
– *Documentation:* To support the integration of the provided components into other Early Warning Systems as well as other information systems supporting decision makers, extensive documentation of the components on a technical level have been formulated.

During the final project phase until mid 2010, the focus will be on the finalization of the Spatial Data Infrastructure including the client-components. This involves fine-adjustment between the on-site sensor-network located at the test area and the Spatial Data Infrastructure components. Based on tests with real seismic data, thresholds for triggering alarm will have to be defined by the EDIM-project partners. These thresholds will be used to define an alarming event triggered by the integrated Web Processing Service.

The components developed in EDIM offer the main building blocks to set up early warning and decision support systems based on spatial data and information. The components are freely available under an Open Source Licence (i.e. GNU Lesser General Public License, Free Software Foundation 2007), which fosters reusability and sustainability. The underlying concept of an Service Oriented Architecture supports loose coupling of the components, thus enhancing the flexibility of the system.

Acknowledgement

The work presented in this paper would not have been possible without the funding within the EDIM project. Funding is provided by the German Federal Ministry of Education and Research within the special programme Geotechnologien, funding code 03G0650E.

References

Botts, M. (Ed.) (2007): OpenGIS Sensor Model Language (SensorML) Implementation Specification.
http://portal.opengeospatial.org/files/?artifact_id=21273

Botts, M., Percivall, G., Reed, C., Davidson, J. (Eds.) (2007): OGC White Paper: OGC Sensor

Web Enablement: Overview and High Level Architecture.
http://portal.opengeospatial.org/files/?artifact_id=25562

Cox, S. (Ed.) (2007): Observations and Measurements – Part 1 – Observation schema. http://portal.opengeospatial.org/files/?artifact_id=22466

Fitzke, J., Greve, K., Müller, M., Poth, A. (2004): Building SDIs with Free Software – the deegree Project. In: Proceedings of GSDI-7, Bangalore.

Foster, I. (2006): Globus Toolkit Version 4: Software for Service-Oriented Systems. IFIP International Conference on Network and Parallel Computing, Springer-Verlag LNCS 3779, pp. 2–13, 2006.

Foster, I., Kesselman, C. (1998): The Grid: Blueprint for a New Computing Infrastructure, San Francisco.

Foster, I., Kesselman, C., Tuecke, S. (2001): The Anatomy of the Grid: Enabling Scalable Virtual Organizations. International Journal of Supercomputer Applications, 15 (3).

Free Software Foundation (Ed.) (2007): GNU Lesser General Public License. Version 3. http://www.fsf.org/licensing/licenses/lgpl.html

Lupp, M., Fitzke, J. (2008): Open Sources # 12: deegree – an SDI framework. GEOconnexion International Magazine: 32–37.
http://www.geoconnexion.com/uploads/opensource_intv7i7.pdf

Na, A., Priest, M. (Eds.) (2007): Sensor Observation Service. Version 1.0.0.
http://portal.opengeospatial.org/files/?artifact_id=26667

Open Geospatial Consortium (Ed.) (2007): OpenGIS Web Processing Service. Version 1.0.0. http://www.opengeospatial.org/standards/wps

Padberg, A., Kiehle, C.(2009): Spatial Data Infrastructures and Grid Computing: the GDI-Grid project. Geophysical Research Abstracts 11 (EGU2009-4242).

Stroink, L., Mossbrugger, V. (2008): Integratives Forschungsmanagement – Vernetzung – am Beispiel des FuE-Programm GEOTECHNOLOGIEN. Wissenschaftsmanagement – Zeitschrift für Innovation, 5/08.
http://www.geotechnologien.de/portal/-;jsessionid=51B368E57793E568071D02610CC1CF94?$part=binar y-content&id=3367768&status=300&language=de

Automated classification of intact road networks in multi-sensorial remote sensing data for near-realtime disaster management

Frey D., Butenuth M., Hinz St.

Institut für Photogrammetrie und Fernerkundung, Englerstr. 7, Universität Karlsruhe

eMail: Stefan.Hinz@ipf.uni-karlsruhe.de

Abstract

In this paper, a near-realtime system for classification of linear infrastructural objects is presented using multi-sensorial imagery. The system provides a framework for the integration of different kinds of imagery as well as any available data sources and spatial knowledge, which contributes information for the classification. The goal of the comprehensive system is the assessment of infrastructure GIS-objects concerning their functionality. It enables the classification of infrastructure into different states as destroyed or intact after disasters such as floodings or earthquakes. The automatic approach generates an up-to-date map in order to support first aid in crisis scenarios. Probabilities are derived from the different input data using methods such as multispectral classification and fuzzy membership functions. The main core of the system is the combination of the probabilities to classify the individual GIS-object. The system can be run in a fully automatic or semi-automatic mode, where a human operator can edit intermediate results to ensure the required quality of the final results. In this paper, the performance of the system is demonstrated assessing road objects concerning their trafficability after flooding. By means of two test scenarios the efficiency and reliability of the system is shown. Concluding remarks are given at the end to point out further investigations.

1. Motivation

A significant increase of natural disasters such as flooding and earthquakes has been observed over the past decades (Kundzewicz et al., 2005). There is no doubt that the disasters' impact on the population has dramatically increased due to the growth of population and material assets. The regrettable death of people is accompanied by heavy economic damage, which leads to a long term backslide of the regions hit by the disaster. This situation calls for the development of integrated strategies for preparedness and prevention of hazards, fast reaction in case of disasters, as well as damage documentation, planning and rebuilding of infrastructure after disasters. It is widely accepted in the scientific community that remote sensing can contribute significantly to all these components in different ways, in particular, due to the large coverage of remotely sensed imagery and its global availability.

However, time is the overall dominating factor once a disaster hits a particular region to support the fast reaction. This becomes manifest in several aspects: firstly, available satellites have to be selected and commanded immediately. Secondly, the acquired raw data has to be processed with specific signal processing algorithms to generate images suitable for interpretation, particularly for Synthetic Aperture Radar (SAR) images. Thirdly, the interpretation of multi-sensorial images, extraction of geometrically precise and semantically correct information as well as the production of (digital) maps need to be conducted in shortest timeframes to support crises management groups. While the first two aspects are strongly related to the optimization of communication processes and hardware capabilities, at least to a large extend, further research is needed concerning the third aspect: the fast, integrated, and geometrically and semantically correct interpretation of multi-sensorial images.

Remote sensing data was already used in order to monitor natural disasters in the year 1969 (Milfred et al., 1969). Particularly, in the case of flooding a lot of studies are carried out to infer information as flood masks from remote sensing data (Sanyal and Lu, 2004). The flooded areas can be derived from optical images (Van der Sande et al., 2003) as well as from radar images (Martinis et al., 2009) via classification approaches. Zwenzner (Zwenzner and Vogt, 2008) estimates further flood parameter as water depth using flood masks and a very high resolution digital elevation model. Combining this results with GIS data leads to an additional benefit of information and simplifies the decision making (Brivio et al., 2002, Townsend and Walsh, 1998). The combination of the GIS and remote sensing data is often carried out by overlaying the different data sources. But, there are only few approaches which use the raster data from imagery to assess the given GIS data. In (Gerke et al., 2004, Gerke and Heipke, 2008) an approach for automatic quality assessment of existing geospatial linear objects is presented. The objects are assessed using automatically extracted roads from the images (Wiedemann and Ebner, 2000, Hinz and Wiedemann, 2004). However, in case of natural disasters the original roads are destroyed or occluded and therefore, it is not possible to extract them using the original methods. Hence, new approaches have to be developed which assesses damaged and occluded objects, too. The integration and exploitation of different data sources, e.g. vector and image data, was discussed in several other contributions (Baltsavias, 2004, Butenuth et al., 2007). However, there is a lack of methods, which assess the GIS data concerning its functionality using imagery (Morain and Kraft, 2003).

In this paper, a classification system using remote sensing data and additionally available information is developed to assess GIS objects. The main goal of the system is the automatic classification and evaluation of infrastructure objects, for example the trafficability of the road network after natural disasters. However, the presented system can be transferred to other scenarios, such as changes in vegetation, because its design is modular. A focus is the integrated utilization of any available information, which is important to ease and speed up the classification process with the aim to derive complete and reliable results (Reinartz et al., 2003; Frey & Butenuth, 2009). Compared to the manual interpretation of images the presented systems is very efficient, which is essential in crisis scenarios. Depending on the type and complexity of the input data, the system can be run in a fully automatic or semi-automatic mode, where a human operator can edit intermediate results to ensure the required quality of the final results.

Section 2 describes the generic near-realtime classification system with the objective to classify and evaluate objects using remote sensing and other available data. In Section 3 the system is applied for road objects in case of natural disasters. Two test scenarios of flooded areas are used to verify the system. By means of manually generated reference data, the applicability and efficiency of the system is evaluated in Section 4. Finally, further investigations in future work are pointed out.

2. System Overview

The goal of the developed classification system is the assessment of GIS-objects using up-to-date remote sensing data. The system is designed in a general and modular way to provide the opportunity to divide GIS-objects into different states. Typical states describe the functionality of infrastructure objects as roads or buildings. The generic system embeds different kinds of image data: multi-sensor as well as multi-temporal data. Additionally, any kinds of available data sources and spatial knowledge, which contributes information for the assessment, can be embedded. Typical examples are digital elevation models (DEM) and further GIS information, e.g. land cover or waterways. The minimum requirement of the system is the objects to be assessed and one up-to-date image, which provides the information for the assessment.

The classification system depicted in Figure 1 can be subdivided into different components. Starting point are the GIS-objects to be assessed and the input data such as imagery or digital elevation models, which contribute the information for the assessment. In the following this information is called *data*. Next component is the classification system itself and, finally, a resulting up-to-date map.

The fusion of multi-sensor images is an important issue, because the co-registration between optical and radar images is still a current research topic (Pohl and Van Genderen, 1998). Methods such as mutual information can be applied for the system (Inglada and Giros, 2004). The system has to deal with multi-temporal images having the possibility to derive important information on time. This leads to an even more complex corregistration process. Change detection algorithms can provide information about the variation of assessed objects. In the following article the temporal factor is neglected, but will be an essential part in future research.

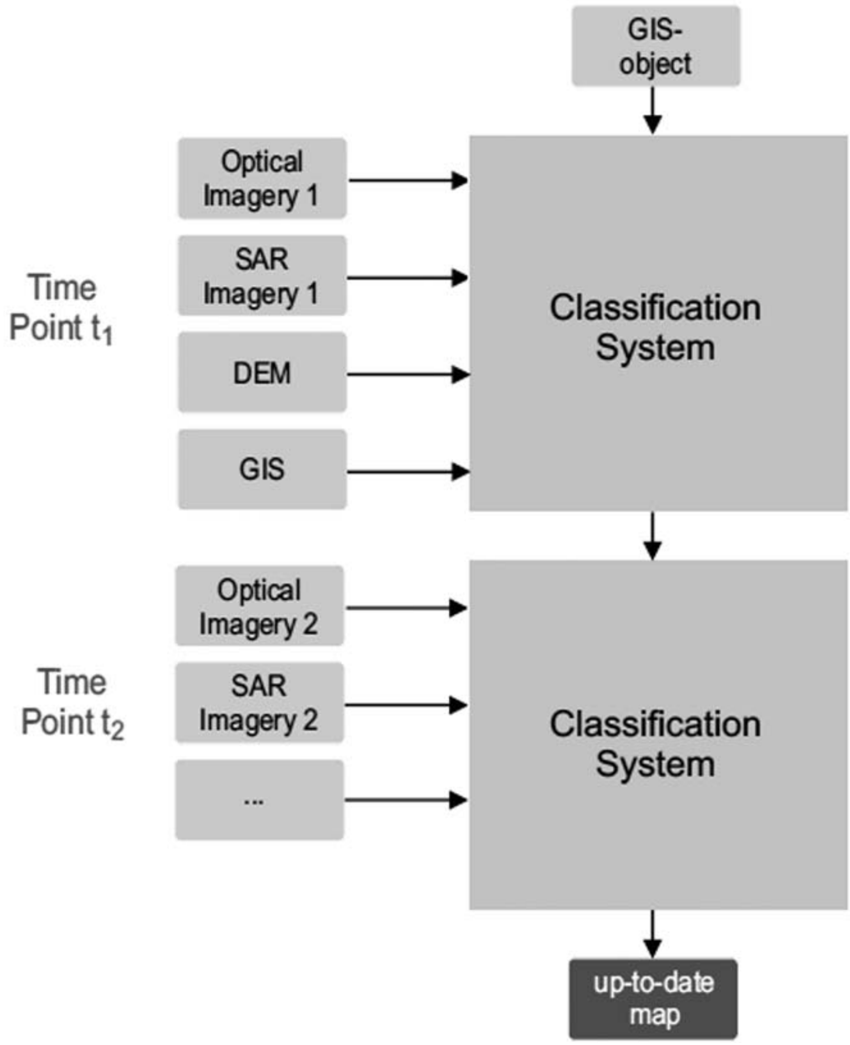

Figure 1: Classification System

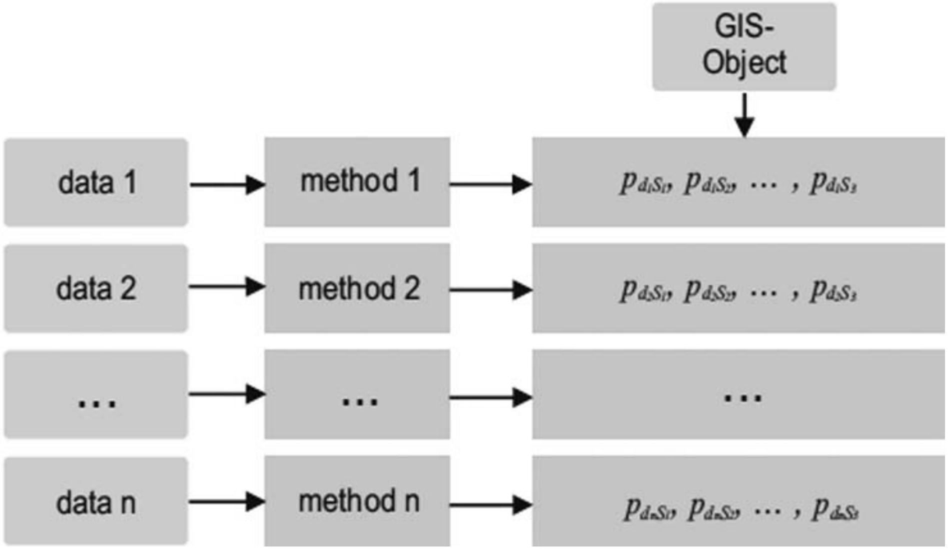

Figure 2: Derivation of probabilities from data using various methods

The classification module represents the core of the system. The goal is to classify each object into different states S_i. For each object, probabilities are derived belonging to a certain state. The methods estimating the probabilities depend on the data. Typical examples for methods are multispectral classification or fuzzy membership functions (Figure 2).

Beside the derivation of the individual probabilities from each data source the combination plays a decisive role:

$$p_{S_1} = p_{d_1,\, S_1} \otimes p_{d_2,\, S_1} \otimes \dots \otimes p_{d_n,\, S_1}$$
$$p_{S_2} = p_{d_1,\, S_2} \otimes p_{d_2,\, S_2} \otimes \dots \otimes p_{d_n,\, S_2}$$
$$\vdots$$
$$p_{S_i} = p_{d_1,\, S_i} \otimes p_{d_2,\, S_i} \otimes \dots \otimes p_{d_n,\, S_i}$$

The variable $p_{d_n,\, S_i}$ denotes the probability that the state S_i occurs given data d_n. The indices i and n describe the number of available states and data, respectively. The result p_{Si} gives the probability that a GIS-object belongs to the state S_i. For given data, weights w_n can be introduced in order to cope with the different influence of information content. Hence, the above equation for one state i leads to:

$$p_{S_i} = w_1 \cdot p_{d_1,\, S_i} \otimes \dots \otimes w_n \cdot p_{d_n,\, S_1}$$

Finally, the object is assigned to the state S_i with the largest probability p_{S_i}. A basic characteristic of the whole system is the combination at the probability level in order to remain flexible concerning the available data.

3. Automatic assessment of road objects

The generic system described above is now specified for the assessment of linear objects, such as roads after flooding. The introduced model is transferable to other linear objects like railways. In a similar sense the context can be adapted to other natural disasters such as avalanches, landslides or earthquakes. In case of natural disasters the GIS-object can be divided into the state *intact/usable* or *not intact/destroyed*. Furthermore, a state between these extrema is possible. Hence, a third state *possibly not intact/destroyed* is introduced, if the automatic approach can not provide a reliable decision. In order to assess roads after a flood disaster following states can be used:

– *Trafficable*
– *Flooded*
– *Possibly Flooded*

For every available data source the probability for each state has to be derived. The methods which are employed to the different data are shown in the following section.

3.1 Evaluation methodologies

A multispectral classification is accomplished in order to derive different classes from imagery. The goal is to assess each linear object individually without taking adjacent linear objects into account, because such kind of topological knowledge about the connectivity of a road network is no more valid in case of road networks hit by a natural disaster. Every linear object is a polygon, which consists of several line segments. Every line segment is assigned to a class using a segment-based multispectral classification. To this end, a buffer is defined around each line to investigate the radiometric image information. In many cases attribute information from a GIS, such as the width of the line object, can be used in order to generate the size of the buffer region.

For the multispectral classification various classes have to be defined depending on the underlying imagery in order to classify the road segments into the three states *trafficable*, *flooded* and *possibly flooded*. In case of optical imagery the class road, water, forest and clouds are convenient, because the class road corresponds to the state *trafficable*, the class water to *flooded* and the classes forest and clouds describe occlusions and therefore belong to the state *possibly flooded*. If radar images are available the class clouds can be neglected. Beside the assignment to a class each individual line segment consists of a probability belonging to a class μ_i. The probability can be formulated as $p_{\mu_i}(g)$, in which g defines the gray values. The length of the vector is equivalent to the number of channels.

Beside the imagery additional information such as digital elevation models or GIS data can be integrated in the system. The methods to derive probabilities depend on the data. One method is membership functions of fuzzy sets (Zadeh, 1965). Membership functions do not describe the likelihood of some event, but they characterize a degree of truth in vaguely defined sets. To emphasize the distinction the membership function is labeled as μ instead of p.

Membership functions $\mu_t(a)$, $\mu_f(a)$ can be generated given a digital elevation model. The

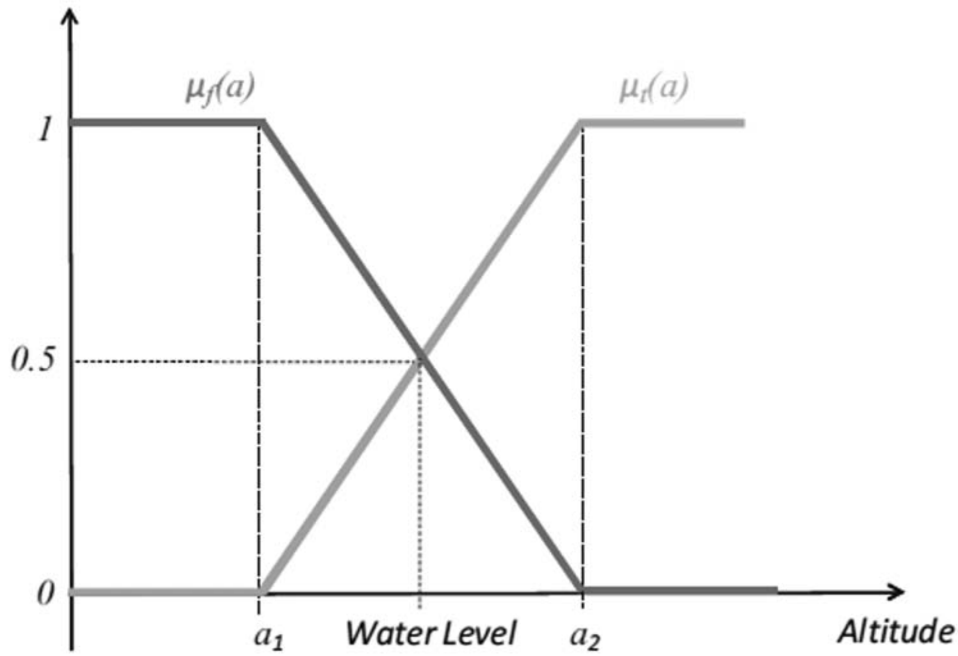

Figure 3: Membership functions for flooded roads and trafficable roads derived from DEM

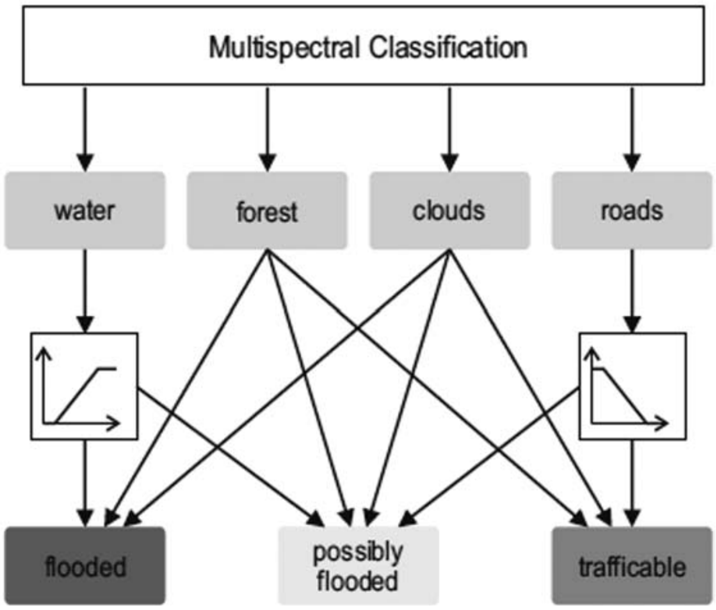

Figure 4: Schematic overview of the classification system

function $\mu_t(a)$ denote the belonging to the state *trafficable t* depending on the altitude *a*. Similarly, $\mu_f(a)$ represents the state *flooded f*. Both functions are illustrated in Figure 3. There are two thresholds a_1 and a_2, which determine the height of very likely flooded or trafficable areas, respectively. The current water level lies between these thresholds, which can be calculated by

$$a_1 = l_l - b_1$$
$$a_2 = l_h + b_2$$

in which l_l is the lowest and l_h is the highest water level in the scene. In order to involve variations due to flows and barriers additional offset-thresholds b_1, b_2 are added.

3.2 Combination of confidence values

The next module of the classification system combines probabilities resulting from a multispectral classification with the results obtained from the membership functions. The combination leads to a value describing again the degree of truth and not a real likelihood. In this section, an example is shown which combines the derived probabilities from optical images with membership functions inferred from a digital elevation model. By means of multispectral classification for each class (water *w*, road *r*, forest *o*, cloud *c*) the corresponding probability $p_{!_i}$ for $i = \{w, r, o, c\}$ can be derived. On the other side, the membership function provide the degree of truth $\mu_t(a)$ and $\mu_f(a)$. Utilizing the knowledge that roads higher than a_2 are definitely trafficable and roads lower than a_1 are very likely flooded a case differentiation is carried out:

$$\mu_f(\vec{g}, a) = \begin{cases} \mu_f(a) = 1 & a \le a_1 \\ \mu_f(a) \cdot p_{w_w}(\vec{g}) & a_1 < a < a_2 \\ \mu_f(a) = 0 & a \ge a_2 \end{cases}$$

$$\mu_t(\vec{g}, a) = \begin{cases} \mu_t(a) = 1 & a \le a_1 \\ \mu_t(a) \cdot p_{w_r}(\vec{g}) & a_1 < a < a_2 \\ \mu_t(a) = 0 & a \ge a_2 \end{cases}$$

Variable *a* denotes the height of a road object. The road is assigned to the state *Flooded* S_F if the degree of truth $\mu_f(g, a)$ exceeds an threshold t_1, which can be pre-estimated via the standard deviation of the likelihood function resulting from the training data for water. The road is assigned to the state *Possibly flooded* S_{PF}, if $\mu_f(g, a)$ is less than t_1. $\mu_t(g, a)$ is treated in an analogous manner. The road is assigned to the state *Trafficable* S_T if $\mu_t(g,a)$ exceeds a pre-determined threshold t_2. Otherwise, the road is again assigned to the state *Possibly flooded* S_{PF}. The road segments which are classified as forest ω_o or Cloud ω_c are assigned to the states in the following way:

$a < a_1 \quad \Rightarrow$ *Floaded* S_F
$a_1 < a < a_2 \quad \Rightarrow$ *Possibly Floaded* S_{PF}
$a > a_2 \quad \Rightarrow$ *Trafficable* S^T

In Figure 4 a schematic overview of the used classification system is depicted. A multispectral classification is carried out to assign the road objects to the different classes. The results of the multispectral classification combined with the membership function leads to the assignment of the road objects to the different states.

4. Results and evaluation

The presented system has been exemplarily tested with two scenarios representing flood disasters. In both cases roads are assessed concerning their trafficability. The first scenario is the Elbe flood in the year 2002 near Dessau, Germany. Three different data sources are used for the assessment: Firstly, an IKONOS-Image with four channels (red, green, blue and infrared), cf. Figure 5. The ground sampling distance of the panchromatic channel is 1 m and of the color-channels is 4 m. As second source a digital elevation model of 10 meters resolution is used. Finally, the objects to be assessed are taken form the ATKIS database, the German Official Topographic Cartographic Information System. The test scene covers an area of 33 km^2 and 5484 line segments are to be assessed.

The second study area covers the Gloucesterhire region in Southeast England, where a record flood level was measured at Tewkesbury in July 2007. During the flooding a 9,5 km^2 TerraSAR-X scene in StripMap mode with a spatial resolution of 3 m was acquired. The polarization is HH, which is more efficient than HV or VV to distinguish flooded areas (Henry et al., 2003). Additionally, linear membership functions from the original rivers are derived and an automatically extracted flood mask is used. 522 road objects taken from OpenStreetMap are assessed in the following. The test scenarios are challenging due to their diverse complex environments and the different kinds of roads. The roads vary from paths to highways. Both test scenarios are evaluated using manually derived reference data. To draw conclusions from the following results, it is important to consider the kind of used reference data. In general, the availability of reference data describing the true state of roads during the flooding is very difficult. One possibility is to derive the reference data from the image itself, which is done for the Elbe scenario. This kind of reference data does not describe the real ground truth, but the information which is possible for a human interpreter to extract from the studied image. In the case of the Gloucesterhire scenario, high resolution airborne image with a resolution of 20 cm are available. This imagery was acquired half a day later than the TerraSAR-X scene, so that quite reliable ground truth is available.

The results of the Elbe scene are depicted in Figure 5. The red lines refer to flooded roads, green lines to trafficable roads and the yellow lines point out, that no decision is possible by the automatic system. In Figure 6 a detail of the original IKONOS image and the assessed roads is shown. Comparing the result with the manually generated reference leads to the numerical results shown in Table 1. »Correct assignment« means that the manually generated classification is identical with the automatic approach. In the case of »Manual control necessary« the automatic approach leads to the state *possibly flooded* whereas the manual classification assigns the line segments to *flooded* or *trafficable*. The other way around denotes the expression »Possibly correct assignment«. »Wrong assignment« means that one approach classifies the line segment to *flooded* and the other to *trafficable*. With the current implementation of the system the approach achieves a correct assignment for 78% of the road objects. Only a very few false assignments are obtained. This result is slightly deteriorated due to the 5% of »Possibly wrong assignments«. Less than 1/5 of all road

Table 1: Results for Elbe example

Possible assignment	Result
Correct assignment	76.99%
Manual control necessary	17.87%
Possibly correct assignment	4.96%
Wrong assignment	0.18%

Table 2: Results for Gloucesterhire example

Possible assignment	Result
Correct assignment	81.22%
Manual control necessary	4.60%
Wrong assignment	14.18%

Figure 5: Automatic assessment of roads using the classification system: flooded roads (red), trafficable roads (green) and possibly flooded roads (yellow)

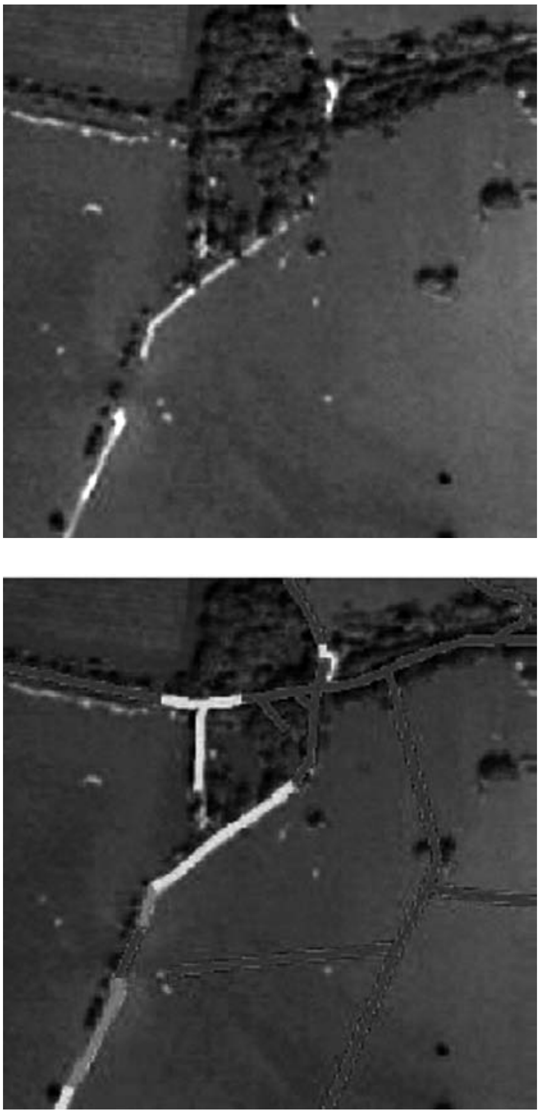

Figure 6: Detail of original and assessed IKONOS scene

segments (17%) should be controlled manually in order to reach a correctness of 95%.

The results are obtained with the threshold parameters t_1 = 0.5 and t t_2 = 0.001. The variations of the parameters are depicted in Figure 7. The parameters are responsible for the amount of road segments which are assigned to the state *possibly flooded* on condition that they are classified to the classes water or road. The decrease of »Wrong assignment« comes along with the decrease of »Correct assignments« and an increase of manual control.

In Figure 8 the combination of $\mu_f(a)$ and $p_{!w}(g)$ is shown. The gray scale bar indicates the combined value $\mu_f(g, a)$. Every star defines a road segment assigned to the class water by multispectral classification, the color shows the state assigned in the reference. Many road segments which are assigned to the state *trafficable* in the reference are wrongly classified by the system to the class water. The reason is the high standard deviation of the probability density function for the class road and, therefore, the overlapping of the class road and water. Road segments in urban areas occluded by shadows are responsible for this effect. The threshold t_1 is depicted in blue separating the assignment of roads into *flooded* and *possible flooded* (Figure 8). Shifting this parameter leads to the results illustrated on the right plot in Figure 7. Furthermore, the improvement of the combined probability is shown in Figure 8. If only one probability is available, threshold t_1 would be drawn as a straight horizontal or vertical line.

The total required time to generate the manual reference is about three hours. Compared to the time needed for the automatic classification (less than one minute) points out the efficiency of the approach. The results of the second test scenario are depicted in Figure 9. A detail of the original TerraSAR-X scene and the assessed road segments is shown in Figure 10.

In the second test scenario the real ground truth is available. Hence, the category *possibly flooded* is not necessary for the reference data. The comparison with the automatic classification system leads to the result shown in Table 2. After checking only 5% of the road segments manually, altogether over 86% are correctly assigned. The value of 14% of wrong assignments is caused by mainly two reasons: Firstly, the resolution of the StripMap mode hardly enables to detect flooded roads in urban areas. Secondly, the geometric accuracy of the used OpenStreeMap road objects is not accurate enough for a correct assignment in many cases.

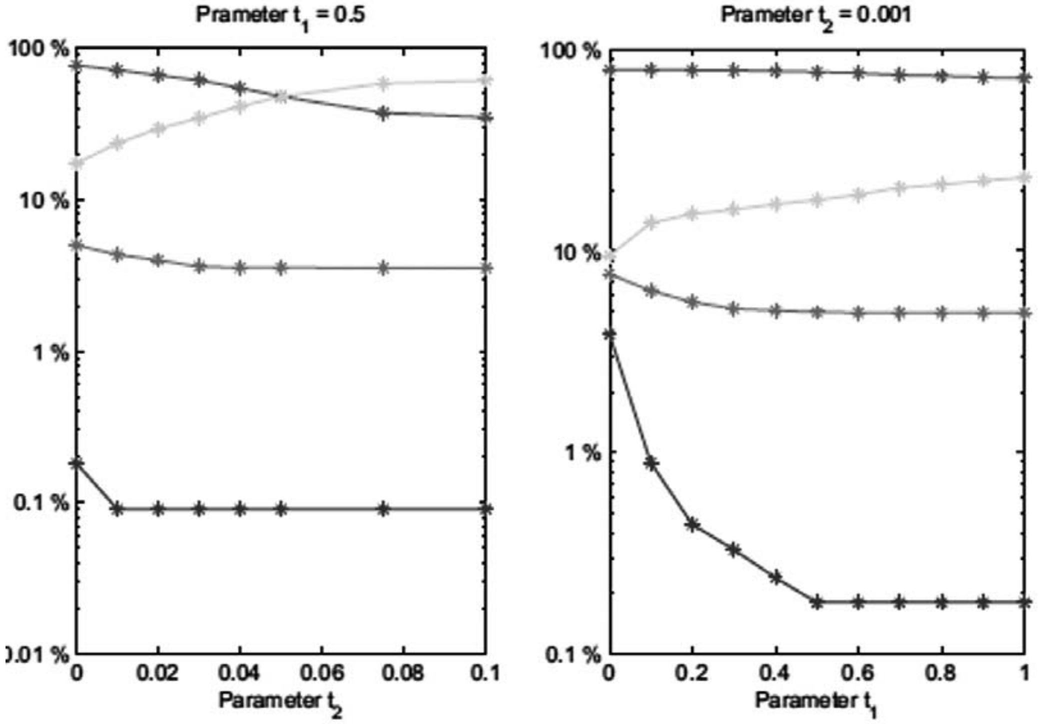

Figure 7: Results dependent on parameter t_1 and t t_2 (red = Wrong, orange = Possibly correct, yellow = Manual control necessary, green = Correct)

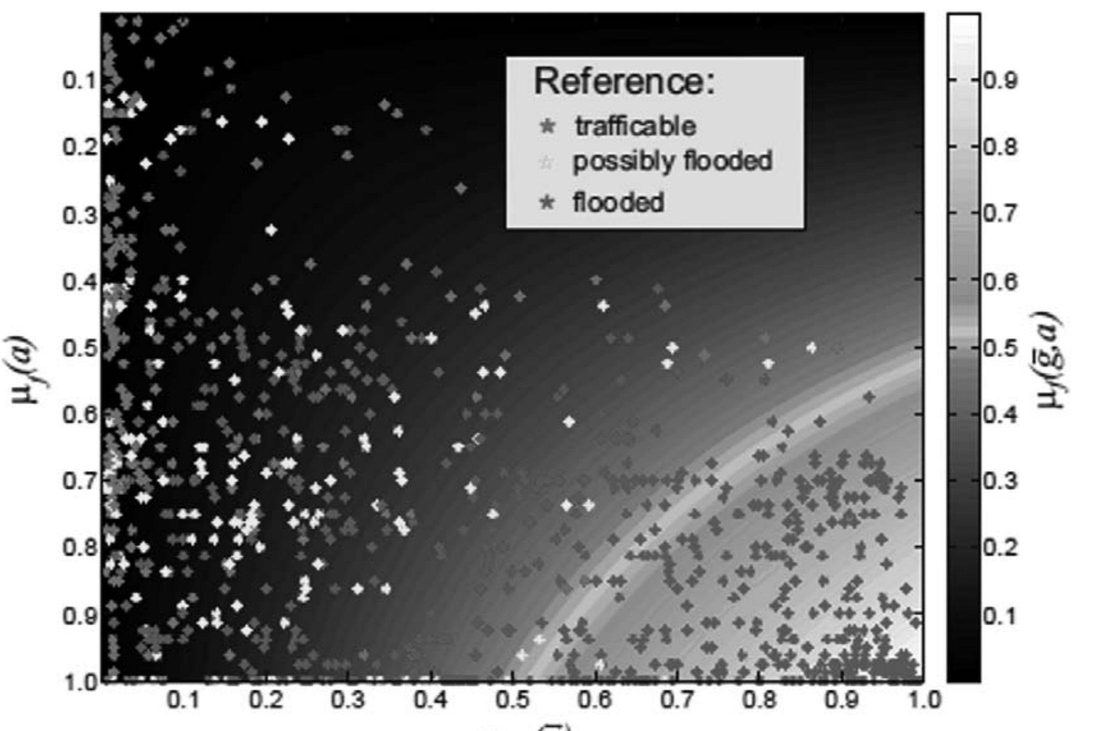

Figure 8: Combination of confidence values and impact of the parameter t_1

Figure 9: Automatic assessment of roads using the classification system: flooded roads (red), trafficable roads (green) and possibly flooded roads (yellow)

5. Conclusions and outlook

We presented a comprehensive classification system to assess linear GIS-objects concerning their current state in the context of a natural disaster. The system is evaluated by means of two test scenarios with the goal to derive the trafficability of roads during a flooding. Both test scenarios show the performance and especially the efficiency of this approach. In future work, the whole system will be evaluated using real ground truth to identify the reliability in disaster scenarios. Moreover, the additional benefit combining different image data types such as optical and radar will be part of further studies. The main attention in future work comprises the development of multi-temporal models to better exploit different image acquisition times including different data types.

Acknowledgment

This work is part of the IGSSE project »SafeEarth« funded by the Excellence Initiative of the German federal and state governments, and part of the project »DeSecure«. The authors would like to thank the Federal Agency for Cartography and Geodesy Sachsen-Anhalt to provide the DEM and the ATKIS road data.

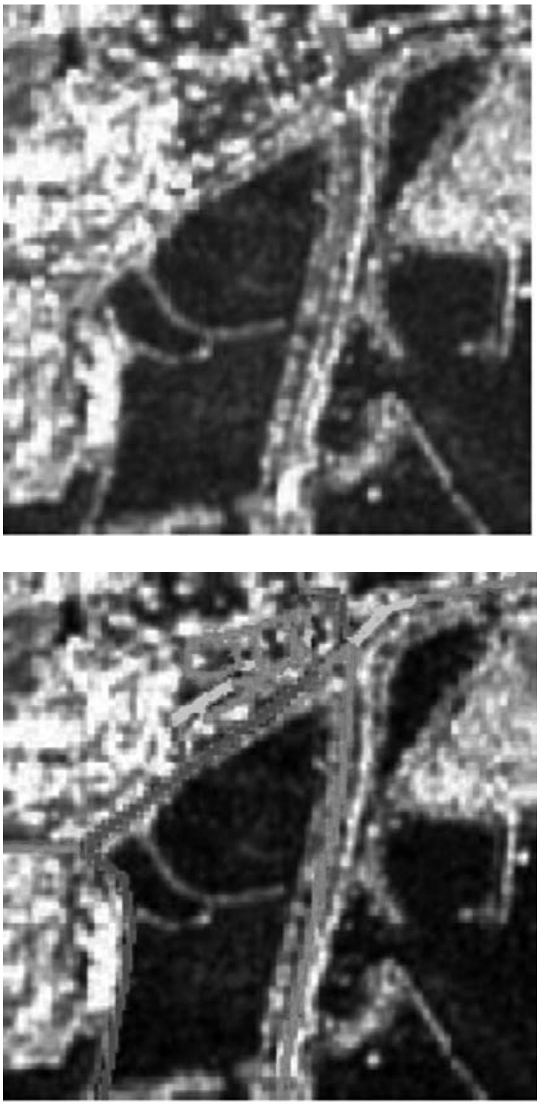

Figure 10: Detail of original and assessed TerraSAR-X scene

References

Baltsavias, E., 2004. Object extraction and revision by image analysis using existing geodata and knowledge: current status and steps towards operational systems. ISPRS Journal of Photogrammetry and Remote Sensing 58(3–4), pp. 129–151.

Brivio, P., Colombo, R., Maggi, M. and Tomasoni, R., 2002. Integration of remote sensing data and GIS for accurate mapping of flooded areas. International Journal of Remote Sensing 23(3), pp. 429–441.

Butenuth, M., Gösseln, G., Tiedge, M., Heipke, C., Lipeck, U. and Sester, M., 2007. Integration of heterogeneous geospatial data in a federated database. ISPRS Journal of Photogrammetry and Remote Sensing 62(5), pp. 328–346.

Frey, D. and Butenuth, M., 2009. Analysis of road networks after flood disasters using multi-sensorial remote sensing techniques. Publikationen der Deutschen Gesellschaft für Photogrammetrie, Fernerkundung und Geoinformation 18, pp. 69–77.

Gerke, M. and Heipke, C., 2008. Image-based quality assessment of road databases. International Journal of Geographical Information Science 22(8), pp. 871–894.

Gerke, M., Butenuth, M., Heipke, C. and Willrich, F., 2004. Graph-supported verification of road databases. ISPRS Journal of Photogrammetry and Remote Sensing 58 (3–4), pp. 152–165.

Henry, J., Chastanet, P., Fellah, K. and Desnos, Y., 2003. ENVISAT multipolarised ASAR data for flood mapping. Proceedings of Geoscience and Remote Sensing Symposium, IGARSS vol. 2, pp. 1136–1138.

Hinz, S. and Wiedemann, C., 2004. Increasing efficiency of road extraction by self-diagnosis. Photogrammetric Engineering and Remote Sensing 70(12), pp. 1457–1464.

Inglada, J. and Giros, A., 2004. On the possibility of automatic multisensor image registration. IEEE Transactions on Geoscience and Remote Sensing 42(10), pp. 2104–2120.

Kundzewicz, Z., Ulbrich, U., Brücher, T., Graczyk, D., Krüger, A., Leckebusch, G., Menzel, L., Pinskwar, I., Radziejewski, M. and Szwed, M., 2005. Summer floods in central europe – climate change track? Natural Hazards 36(1), pp. 165–189.

Martinis, S., Twele, A. and Voigt, S., 2009. Towards operational near real-time flood detection using a split-based automatic thresholding procedure on high resolution TerraSAR-X data. Natural Hazards and Earth System Science 9(2), pp. 303–314.

Milfred, C., Parker, D. and Lee, G., 1969. Remote sensing for resource management and flood plain delineation. 24thMidwestern States Flood Control and Water Resources Conference.

Morain, S. and Kraft, W., 2003. Transportation lifelines and hazards: Overview of remote sensing products and results. Proceedings of Remote Sensing for Transportation 29, pp. 39–46.

Pohl, C. and Van Genderen, J., 1998. Multisensor image fusion in remote sensing: concepts, methods and applications. International Journal of Remote Sensing 19, pp. 823–854.

Reinartz, P., Voigt, S., Peinado, O., Mehl, H. and Schröder, M., 2003. Remote sensing to support a crisis information system: Mozambique rapid flood mapping system, river elbe flood: Germany 2002. Proceedings of Remote Sensing of Environment pp. 10–14.

Sanyal, J. and Lu, X., 2004. Application of remote sensing in flood management with special reference to monsoon Asia: a review. Natural Hazards 33(2), pp. 283–301.

Townsend, P. and Walsh, S., 1998. Modeling floodplain inundation using an integrated GIS with radar and optical remote sensing. Geomorphology 21(3–4), pp. 295–312.

Van der Sande, C., De Jong, S. and De Roo, A., 2003. A segmentation and classification approach of IKONOS-2 imagery for land cover mapping to assist flood risk and flood damage assessment. International Journal of Applied Earth Observations and Geoinformation 4(3), pp. 217–229.

Wiedemann, C. and Ebner, H., 2000. Automatic completion and evaluation of road networks. International Archives of Photogrammetry and Remote Sensing 33(B3/2–3), pp. 979–986.

Zadeh, L., 1965. Fuzzy sets. Information and Control 8(3), pp. 338–353.

Zwenzner, H. and Vogt, S., 2008. Improved estimation of flood parameters by combining space based SAR data with very high resolution digital elevation data. Hydrology and Earth System Sciences Discussions 5(5), pp. 2951–2973.

Geocoding Sensor Data – Applying OGC's Sensor Web Enablement Specifications

Walter K.
Rostock University, Faculty of Agricultural and Environmental Sciences,
Institute for Management of Rural Areas, Chair of Geodesy and Geoinformatics
Justus-von-Liebig-Weg 6, 18059, Rostock, Germany
eMail: kai.walter@uni-rostock.de

Introduction

The Open Geospatial Consortium (OGC) addresses the requirement of integrating sensor information into spatial information infrastructures by developing service interfaces, protocols and data types in the Sensor Web Enablement (SWE) specification series. Using web-based services as tools for interdisciplinary data exchange, as well as for the extensive usage of heterogeneous data resources is an important step towards addressing today's larger scale environmental problems (Bacharach, 2008). By making measurements and results discoverable and accessible over the internet, data producers can reduce data redundancy and existing data sets can be used to their full capacity.

Even though SWE services are designed to be a foundation for »plug&play« access to sensors and sensor networks, questions about how to apply standards for information providers still have to be answered. Compared to the »state of the art« of specialised mass-market ready sensor and communication technology, SWE standards appear bloated, impractical and hard to implement. The project SLEWS (**S**ensor-based **L**andslide **E**arly **W**arning **S**ystem) uses existing commercial sensor products, implementing SWE technologies on top as a middleware layer to provide the data in an open and interoperable manner as a proof-of-concept. Results of the project's work outline approaches to improve the process of providing sensor data in a SWE-enabled format using today's commonly used internet technologies.

Sensor-based Landslide Early Warning System

The collaborative research project SLEWS aims for the systematic development of a prototype alarm and early warning system for mass movements. Project partners are the Department of Engineering Hydrogeology at RWTH Aachen, the Federal Institute for Geosciences and Natural Resources (Hannover), the Chair of Geodesy and Geoinformatics at Rostock University and ScatterWeb GmbH (Berlin). Early warning and alarm systems are an effective tool to reduce risks from landslides (Fernandez-Steeger et al., 2008). The main goals of SLEWS are the utilisation of ad hoc wireless sensor networks and spatial data infrastructure technologies according to OGC guidelines to produce a low-cost, interoperable and performant early warning system. Methods of data access, communication and visualisation are to be implemented using SWE specifications, concurrently offering information resources via open standards to external applications while importing interoperable resources in return (Bill et al., 2008).

System Architecture

Wireless Sensor Network

Wireless sensor networks (WSN) provide an inexpensive and easy to implement monitoring system for landslide events. Sensor nodes are fitted with sensors such as tilt meters and pressure, acceleration and displacement detectors specifically chosen to monitor engineering-geological parameters of landslide events. Due to improved manufacturing processes and progress in the area of micro sensor systems, small but precise low-cost sensors can be integrated in such systems.

The WSN used in SLEWS is constructed by the project partner ScatterWeb. As a modern and autonomous ad hoc wireless sensor network it is characterised by self-organisation and self-healing capacity. Data packages from each node are sent via radio waves directly or via other nodes (multi-hop) to a collection point (gateway). Energy efficiency is achieved by reducing transmission power to only communicate with adjacent nodes. The bi-directional structure of the system enables data transfer from each node via the gateway interfaces to the main computer unit (PC, laptop, server) and also allows the transmission of commands such as data requests and software-updates to individual nodes or to a group of nodes (Arnhardt et al., 2007).

Measurement data is retrieved from the WSN via a specialised gateway node. To read out the data the gateway node has to be connected to a computer unit (gateway server, see Figure 1) via wired or wireless connection. An application running on the gateway server can access the data stream arriving at the gateway node, consisting of text output representing data packages received from sensor nodes.

SWE Services

Sensor Observation Service

A Sensor Observation Service (SOS) offers a web-based interface to retrieve measurement data and sensor information via HTTP-based spatial and temporal queries (OGC, 2008). Response formats of the SOS are the XML-based data encoding schemes SensorML and Observation & Measurement (O&M):

SensorML is used to describe and formalise the parameters of a sensor or data producer. The way sensors are described in SensorML is strictly process-based and can be used to capture sensor metadata, operation sequences as well as software patterns of data-related operations. Every procedure a SOS offers data from has to be described by a particular SensorML document, which will be returned in response to a *DescribeSensor* query. SensorML is thus used to enable interoperability of sensors by allowing a client to discover new sensors and to prepare for the interpretation of measurements in a hardware-independent manner.

O&M is used for the exchange of actual measurements and observations. O&M output documents can be requested using the *GetObservation* operation with options to filter all available observations by time, location, observed phenomenon or sensor. O&M is comparable with the well-established OGC format for vector data, Geography Markup Language (GML). Elements of GML are already used in O&M and the OGC SWE working group is currently attempting to fully harmonise both standards.

To understand the functionality of a SOS it is helpful to outline the SWE spatial view on the conventional sensor/measurement concept. Consistent to well-established OGC models, a sensor, as one of many possible data producers called *procedure*, is well-defined by a location called *feature of interest*. At a location an *observation* is recorded which represents a certain *phenomenon* at a certain time.

Sensor Planning & Sensor Alert Service

Bi-directional communication with the WSN to remotely control functions such as energy management or measurement cycle rate is possible by sending instructions via the gateway node. The process of communicating these instructions to the WSN can be encapsulated using a Sensor Planning Service. A SPS offers the execution of a set of instructions via standardised web-based interface. Users of the SOS can thus remotely adapt the process of

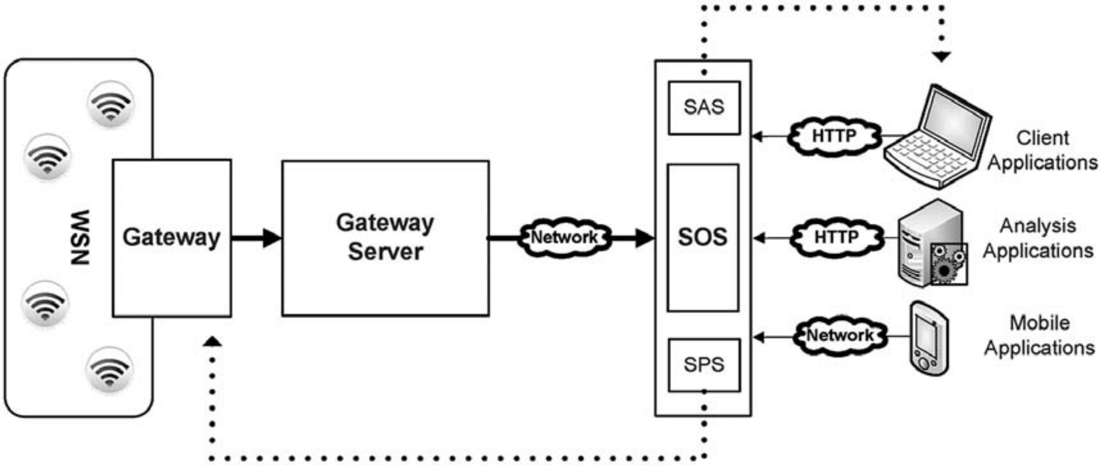

Figure 1: Current SLEWS information infrastructure (SAS = Sensor Alert Service, SOS = Sensor Observation Service, SPS = Sensor Planning Service)

data gathering without the requirement of knowing details of the WSN's operations.

Another aspect of bi-directional communication with the WSN is the need for event-based notification to users without having to continuously »poll« the SOS for new information. A Sensor Alert Service (SAS) allows the subscription of clients to messages coming from a sensor system matching certain criteria. Users are then able to receive messages about threshold exceedance or sensor malfunction asynchronously, being notified to request more detailed information from the SOS or to heighten the WSN's measuring sensibility via SPS.

Methods

Geocoding WSN Data

To be processable by the SOS and SAS, measurement data coming from the gateway node have to be transformed to fit the appropriate SWE data model. This process is also called formalising or geocoding sensor data. A manufacturer-specific application running on the gateway server is used to access the data stream arriving at the gateway node, consisting of text output representing data packages received from the WSN. A typical measurement string has the form

S4 20 2008-08-13#16:14:12 2696

where *S4* is the network identification number (node number 4), *20* is the sensor identification number for the specific node, followed by sampling date, time and the actual sampling value (*2696*, sensor specific hexadecimal form). While date, time and value can be adopted almost unchanged, network and sensor identification numbers have to be resolved using previous knowledge. Knowing the identification numbers, information such as sensor location (*feature of interest*), sensor properties (*procedure*) and observed phenomena (*phenomenon*) can be determined.

Another application running on the gateway server parses the incoming data strings, dividing them into tokens using look-up tables (shown simplified in Table 1) to determine adequate SWE parameters. Most parameter values must be expressed in a certain XML-based form, e.g. values for *procedure* and *phenomenon* are used in Uniform Resource Name (URN) notation. URNs, as specialised cases of Uniform Resource Identifiers (URI – W3C, 2006), serve in XML-based O&M or SensorML documents to unambiguously identify information resources and phenomenon definitions by semantic descriptions.

Making WSN Data Accessible

Within the SLEWS project, the determined »SWE-enabled« data set can be inserted in the

Table 1: Simplified look-up table for SWE-based parameters

SWE parameter	Node-ID: **(S4)**	Sensor-ID: **(20)**
procedure	**urn:ogc:object:feature: Sensor:SLEWS:slewsMote_0.1.1**	
offering		**Atmospheric_Temperature**
phenomenon		**urn:ogc:def:phenomenon: OGC:1.0.30:temperature**
feature of interest	**locationID: id001** **descr.: Aachen sampling point 1** **coord.: 50.776208,6.080085**	

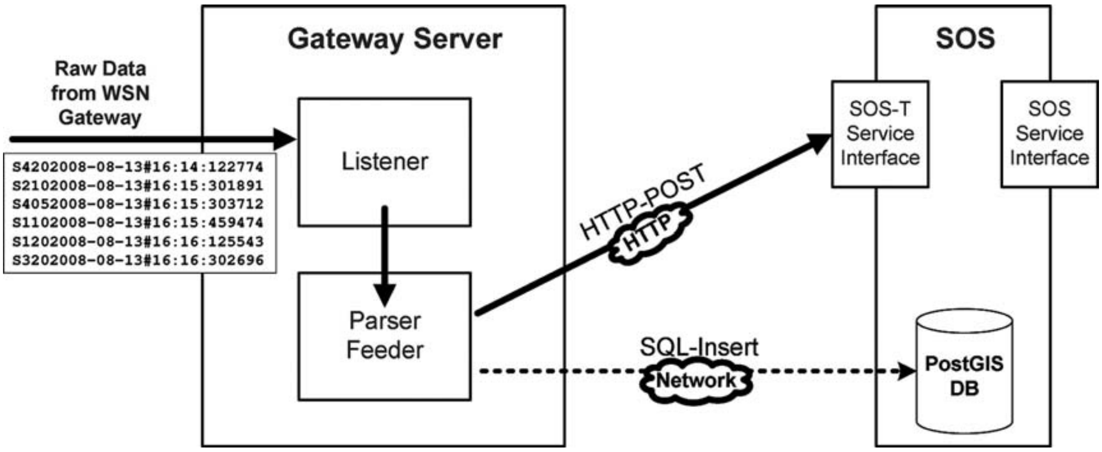

Figure 2: Importing data from the WSN into the Sensor Observation Service

SOS database by a feeder application running on the gateway server (see Figure 2). Even though this way of data transmission shows very good performance, it is not further discussed because of its lack of interoperability. In order to be able to insert data directly the database has to be remotely accessible and a considerable amount of detailed knowledge (access parameters, access permission, database structure) is required. Another way to transmit data is using the SOS interface itself. For this, the transactional SOS operations (*RegisterSensor*, *InsertObservation)* require data sets to be O&M- (and SensorML-) formatted. Any data provider using proper HTTP-requests is able to register with the SOS and supply it with data sets without previous knowledge. As a result the parser/feeder applications running on the gateway server were modified to support transactional SOS operations. The transmission performance is currently under evaluation.

Discussion

Even though the use of web-based interfaces to supply SWE services with data benefits interoperability, extending and reformatting sensor-specific data to fit a SWE-based layout still requires a high amount of training and the implementation of highly specialised software applications. Within the SLEWS project significant customisation has proven to be necessary, however building an Early Warning System on top of SWE services makes very specific demands. In order to advance the widespread usage of SWE standards in the sensor community, more intuitive methods to interface sensor data and SWE services should be devel-

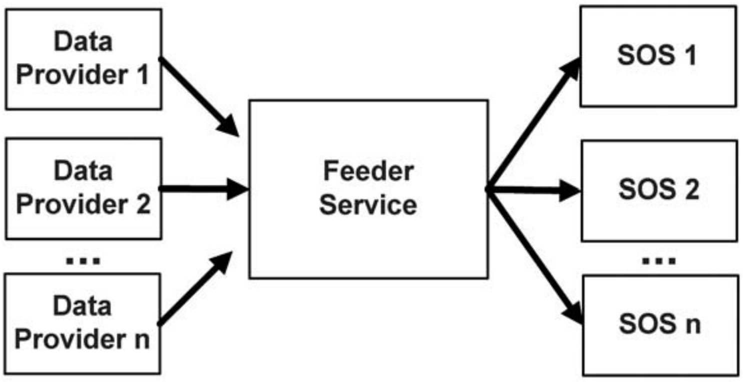

Figure 3: Using a feeder service a single entry point to supply different Sensor Observations Services with data

oped. »Casual« users and data providers should not directly be confronted with the production of feeder software, XML code or SWE semantics, thus the technical encapsulation of services with easy-to-use web-based applications functioning as mediating middleware seems to be a feasible approach. Here we present a potential model for future developments. Another more specialised sensor-system layer based formalisation model is described in (Walter et al., 2009) and will not further be discussed.

SWE Feeder Service

Using dedicated feeder web services (e.g. see 52° North, 2008) to transfer data from provider applications or sensor systems to SWE services is an important step towards »plug&play«-capability. Single feeder services can serve as an entry point for the data import in several transactional or non-transactional SOS (Figure 3). To publish their services, each SOS provider can register with the feeder service to provide the necessary information such as database access or the web address of the transactional interface. Potential data providers can supply a SOS with data without the requirement to know technical details. In addition, feeder services can hierarchically or thematically organise different SOS and present them to the user. However, at this point the data transmitted from the feeder service to the SOS must already be fully SWE compatible and O&M formatted so the process of geocoding raw sensor data has to take at place an earlier stage.

SWE Connector Client

Even when using middleware between SWE services and data provider, and considering the large number of different sensor systems, implementing solutions to convert a proprietary sensor format into a SWE-based format is still unavoidable and requires detailed knowledge. In order to overcome this problem, we propose that a dedicated »SWE connector« application should be developed. The application is proposed to act as a client to the previously described feeder web service, supporting the data provider in the process of geocoding the sensor data and transmitting it to a SOS via the feeder service. The SWE connector client, designed to be a user-friendly frontend to the feeder web service, should be implemented as a browser-based application. The use of JavaScript/AJAX technology would offer the user a vey intuitive interface rich in features previously available only in desktop applications.

The client has to support the option to upload raw data from different sources supplying generic tools for database-, file- or stream-based access. As a basic but widespread example, the CSV format (comma separated values) is very often used by sensor (network) operators as a file-based exchange format. The SWE connector application could easily implement functionality to upload and parse CSV or other file types. In a next step the user would have to provide a number of SWE parameters to expand the data model of the provided raw sensor data. A combination of user-friendly

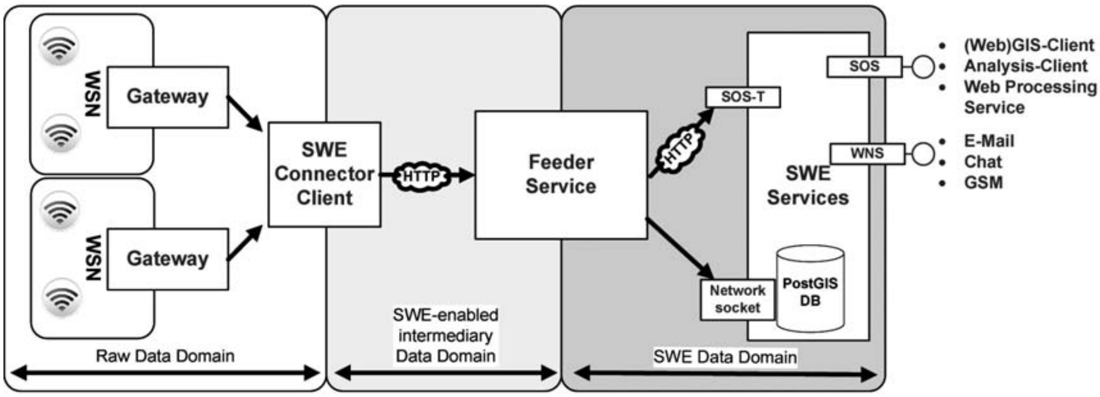

Figure 4: Layout of a middleware layer based SWE standardisation process (SOS-T: transactional SOS; WNS: Web Notification Services)

browser selection menus on top of SWE parameter dictionaries (e.g. for. phenomenon, sensor and location definition) would provide a sufficient tool to create complete SWE-based data sets. However, for transmitting the data from the SWE connector client to the feeder service, taking the overhead of uncompressed XML data traffic into account, the exchange format should not necessarily be O&M-based but in an intermediary lightweight format. Using JSON (JavaScript Object Notation) as a structured but compact data exchange format is a feasible approach. SWE parameters in the form of placeholder identification codes could be transmitted together with the sensor data as a data block which could easily be parsed and remodelled by the feeder service (Figure 4).

Conclusions and Future Work

The vision of the SWE-initiative is to create standards as a foundation for »plug&play" web-based sensor networks (Botts, 2007). The services and models produced provide effective tools to realise the concept envisioned by the OGC of uncoupling sensor information from the way they are collected and to make this information available over the web using standardised formats and interfaces. However connecting sensors to SWE services remains a difficult task requiring detailed knowledge of both the sensor system and of the SWE standards, and off-the-shelf WSN as used in the SLEWS project do not support SWE standards. As the experience in the project, shown in detail in the previous sections, this leaves an interoperability and usability gap which must be bridged by anyone wishing to provide data via SWE services.

First steps towards closing the gap are being taken with the utilisation of transactional SOS and multifunctional web service-based feeder services, mapping sensor data to the data model of the service backend. Further efforts in this process must be made focussing on the earlier stages of the data delivery chain. The result should be an easier way of providing sensor data from a large number of different sensor-native formats to a SWE-enabled format. Therefore we suggest a lightweight »SWE connector« web service application working as a frontend for feeder web services, providing a generic toolbox which can be adapted to import different raw data and exchange formats and transform them to a SWE-based data model. Taking system performance and limited communication resources into account, data transfer between services should not necessarily use O&M but rather a structured lightweight intermediary format such as JSON. Customised import plug-ins could be designed for a wide range of different data formats.

Current work within the SLEWS project is concentrating on the evaluation of different specialised as well as generic approaches. Different architectures and application implementations will focus on interfacing WSN and SWE services effectively. In the context of a time-aware alarm and monitoring system the principle usefulness of SWE technologies have to be determined. Furthermore, implementation of landslide event-based data analysis and decision management processes will be tested using a system architecture based on the coupling of SWE services with further OGC web service-based visualisation and notification technologies.

Acknowledgements
This work was funded by the German Federal Ministry for Research and Education under grant number FKZ: 03G0662A. The author would also like to thank colleagues from within the SLEWS project who have assisted with aspects of this work.

References
52° North Initiative for Geospatial Open Source Software GmbH (2008): Integration of different data sources into 52N SOS. URL: http://www.gi-tage.de/archive/2008/downloads/Material/geosensornetworks/52N_SWE_SOS_Feeder.pdf (accessed 14/01/2009)

Arnhardt, C.; Asch, K.; Azzam, R; Bill, R.; Fernandez-Steeger, T. M.; Homfeld, S. D.; Kallash, A.; Niemeyer, F; Ritter, H.; Toloczyki, M.; Walter, K. (2007): Sensor based Landslide Early Warning System – SLEWS. Development of a geoservice infrastructure as basis for early warning systems for landslides by integration of real-time sensors. – GEOTECHNOLOGIEN Science Report 10. Early Warning Systems in Earth Management, 75–88.

Bacharach, S. (2008): Sensors and the Environment. In: Vector 1 Magazine – Promoting Spatial Design for a Sustainable Tomorrow. URL: http://www.vector1media.com/article/feature/sensors-and-the-environment/(accessed 14/01/2009).

Bill, R.; Niemeyer, F.; Walter, K. (2008): Konzeption einer Geodaten- und Geodiensteinfrastruktur als Frühwarnsystem für Hangrutschungen unter Einbeziehung von Echtzeit-Sensorik. GIS, Zeitschrift für Geoinformatik 1/2008 26–35.

Botts, M. (2007): OGC White Paper – OGC Sensor Web Enablement: Overview and High Level Architecture. – Version 3. URL: http://www.opengeospatial.org/pressroom/papers (rev.: 28.12.2007). OGC 07-165.

Fernandez-Steeger, T. M.; Arnhardt, C.; Niemeyer, F.; Haß, S. E.; Walter, K.; Homfeld, S. D.; Nakaten, B.; Post, C.; Asch, K.; Azzam, R.; Bill, R.; Ritter, H.; Toloczyki, M.: Current Status of SLEWS – a Sensor Based Landslide Early Warning System. In: Universitätsgesellschaft Osnabrück e.V.: R & D – Programme Geotechnologien Status Report. Early Warning Systems in Earth Management, 2008

OGC (2008): Sensor Observation Service/Na, Arthur (IRIS Corp.); Priest, Mark (3eTI). URL: https://portal.opengeospatial.org/modules/admin/license_agreement.php?suppressHeaders=0&access_license_id=3&target=h ttp://portal.opengeospatial.org/files/index.php?artifact_id=26667 (rev.: 26.10.2007, accessed 14/01/2009).

W3C (2006): Naming and Addressing: URIs, URLs, ...URL: http://www.w3.org/Addressing/ (accessed 14/01/2009).

Walter, K.; Nash, E.: Coupling Wireless Sensor Networks and the Sensor Observation Service – Bridging the Interoperability Gap. In: Proceedings of AGILE 2009, Hannover. *(accepted)*

Index of Authors

Early Warning Systems for Transportation Infrastructures Workshop (Karlsruhe, 9–10 February 2009

Exhibitors

INFAP, Munich (Industrial fiber applications)
Fürstenrieder Str. 279 a,
81377 München, Germany
www.infab.de
manfred.resch@infap.de

edilon)(sedra, Munich (Embedded rail systems)
Kistlerhofstr. 168, 81379 München, Germany
www.edilonsedra.com
g.schnellboegl@edilonsedra.com

INNOtec Systems GmbH, Worms (In-situ measurement of rail bending forces)
Pfeddersheimer Str. 95,
67549 Worms, Germany
www.innotec-systems.de
hv@innotec-systems.de

System and Data Research Co., Ltd., Tokyo (Earthquake early warning system)
SDR Bldg., 3-25-3 Fujimi-dai, Kunitachi-shi,
186-0003 Tokyo, Japan
www.sdr.co.jp
yutaka@sdr.co.jp

Geoforschungszentrum, Potsdam
(Project EDIM: Self-organizing seismic early warning information network)
Telegrafenberg, 14473 Potsdam, Germany
www.gfz-potsdam.de
picoz@gfz-potsdam.de

GEOTECHNOLOGIEN Science Reports – Already published/Editions

No. 1 Gas Hydrates in the Geosystem – Status Seminar, GEOMAR Research Centre Kiel, 6–7 May 2002, Programme & Abstracts, 151 pages.

No. 2 Information Systems in Earth Management – Kick-Off-Meeting, University of Hannover, 19 February 2003, Projects, 65 pages.

No. 3 Observation of the System Earth from Space – Status Seminar, BLVA Munich, 12–13 June 2003, Programme & Abstracts, 199 pages.

No. 4 Information Systems in Earth Management – Status Seminar, RWTH Aachen University, 23–24 March 2004, Programme & Abstracts, 100 pages.

No. 5 Continental Margins – Earth's Focal Points of Usage and Hazard Potential – Status Seminar, GeoForschungsZentrum (GFZ) Potsdam, 9–10 June 2005, Programme & Abstracts, 112 pages.

No. 6 Investigation, Utilization and Protection of the Underground – CO_2-Storage in Geological Formations, Technologies for an Underground Survey Areas – Kick-Off-Meeting, Bundesanstalt für Geowissenschaften und Rohstoffe (BGR) Hannover, 22–23 September 2005, Programme & Abstracts, 144 pages.

No. 7 Gas Hydrates in the Geosystem – The German National Research Programme on Gas Hydrates, Results from the First Funding Period (2001–2004), 219 pages.

No. 8 Information Systems in Earth Management – From Science to Application, Results from the First Funding Period (2002–2005), 103 pages.

No. 9 1. French-German Symposium on Geological Storage of CO_2, Juni 21./22. 2007, GeoForschungsZentrum Potsdam, Abstracts, 202 pages.

No. 10 Early Warning Systems in Earth Management – Kick-Off-Meeting, Technical University Karlsruhe, 10 October 2007, Programme & Abstracts, 136 pages.

No. 11 Observation of the System Earth from Space – Status Seminar, 22–23 November 2007, Bavarian Academy of Sciences and Humanities, Munich, Programme & Abstracts, 194 pages.

No. 12 Mineral Surfaces – From Atomic Processes to Industrial Application – Kick-Off-Meeting, 13–14 October 2008, Ludwig-Maximilians-Universtität, Munich, Programme & Abstracts, 133 pages.

No. 13 Early Warning Systems in Earth Management – Status Seminar, 12–13 October 2009 Technische Universität München, Programme & Abstracts, 165 pages.

No. 14 Die dauerhafte geologische Speicherung von CO_2 in Deutschland – Aktuelle Forschungsergebnisse und Perspektiven, Herausgegeben von: Ludwig Stroink, J. Peter Gerling, Michael Kühn, Frank R. Schilling, 140 Seiten.

Notes

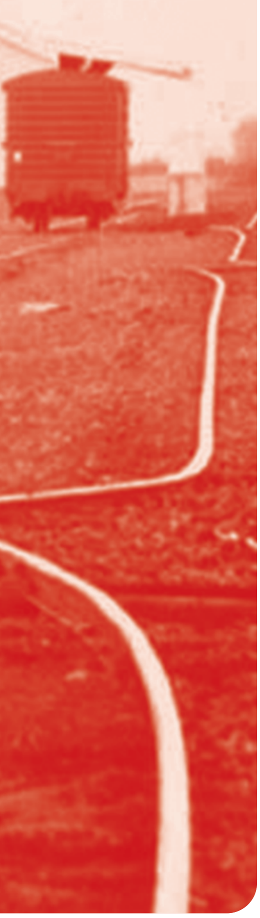

Early Warning Systems for Transportation Infrastructures

Transportation infrastructures are the backbone of modern society. Especially in metropolitan areas, millions of people use land-based transportation systems for commuting to work and for distributing goods, everyday. Hence, transportation infrastructures are justly called lifelines. In earthquake-prone areas, sustained integrity and fast repair is crucial for mitigating the consequences of a natural disaster. In this case, an intact transportation network is vital for providing rapid access to affected areas and for rescuing injured people.

On February 9-10, 2009 an international Workshop on »Early warning systems for transportation infrastructures« was held at the Fraunhofer Institute for Information and Data Processing (IITB) in Karlsruhe. The Workshop was organized by the Karlsruhe Institute of Technology (KIT) and Fraunhofer IITB. The meeting was funded by the geoscientific research and development programme GEOTECHNOLOGIEN.

The Workshop's focus was on the specific safety requirements of railbound transportation systems. For two days international experts from the fields of seismology, sensor technology, railway engineering, computer science, and railway safety reviewed the state of the art and the potential of early warning for transportation systems. Major workshop topics were

- seismic early warning and sensors,
- early warning of endangered trains,
- damage assessment for railway infrastructure,
- modern geo-standard based information systems,
- train control and safety strategies.

Another purpose of the workshop was to delineate the possibilities and limitations of a railway infrastructure integrated network of accelerometers that can be used for permanent structural health monitoring and earthquake early warning.

Bundesministerium
für Bildung
und Forschung

DFG

The GEOTECHNOLOGIEN programme is funded by the Federal Ministry for Education and Research (BMBF) and the German Research Council (DFG)

ISSN: 1619-7399